# Baculovirus surface display of influenza virus haemagglutinin and its potential as a vaccine

**RIYADH ABDULJABBAR ABDULSAHIB ALAKEELY**

A thesis submitted in partial fulfilment of the requirements for University of Oxford Brookes for the degree of

Doctor of Philosophy

September 2018

# Abstract

Based on data obtained from the World Health Organization (WHO), influenza (or flu) is responsible for highly contagious, acute respiratory diseases in humans. These diseases are caused by influenza viruses and result in 250,000 to 500,000 deaths globally every year from seasonal flu. In addition, outbreaks of new influenza subtypes occur that on occasion quickly spread to become an epidemic or pandemic. Prevention and control of the spread of these diseases are mainly based on an effective vaccination regime. To date, the vast majority of influenza vaccines are manufactured using conventional technology based on embryonated hen's eggs that takes several months to produce. However, the threat of influenza virus outbreaks emphasizes the need for a novel, rapid vaccine technology that can respond quickly to stop or reduce the threat of epidemic and pandemic influenza.

Sub-unit vaccines based on baculovirus surface display technology are an option for the development and generation of safe human vaccines due to the lack of pre-existing immunity, toxicity and ability to replicate in mammalian systems. Furthermore, this technology may provide an efficient way to produce a large amount of influenza vaccine within a short time frame with a relatively low cost. Haemagglutinin (HA), the surface glycoprotein of influenza virus, is the preferable target for recombinant vaccine studies as it is known to be responsible for new influenza subtypes that may cause pandemic outbreaks and is the key immunogenic protein that can elicit protective neutralising antibody in the host.

The research in this thesis was focused on investigating baculovirus surface display technology as a novel approach to develop a recombinant influenza vaccine. Several surface display expression vectors were constructed, using either a truncated or full-length HA, to optimise glycoprotein incorporation into the budded virus (BV) envelope of three recombinant baculovirus variants: BacPAK6, BacPAK6 (high-titre) and *flash*BACULTRA (FBU).

Surface display of HA was found to be improved when the native HA signal peptide and transmembrane domain (TMD) were used; replacement of these domains with baculovirus GP64 signal peptide and TMD reduced HA display. The displayed HA was shown to be biologically active by haemadsorption assay and haemagglutination of chicken red blood cells (RBCs). Analysis of HA display by immunoblotting suggested that HA was incorporated into the BV surface envelope in recombinant virus-infected Sf9 and Tni Hi5 cells and that the levels of display varied between the expression vectors and virus promoters tested. This thesis demonstrates the benefits of using the FBU vector with the polyhedrin gene promoter in Tni Hi5 cells for producing HA incorporated into BV. Interestingly, use of the late *p6.9* promoter did not result in increased levels of HA displayed in BV. Initial investigations also demonstrated the promise of RNAi technology to improve HA display by reducing GP64 synthesis and incorporation into the BV surface.

The ability of baculovirus displayed HA to elicit an antibody response was assessed in an initial immunisation study using BALB/c mice. Preliminary results showed a strong immune response using ELISA and the antibodies generated were able to prevent haemagglutination in an inhibition assay. Overall, this study suggests that baculovirus display of HA is efficacious and may offer a novel approach for rapid and large-scale production of influenza subunit vaccines to control influenza outbreaks.

# Publications and Presentations

## Publications

Graves, L., Aksular, M.; **Alakeely, R. A.**, Ruiz Buck, D.; Chambers, A., Murguia-Meca, F., Plata-Muñoz, J., Hughes, S., Johnson, P., Possee, R., King, L. (2018) Improved Baculovirus Vectors for Transduction and Gene Expression in Human Pancreatic Islet Cells. Viruses 10(10):574. https://doi.org/10.3390/v10100574.

## Oral Presentations

**Alakeely, R. A.**, Irons, S. L., Possee, R. D., & King, L. A. (2015) Development of a novel BacMam gene delivery and display vectors using Occlusion-Derived baculovirus particles(ODV). Postgraduate Research Student Symposium, Oxford Brookes University, Oxford, UK.

**Alakeely, R. A.**, Irons, S. L., Possee, R. D., & King, L. A. (2018) Development of novel baculovirus surface display vectors for virus glycoproteins and vaccine production. Biological and Medical Sciences Seminar Series. Oxford Brookes University, Oxford, UK.

## Posters

**Alakeely, R. A.**, Irons, S. L., Possee, R. D., & King, L. A. (2016) The structure of baculovirus occlusion bodies (OB). Graduate College Annual Event. Oxford Brookes University, Oxford, UK. **Winner of 1$^{st}$ place prize for a best student poster presentation.**

**Alakeely, R. A.**, Irons, S. L., Possee, R. D., & King, L. A. (2016) The structure of baculovirus occlusion bodies (OB). Iraqi Cultural and Scientific Conference at Reading University, Reading, UK.

**Alakeely, R. A.**, Irons, S. L., Possee, R. D., & King, L. A. (2016) Baculovirus ODV occluded by polyhedra in different insect cell lines. 49$^{th}$ Annual Meeting of the Society for Invertebrate Pathology, Tours, France.

**Alakeely, R. A.**, Irons, S. L., Possee, R. D., & King, L. A. (2016) Baculovirus ODV occluded by polyhedra in different insect cell lines. Postgraduate Research Student Symposium, Oxford Brookes University, Oxford, UK

**Alakeely, R. A.**, Irons, S. L., Possee, R. D., & King, L. A. (2017) Baculovirus ODV occluded by polyhedra in different insect cell lines. Graduate College Annual Event. Oxford Brookes University, Oxford, UK.

**Alakeely, R. A.**, Irons, S. L., Possee, R. D., & King, L. A. (2019) Baculovirus surface display of influenza virus haemagglutinin and its potential as a vaccine. European Congress of Virology, Rotterdam, Netherlands.

Graves, L., Aksular, M., Ruiz Buck, D., Chambers, A., Murguia-Meca, F., **Alakeely, R. A.**, Plata-Muñoz, J., Hughes, S., Johnson, P., Possee, R. D., & King, L. A. (2019) Development and characterisation of BacMAM vectors as a gene delivery tool for human pancreatic islets. European Congress of Virology, Rotterdam, Netherlands.

Page intentionally left blank

# Dedication

**I would like to dedicate this thesis.**

**First, to the precious homeland, the cradle of civilizations, Mesopotamia, *IRAQ*.**

**To the souls of our martyrs who sacrificed their pure blood for our dear homeland.**

**To my beloved mother, ask Allah Almighty to prolong her life and give her health and wellness.**

**To the soul of my father and my grandparents who were the source of inspiration, strength and encouragement to love science and perseverance to achieve the desired goal since my childhood.**

**To my wife and the gift of Allah for me, my little angels, *Muhammad and Zahraa*.**

**To my brothers, sisters, relatives, and all my friends.**

Riyadh A. Alakeely

# Acknowledgements


## "In the name of Allah, the most beneficent, the most merciful"

PhD journey is a great challenge and it would have been a much more difficult task without the guidance, the help and the support that I received from several people. Therefore, I take this opportunity to extend my sincere gratitude and appreciation to all those who made this PhD thesis possible.

First and foremost, I would like to extend my sincere gratitude to Allah Almighty for the guidance, strength, power of the mind and for the continuation of health and wellness.

I would like to say thank you so much, Professor Linda King, Professor Robert Possee and Dr Sarah Irons for your valuable support and continuous professional guidance throughout the whole period of my study, your help was greatly appreciated.

I gratefully acknowledge my homeland, IRAQ for providing me with this scholarship.

IVRG and Oxford Expression Technologies members, Elisabetta, Carina, Raquel, Adam, Mine, Leo, Olga, Daria, Daniel, Durva, Cassandra, Leonie, Laura, Alice, Becky, thank you so much all for your help, support and friendship. It was a great opportunity to have such lovely friends like you during these four years.

I would also like to extend my thanks to Oxford Expression Technologies Ltd (OET) for collaborating with vaccination experiments.

I am also very grateful to all my friends in Iraq and in the UK. I am especially grateful to my very close friend Dr Rafid Wasfi, for always being there praying for me. I also would like to thank my colleagues, Dr Khalid, Dr Wisaal and Mr Deyaa at Biotechnology Department, College of Sciences, University of Baghdad, Iraq for their help and support to get this scholarship.

Very special words of thanks should go to my friend Raheem Al-Abedi and his family for their generosity in letting me live in their house in Oxford to finish my writing when they were away in Iraq.

Special thanks to my brother in law Moayed and his family for all the pray, help and support during my PhD journey.

My deep appreciation goes out to the people who were physically far apart but the ones closest to my heart, my family. Your love, pray, support and encouragement make me pass all the difficulties I faced during my PhD study.

Lastly, my wife, my sweet daughter, Zahraa and my big boy, Muhammad, great thanks for being patient during my PhD study.

*Riyadh A. Alakeely*

# List of Contents

# List of Figures

# List of Tables

# List of Abbreviations

| | |
|---|---|
| aa: | Amino acid |
| AcMNPV: | Autographa californica multicapsid nucleopolyhedrovirus |
| β-galactosidase gene | *lacZ* |
| BAC: | bacterial artificial chromosome |
| BEVS: | Baculovirus expression vector systems |
| bp: | Base pairs |
| BSA: | Bovine serum albumin |
| BV: | Budded virus |
| CMV: | Cytomegalovirus |
| C-terminal: | Carboxy-terminal |
| DAPI: | 4',6-diamidino-2-phenylindole |
| DMF: | Dimethylformimide |
| DMSO: | Dimethylsulphoxide |
| DNA: | Deoxyribonucleic acid |
| dsRNA: | Double-stranded RNA |
| dNTP: | Deoxynucleotide triphosphate |
| dpi: | Days post infection |
| dpv: | Day post vaccination |
| dsDNA: | Double-stranded deoxyribonucleic acid |
| *E.coli*: | *Escherichia coli* |
| EDS: | Electron-dense spacer |
| EGFP: | Enhanced green fluorescent protein |
| ELISA: | Enzyme-linked immunosorbent assay |
| EM: | Electron microscopy |
| FB: | *flash*BAC™ |
| FBG: | *flash*BACGOLD™ |
| FBS: | Foetal bovine serum |
| FBU: | *flash*BACULTRA™ |
| GV: | Granulovirus |
| HA: | Haemagglutinin |
| HEK293: | Human embryonic kidney cells 293 |
| Hi5: | BTI-Tn-5B1-4 (High Five™) |
| hpi: | Hours post infection |
| *ie1:* | immediate early 1 |
| INM: | Internal nuclear membrane |
| kDa: | kilo Dalton |

| | |
|---|---|
| kbp: | Kilobase pair |
| MAP: | Microtubule-associated protein |
| MNPV: | Multi-capsid nucleopolyhedrovirus |
| MOI: | Multiplicity of infection |
| NPV: | Nucleopolyhedrovirus |
| OBs: | Occlusion bodies |
| ODV: | Occlusion-derived virus |
| ORF: | Open reading frame |
| P10: | The baculovirus 10 kDa protein |
| *p10*: | The baculovirus 10 kDa protein gene |
| PBS: | Phosphate buffered saline |
| PCR: | Polymerase chain reaction |
| PE: | Polyhedral envelope |
| PEP: | Polyhedral envelope protein |
| pfu: | Plaque forming units |
| PIF: | *Per os* infectivity factor |
| *polh*: | polyhedrin |
| RNA: | Ribonucleic acid |
| rpm: | Rotations per minute |
| RT: | Room temperature |
| SDS: | Sodium dodecyl sulfate |
| SDS-PAGE: | Sodium dodecyl sulfate polyacrylamide gel electrophoresis |
| Sf: | *Spodoptera frugiperda* |
| Sf21: | IPLB-SF-21 cell line |
| SNPV: | Single-capsid nucleopolyhedrovirus |
| Tni: | *Trichoplusi ni* |
| TEM: | Transmission electron microscopy |
| TE: | Tris-Ethylenediaminetetraacetic acid |
| TMD: | Transmembrane domain |
| X-gal: | 5-Bromo-4-chloro-3-indolyl β -D-galactopyranoside |

# Chapter 1
# Introduction

## 1.1 Baculoviruses

It has been established from fossils 100 million years old that huge numbers of baculovirus occlusion bodies (OBs) were present in arthropods at that time (reviewed by Poinar and Poinar, 2005). Baculoviruses are a group of viruses that are widely spread in the environment and they mainly infect arthropods of the insect order. However, they have been isolated from over 600 host insect species that belong to different orders such as Diptera (mosquitoes), Lepidoptera (butterflies and moths) and Hymenoptera (wasps) (Herniou *et al.*, 2003). The majority of lepidopteran baculoviruses species are well known and among the best identified, in contrast to other baculoviruses species isolated from other arthropod orders (Hiscock and Upton, 2000). The name baculovirus was first suggested by Mauro Martignoni according to the rod-shaped virion, which derived from the latin word “baculum” (cane, walking stick). Martignoni also suggested naming of the baculovirus family (Baculoviridae) in 1973 based on the type of genome and virion morphology (reviewed by Rohrmann, 2013a).

The previous taxonomy, based on the life cycle characteristics and virion morphology, classified the family Baculoviridae into two genera: Nucleopolyhedrovirus (NPV) and Granulovirus (GV) (Murphy *et al.*, 1995). Based on the virus species, NPV could either comprise a single nucleocapsid (single nucleopolyhedrovirus, SNPV) or multiple nucleocapsids (multiple nucleopolyhedroviruses, MNPV). Whereas GV virions comprise a single nucleocapsid only (reviewed by Rohrmann, 2013a). Later, based on morphological, biological and phylogenetic characteristics, the Baculoviridae family was classified into four genera: Alphabaculoviruses and Betabaculoviruses in which both infect Lepidoptera and include NPVs and GVs, respectively (Jehle *et al.*, 2006). While baculoviruses that infect Hymenoptera and Diptera are known as Gammabaculoviruses and Deltabaculoviruses, respectively (Jehle *et al.*, 2006). In addition, the Alphabaculovirus can be divided into two subgroups: group I and group II based on the envelope fusion protein type incorporated into the budded virus (BV) (Jehle *et al.*, 2006). All group I baculoviruses have the GP64 glycoprotein on their BV envelope, while group II has furin-cleaved (F) protein instead (Herniou and Jehle, 2007).

Generally, baculoviruses are known as having a limited host range, capable of infecting one species only or its closest relatives within a single genus or family. However, Autographa californica multiple nucleopolyhedroviruses (AcMNPV) is an exception, able to infect approximately 39 species among 13 families of Lepidoptera (Entwistle and Evans, 1985; Bonning and Hammock, 1992). AcMNPV is a type I alphabaculovirus and was first isolated in 1971 from alfalfa looper larva and it is the model baculovirus for this study. Baculoviruses

capsid size varies between species ranging from 40–50 nm in diameter and 200–400 nm in length and encloses a large circular, double-stranded DNA, which also varies between species with size ranging from approximately 80 to 180 kilobase pair (kbp) in length (Funk *et al.*, 1997).

The first completely sequenced baculovirus prototype was AcMNPV and it was found to be around 134 kbp in size and harbour about 154 predicted open reading frames (ORFs, (Ayres *et al.*, 1994). This prototype has received the greatest attention among other baculoviruses. Baculoviruses have been exploited for human benefit first as a biocontrol agent against the agricultural pests. However, their use has been expanded over the last two decades to applications such as the production of recombinant proteins (Kost *et al.*, 2005). Currently, they are also used as vectors to deliver target gene(s) to mammalian cells for gene therapy or as a surface display for various target proteins (Airenne *et al.*, 2013).

## 1.2 The structure of occlusion bodies

The occlusion body (OB) structure plays an important role in the Baculoviridae family classification. The OB polyhedra structure can be easily observed under the light microscope due to its refractory nature and larger size (reviewed by Adam and McClintock, 1991). Polyhedrin is the main OB protein component and it is about 30 kDa, which gives the OB the polyhedra shape with size ranging from 0.6 to 2 μM in diameter (reviewed by Rohrmann, 2013a). On the other hand, the OB of the GV genus has a granule structure. Granulin is the main GV OB protein component and it is about 30 kDa, which gives the OBs the oval shape that is range about 0.5 μM in length and 0.2 μM in width. Therefore, it is very difficult to be observed under the light microscope (reviewed by Rohrmann, 2013a). Electron microscope (EM) images of both NPV and GV OBs are shown in Figure 1.1. The NPV polyhedra usually contain several occlusion-derived viruses (ODVs), which comprise either single or multi nucleocapsids (Figure 1.1A; Summers and Arnott, 1969). In contrast, the vast majority of the GV include only one ODV, which comprise a single nucleocapsid (Figure 1.1B; Summers and Arnott, 1969). It has been found that during OB formation of both genera, they are surrounded by a glycoprotein multi-layered lattice structure called the calyx or polyhedral envelope (PE) (Whitt and Manning, 1988; Adam and McClintock, 1991). Baculoviruses enveloped in OB can stay viable and stable in the environment in the soil or on plant surfaces for decades, unlike other enveloped viruses, which can lose their viability due to harsh environmental factors such as UV light and high temperatures (Rohrmann, 2013a). It has been found that in the absence of the PE, the OB surface appears to be uneven and pitted, and are prone to losing ODVs (reviewed by Chambers, 2012). The PE

formation process is still not clear but it is thought that both P10 and electron dense spacers (EDS) may play important role in the OB construction (Gross *et al.*, 1994).

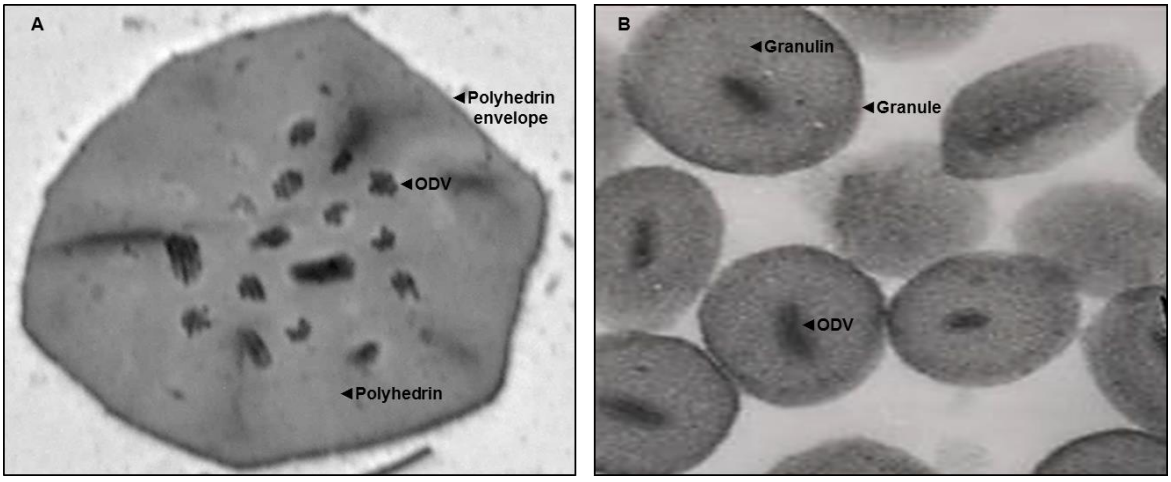


**Figure 1.1: Purified baculovirus occlusion bodies as observed by transmission electron microscopy (TEM).**
Two structural forms of OB as they appear under the TEM. A: Autographa californica multiple nucleopolyhedroviruses (NPV, AcMNPV) includes single or multiple nucleocapsids in OB, (EM image produced in this study). B: Plodia interpunctella granulovirus (GV) granulin includes a single nucleocapsid in OB, EM image (Image kindly provided by R. Possee). The OB of NPV and GV consists of polyhedrin and granulin, respectively.

## 1.3 The life cycle of baculovirus

Two distinct virion phenotypes are produced during the bi-phasic life cycle of the baculovirus: budded virus (BV) and occlusion-derived virus (ODV) (Blissard and Rohrmann, 1990). These two phenotypes play different roles during the baculovirus life cycle. In addition, each phenotype is produced in a different location inside the host cell and at different times after infection. The BV are produced during the late phase of infection and it includes a single nucleocapsid surrounded by virion envelope (Figure 1.2A). Nucleocapsids bud through the plasma membrane of the host cell, acquiring the GP64 enriched envelope, which is the major protein for BV attachment and for spreading the virus from cell to cell inside the host insect or during the virus amplification in cell culture (reviewed by Rohrmann, 2013b).

Compared to BV, the ODV are produced in the very late phase of infection. The ODV include either single or multiple nucleocapsids surrounded by a lipid bi-layer envelope that are packaged together in a protein crystal called the polyhedron. (Figure 1.2B; reviewed by Slack and Arif, 2007). These comprise the OBs, which are responsible for virus stability outside the host insect and for delivering the infectious virus to insect midgut cells during the horizontal transmission between insect hosts (reviewed by

Rohrmann, 2013b). The ODV envelope is more rigid than the BV envelope due to the high content of saturated fatty acid phospholipids. Furthermore, the ODV envelope contains phosphatidylcholine, which is replaced by phosphatidylserine in the BV envelope (Slack and Arif, 2007). In addition, the ODV envelope viral proteins are more diverse than the BV envelope proteins. Most of these proteins are non-glycosylated (Slack and Arif, 2007).

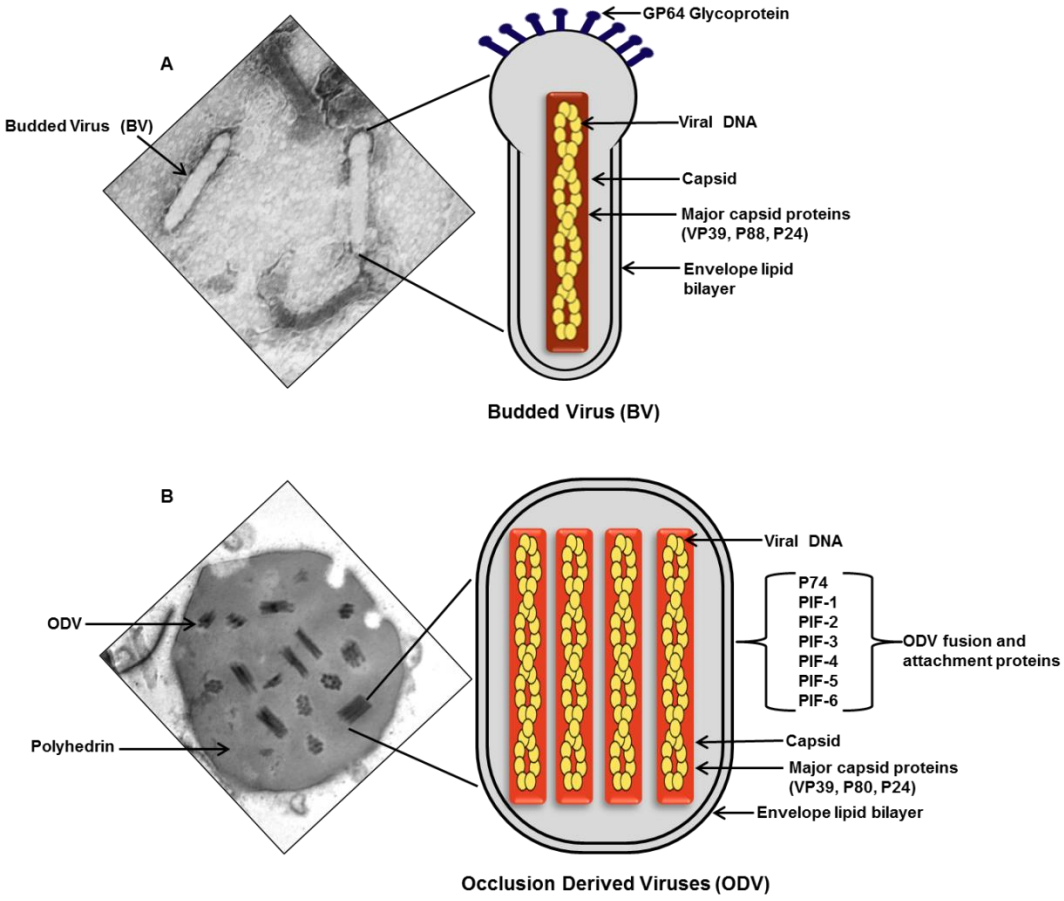


**Figure 1.2: Schematic representation of the baculoviruses two distinct virion phenotypes.** **A:** Illustrates the AcMNPV budded virus (BV) EM image and it's model structure. The BV includes a single nucleocapsid that is enclosed in a lipid bilayer and it has GP64 envelope protein at the apical ends. **B:** AcMNPV occlusion body (OB) EM image including multiple occlusion-derived viruses (ODV) and their structures; the ODV includes multi nucleocapsids that are enclosed in a lipid bilayer.

The ODV envelope contains several different proteins (Figure 1.2 B; Braunagel and Summers, 2007) including seven highly conserved proteins among all baculoviruses (PIF1, PIF2, PIF3, PIF4, PIF5, PIF6 and P74), which are distributed on the outer ODV envelope. These proteins are known as "*per os*" infectivity factors (PIFs) and they play an essential role in oral infectivity. Any mutation or deletion of these genes from the baculovirus genome can result in loss of oral infectivity. However, viral replication in cell culture is not affected (Peng *et al.*, 2010). It has been found that PIF1-PIF3 with P74 form a stable complex of proteins, which is believed to play an essential role in ODV binding to the host midgut. This

binding facilitates the nucleocapsids releasing into the cytosol (Horton and Burand, 1993; Haas-Stapleton *et al.*, 2004; Braunagel and Summers, 2007; Slack and Arif, 2007). Despite the difference in the BV and ODV envelope membrane in terms of lipid and protein components, both share the same nucleocapsid structure (Figure 1.2 A and B; Funk *et al.*, 1997). The two virus phenotypes differ in biochemical, biological and biophysical properties, however, both are present in the infected insect larva and when the virus is propagated in cell culture.

### 1.3.1 Baculovirus life cycle in insect larva

The baculovirus replication cycle starts when the insect larva inadvertently consumes OB-contaminated plant parts (Figure 1.3 page 7; Keddie *et al.*, 1989). Following ingestion, the OBs naturally move through the foregut into the insect midgut. The high alkaline conditions (pH 10-11) and the proteases present in the host midgut result in dissolution of the protein matrix that comprises the OB (Harrap, 1972; Pritchett *et al.*, 1984). As a result, ODV are released from the polyhedra into the host midgut lumen after about 12 minutes of entry and bind to columnar epithelial cells (Adam and McClintock, 1991). Then the ODV penetrate the peritrophic membrane of midgut cells by PIF factors and enter the cells via the apical ends of the microvilli, by clathrin-mediated adsorptive endocytosis. (Federici and Hice, 1997). Once the ODV enter the epithelial cells, nucleocapsids are unpackaged and released into the cytosol and journey to the nuclear membrane by actin polymerisation and enter the nucleus via nuclear pores (Figure 1.3; Charlton and Volkman, 1991; van Loo *et al.*, 2001).

Four different successive phases of gene expression occur in the nucleus: immediate-early (ie), which is active from virus contact with the cells 0-3 hours post infection (hpi), delayed early (3-6 hpi), late (6-24 hpi) and very late (18-72 hpi) (reviewed by Miller, 1997; Figure 1.4 page 8 ). The first two phases start when the viral DNA in the nucleus becomes uncoated and triggers the early viral genes for immediate transcription by host RNA polymerase (reviewed by Rohrmann, 2013b). The early proteins resulting from this process are crucial for early transcription, the replication of viral DNA and inhibition of host cell apoptosis.

The expression of the *ie* genes such as *ie-0*, *ie-1*, *ie-2* and *pe-38* are started first and transcription of foreign gene(s) in non-infected host cells can be driven by these gene promoters (Figure 1.4). It has been suggested that *ie-1* expressed in the early and late phases of the host infection play an important role in baculovirus gene expression regulation. For example, the delayed-early genes and some of the late genes such as the late capsid protein gene (*vp39*) and the very late *polh* can be triggered by the activity of the IE-1 multifunctional transcriptional regulatory protein (Passarelli and Miller, 1993).

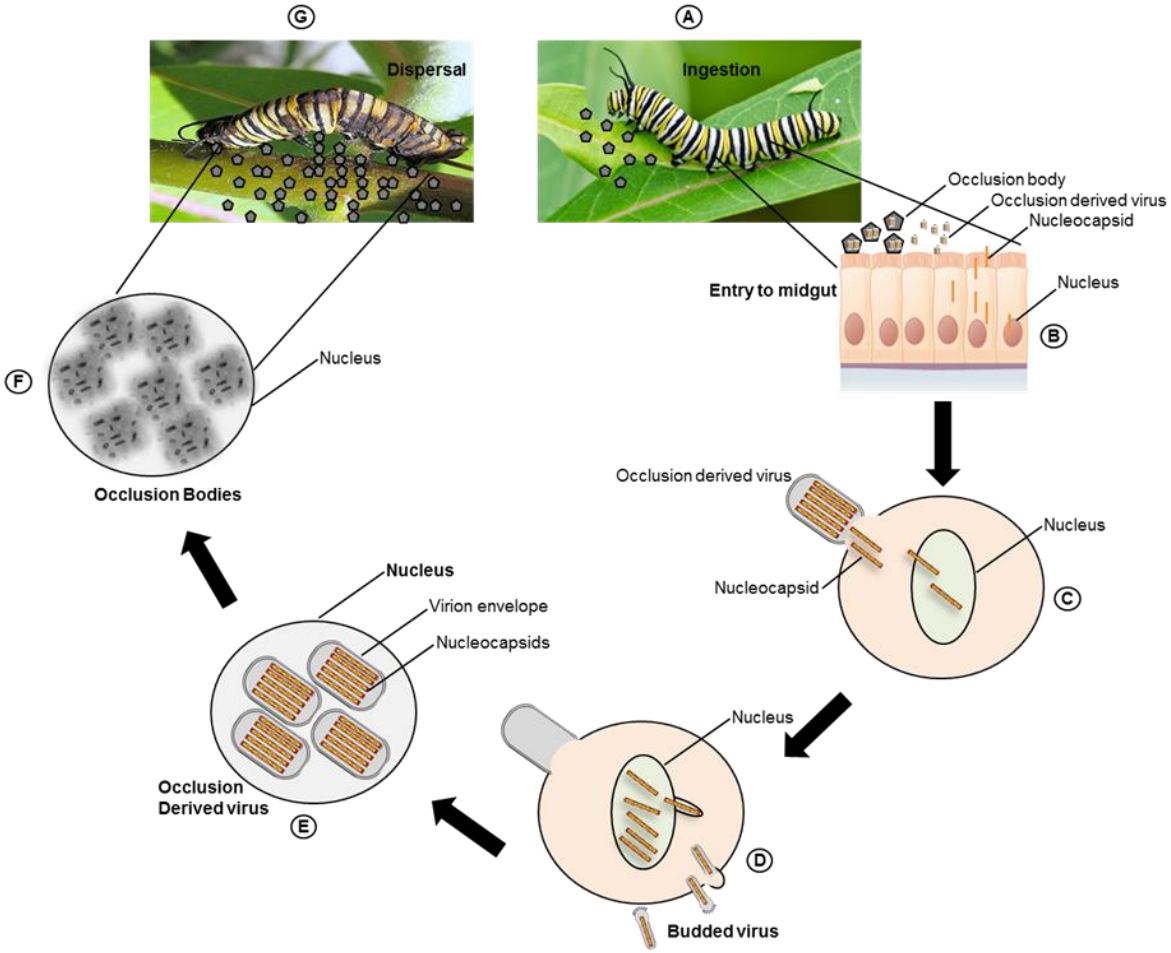


**Figure 1.3: Schematic representation of the baculovirus life cycle in vivo.**
The virus life cycle begins when the insect larvae ingest food contaminated with OBs (A). The OBs dissolve in the high alkaline condition of the insect midgut (pH 10-11), followed by the release of the ODVs resulting in a primary infection (B). The nucleocapsids are transported from the cell cytoplasm into the nucleus and the viral DNA transcription and replication begin (C). Two distinct virion phenotypes are produced in this single infection cycle, budded virus (BV), which is responsible for spreading the virus infection from cell to cell inside the host insect (D). Occlusion derived viruses (ODVs) are produced in the very late phase of the infection in the nucleus (E), they are further packaged in a protein crystal called the polyhedra (F). These comprise the occlusion bodies (OBs), which are responsible for virus stability outside the host insect and for delivering the infectious virus to insect midgut cells (G).

The replicated viral genomes are then enveloped to assemble into new nucleocapsids (Granados, 1978; Slack and Arif, 2007), which first bud out through the nuclear membrane and finally via the host cell membrane where they acquire their envelope GP64 glycoprotein (Figure 1.3). The BVs are infectious and can transmit the infection from the host cells midgut, via tracheal cells or the haemolymph to entire larval tissue, this is called secondary infection (Federici and Hice, 1997; Volkman, 1997). The production of BV then declines from about 24 hpi (Shi *et al.*, 2015).

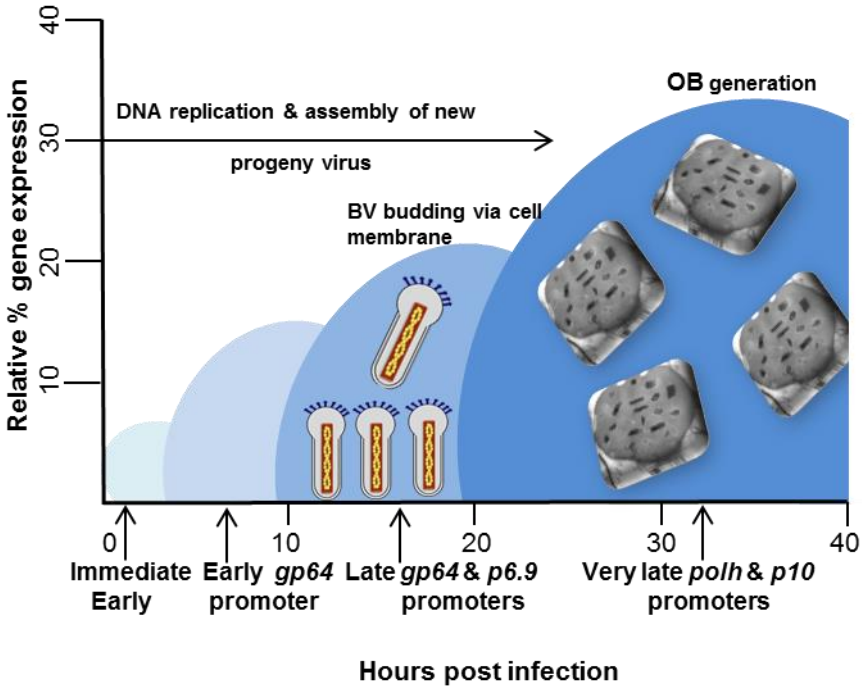


**Figure 1.4: Schematic representation of baculovirus phases of gene expression.**
Baculovirus infection cycle involves four successive gene expression phases: immediate early, early, late and very late. During the early phases of host infection, virus genes transcription relies on the host RNA polymerase, which then shifts to viral RNA polymerase after viral DNA replication. BV are produced following the late genes transcription between (6-24 hours), while ODV produced after the very late gene transcription, which starts from 18 hours onwards. The graph also shows the gene promoters activity during infection stages: *gp64* promoter is active in early and late phases of host infection while *p6.9* promoter is active during the late phase. In contrast, *polh* and *p10* expression start in the very late phases of host infection resulting in the generation of OB and nuclear lysis, respectively.

The accumulation of the ODV envelope proteins during the late and very late phases of the viral infection leads to envelopment of the nucleocapsids within the nucleus. It has been suggested that this process could stop the nucleocapsids leaving the nucleus to form the BV (Rohrmann, 2013b), It is still of speculation how the ODV envelope is synthesized. It could be either synthesized *de novo* or may be derived from the internal nuclear membrane (INM). During the late stage of the host infection, the ODV envelope proteins and INM are modified and invaginated as microvesicles into the nuclear ring zone. If this hypothesis is used, the virus must induce "*de novo*" INM synthesis to produce adequate material during infection for all nucleocapsid envelopment to be ODV. It has been found that the ODV nucleocapsids are enclosed in a proteinaceous virus-derived envelope first before they become ODV. Following, the ODV start to appear within the nuclear ring zone and then are occluded into the OBs starting from 24 hpi (Slack and Arif, 2007).

During the very late phases of infection, the OBs are surrounded by a polyhedrin envelope (PE)/calyx. Then, the mature OBs accumulate within the nucleus of the infected larval cells (Jarvis *et al.*, 1991; Carstens *et al.*, 1992) as shown in (Figure 1.3). During the very late phases of larval infection, another protein is also hyper-expressed, which is known as P10. The P10 protein plays important role in the assembly of tubule-like structures initiated within the cell cytoskeleton, which leads to penetration of the cytoplasm and the nucleus of the infected cells (Patmanidi *et al.*, 2003; Carpentier *et al.*, 2008). It has been found that P10 also play an essential role in PE construction and OB maturation (Lee *et al.*, 1996).

The release of OBs from the nuclei of the infected larva cells begins from 48 hpi due to the viral cathepsin protein activity, which also plays a role in the infected larva liquefaction (Figure 1.3). It has been demonstrated that cells in a culture infected with an AcMNPV cathepsin-deletion mutant are unable to release OBs into the media (Slack *et al.*, 1995). P10 is also found to play a role in cell lysis and host cell microtubule interaction (Patmanidi *et al.*, 2003). Releasing the OBs from host cell nuclei into the tissue results in enlargement and weakening of the infected larva basal lamina, which eventually causes the infected larva to die and liquefy within 5-10 days (Figure 1.3). The OBs are then released into the environment in which a new infection cycle can occur when they ingested by new larvae (Blissard and Rohrmann, 1990).

### 1.3.2 Baculovirus life cycle in cell culture

The baculovirus replication cycle in both insect larval cells and in insect cell lines are similar. However, it is essential to infect cultured insect cells with BV as the infectivity of ODV in cell culture is about 1,800 fold lower (Volkman *et al.*, 1976). The most common insect cell lines used for AcMNPV research are those isolated from *Spodoptera frugiperda* IPLB-Sf21-AE (Sf21), *S. frugiperda* (Sf9) or *Trichoplusia ni* (T.ni) (Wickham *et al.*, 1992; Patterson *et al.*, 1995). Sf21cells are a continuous cell line, which was originally isolated from pupal ovarian tissue of the fall army worm, *S. frugiperda* (Vaughn and Fan, 1997) and the Sf9 is a clonal cell line that was developed from Sf21 cells. High Five (Hi5) cells were derived from the cabbage looper *Trichoplusia ni* egg cell homogenates and are also used for protein production (Wickham and Nemerow, 1993; Granados *et al.*, 1994).

The first step of the cell culture infection is when the BV attaches to a receptor on the cell surface membrane (Figure 1.5 page 10). This process is mediated by the envelope fusion glycoprotein GP64 (Okano *et al.*, 2006). Subsequently, following binding, the virus enters the cells via clathrin-mediated endocytosis (Long *et al.*, 2006). The stimulation of endocytitic processes leads to an increase of clathrin concentration inside the cell plasma membrane

at the point of BV attachment, which allows BV uptake within vesicles (Figure 1.5). Vesicles are then transported into endosomes using the cell cytoskeleton network. The BV escapes and merges with the endosome membrane, due to a conformational change in the GP64 viral envelope protein that results from endosome acidity (pH 5.9-6.0) (Charlton and Volkman, 1993; Plonsky *et al.*, 1999).

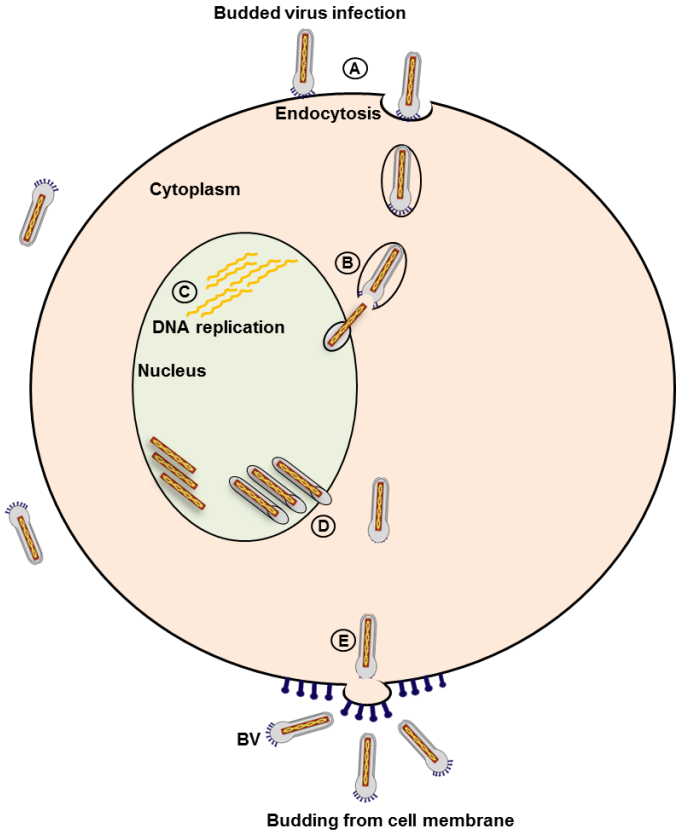


**Figure 1.5: Schematic representation of the baculovirus life cycle insect cell culture.**
Baculovirus life cycle in cell culture begins when the budded virus (BV) attaches to the cell membrane and enter by endocytosis (A). The BV is transported within a vesicle into the nucleus to start the gene expression and viral replication and new progeny BVs are produced (B-D). Finally, BV acquire their GP64 envelope protein when they bud through the cell membrane (E) and start a new infection.

This process leads to the release of the uncoated nucleocapsids into the cell cytoplasm, where they then migrate to the nucleus to start gene expression and viral replication (Figure 1.5; Rohrmann, 2011). It has been found that the GP64 conformational change in acidic conditions allows direct BV fusion with the host cell plasma membrane with no need for endocytosis. However, it is highly unlikely that the BV could face these conditions outside the cells within the host insect larvae (Dong *et al.*, 2010).

The success of baculovirus infection in cell lines depends on the following factors. The first factor is the multiplicity of infection (MOI, the number of BVs used to infect a cell) (Licari

and Bailey, 1991). Using a high MOI leads to most of the cells in the culture being infected at the same time. The second factor that can affect virus infection is the cell cycle phase. In general, the infection of host insect cells with BV leads to the arrest of the cell cycle in the G2/M phase (reviewed by Monteiro *et al.*, 2012). Lynn and Hink (1978) demonstrated that the cells infected at either the G1 or S phase show a higher percentage of cell infection than those infected in the G2 phase. Later, a study by Kioukia and colleagues demonstrated that Sf9 infection with baculovirus in S phase was significantly more efficient (Kioukia *et al.*, 1995). Saito *et al.* (2002) also confirmed these results, when they compared the yield of cell infection in G1/S phase with cells infected at G2/M phases. Finally, the number of baculovirus passages in cell culture can cause mutation in the viral genome (Cheng *et al.*, 2013). Generally, this mutation occurs in the *fp25k* gene location leading to a new baculovirus phenotype that produced few polyhedra (FP) within the nucleus of the infected cell.

## 1.4 GP64 baculovirus envelope glycoprotein

It has been shown that after infection of insect cells, purified AcMNPV BV can be neutralized with the AcV1 monoclonal antibody (Hohmann and Faulkner, 1983). In addition, Mangor *et al.* (2001) demonstrated that GP64 is the main BV envelope glycoprotein; it is present in all group I baculoviruses and it has an essential role in BV infectivity. Furthermore, AcMNPV mutants deficient in *gp64* are unable to infect other cells lines. Moreover, occluded virions produced from the mutant *gp64* AcMNPV are unable to initiate a productive (lethal) infection in larvae as the BV cannot spread the infection from cell to cell inside the infected larval body (Monsma *et al.*, 1996). *In vitro* biosynthesis analysis and DNA sequencing (Whitford *et al.*, 1989) showed that the synthesis of the AcMNPV GP64 glycoprotein occurred in both the early and late infection phases (Figure 1.4). In addition, the biosynthesis analysis showed that GP64 includes an N-linked glycosylation site in its structure, which is essential for surface expression and for infectious BV production (Stiles *et al.*, 1983; Charlton and Volkman, 1986; Jarvis and Garcia, 1994).

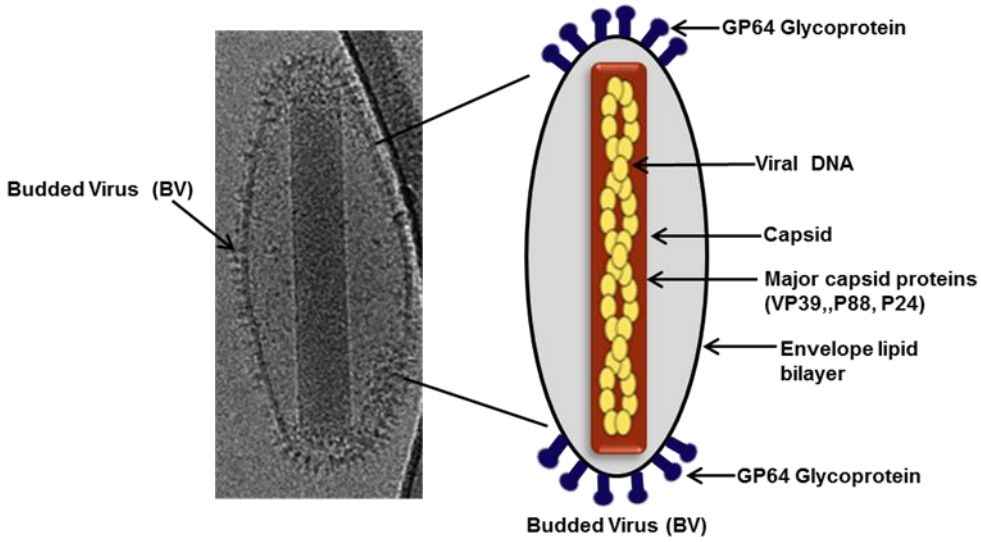


**Figure 1.6: Schematic representation of the Cryo-EM image of AcMNPV budded virus.** Illustrates the recent AcMNPV BV ovoid-shaped and its model structure. The BV includes a single nucleocapsid that enclosed in a lipid bilayer and it has GP64 envelope protein at both apical ends. The EM image is taken from Wang *et al*. (2016) based on the permission rights obtained from ScienceDirect.

Oomens and Blissard (1999) demonstrated that the GP64 protein exists as a disulphide linked trimer of proteins in which each one has a signal peptide at the amino-terminus (N-terminal) and an anchor domain at the Carboxy-terminal (C-terminal). The GP64 was also found to be distributed on the infected cell plasma membrane in the form of spikes and incorporated into the BV envelope surface when it buds out via the cell membrane (Figure 1.3 and 1.4) (Volkman *et al.*, 1984). Ultra-structural studies of AcMNPV using EM, confirmed the existence of the GP64 envelope protein on the apical end of the rod-shaped BV (Figure1.2 A; Fraiser, 1986). However, Wang *et al.* (2016) more recently demonstrated that the BV imaged by cryo-EM has an oval shape with the GP64 envelope proteins distributed on both polar ends (Figure 1.6).

## 1.5 Baculovirus expression vector system

### 1.5.1 Introduction to baculovirus expression vector systems

In the early 1980's, AcMNPV was first exploited as an expression vector by Smith *et al.* (1983). In this study, they demonstrated that the expression of the human β-interferon protein in insect cell cultures significantly increased and reached high levels, when the gene was inserted into the AcMNPV genome under control of the *polh* promoter, due to the hyper-expression of this promoter during the late and very late phase of insect cells infection. Within a short time following this publication, Miller and co-workers published similar results, this time on *Escherichia coli* β-galactosidase expression (reviewed by van Oers *et al.*,

2015). These publications highlighted the birth of the baculovirus expression vector system (BEVS). During the three decades since these findings, several developments have been achieved over the original BEVS.

The earliest construction of BEVS was dependent on polyhedra-negative viruses, in which the *polh* coding region was replaced with the target gene for recombinant baculovirus production. The expression of the target gene(s) was under the control of the strong *polh* promoter. The BEVS has become an attractive expression system because of its ability to infect insect cell lines, which can achieve recognisable post-translational modifications necessary for the biological activity of complex proteins, such as phosphorylation, glycosylation and disulfide bond formation (Klenk, 1996; Geisler and Jarvis, 2009). As a result, recombinant proteins have similar features to the native ones in both structure and function (Hoss *et al.*, 1990). In addition, recombinant proteins produced in insect cell culture using this system can be easily scaled up and high concentration propagation can be achieved by using these cells (Elias *et al.*, 2000). The genome size of AcMNPV is generally too large for the direct insertion of the target gene(s). Hence, transfer vectors must be used for target gene insertion, which contain sequences that flank the *polh* gene.

### 1.5.2 Development of the baculovirus expression vector systems

#### 1.5.2a BacPAK6 system

BacPAK6 viral DNA is based on the AcMNPV genome in which the *polh* gene-coding region has been replaced with the *lacZ* gene. This system involves three *Bsu*36I restriction sites, the first one in the *lacZ* gene whereas the others are located in the two genes flanking *lacZ* (Kitts and Possee, 1993). Restriction digest of the BacPAK6 virus DNA with *Bsu*36I restriction enzyme removes the *lacZ* gene in addition to part of an essential gene (ORF1629) leading to the production of a linear virus DNA, which is unable to propagate in transfected insect cells. The BacPAK6 system produces recombinant baculoviruses by the co-transfection of insect cells with the linearized baculovirus DNA and the transfer vector. Homologous recombination replaces the *orf1629* in addition to the target gene insertion into the genome of the virus, which leads to recovery of circular virus DNA and infectious virus containing the target gene (Figure 1.7 page 14; Kitts and Possee, 1993). This process leads to recovery of about 90% of recombinant virus, and 10% original parental virus. Therefore, the culture medium containing BV needs to be purified using a plaque assay to separate the recombinant from parental virus (Kitts and Possee, 1993). This assay is considered very time consuming and in addition, requires technical proficiency (Kitts *et al.*, 1990). This system is now available commercially from Oxford Expression Technologies Ltd (OET).

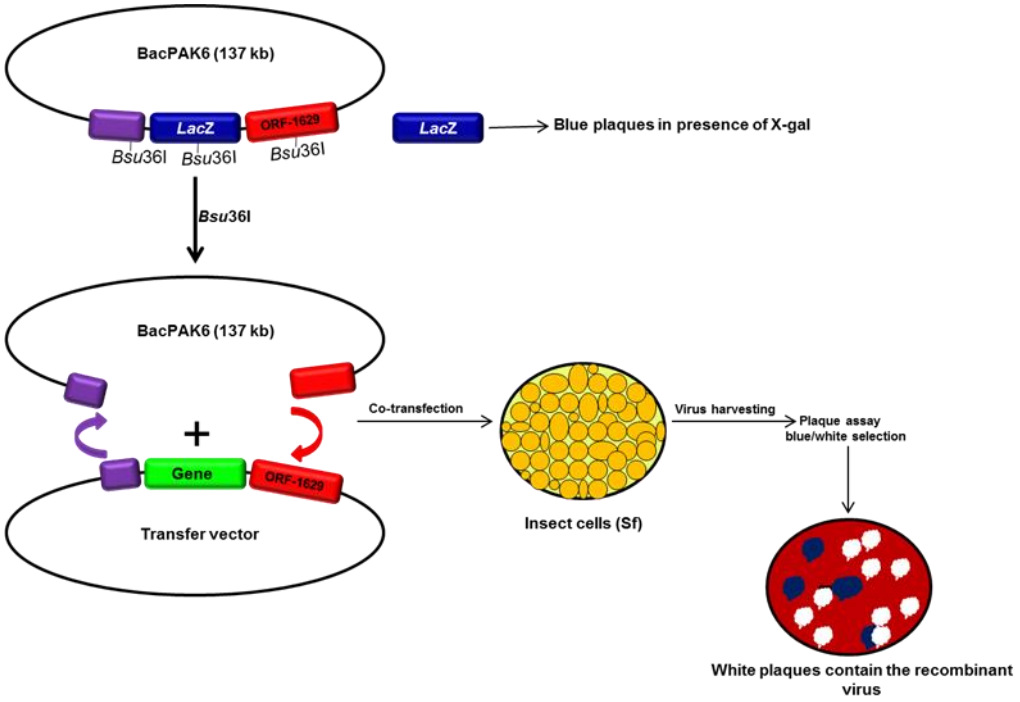


**Figure 1.7: Schematic representation of the recombinant virus generation.**
The BacPAK6 system produces recombinant baculoviruses by the co-transfection of Sf insect cell lines with the linearized baculovirus DNA and transfer vector. Homologous recombination replaces the *orf1629* in addition to the target gene insertion into the genome of the virus, which results in recovery of the circular baculovirus DNA and infectious virus containing the target gene. The recombinant virus is purified by blue/white plaque assay in the presence of X-gal. White plaques contain the recombinant virus.

### 1.5.2b BacPAK6$^{HT}$ system

It has been found that the number of AcMNPV passages in the cell culture using a high multiplicity of infection (MOI) can cause mutation in the viral genome (Cheng *et al.*, 2013). Generally, this mutation occurs in the *fp25k* gene location leading to a new baculovirus phenotype that produces few polyhedra (FP) within the nucleus of the infected cell. Furthermore, the number of polyhedra in AcMNPV *fp25*k mutants is decreased due to the reduction in *polh* promoter activity, which was particularly noticeable in Tni cells (Katsuma *et al.*, 1999; Cheng *et al.*, 2013). These mutations also lead to a significant increase in the number of BV in cell culture medium, which varies between insect cell lines (Harrison and Summers, 1995). For example, this phenotype was clearly noticed in Hi5 and Sf9 cells but not in Sf21 cells (Cheng *et al.*, 2013). This mutation may be more beneficial than the normal BV phenotype in some studies such as vaccine production and gene therapy that require high BV virus titre (Fraser *et al.*, 1995; Cheng *et al.*, 2013). The mutant virus genome has been called (high-titre) BacPAK6$^{HT}$, however, the *polh* promoter in BacPAK6$^{HT}$ is less efficient than in BacPAK6 (personal communication, R. Possee OET Ltd). The *p10* promoter is not affected by the *fp*25K mutation, therefore, it can be used to drive the foreign gene

expression. Recombinant baculoviruses produced using the BacPAK6$^{HT}$ system use the same protocols as described previously for the BacPAK6 system (1.5.2a), except the transfer vector should have a *p10* promoter, not *polh*.

### 1.5.2c Bac-to-Bac$^{TM}$ expression system

In order to omit the plaque purification step from the isolation of recombinant virus, an AcMNPV bacmid vector has been generated by insertion of *lacZ* gene as a selection marker and Tn7 transposition sites into the baculovirus genome. This genome can be maintained inside competent DH10BAC *E.coli* cells instead of insect cells using a mini-F replicon (Luckow *et al.*, 1993). The transfer vector encodes the target gene and Tn7 transposase. The transposition occurs inside *E.coli* cells in which the *polh* coding region is replaced with the target gene(s) in the position located between the Tn7 left and right arms, leading to destruction the *lacZ* gene (Figure 1.8).

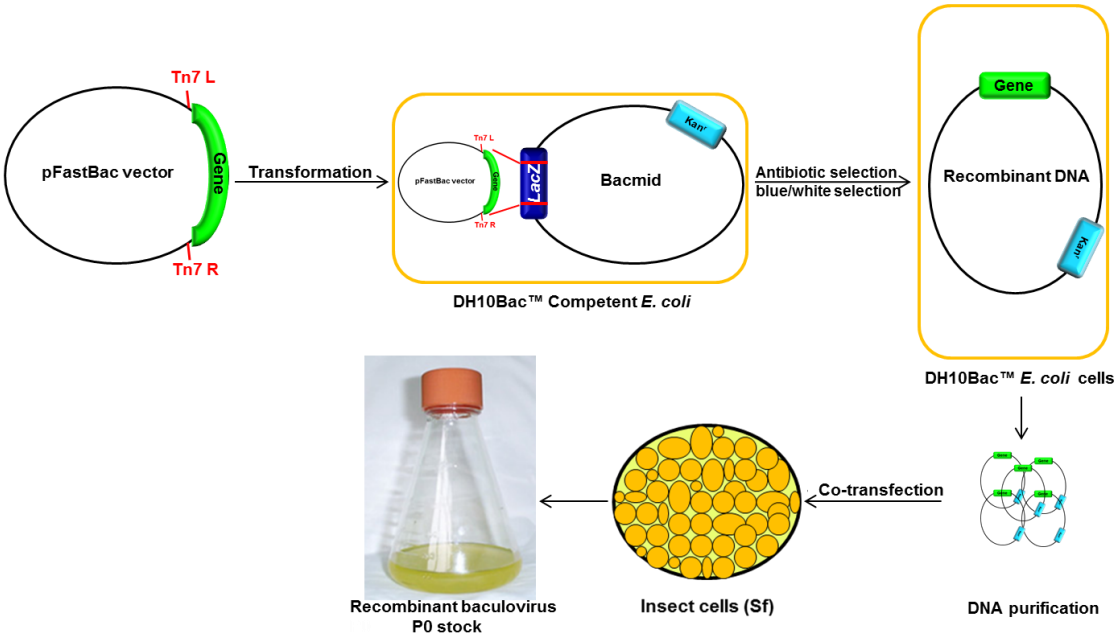


**Figure 1.8: Schematic representation of the recombinant virus generation using Bac-to-Bac$^{TM}$ system.**
Baculovirus shuttle vector (bacmid) includes the *lacZ* gene, Tn7 transposition sites (red) and kanamycin resistance gene (light blue). The insertion of the gene of interest into the baculovirus bacmid results in *lacZ* disruption. The transformed bacteria will then plate on agar media containing kanamycin antibiotic and X-gal for blue/white colony selection due to the activity of β-galactosidase. The purified recombinant bacmid is then used to transfect Sf insect cell lines to generate the P0 stock of recombinant baculovirus.

The transformed bacteria are then plated on agar media containing a suitable antibiotic and X-gal for blue/white colony selection due to the activity of β-galactosidase. The white colonies are selected and propagated followed by recombinant DNA extraction by an

alkaline lysis protocol. Finally, insect cells are transfected with the recombinant viral bacmid DNA in order to produce the recombinant BV (Figure 1.8; Luckow *et al.*, 1993). This system has been commercialized by Invitrogen Ltd as Bac-to-Bac™.

### 1.5.2d *flash*BAC™ system

The *flash*BAC™ (FB) system has been developed by OET Ltd. by generating an AcMNPV genome that lacks part of an essential gene (*ORF 1629*) and by replacing the *polh* coding region with a bacterial artificial chromosome (BAC). These changes prevent the replication of the parental virus within insect cell lines and allow recombinant baculovirus generation in a single step without the need for plaque purification. In addition, *flash*BAC circular DNA can be easily amplified and maintained in *E.coli* cells. Therefore, there is no need for DNA linearization using restriction enzymes before the recombination step (Figure 1.9; (Possee *et al.*, 2008). Insect cells are co-transfected with the *flash*BAC circular DNA and the transfer vector, which includes the gene of interest. Homologous recombination between *flash*BAC circular DNA and the transfer vector results in replacement of the BAC with the target gene to be under the control of the *polh* promoter and at the same time restoring the function of *ORF1629*, which enables the virus DNA replication to produce BV.

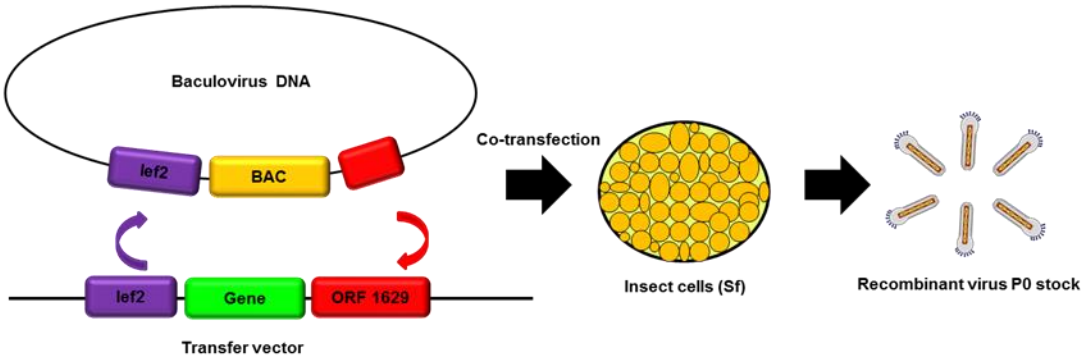


**Figure 1.9: Schematic representation of the recombinant virus generation using the *flash*BAC™ system.**
The *flash*BAC™ system produces recombinant baculoviruses in a single step without the need for plaque purification by the co-transfection of Sf insect cell lines with the transfer vector, which includes the gene of interest and *flash*BAC DNA. Homologous recombination replaces the *polh* coding region with a bacterial artificial chromosome (BAC). The BV can be harvested from the culture medium and considered as a seed stock of recombinant virus.

The BV can be harvested directly from the culture medium and considered as a seed stock of recombinant virus (Hitchman *et al.*, 2007a). The *flash*BAC™ system has been further improved into two forms: The first form *flash*BACGOLD™ (FBG), where the *chiA* and *v-cath* genes were deleted from its genome. The second form is *flash*BACULTRA™ (FBU), where the *p10, p74, p26,* in addition to *chiA* and *v-cath* genes were deleted from its genome

(Hitchman *et al.*, 2011). In both systems, the modifications result in improving the secretory pathway efficacy and enhancing the quality and the yield of membrane-bound or secreted targeted recombinant proteins (Hitchman *et al.*, 2007a, 2009; Hitchman *et al.*, 2010b).

## 1.6 Applications of baculoviruses in biotechnology and medicine

Baculoviruses have a significant role in the ecosystem by controlling insect population size (Odindo, 1983). Abundant molecular studies have been carried out to exploit baculoviruses in order to use them for pest control. Baculoviruses have been effectively exploited for biocontrol against various agricultural and forest insect pests for several decades. They have been used as insecticides to control insects like the velvet bean caterpillar *Anticarsia gemmatalis* (Moscardi, 1999) cotton bollworm *Helicoverpa zea* (Zhang, 1994) and gypsy moth *Lymantria dispar* (Cook *et al.*, 2003). Baculoviruses have been considered as successful candidates for biocontrol due to their ability to infect a particular type of host insect, little environmental impact and in addition they are non-harmful for humans (Bonning and Hammock, 1992).

## 1.7 BEVS and vaccine development

It has been found that baculoviruses can be used safely because they do not have any toxic effect toward mammalian cells and they do not affect the growth of transduced cells even when used at high MOI (Gao *et al.*, 2002; Zeng *et al.*, 2007). On the other hand, they are able to transduce human cells and deliver the gene of interest to the nuclei with no immunogenic response, unlike other viruses such as adenoviruses and poxviruses (Madhan *et al.*, 2010). Currently, the BEVS has been successfully employed to produce numerous commercial vaccines and pharmaceutical recombinant proteins, some of them are under use while others are still undergoing clinical testing. In addition, they are also used to produce several recombinant proteins for research purposes (Chen *et al.*, 2013).

Because of all the advantageous and attractive characteristics above, BEVS was selected to be used as a vaccine generation platform. It is also very important to produce a particular vaccine within a short time during a pandemic or outbreak of an emerging disease, which can be achieved by using BEVS. For example, Zaire ebola virus glycoprotein nanoparticle vaccine has been produced successfully using this system within three months from project initiation to a clinical batch (Hahn *et al.*, 2015). Approval of several commercial human and veterinary vaccines in addition to human therapeutic agents (Table 1.1 and Table 1. 2) has also confirmed the safe use of BEVS for vaccine production (Cox, 2012; Felberbaum, 2015; van Oers *et al.*, 2015).

**Table 1.1: Overview of approved human vaccines and therapies using the baculovirus expression system**

| Product name | Company | Target protein | Product form/ Purpose of use | Reference |
|---|---|---|---|---|
| Cervarix | GlaxoSmith Kline | papillomavirus L1 protein (serotypes 16 and 18) | VLP-based vaccine against cervical cancer | Harper, 2008 |
| Flucelvax | Novartis | Influenza HA | Annual quadrivalent flu vaccine | Thompson *et al.*, 2015 |
| Flublok | Protein Sciences | Influenza HA | Annual quadrivalent flu vaccine | ISBiotech 2018 |
| Provenge (sipuleucel-T) | Dendreon | PAP-GM-CSF | Immunotherapy against prostate cancer | Kantoff *et al.*, 2010 |
| Glybera | UniQure | AAV vector with lipoprotein lipase transgene | Gene therapy against familial lipoprotein lipase deficiency | Haddley, 2013 |

**Table 1.2: Overview of approved veterinary vaccines using the baculovirus expression system**

| Product name | Company | Target protein | Product form/ Purpose of use | Reference |
|---|---|---|---|---|
| Bayovac CSF E2 | Bayer Biologicals/Pfizer Animal Health | E2 glycoprotein | Subunit vaccine against classical swine fever | Hulst *et al.*, 1993 |
| Porcilis Pesti | MSD Animal Health | | | Moormann *et al.*, 2000 |
| Porcilis PCV | MSD Animal Health | Porcine circovirus ORF2 | VLP vaccine against porcine circovirus type | Blanchard *et al.*, 2003 |
| CircoFLEX | Ingelvac | | | Fachinger *et al.*, 2008 |
| Circumvent PCV | MSD Animal Health | | | Kristensen *et al.*, 2011 |

## 1.8 BacMam discovery

BacMam refers to the use of mammalian cell-active promoter elements to construct recombinant baculoviruses vectors, which can control the expression of the target gene(s) in transduced mammalian cells. BacMam vectors are appropriate for use in multimeric complex expression (Figure 1.10 page 19; reviewed by Mansouri and Berger, 2018). The ability of AcMNPV to transduce mammalian cells lines like human lung carcinoma A427 was first reported by Volkman and Goldsmith (1983). Two years later, Carbonell *et al.* (1985) showed that AcMNPV had the capability to transduce mouse L929 cell lines and express the chloramphenicol acetyltransferase (CAT) gene derived from *E.coli* at a minimum level under the Rous sarcoma virus (RSV) promoter. This study indicated that baculovirus can be used as a gene delivery vector. Earlier studies by Hofmann *et al.* (1995) and Boyce and Bucher (1996) demonstrated that recombinant baculovirus with a mammalian expression cassette, including either Rous Sarcoma Virus (RSV) or Cytomegalovirus (CMV) promoter to control the expression of target genes, were able to transduce hepatocytes of various mammalian cell lines. Such cell lines derived from mouse, rabbit and human have been shown to produce recombinant proteins efficiently.

Additional studies have exploited recombinant AcMNPV involving the target gene under the control of a stronger CMV promoter to express to high levels recombinant proteins in both hepatocyte and non-hepatocyte cell lines (Shoji *et al.*, 1997; Condreay *et al.*, 1999). Subsequent studies have added more cell lines that can be transduced by recombinant baculoviruses, such as cells derived from rat, monkey, porcine, shrimp, fish and frog tissues (reviewed by Kost *et al.*, 2005). Furthermore, it has been reported that recombinant baculoviruses are able to transduce mesenchymal stem cells (MSC) derived from human umbilical cord blood and bone marrow, MSC-derived adipogenic and human embryonic stem (ES) cells and deliver the genes of interest into these cells efficiently (Ho *et al.*, 2005; Tsai *et al.*, 2009; Bak *et al.*, 2011).

The entry mechanism of baculovirus into the mammalian cells is still not clear. At first, it was believed that there was a specific binding site on the cell membrane for virus uptake (Wang *et al.*, 1997). Some studies proposed that baculovirus uptake might occur through electrostatic interactions, heparan sulphate or phospholipids (Duisit *et al.*, 1999; Tani *et al.*, 2001). Other studies suggested that baculovirus could enter cells via clathrin-mediated endocytosis or macropinocytosis (Matilainen *et al.*, 2005; Long *et al.*, 2006) or via phagocytosis (Laakkonen *et al.*, 2009). Further studies demonstrated that baculovirus could transduce mammalian cells via the direct fusion pathway of the GP64 envelope protein, when the BV virus attaches to the cell surface (Kaname *et al.*, 2010; Kataoka *et al.*, 2012). The study by Makkonen *et al.* (2013) reported that baculovirus could enter mammalian cells through the interaction with 6-O and N-sulphated chains of the heparan sulphate proteoglycans (HSPG) and bind to the receptor syndecan-1, which mediates virus entry into the transduced cells. BacMams are a good choice for multimeric complex expression due to the large gene(s) of up to 40 kb that can be inserted into its genome. The expression of the target gene(s) in the transduced cells generally needs four days maximum, without application of any selection force. Nevertheless, gene expression may take up to 16 days (Chen *et al.*, 2002). Studies demonstrated that very high transduction efficiency and flexibility could be achieved up to 100% by using high MOI (Haase *et al.*, 2013).

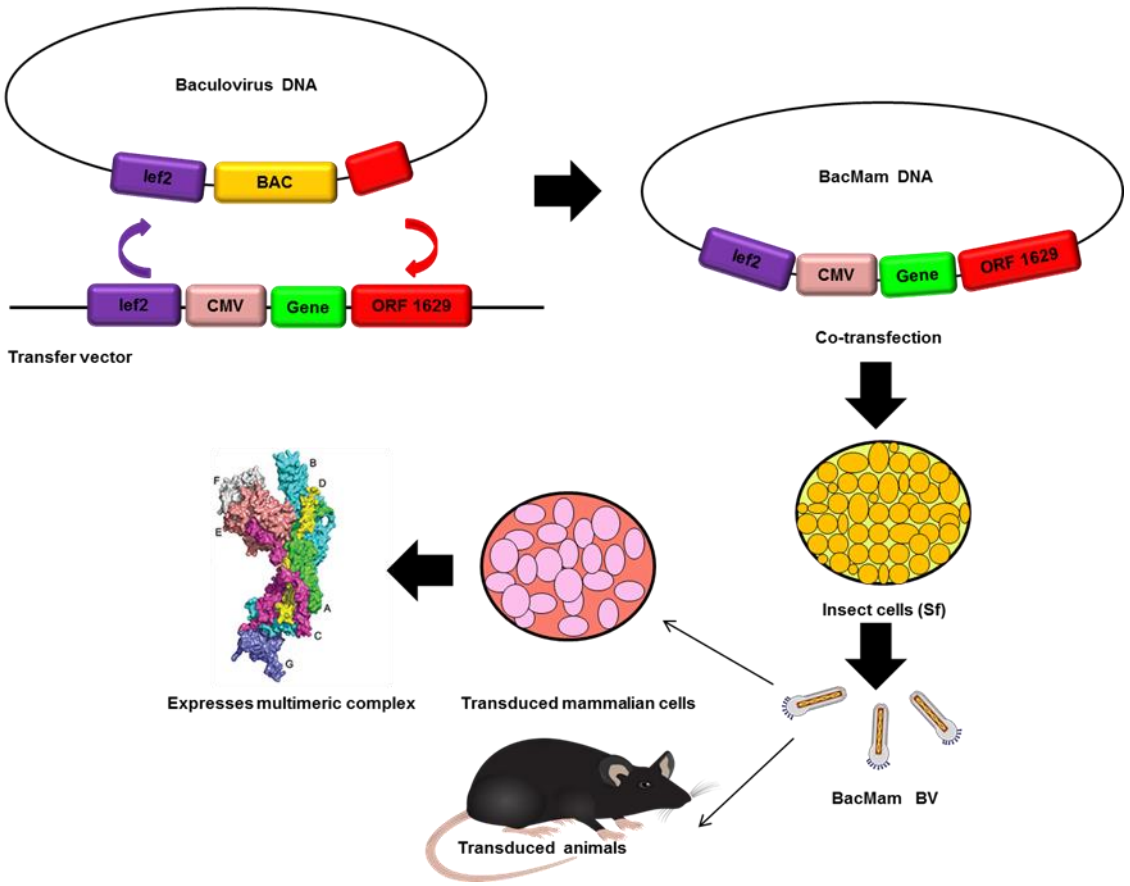


**Figure 1.10: Schematic representation of the BacMam virus generation.**
BacMam viruses produced by the co-transfection of Sf insect cell lines with the transfer vector, which includes mammalian active expression cassette and baculovirus DNA. Homologous recombination replaces the *polh* coding region with a bacterial artificial chromosome (BAC). The BacMam virus can be harvested from the culture medium. The BacMam viruses can be used to transduce mammalian cell culture leads to the expression of the recombinant protein(s). BacMam viruses can be also used to transduce mammalian organisms.

## 1.9 Baculovirus surface display

Baculovirus surface display technology has been exploited with additional advantages over phage display and conventional vectors in this project. Firstly, recombinant proteins of eukaryotic origin produced by baculovirus-infected insect cells are biologically active and have the correct fold due to the proper complex post-translational modifications (reviewed by Aksular, 2017). Furthermore, the ability to insert a large fragment of the target gene(s) into the baculovirus genome and most importantly, the nonpathogenic and nontoxic nature of baculovirus for human and vertebrates encourages the development of this technology (Grabherr *et al.*, 2001). The protein of interest is presented on the BV envelope surface in a similar way to that of phage display. In both technologies, it should be presented on the surface as a fusion to the viral surface protein(s) (Smith, 1985; Boublik *et al.*, 1995).

Target peptides or proteins that can be displayed on the surface of virus particles have been used in various life sciences applications, including the study of protein structure/function and clinical studies such as vaccine improvement and gene therapy (Musthaq *et al.*, 2014). Baculoviruses have been extensively used to improve display strategies of target proteins and peptides. Various surface display strategies of target proteins or peptides on the surface of baculovirus have been improved by merging the target proteins or peptides to the main virus envelope glycoprotein GP64, leading to localisation of the target proteins or peptides on the baculovirus envelope (Haase *et al.*, 2013). This strategy is very powerful and successful in the production and maturation of binding properties like antigenic recognition (Grabherr and Ernst, 2010).

The design of vectors aiming to use BV surface display must include both recombinant GP64 and the wild-type GP64 molecules (Figure 1.11 A) to ensure the BV infectivity and replication in insect cell lines. In addition, proteins targeted to GP64 on the surface of baculovirus are considered very successful immunogens and can be used efficiently to produce antibody responses and antibody production, in addition to vaccine development (Xu *et al.*, 2008; Xu and Liu, 2008; Xu *et al.*, 2009; Xu *et al.*, 2011). Because baculoviruses are able to induce a strong innate immune response via activation of Antigen Presenting Cells (APCs). It is predicted that recombinant viruses which display heterologous antigens on their envelopes can induce a targeted immune response against the displayed antigen (Haase *et al.*, 2013). Another baculovirus display strategy was developed by Kukkonen *et al.* (2003) called capsid display, in which the protein of interest is inserted directly into N or C terminus of the baculovirus VP39 capsid protein (Figure 1.11 B).


**Figure 1.11: Schematic representation of the baculovirus display technologies.**
**A:** Illustrates surface display technology where the target gene inserts into baculovirus GP64 envelope protein sequences between the signal peptide and the transmembrane domain; the BV includes both the wild-type GP64 and the recombinant one. **B:** Illustrates capsid display technology where the target gene inserts into the baculovirus VP39 capsid protein sequence directly into either the N or C terminus, the BV includes both the wild-type VP39 and the recombinant one.

A transfer vector that has been widely used for surface display on the baculovirus envelope was constructed first by Boublik *et al.* (1995). They suggested that the target gene(s) should be inserted between the GP64 signal peptide and the TMD to form a chimeric protein with GP64. It has also been reported that Vesicular Stomatitis Virus G Glycoprotein (VSV-G) can be presented on the surface of the baculovirus using its own domains for membrane incorporation (Barsoum *et al.*, 1997). Another study by Chapple and Jones (2002) reported that VSV-G could also be used like GP64 to display proteins of interest on the baculovirus envelope surface.

## 1.10 Influenza disease

Influenza (flu) is an acute, highly infectious and deadly respiratory sickness caused by influenza viruses. People infected with influenza virus can be identified through several symptoms such as a runny nose or a dry cough, fatigue, pain, sore throat, fever and headache (Cox and Subbarao, 2003). Epidemics of influenza usually happen worldwide seasonally and annually and hit a peak of activity during the winter in northern temperate climates, while in the tropical climates it occurs throughout the year (Cox and Subbarao, 2003). In 2018, three to five million people around the world are estimated to have severe clinical illness from influenza epidemics and between 290,000 to 650,000 deaths occur (WHO, 2018). Influenza can infect people from any age group but elderly people over 65 years with medical problems, pregnant women in addition to children under five years old are at greater risk of severe clinical illness than others (WHO, 2018). The most deadly influenza outbreak was Spanish influenza in 1918, caused by H1N1 influenza virus type A.

### 1.10.1 Influenza virus structure

Influenza viruses can be divided into three different types A, B, C depends on their nucleoproteins and matrix (NP and M). Furthermore, these influenza viruses are different in morphology, host range, genome organization as well as in surface glycoprotein variability (Lamb and Krug, 2001). All these types of influenza viruses can result in human's infection but epidemics of influenza illness are caused by influenza A virus and influenza B (Lamb and Krug, 2001). In nature, influenza virus particles are usually filamentous or spherical with a diameter between 80-120 nm. This particle includes a segmented genome of eight linear single-stranded, negative polarity ribonucleic acids (RNA) (Figure 1.12) and is classified in the family Orthomyxoviridae (Jin *et al.*, 1997; Lamb and Krug, 2001).

The viral particles are enveloped and consist of nine or ten structural proteins as in Influenza B or Influenza A viruses respectively. The subunits of the viral polymerase are represented by three large proteins (PB1, PB2 and PA), which are essential for RNA transcription and

virus replication. The M1 protein plays an essential role in viral protein structure, surrounding the virus particle under the viral envelope as well as for virion morphogenesis (Figure 1.12).

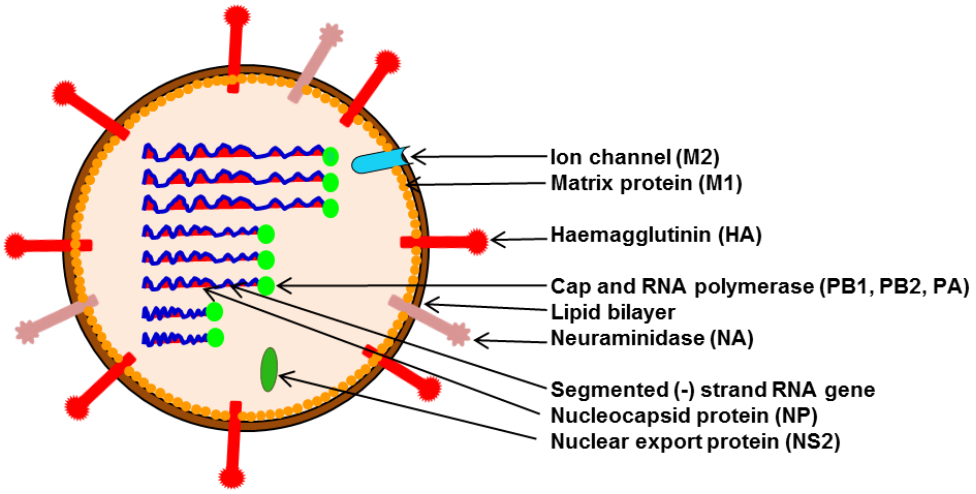


**Figure 1.12: Influenza A virus structure.**
Schematic representation of influenza A virus illustrates the virus structure. Two different glycoproteins HA and NA are distributed on the virus envelope. In addition, the influenza virus type A includes a segmented genome of eight linear single-stranded negative polarity ribonucleic acids (RNA). Six different proteins are expressed from the viral genome (nucleoprotein (NP), transcriptases (PB2, PB1, and PA) and two non-structural proteins (NS2).

The influenza virus envelope includes two distinct surface glycoproteins neuraminidase (NA) and Haemagglutinin (HA) (Figure 1.12). The HA glycoprotein plays a major role in virus attachment to sialic acid receptors on the host cell surface ending with a fusion between the influenza virus and the infected cells, whereas the NA glycoprotein is important for new virions releasing from the infected cell surface by the cleavage of neuraminic acid glycoside bond (Samji, 2009). The influenza A virus nomenclature depends on the antigenic variation of the HA and NA glycoproteins (Bouvier and Palese, 2008). To date, there are about 18 HA subtypes (H1-H18) and 11 NA subtypes (N1-N11), however, only H1-H3 and N1-N2 have been isolated from both human and swine infections (CDC, 2018). It has been found that birds are the major reservoirs for all influenza viruses. However, H3, H7, N7 and N8 have been reported in horses (Lamb and Krug, 2001). The H17 and H18 influenza A viruses subtypes were isolated from fruit bats in 2013 as reported by NHS (2012).

### 1.10.2 Influenza virus haemagglutinin glycoprotein

Haemagglutinin (HA) is the major influenza glycoprotein with a molecular mass around 64 kDa. It is a trimeric fusion glycoprotein that has a cylinder shape with length about 13.5 nm and it is essential for attachment to the receptors of the monosaccharide sialic acid, which

is present on the surface of the host cells (Segal *et al.*, 1992). The structure biologically active HA glycoprotein includes two regions: The globular head, which includes the HA1 subunit in addition to the sialic acid binding site and the main sites of the antibody binding (Figure 1.13 A and B; Wilson *et al.*, 1981). The second region includes the fibrous stem domain known as HA2. HA2 includes the membrane fusion peptide and transmembrane domain (Figure 1.13 A and B; Wilson *et al.*, 1981). The influenza HA was used in this study as a model system for glycoprotein production and surface display vaccine development.

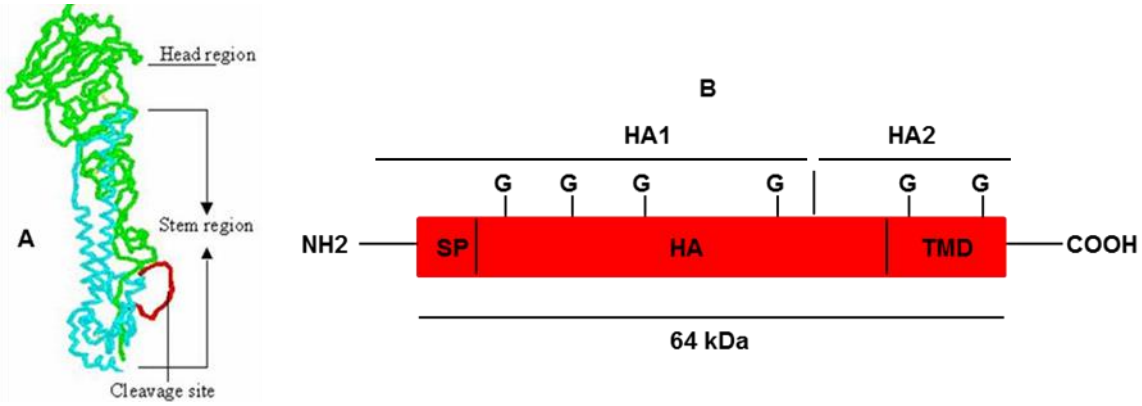


**Figure 1.13: Influenza virus haemagglutinin HA surface glycoprotein.**
**A:** 3D structure of globular HA protein. HA undergoes proteolytic cleavage into 328 amino acid HA1 (green) and 222 amino acid HA2 subunits (cyan) (structure from Rachakonda, 2006). **B:** Schematic representation of the HA protein. HA has an amino-terminal signal peptide (SP) and a carboxy-terminal transmembrane domain (TM) followed by a short cytoplasmic domain. HA1 has several glycosylation sites (G).

## 1.11 Influenza virus surveillance

The isolation and characterisation of human influenza viruses spread around the world have been conducted through the World Health Organization (WHO) and Global Influenza Surveillance and Response System (GISRS) for more than 60 years. Recently, there are 144 institutions in 114 WHO member states, which are recognized as National Influenza Centres (NICs) by WHO. All working groups and collaborating laboratories in these centres are working together to tackle specific emerging issues (WHO, 2018). WHO reported that influenza virus activity between September 2017 and January 2018 was co-circulated in all regions around the world, with influenza A (H1N1), A (H3N2) and influenza B viruses as mentioned in WHO report (Europe, 2018). For instance, during week 6/2018, the WHO and collaborating laboratories tested 3,603 sentinel respiratory specimens obtained from different parts of Europe including the UK. 1,837 (51%) of these tests were positive for both

influenza virus type A and type B. Of these, 27.8% were type A and the vast majority of observed severe cases 72.2% belonged to influenza virus type B.

In addition, of 377 subtyped influenza A viruses, 67.9% were influenza A (H1N1) pdm09 and 30.1% A (H3N2). Furthermore, of 600 subtyped influenza B viruses, 99% were B/Yamagata and 1% B/Victoria. Most cases were detected in the age group over 65 (WHO, 2018). During the vaccine composition meeting held on 19-21 February 2018, organised by representatives from WHO and the reference collaborating laboratories, the available surveillance data was reviewed and the decision made for the composition of the annual vaccine formulation. It was recommended that quadrivalent vaccines are used in the 2018-2019 northern hemisphere influenza season. The vaccine should contain the following candidate influenza strains: an A/Michigan/45/2015 (H1N1) pdm09-like virus, A/Singapore/INFIMH-16-0019/2016 (H3N2)-like virus, B/Colorado/06/2017-like virus (B/Victoria/2/87 lineage) and B/Phuket/3073/2013-like virus (B/Yamagata/16/88 lineage) (Europe, 2018).

## 1.12 Influenza illness treatment

Antiviral drugs can be used for influenza illness treatment. Several antivirals have been approved for this purpose such as Amantidines, Tamiflu and Relenza. However, there is a limitation of using these drugs as they are effective only when used 24-48 hours post-infection and in addition influenza virus may become resistance to them (Anthony *et al.*, 2008). The most effective way to prevent influenza virus spread of infection and the development of severe illness is by vaccination (LaMontagne *et al.*, 1983; Nichol *et al.*, 1994; Nichol *et al.*, 2003). Influenza virus surface glycoproteins (HA and NA) are recognised by the host cells as antigens for both natural infection and vaccination. To prevent influenza infection, antibodies neutralising HA must be evoked in the immune response. Preventing virus entry could be due to interfering with the attachment of the virus either with the host cell surface receptors or with viral and endosomal membranes fusion (Kida *et al.*, 1983; Yoden *et al.*, 1986).

Influenza vaccine formulation made by WHO annually depends on the prediction of the influenza strains circulating during the infection season. Occasionally, incorrect identification of virus pathogenic strains result in a dramatic reduction in vaccine efficacy. Furthermore, influenza prevention programs can be effected by the appearance of novel influenza strains, which result in pandemic disease (Neumann *et al.*, 2009). The new variants of influenza A viruses can arise as a result of the continual antigenic changes (antigenic drift), which result from the accumulation of point mutations that occur during the

virus life cycle leading to different changes in the haemagglutinin amino acid sequence (Cox and Subbarao, 2003). In addition, it has been found that antigenic shift is caused by the re-assortment of RNA molecules between virus strains and can result in introducing new HA and/or NA into the circulating virus leading to virus pandemic (Cox and Subbarao, 2003).

It has been found that inactivated influenza virus vaccines can elicit a humoral immune response and increase the levels of protection of 70 to 90% in healthy adult recipients (LaMontagne *et al.*, 1983). Furthermore, the hospitalization and death risk for the elderly can be reduced by about 50% and 75%, respectively, using influenza vaccination (Nichol *et al.*, 1994). The efficiency of the seasonal influenza vaccine to prevent the laboratory-confirmed influenza diseases depend on the match between the circulating virus and the produced vaccine. In addition, it has been found that when the match is close, the vaccine efficacy reached about 40-60%. However, even with poor matching, vaccination can decrease the hospitalization and death caused by influenza illness. For example, the efficacy of the influenza vaccine against the circulating influenza A and B viruses during 2016-2017 seasons was overall adjusted up to 42% (Belongia *et al.*, 2016; Flannery *et al.*, 2017).

The most popular licensed influenza vaccines have been commercially produced by infecting embryonated chicken eggs with the selected influenza virus to produce a high yield of this virus after serial passages. Then purification of influenza virions from the allantoic fluid is followed by virus inactivation (Chiron, 2002). However, there are several disadvantages for using this process. Firstly, it is very difficult to produce huge amounts of the required vaccine during pandemics within a short time using the egg-based system. Secondly, it is considered an expensive process, because it requires a large supply of pathogen-free eggs annually (Reperant *et al.*, 2014). Furthermore, it has been found that egg proteins present in this vaccine can cause allergic reactions in some people (reviewed by Hsieh *et al.*, 2018). Moreover, the duration of the manufacturing process of influenza virus vaccine from the egg to vaccine formulation and delivery takes approximately six months (Chiron, 2002). Finally, it has been found that some changes could occur in the influenza virus HA glycoprotein during the production process resulting in a reduction of vaccine efficiency (Katz *et al.*, 1987; Wang *et al.*, 1989; Rajakumar *et al.*, 1990).

## 1.13 Alternative vaccines to control influenza diseases

To overcome the drawbacks of egg-based influenza vaccines, several efforts have been made by different pharmaceutical companies to develop influenza vaccine production using cell culture technologies. For instance, influenza vaccines have been produced using Madin

Darby Canine Kidney (MDCK) cells by Novartis, GSK and Solvay (Brands *et al.*, 1999; Doroshenko and Halperin, 2009). Sanofi Pasteur has employed a human retina cell line (Per.C6) to produce a vaccine (Paul *et al.*, 2001). African Green Monkey Kidney (VERO) cells have been used for the same purpose by the Baxter company (Barrett *et al.*, 2009). To date, none of these vaccines has been successfully commercialised due to the challenges that face influenza vaccine production based on cell culture. However, in 2012 the U.S. Food and Drug Administration (FDA) approved the first influenza vaccine Flucelvax based on MDCK by Novartis (reviewed by Thompson *et al.*, 2015). Due to resistance to the influenza vaccines associated with anti-HA antibody levels in serum, the recombinant vaccines based on influenza HA glycoprotein would be an attractive choice to replace the previous technologies (Choi *et al.*, 2017). Rapid cloning of influenza virus HA genes has been achieved in the last decade due to progress in recombinant DNA technology. However, to reach high gene expression of biologically active and correctly folded HA glycoprotein, an appropriate expression system must be selected. Several advantages could be obtained from producing influenza vaccines based on recombinant DNA technology. For instance, the recombinant HA antigen cloning, expression and manufacturing processes are less time consuming than the conventional procedures, which means a correct vaccine could be produced later in the year based on more accurate and reliable epidemiological data. Moreover, large amounts of influenza HA antigens could be produced by the fermentation process under sterile and completely controlled conditions. Furthermore, highly purified influenza vaccine with no egg contaminants will eliminate the allergic reaction towards egg-based vaccines (Choi *et al.*, 2017). Finally, no denaturing effects or safety issues are accompanied with recombinant influenza vaccines purification as it does not need virus inactivation or organic extraction methods (Cox and Hollister, 2009). Baculovirus expression systems have been advantageously used in overexpression of the recombinant proteins in insect cells for several years. The Protein Science Corporation has successfully exploited this technology to produce the first effective trivalent influenza vaccine known as Flublok, which was approved by the FDA in 2013 (reviewed by Thompson *et al.*, 2015). It was demonstrated in 2012 that the HA antigen production yield using BEVS was four to seven-fold higher than the HA produced in MDCK, which also reduced the vaccine cost production (Cox, 2012).

## 1.14 Aims of Thesis

The main aims of this thesis were to construct novel recombinant baculovirus vectors that can be used for vaccine development and gene delivery into mammalian cells using surface

display technology, via either using ODV for BacMam display of proteins or by improving the conventional display system using BV.

- To investigate the potential of baculovirus ODV as a gene delivery system for mammalian cells and as a vector for protein display
- To determine the optimal system for the surface display on BV of influenza virus HA including

  A- HA gene construct
  B- Genetic composition of the baculovirus expression vector including a comparison of late vs very late gene promoters
  C- The optimal host cells (Sf9 vs Tni Hi5)
- To assess the feasibility of downregulating AcMNPV GP64 synthesis to enhance HA surface display

- Finally, this study aimed to investigate the potential of HA-surface display baculoviruses as vaccines via exploring whether the HA displayed on the baculovirus envelope or the HA expressed by Tni Hi5 cells could serve as an immunogen *in vivo* by immunizing mice, this work was achieved by BioServ Ltd, Sheffield, UK through collaboration with Oxford Expression Technologies Ltd, Oxford, UK.

# Chapter 2

# Materials and Methods

## 2.1 Materials

The chemicals used in this thesis were purchased from the following companies unless stated otherwise: Sigma-Aldrich, BDH Chemicals Ltd or Fisher Scientific. The reagents used in molecular biology experiments were supplied by New England Biolabs (NEB), Fermentas, Qiagen or Invitrogen. The media used for cell lines culture were purchased from OET Ltd and Gibco. The antibodies and antigens were purchased from Abcam, Gene script, Jackson Immuno Research, Life technologies, Native Antigen and BioRad (all based in the UK). The sterilization of the internally prepared media and solutions was performed either by autoclaving for 15 minutes (15 pounds per square inch (p.s.i.)) or by filtration using 0.2 µm or 0.45 µm filters. Milli-Q ultrapure (>18 mega ohms) water was used in all preparations. All the reagent percentages were prepared as w/v unless otherwise stated. Table 2.1 presents the plasmids used in this thesis. The viruses used in this thesis are presented in Table 2.2 and the *Escherichia coli* (*E. coli*.) DH5α strain used for cloning is described in Table 2.3. Finally, Table 2.4 presents the baculovirus expression systems used in this thesis.

**Table 2.1: Plasmids used in this thesis**

| Plasmid | Source |
|---|---|
| pEGFP-N1 | Clontech |
| pAcUW21 | Addgene |
| pEGFP-N1-*Xba*I | Riyadh Alakeely, this thesis |
| pAcUW21-*Not*I | Riyadh Alakeely, this thesis |
| pAcCMV-GFP | Riyadh Alakeely, this thesis |
| pBACsurf-1-*polh* | Dr. Mine Aksular, Oxford Brookes University |
| pAcMPHA$^{p6.9}$ | Profssor Robert Possee, Oxfrod Expression Tecnologies |
| pAcUW3HA$^{p10}$ | Profssor Robert Possee, Oxfrod Expression Tecnologies |

**Table 2.2: Viruses used in this thesis**

| Virus | Source |
|---|---|
| WT AcMNPV | Prof Robert Possee, OET Ltd |
| AcRP19HA$^{polh}$ | Prof Robert Possee, OET Ltd |
| AcHA$^{p6.9}$ | Riyadh Alakeely, this thesis |
| Ac$^{HT}$HA$^{p6.9}$ | Riyadh Alakeely, this thesis |
| FBUHA$^{p6.9}$ | Riyadh Alakeely, this thesis |
| AcHA$^{p10}$ | Riyadh Alakeely, this thesis |
| Ac$^{HT}$HA$^{p10}$ | Riyadh Alakeely, this thesis |
| FBUHA$^{p10}$ | Riyadh Alakeely, this thesis |
| AcSurf-HA51$^{polh}$ | Riyadh Alakeely, this thesis |
| HTSurf-HA51$^{polh}$ | Riyadh Alakeely, this thesis |
| FBUSurf-HA51$^{polh}$ | Riyadh Alakeely, this thesis |
| AcCMV-GFP | Riyadh Alakeely, this thesis |

**Table 2.3: *Escherichia coli* DH5α strain**

| *E. coli* strain | Genotype | Source |
|---|---|---|
| DH5α | F- Φ80lacZΔM15 Δ(*lac*ZYA-argF) U169 recA1 endA1 hsdR17($r_k m_k^+$) phoA sup E44 thi-1 gyrA96 relA1 λ- | Thermo FisherScientific |

**Table 2.4: Baculovirus expression systems**

| Baculovirus expression system | Genotype | Source |
|---|---|---|
| *flash*BAC ULTRA | Δ*p*74, Δ*p*10, Δ*p*26, Δ*v-cath*, Δ*chiA* | OET Ltd |
| BacPAK6 | Wild-type (WT) | OET Ltd |
| BacPAK6$^{HT}$ | *fp*25 | OET Ltd |

## 2.2 Cell lines and viruses

### 2.2.1 Cell lines

Several cell lines were used in this study either for protein production or for virus amplification: Human embryonic kidney (HEK-293), Sf21, Sf9 and Tni Hi5). The HEK-293 cell line was maintained in Dulbecco's Modified Eagle's medium (DMEM; Gibco) supplemented with 10% (v/v) foetal bovine serum (FBS). The Sf9 and Tni Hi5 cells were maintained in serum-free media (ESF 921; OET), while Sf21 cells were maintained in TC100 medium (Gibco) supplemented with 10% (v/v) FBS as described by King and Possee (1992). In order to maintain the cells in log-phase and to prevent them reaching stationary phase, the cells were passaged on a regular basis every 3-4 days by seeding at a lower density into the fresh culture medium.

### 2.2.2 Amplification of viruses

All virus stocks were amplified according to the protocol described by King and Possee (1992). Briefly, Sf9 cells (2 x $10^6$ cells/ml) shaking cultures were infected at a multiplicity of infection (MOI) of 0.1 pfu/cell and the cultures then incubated at 28ºC for 4-5 days on a shaking platform. Following the incubation, the culture medium containing BV was harvested and clarified by centrifugation (4000 rpm for 15 minutes at 4ºC, TY-JS 4.2 rotor, J6-MI Beckman centrifuge) to remove the cells and cellular debris. BV was stored at 4ºC in the dark in the presence of 2% (v/v) FBS to prevent the reduction in the virus stock titre during the long-term storage. Aliquots of 1 ml BV stock were also stored at -80ºC for long-term storage.

### 2.2.3 Co-transfection of insect cells to generate recombinant baculoviruses

To generate the recombinant baculoviruses, three different baculovirus expression systems were used (*flash*BACULTRA™, BacPAK6, or BacPAK6$^{HT}$; Table 2.4) following the supplier's protocol (Oxford Expression Technologies (OET) Ltd; Possee *et al.*, 2008). Sf9

cells were transfected with 100 ng of viral DNA and 500 ng of the recombinant transfer plasmid vector, which was quantified using a NanoVue™ spectrophotometer (GE Healthcare). The virus DNA and the recombinant transfer plasmid vectors were prepared in 100 µl of ESF 921 serum-free media in 1.5 ml Eppendorf tubes, which were then mixed with 1.2 µl TransIT®-insect transfection reagent (Mirus®) and incubated at room temperature (RT) for 20 min in order to allow the DNA complexes to form. One ml of medium was removed from a 35 mm dish that was previously seeded with 1 x $10^6$ cells/dish of Sf9 cells then the total transfection mixture was added to the cells. The transfected cells were incubated at 28ºC for overnight, later 1 ml of ESF 921 (OET) medium was added and the cells were incubated for a further 4 days at 28ºC. Then the recombinant virus was harvested from the culture media of the transfected cells. This sample was considered as the P0 virus stock, which was later used as a source to amplify large stock of P1 virus amplification as described in section 2.2.2.

### 2.2.4 Virus titration

In order to titre the virus stocks, either a plaque assay protocol (King and Possee, 1992) was used or a quantitative real-time PCR (qPCR) based titration system using the *baculo*QUANT™ ALL-IN-ONE (OET Ltd; Hitchman *et al.*, 2007b).

#### 2.2.4a Recombinant virus titration by plaque assay

To titre the recombinant virus stocks using plaque assay, 12-well or 6-well plates were seeded with Sf21 at a density of 0.5 x $10^6$ cells/well or 1.4 x $10^6$ cells/well, respectively. The plates were then left on the flat surface for the cells to settle and establish a monolayer at 28ºC for 1-2 hours. Ten-fold serial dilutions of the virus to be titrated were made in TC100 (Gibco) medium supplemented with 10% (v/v) (FBS) for each recombinant virus stock to be titrated. Then the overlay media was removed and replaced with 100 µl of virus inoculum at the required dilution and the plates were left on a rocker at RT for 1 hour. Following, the recombinant virus inoculum was removed and replaced with 1 ml for 12-well plates or 2 ml for the 6-well plates of 2% low melting agarose temperature (LGT, Lonza) diluted in an equal volume of TC100 medium supplemented with 10% (v/v) FBS.

The plates then were placed on a flat surface for 15-20 min to allow agarose solidification at RT. When the agarose was set, 1 ml of TC100 medium supplemented with 10% (v/v) of FBS overlay was added to each well and the plates were incubated at 28ºC for 4-5 dpi. After this period 1 ml of 1:20 dilution of neutral red in PBS was added to each well. After incubation of the plates at 28ºC for 4 hours or overnight, the stain was removed into 1% Virkon disinfectant and the plates were wrapped with aluminium foil and inverted at RT for

overnight in order to distinguish between the live cells, which will be stained with neutral red and dead cells, which will be identified as clear plaques. The clear plaques were counted and the titre calculated based on dilution of the virus and the volume of the virus inoculum used in this assay. Virus stock titres were generally in the range 1-2 x $10^8$ pfu/ml.

### 2.2.4b Recombinant virus titration by qPCR

To titre the recombinant viruses by qPCR, an Applied Biosystems 7500 Real-Time PCR was used according to the supplier's recommended protocol. A serial (1 in 10) dilution of a known standard virus (1.2 x $10^8$ pfu/ml) was prepared in RNase-free water by placing aliquots of 90 µl of water into five 1.5 ml Eppendorf tubes then 10 µl of the standard virus was added to the first tube to get 1 x $10^7$ pfu/ml. Following, the tube was vortexed and 10 µl taken from this tube and added into the second tube to get (1 x $10^6$ pfu/ml) dilution, virus was mixed well and the previous steps were repeated for the standard virus until the last tube in which the dilution will be equal to 1 x $10^3$ pfu/ml. After preparing the serial dilutions, an aliquot of 80 µl from each dilution was added into PCR tubes in addition to 80 µl of the viruses to be titrated. Then the BV was pelleted by centrifugation at 13,000 rpm for 5 minutes. The BV pellets were re-suspended in 20 µl of DLS6 lysis buffer by vortexing and applied into a SureCycler 8800 thermal cycler to run the pre-set lysis program (Table 2.5). When the lysis program was completed, samples were either titrated directly by qPCR or stored at -20ºC overnight.

**Table 2.5: Thermal cycler conditions for virus lysis**

| Step | Temperature | Duration (minutes) |
|---|---|---|
| 1 | 65ºC | 15 |
| 2 | 96ºC | 2 |
| 3 | 65ºC | 4 |
| 4 | 96ºC | 1 |
| 5 | 65ºC | 1 |
| 6 | 96ºC | 0.5 |
| 7 | 20ºC | Hold |

A master mix of 23 µl per sample was prepared for the qPCR reaction, which includes (12.5 µl) of qPCR Low ROX mix, (7.5 µl) of RNase free water, (1 µl) of each SensiFAST™ lo-ROX probe (Bioline) and a forward and reverse primer, as supplied in the *baculo*QUANT™ virus titration kit. For the qPCR, 23 µl of the master mix was aliquoted into each well of a 96-well PCR plate and then 2 µl of unknown and standard virus DNA added into triplicate wells containing a master mix. RNase free water was added as a negative control instead of viral DNA. The plate was then sealed and centrifuged at 1000 rpm for 1-2 minutes and the virus titrated by Applied Bio-systems 7500 Real-Time PCR machine according to

supplier's protocol for fluorescent dyes (6 FAM and TAMRA) and the thermo-cycling conditions listed in Table 2.6.

**Table 2.6: Applied Bio-systems 7500 Real-Time PCR cycling conditions**

| Step | Temperature | Duration | Cycles |
|---|---|---|---|
| Enzyme activation | 95ºC | 10 Minutes | 1 |
| Denaturation | 95ºC | 15 Seconds | 40 |
| Annealing | 60ºC | 60 Seconds | 40 |

### 2.2.5 Plaque purification of recombinant viruses

It was essential to plaque-purify the recombinant viruses that were constructed by using BacPAK6 (BEVS) as described by King and Possee (1992) to separate the recombinant virus from the parental one. The virus was titrated by plaque assay as described in section (2.2.4a) with dilutions ranging from neat to $10^{-4}$. The plate was incubated for 3-5 dpi, then 15 µl/ml of 5% w/v X-gal (5-Bromo-4-chloro-3-indolyl β-D-galactopyranoside) in N,N-Dimethylformamide (DMF) was added to 0.5% w/v neutral red diluted in phosphate-buffered saline (PBS) with a ratio 1:20. One ml of this mixture was then added to each well and the plate incubated for 5-16 hours for plaque to develop.

After this period, the stain was removed and the plate inverted and wrapped with aluminium foil and left at room temperature. There were two kinds of plaque in the plate, clear plaques, which refer to the recombinant virus due to disruption of *lac*Z location via target gene insertion or blue parental plaques as a result of β-galactosidase expression from the *lac*Z gene. Clear plaques of recombinant BV were then picked and transferred to 0.5 ml of TC100 (Gibco) media supplemented with 10% FBS (v/v) to apply for other rounds of plaque assay until all the plaques obtained were clear. Finally, 35 mm dishes were seeded with Sf9 cells at a density of 1 x $10^6$ cells/dish and the cells were infected with the BV from the final plaque pick to produce the P0 recombinant virus stock. The P0 virus was harvested at 4 dpi and used to produce (P1 and P2) virus stock as described in section 2.2.2.

### 2.2.6 Budded virus amplification and purification

Tni Hi5 cells were diluted to 1 x $10^6$ cells/ml in the required volume of 200-500 ml ESF 921 culture media in a shaking flask and infected with virus stock at MOI of 0.1 pfu/ml to produce the required recombinant BV. The flask was incubated at 28ºC on a shaking platform for 5 days, then the culture was centrifuged at 4000 rpm for 15 minutes at 4ºC (TY-JS 4.2 rotor, J6-MI Beckman centrifuge), cell pellets were washed twice with PBS and then stored at -80ºC until required. The culture media including the BV was centrifuged at 14000 rpm for 1 hour at 4C (JA-14 rotor, Avanti J-25i Beckman centrifuge) in order to pellet the BV particles.

Then, the culture media was removed and the BV pellet soaked in 1 x TE buffer (10mM Tris-HCl, pH 8.0; 1 mM EDTA) overnight at 4C prior to resuspension.

The following day, virus particles were re-suspended in TE buffer by pipetting gently up and down to prevent BV damage and then loaded on to a discontinuous sucrose gradient 10-50% (w/w) in 1 x TE buffer in ultra-clear tubes. The tubes were centrifuged at 30000 rpm for 1 hour at 4ºC (SW32TI rotor, Optima LE-80K Beckman Ultracentrifuge). The white band in the middle of the tube, which represented the BV fraction was harvested gently from the sucrose gradient using a p1000 pipette into a 7ml Bijoux tube. Next, the BV particles were dialysed against three changes of 500 ml of 1 x PBS stirring at 4ºC for overnight in the dark to remove the residual sucrose. The purified BV was harvested and stored at 4ºC until use.

## 2.3 Bacterial protocols

### 2.3.1 *E.coli* DH5α ultra-competent cells preparation-Inoue method

The Inoue protocol described by (Sambrook and Russell, 2006) was used to produce *E.coli* DH5α strain ultra-competent cells. Twenty-five ml of SOB medium (5 g Yeast extract, 20 ng Bacto-tryptone, 0.5 g NaCl in 1 L of distilled water ($dH_2O$) and 10 ml of 250 mM KCl was added, pH adjusted to 7.0 and the media was autoclaved and 5 ml 2 M MgCl2 added. Then a single colony of *E.coli* cells (2-3 mm in diameter) was picked from fresh cultured plate to inoculate the SOB media and the media was incubated at 37ºC in a shaker at 200 rpm for 6-8 hours. The culture was used to inoculate three conical flasks of 250 ml SOB with either, 2 ml, 4 ml or 10 ml of bacterial culture. The flasks were incubated at 18ºC in a shaker at 180 rpm overnight. The bacterial cell density was monitored in each flask using spectrophotometer (DU 730, Beckman) until one of them reached 0.45-0.5 at $OD_{600.}$ This culture was then chilled in an ice-water bath for 10 minutes, and then the bacterial cells were harvested by centrifuge in a pre-chilled rotor at 3000 rpm for 10 minutes at 4ºC. The supernatant was discarded and the cell pellets were resuspended gently in 80 ml ice-cold Inoue transformation buffer (55 mM $MnCl_2$, 15 mM $CaCl_{2,}$ 250 mM KCl, 10 mM PIPES, pH6.7). The bacterial cells were centrifuged again and the pellets resuspended gently in 20 ml ice-cold Inoue buffer. Finally, 1.5 ml of DMSO was added and (250-750 µl) of ultra-competent cells aliquot were placed into 1.5 ml Eppendorf tubes and immediately frozen by immersing into liquid nitrogen and stored at -80 ºC until used.

### 2.3.2 *E. coli* DH5α transformation with plasmid DNA

The *E.coli* competent cells prepared in section 2.3.1 were thawed in an ice bath and 50 µl of cells were used for each transformation reaction, 2-5 µl of ligation mixture or 5-10 ng of plasmid DNA was added to the competent cells and mixed gently by flicking. Then the

mixture was incubated in an ice bath for 30 minutes prior to heat-shock at 42°C for 45 seconds. The cells were allowed to recover by incubation in an ice bath for 2 minutes. After that, 950 µl of SOC media (SOB media + 20 µl/ml 1 M glucose) were added to each transformation reaction tube and incubated at 37°C for 45-60 minutes in a shaker incubator at 200 rpm. Then 100 µl from each reaction was plated on Luria broth (LB) nutrient agar plates supplemented with appropriate antibiotic based on the plasmid antibiotic resistance marker by disposable plastic spreaders. Finally, the plates were incubated at 37°C for overnight and then the plates were stored at 4°C until used.

### 2.3.3 Purification of plasmid DNA from transformed *E.coli* DH5α cells

To purify the recombinant plasmid DNA from transformed cells, a single colony was picked from (LB) nutrient agar plates (section 2.3.2) to inoculate 5 ml of Luria broth (LB) media with appropriate antibiotic. The cultures were incubated overnight at 37°C in a shaker incubator at 180 rpm. The transformed cells were then pelleted by centrifugation at 3000 rpm for 5 minutes for plasmid DNA purification. The recombinant plasmid DNA was purified by QIAprep Spin Miniprep kit (Qiagen®) according to the supplier's protocol (Qiagen®).

## 2.4 Molecular biology protocols

### 2.4.1 Digestion with restriction enzymes

In order to examine or to aid DNA cloning, restriction enzymes (RE) were used. Two µl of DNA for checking or 10 µl of DNA for cloning were digested by restriction enzymes according to the supplier's recommended protocol (NEB). Unless otherwise stated, all the digestion reactions were incubated at 37°C for 1-2 hours for DNA examination or overnight if the DNA was for cloning. The enzyme activity was stopped by heat-inactivation according to the supplier protocol and 1:5 volumes of 5 x loading buffer (40% sucrose, 5 x TAE (40 mM Tris-Acetate, 1 mM EDTA, 2.5% SDS, and 0.1% bromophenol blue dye) added for DNA examination or the DNA was purified according to the supplier's protocol (Qiagen®) prior to cloning experiments. The DNA samples were then analysed using 1% agarose gel electrophoresis (section 2.4.2).

### 2.4.2 Agarose gel electrophoresis

Different concentrations of high gelling temperature agarose (Fisher Scientific) 0.8-3% in 1 x TAE buffer were prepared according to the DNA size to be analysed. Ethidium bromide (EBr) at 0.5 µg/ml was added to the agarose before it solidifies in order to visualise the DNA under UV light. The DNA samples were mixed with loading buffer (section 2.4.1). Then the agarose gels were run at 100-120 volts for 40-70 minutes, after that the DNA was visualised

using a UV transilluminator (Bio-Rad, Chemi Doc™ Imaging Systems). De-staining "tea bags" (Fisher) were used to absorb the EBr from the electrophoresis buffer. The buffer and the gel containing EBr were then disposed into cytotoxic waste for incineration off-site.

### 2.4.2a DNA purification from agarose gel

DNA digested with RE were purified from 1% agarose gel after electrophoresis was completed (section 2.4.2.). The target DNA fragment was visualised under the UV light first and carefully excised from the gel using a new scalpel. The DNA fragment was then purified by QIAquick™ Gel Extraction Kit, according to suppliers protocol (Qiagen).

### 2.4.2b De-phosphorylation of the DNA vector

In order to use the purified DNA vector in cloning experiments, it was important that the vector should be dephosphorylated to improve the cloning efficacy by preventing vector self-ligation. DNA de-phosphorylation was achieved according to the supplier's recommended protocol (NEB): 1 µl Antarctic Phosphatase (AnP) and 1:10 volumes of the AnP reaction buffer was added to the purified sample and the mixture was incubated 37°C for 15-30 minutes. Then the reaction was heat-inactivated by incubation of the mixture in a water bath at 70°C for 5 minutes.

### 2.4.3 DNA ligation

In order to ligate the gene of interest into the cloning vector, 25-50 ng of DNA vector was mixed with 75-150 ng of the gene of interest. Then 0.5 µl of T4 DNA ligase and 1 µl 10 x ligase buffer (NEB) were added to the reaction mixture and the total volume of the mixture was adjusted to 10 µl using $dH_2O$ as required. Following the reaction was incubated for 3-4 hours at RT before transformation as described above (section 2.3.2.).

### 2.4.4 DNA amplification using polymerase chain reaction (PCR)

Several primers were designed by the author and synthesized as synthetic oligonucleotides by Eurofins MWG Operon in this study to be used in the PCR reaction to amplify the target gene. Primers were supplied as a lyophilised powder and were re-suspended in the recommended volume of $dH_2O$ by the supplier to make a stock concentration of 100 pmol/µl. Then the stock primers were stored at -20 °C. All primers used in this study are listed in Table 2.7. For each PCR reaction, 0.25 µl of the individual primer stock (100 pmol/µl) was used (forward and reverse primer). In addition, the mixture included 0.25 µl 10 mM dNTPs, 2.5 µl 1 x thermo-polymerase buffer, 0.2-0.5 µl DNA template, 0.125 µl of either Taq DNA

polymerase or Q5 High-Fidelity DNA Polymerase (Q5 HF polymerase, NEB), dependent on the proof-reading activity, which can be provided only by using the Q5 HF polymerase.

The total volume of the reaction was adjusted to 25 µl by adding the required amount of $dH_2O$. For each PCR experiment, a negative control was included in which the reaction included $dH_2O$ instead of DNA template. To start the DNA amplification, the PCR mixture was applied to thermocycler (RoboCycler gradient 96, Stratagene) depending on a programme set out according to the enzyme supplier protocol. When the cycles completed, 1 µl of PCR sample was mixed with 9 µl dH2O and 2 µl loading buffer and analysed on a 1% agarose gel as described in section 2.4.2.

**Table 2.7: Primers used in this thesis.**

| Primer Name | Primer sequence (5'-3') |
|---|---|
| | Chapter 3 |
| Linker oligo (RA1) | GATCTTGGCGGCCGCCAT |
| Linker oligo (RA2) | CTAGATGGCGGCCGCCAA |
| Linker oligo (RA3) | TAGCTAGTCTAGACTAGC |
| EGFP F | ATGGTGAGCAAGGGCGAGGAA |
| YGFP R | GGGCATGGCGGACTTGAAG |
| | Chapter 4 |
| HA *Kpn*I F | TGCGGTACCCACAATATGTATAGGCTACCATGCGAAC |
| HA *Xma*I R | CGCCCCGGGGTTCCCTGTTCAACTTTGACTCTTCTGA |
| RDP213B | TGAGACGCACAAACTAATATCACAAAC |
| RDP214B | ATACGTACAACAATTGTCTGTAAATCAAC |

### 2.4.5 DNA Sequencing

When necessary, plasmid constructs were sent to Source Bioscience, Oxford, UK for sequencing. The received data were analysed by using SnapGene® software version 3.2.1.

## 2.5 Protocols for protein analysis

### 2.5.1 Infecting cell lines

To examine the production of recombinant proteins, an expression test was carried out in HEK-293 mammalian cell lines or Sf9/Tni Hi5 insect cell lines. To achieve that, the cell lines were seeded at 0.2 x $10^6$ cells/35 mm dish, 1 x $10^6$ cells/35 mm dish or 0.5 x 1 $0^6$ cells/35 mm dish, respectively. The dishes seeded with insect cell lines were incubated at 28ºC, whereas HEK-293 cells were incubated at 37°C in a humidified incubator for 1 hour or until the cells had settled down. Following the cell lines were infected with the corresponding virus at the required MOI after it was diluted in the optimum culture media to a final volume of 100 µl/well. The infected cells were incubated for 1 hour on a rocker at room temperature and then the virus inoculum was removed and replaced with 2 ml of the appropriate fresh culture media. The cells were incubated at optimum temperature until the harvesting time.

The cell pellets were harvested by centrifugation at 4000 rpm for 15 minutes and the budded virus was harvested from the culture media by centrifugation at 15000 rpm for 30 minutes at 4ºC.

### 2.5.2 Protein analysis by SDS-PAGE

The standard dodecyl sulfate polyacryamide gel electrophoresis (SDS-PAGE) protocol as described in Sambrook and Russell (2001) was employed to analyse the protein samples in which the SDS-PAGE gel was prepared at 10% according to this protocol. Various protein samples obtained from either whole infected cell lysates or from BV particles were analysed. Briefly, the samples were resuspended in 1/5$^{th}$ volume of 6 X Laemmli SDS-PAGE loading buffer (10% SDS, 50% (v/v) glycerol, 250mM Tris-HCl pH 6.8, 0.05-0.5% bromophenol blue and 25% (v/v) β-mercaptoethanol, added just before use) and the total volume was adjusted by adding $dH_2O$. The samples were then boiled in a water bath for 5 minutes and loaded into the SDS-PAGE gels using the mini-protein vertical gel electrophoresis system (Bio-Rad) at 100V for 10 minutes for the stacking gel and then at 150V for 50-60 minutes for the resolving gel. Finally, the gels were either directly Coomassie stained (2.5.2a) or processed for western immunoblotting (2.5.2b).

#### 2.5.2a Coomassie staining

Coomassie stain, (0.25% Coomassie Brilliant Blue R-250 dissolved in 50% (v/v) methanol, 10% (v/v) glacial acetic acid), was used to stain the SDS-PAGE gel for 2 hours or overnight. In order to obtain a clear gel background, the stain then was removed from the gel using de-staining solution (30% (v/v) methanol, 10% (v/v) glacial acetic acid). Following, the gel was washed with $dH_2O$ and imaged using a Chemi Doc$^{TM}$ Imaging System (Bio-Rad).

#### 2.5.2b Western immunoblotting analysis

The proteins were transferred from the SDS-PAGE gel into a nitrocellulose membrane using Towbin transfer buffer (25 mM Tris, 192 mM glycine and 20% (v/v) methanol) and the Trans-Blot Turbo blotting system, according to the supplier's instructions (Bio-Rad). Following, the membrane was incubated for 30 minutes with blocking buffer (5% skimmed milk powder in PBS-T (PBS+ 0.1% (v/v) Tween 20)) at RT on a horizontally rotating platform. After that, the membrane was incubated with primary antibody at required dilution (Table 2.8) in blocking buffer for 1 hour at RT or overnight at 4ºC temperature depending on the primary antibody on a horizontally rotating platform. Next, the membrane was washed three times for 5 minutes each with 12 ml of PBS-T buffer with shaking. Then the membrane was incubated with a secondary antibody at required dilution (Table 2.8) in blocking buffer for 1

hour at 4ºC on a horizontally rotating platform. The secondary antibody was removed and the membrane washed three times for 5 minutes each with 12 ml of PBS-T buffer and then developed using the alkaline phosphatase protocol according to the supplier's recommended instructions (Merck). Finally, the developed membrane was visualised and imaged by Chemi Doc™ Imaging System.

**Table 2.8: Antibodies used for western blotting**

| Antibody target | Source species | Working dilution | Supplier |
|---|---|---|---|
| Anti-GFP | Mouse | 1:2000 | Abcam |
| Anti-VP39 | Rabbit | 1:5000 | Gene script |
| Anti-GP64 AcV5 | Mouse | 1:1000 | Sigma |
| Anti-Avian Influenza A Hemagglutinin antibody [1G7] | Mouse | 1:1000 | Abcam |
| Anti-mouse IgG conjugated to alkaline phosphatase | Goat | 1:25000 | Jackson Immuno Research |
| Anti-rabbit IgG conjugated to alkaline phosphatase | Goat | 1:25000 | Sigma |

### 2.5.3 Post-translational modifications analysis

In order to analyse the protein glycosylation, duplicate samples of purified BV (2 ml) particles from infected cell lines culture media were pelleted using an Eppendorf bench-top centrifuge at 15000 rpm for 15 minutes at 4ºC. The first sample was re-suspended in $dH_2O$ to be used as a negative control in this analysis, the other sample was applied to the corresponding buffers of specific enzymatic treatments according to the supplier's recommended protocol (NEB). The analysis of de-glycosylation was carried out using *PNG*ase F or Endo H enzyme.

## 2.6 Microscopy protocols

### 2.6.1a Immunofluorescence assay

To perform an immunofluorescence assay, Sf9 cells were seeded on sterile coverslips in 6-well plates. The cells then were infected with the target virus as described in section 2.5.1. The culture media were removed from each well after the required time post- infection and the infected cells were washed twice with 2 ml of 1 x PBS buffer. After that, the cells were fixed using 1 ml of 4% (v/v) paraformaldehyde diluted in PBS buffer for 1 hour at room temperature. Following, the cells were washed twice with 1 ml of 1 x PBS buffer, then the cells were permeabilised by incubation for 10 minutes with 1 ml of PBS buffer containing 1% BSA (Sigma Aldrich) and 0.1% Triton X-100. After that, the permeabilised cells were washed twice with 2 ml of PBS buffer followed by blocking for 30 minutes in 2 ml of PBS-1% BSA.

Next, 200 µl/well of required primary antibody (Table 2.9) was added to the cells and the plates were incubated at RT for 1 hour. The cells then washed three times with 2 ml of PBS-BSA 1% buffer and 200 µl/well of required secondary antibody (Table 2.9) was added and the cells incubated at RT for 1 hour. To remove the residual secondary antibody, the cells were washed 5 times with 2 ml of PBS-BSA 1% buffer. Finally, the coverslips were mounted on to microscope slides with a glycerol-based mounting media (Vectashield, Vector Laboratories), the coverslip edges were sealed with clear nail varnish and the slides were stored at 4ºC in dark to be protected from the light until examination by confocal microscope.

**Table 2.9: Antibodies used for immunofluorescence**

| Antibody target | Source species | Working dilution | Supplier |
|---|---|---|---|
| Anti-Avian Influenza A Hemagglutinin antibody [1G7] | Mouse | 1:100 | Abcam |
| Anti-GP64 AcV5 | Mouse | 1:100 | Sigma |
| Anti-mouse IgG conjugated to Alexa Fluor 488 | Goat | 1:200 | Life technologies |

### 2.6.1b Confocal microscopy

The cells prepared in section 2.6.1a were imaged by Zeiss LSM 510 meta laser scanning microscope at the 488 nm excitation line of the argon laser and using a 488/543 nm dichroic beam splitter and a 505-530 nm band-pass filter for Alexa-Fluor 488® fluorescence detection. An oil immersion objective; Plan-Apochromat 63 X (1.4 numerical aperture) was used to acquire the images. LSM 880 Image Browser (Zeiss) was used for Post-acquisition image processing and Z-stack image projections.

### 2.6.2 Transmission electron microscopy (TEM)

### 2.6.2a Samples preparation for microscopy

For transmission electron microscopy, 35 mm tissue culture dishes were seeded with the Sf9 cell at 3 x $10^6$/ flask. The cells were infected with AcMNPV or AcCMV-GFP viruses at MOI of 1 pfu/cell and incubated at 28ºC for three days. The cells then were either scraped off or tapped and pelleted at 1000 rpm for 5 minutes in 1.5 ml Eppendorf tubes. The cell pellet was washed two times with PBS buffer and then fixed by incubation at RT for 30 minutes on a rocker table in 500 µl of primary fixative (2% w/v paraformaldehyde and 2.5% v/v glutaraldehyde in 0.2 M w/v sodium cacodylate buffer (pH 7.4), 0.1% w/v tannic acid). The pellet was washed with 0.1 M sodium cacodylate buffer (pH7.4) (mixed 1:1 with dH20) four times for 5 minutes and centrifuged at 3000 rpm for 1 minute if required.

The pellet was then fixed and osmicated by incubation with 500 µl of 1% v/v osmium tetroxide in 0.2 M sodium cacodylate buffer (1:1 mix) for 1 hour at RT on a rocker table.

Following, the pellet was sequentially dehydrated in 500 µl of 10%, 30% and 50% v/v ethanol (diluted in $dH_2O$) for 30 minutes for each dehydration step. The ethanol was removed from the pellet after each step and the sample centrifuged to avoid sample loss. After 50% v/v ethanol, 500 µl of 70% v/v ethanol containing 2% v/v uranyl acetate was passed through a 0.2 µm filter and added to the pellet and incubated at 4ºC for overnight. Then the mixture was removed and the pellet washed twice with 70% v/v ethanol for 15 minutes. One dehydration step with 90% v/v ethanol followed with three steps with 100% v/v ethanol for 30 minutes incubation each. Finally, 100% v/v of dried ethanol was added to the pellet and incubated for 30 minutes before it was removed.

The final step of the sample preparation for microscopy was infiltration, which was achieved by adding 500 µl mixture of Epon 812 epoxy resin in 100% dried ethanol at different ratios (1:3, 1:1 and 3:1 v/v) followed by incubation at RT for 60 minutes for each ratio. Then several changes of 100% Epon 812 fresh resin were applied to the sample with incubation for 60 minutes each. To aid infiltration of resin, the sample was centrifuged after each change at 3000 rpm for 5 minutes. After adding the resin in the final change, the sample was incubated at 70ºC overnight for polymerisation and stored at RT until sectioning by ultra-microtome.

### 2.6.2b Sample sectioning and post-staining

To examine and image the samples by TEM, ultrathin 80-100 nm sections of sample block were cut by a diamond knife with water-filled trough using the PT-PC PowerTome Ultramicrotome (RMC™). After that, the sections were collected on formvar-coated grids, allowed to dry and then washed (grid on the drop) in $dH_2O$ then stained with 2% w/v aqueous uranyl acetate filtered via a 0.2 µm filter (grid on the drop) for 10-15 minutes. The grids were washed three times with $dH_2O$, then the grids were placed on a drop of 10% w/v lead citrate (1.33 g $Pb(NO_3)_2$, 1.76 g $Na_3(C_6H_5O_7)$, ~42 ml $dH_2O$, 8 ml 1M $NaOH_2$) in a Petri dish. Sodium hydroxide pellets surrounded the grids to prevent the precipitation. The next step was to rinse the grids with 1 M sodium hydroxide followed by three times washing with $dH_2O$. Finally, the grids were stained with uranyl acetate for 5-8 minutes and washed three times with $dH_2O$ and left to dry at RT prior to examining and imaging by Hitachi H7650 electron microscope. Sample images were taken at 100 kV with different magnifications.

### 2.6.3 Small-scale infection of cells

Tni Hi5 or Sf9 cells were seeded in 35 mm tissue culture dishes (0.5 x $10^6$ cells/ml or 1 x $10^6$ cells/dish), respectively and left 1 hour at RT for cells to attach to the surface. Then the virus inoculum was diluted in appropriate medium to the MOI of 1puf/cell. The medium was removed and replaced with 100 µl of the relevant virus. The inoculated cells were incubated

at RT on a rocker platform for 1 hour. Following, the virus inoculum was removed and 2 ml of relevant media were added to the infected cells. The infected cells were incubated at 28ºC for the required time until harvest or imaging.

### 2.6.4 Polyhedra production and ODV purification

To purify the ODV, Tni Hi5 cells were seeded in 500 ml conical flasks at 1 x $10^6$ cells/ml. The cells were infected with BacMam at MOI of 1 pfu/cell and incubated at 28ºC for 5 days. Then the infected cells were harvested from the culture media by centrifugation at 4000 rpm for 15 minutes and the cell pellets were washed with PBS buffer. The cells were then lysed with SDS 0.5% w/v in distilled water and incubated for 30 minutes at RT on a rocker table. The cells were checked under the light microscope to confirm full lysis and polyhedra release. The polyhedra were harvested by centrifugation at 4000 rpm for 20 minutes and washed with PBS to remove the residual SDS. The yield of polyhedra was calculated using a C-chip haemocytometer (Labtech) with triplicate count per sample using a light microscope at X400 magnification.

Polyhedra were purified using a 50-60% (w/w) sucrose gradient in 1 x of Tris-Ethylenediaminetetraacetic acid (TE) buffer in ultra-clear tubes and centrifuged at 32000 rpm for 1 hour at 4ºC (SW32TI rotor, Optima LE-80K Beckman Ultracentrifuge). The polyhedra band was collected gently from the gradient using a P1000 pipette and washed twice with PBS buffer and re-suspended in the same buffer. Samples were then dissolved in an alkaline buffer to release ODV, which were then purified using continuous 30-60% (w/w) sucrose gradient in 1 x TE buffer in ultra-clear tubes and centrifuged at 32000 rpm for 1 hour at 4ºC (SW32TI rotor, Optima LE-80K Beckman Ultracentrifuge). Following, the bands representing ODV were gently collected from the gradient using a P1000 pipette into 2 ml Eppendorf tubes. ODVs were then dialysed against 750 ml of 1 x PBS buffer with stirring for 1-2 days at 4ºC to remove residual sucrose. The PBS buffer was replaced twice and the purified ODV were stored at 4ºC until use.

### 2.6.5 Transduction of mammalian cells

To transduce the mammalian cells HEK-293 with ODV or BV of the BacMam virus, the cells were seeded in 6-well plates at the appropriate cell density and incubated at 37°C in a 5% $CO_2$ incubator for overnight. Cells were then transduced with either AcCMV-GFP BV at MOI of 10, 30, or 100 pfu/cell or with AcMNPV-GFP ODV at MOI of 100, 250 or 400 qpfu/cell as protocol described in section 2.5.1 and incubated at 37°C in a 5% $CO_2$ incubator for 24 or 48 hours. Finally, the transduced cells were harvested and applied to SDS-PAGE followed by immuno western blot as described in section 2.5.2b.

### 2.6.6 Statistical analysis of data

Microsoft Office Excel 2010 was used to analyse the data and ImageJ software (Schindelin *et al.*, 2015) was used for the enumerated polyhedra and their size comparisons. A T-test ($\alpha$=0.05) was used for statistical comparisons when comparing two population means.

## 2.7 Haemagglutinin (HA) activity assays

### 2.7.1 Chicken red blood cell preparation

Adult chicken red blood cells (RBCs) in Alsever`s solution supplied by (TCS Biosciences) were used in this study. First, 4 ml of chicken blood was added into a 15 ml conical tube and then 11 ml of PBS buffer was added and gently mixed by inverting (avoiding use vortex mixer) in order to wash the blood cells. The blood mixture was centrifuged at 1000 rpm at 4ºC for 10 minutes to precipitate the RBCs. After that, the supernatant was aspirated gently without disturbing the blood cells. The wash step was repeated three times and after final wash, the supernatant was aspirated and 10% stock solution of RBCs in PBS was prepared. This solution can be used within one week. Finally, a working solution of 1% or 0.5% RBCs in PBS buffer was prepared for haemagglutination and haemadsorption assays respectively.

### 2.7.2 Haemagglutination assay

To examine the HA haemagglutination activity of recombinant viruses, Tni hi5 cells were seeded in 35 mm dishes at a density of 0.5 x $10^6$ cells/dish and then infected with the target virus at MOI of 5 pfu/cell as protocol described in section 2.5.1. The infected cells were harvested after 48 hpi by centrifugation at 2000 rpm for 10 minutes at 4ºC, the culture medium was removed and stored at 4ºC as a source for BV and the cell pellets were resuspended in 2 ml of PBS buffer. The cell suspension was divided into two samples; the first one was disrupted by using 10-second interval pulsar cycle timer (XL2020 ultrasonic liquid processor), while the second sample was kept without treatment (whole infected cells). BV obtained from the culture medium were pelleted by centrifugation at 15000 rpm for 40 minutes at 4ºC and re-suspended in 150 µl of PBS buffer.

Then 50 µl of PBS buffer was added to each well of a round-bottomed 96 well plate and two-fold serial dilutions were prepared. After that 50 µl samples of sonicated, whole cells or BV were added into the first well column of a 96-well plate and mixed well with the PBS buffer, then 50 µl was transferred to the next well on its right. Mixing and transferring of 50 µl was repeated, the length of the plate and 50 µl from the last well was discarded into 1% Virkon solution. Following, 50 µl of 1% RBCs solution was added to each well and mixed gently by pipetting up and down, the plate was incubated at RT for 60-90 minutes to allow

haemagglutination. This was expressed using the haemagglutination activity unit (HAU), which is the highest sample dilution that can result in a visible haemagglutination/well. The plate showed positive results as a reddish colour of cross-linked matrix across the well or negative results as red dots in the well centre where cells had pelleted. Tni Hi5 cells infected with wild-type baculovirus or PBS buffer was used as a negative control.

### 2.7.3 Haemadsorption assay

To determine the haemadsorption activity, Sf9 cells were prepared and infected using the protocol described in section 2.8.2 with an exception of cell density at 0.5 x $10^6$ cells/dish. After the required incubation time post-infection, the culture media were removed and the cells were washed three times with 2 ml PBS buffer. Then 1 ml of 0.5% RBCs was added into each dish and incubated for 30 minutes at RT, after that the RBCs were removed and the cells were washed 4-5 times with PBS buffer to remove any an adsorb RBCs. Finally, the cells were examined and imaged using a light microscope, Zeiss Axiovert 135, at 24 and 48 hpi to show the RBCs haemadsorption on the infected cell surface (100X).

### 2.7.4 Evaluation of HA-specific antibodies in vaccinated mice sera

An indirect Enzyme-linked immunosorbent assay (ELISA) was performed to detect HA-specific antibodies in the sera from vaccinated mice. Briefly, 96-well ELISA plate was coated with purified HA protein of H1N1 virus (20 ng/well, (NativeAntigen) diluted in 0.05M carbonate/bicarbonate buffer, pH9.6 (Sigma, C3041) overnight at 4ºC. After that, the wells were washed four times with PBS+0.05% (v/v) Tween 20 (PBST) buffer using a microplate washer (LT-3500) and blocked with 5% skimmed milk in PBST at 37ºC for 1 hour. Subsequently, serum samples from each vaccinated group at 1 in 10000 dilutions were added at 50 µl/well and the plate was incubated at 37ºC for 1 hour. Wells were washed four times with PBST and HRP-conjugated anti-mouse secondary antibody 1:2000 (Jackson Immunoresearch) was then added to each well and the plate was incubated at 37ºC for 1 hour. Following, the secondary antibody was washed four times with PBST buffer. Then the plate was developed with 50 µl/well of TMB substrate (3, 3′, 5, 5′ Tetramethylbenzidine Liquid Supersensitive Substrate, T4444 Sigma) and incubated at room temperature in a dark place for 5 minutes. To stop the colour reaction 50 µl/well of stop solution (N600, Thermo Scientific) was added and the optical density (OD) was read at 450 nm using a microplate reader (LT-4500).

### 2.7.5 Analysis of the humoral immunity induced in mice vaccinated with HA antigens

A Haemagglutination inhibition assay (HAI) was carried out to assess the immune responses against H1N1influenza A virus haemagglutinin (Bio-Rad). Briefly, sera samples

from 21 days after boost vaccination were collected and serially diluted 2-fold in 96-well round-bottom plates, mixed with an equal volume of influenza virus (4 HAU) and incubated at RT for 30 minutes. After that, 50 µl of 1% of chicken RBCs was added into each well and gently mixed and the mixture incubated at room temperature for 30 minutes. The HAI was presented as the last serial dilution able to prevent RBCs haemagglutination.

## 2.8 Knockdown of GP64 glycoprotein

### 2.8.1 Double-stranded RNA (dsRNA) synthesis

The *p35* and *gp64* glycoprotein DNA sequences were amplified from AcMNPV entire DNA by PCR using specific primers Table 2.7. These sequences were used as a template for the in vitro transcription to obtain the dsRNA, which targets the *p35* or *gp64* with the T7 polymerase. The dsRNA was synthesised *in vitro* according to the supplier's recommended protocol using a HiScribe™ T7 High Yield RNA Synthesis Kit (NEB). DNA templet provided with the kit was used to synthesise the control dsRNA. In brief, to assemble the reaction it was necessary first to thaw the kit components and mix them well followed by pulse centrifuge to collect the solutions at the tube bottom and then to store the tubes on ice. The reaction mixture should be in the order shown (Table 2.8), the reaction was then mixed thoroughly and pulse centrifuged. After that, the reaction mixture was incubated at 37ºC for 2 hours using a PCR machine. The reaction mixture was usually 20 µl. The dsRNAs were purified using RNeasy MinElute Cleanup Kit according to the supplier's recommended protocol (Qiagen®).

**Table 2.10: dsRNA synthesis reaction mixture**

| Component | Volume (µl) |
|---|---|
| Nuclease-free water | X |
| 10X Reaction Buffer | 2 |
| ATP (100 mM) | 2 |
| GTP (100 mM) | 2 |
| UTP (100 mM) | 2 |
| CTP (100 mM) | 2 |
| Template DNA | X |
| T7 RNA Polymerase MiX | 2 |
| Total reaction volume | 20 |

### 2.8.2 Transfection of insect cell lines with dsRNA

To compare the transfection efficiency, three different transfection reagents were used according to the supplier's recommended protocol (Lipofectine®, Lipofectamine™ RNAiMAX (Invitrogen)) or TransIT®-Insect Transfection Reagent (Mirus). Firstly, Sf21 cells

were seeded in 6-well tissue culture plate at a density of 1 x $10^6$ cells/well and then the cells were transfected with 1 µg of dsRNA under investigation or standard dsRNA as a control. The cells were then incubated overnight at 28ºC. The following day, cells were infected with the AcMNPV virus at MOI of 1 pfu/cell and the virus was harvested from the culture media after different post-infection times (24, 48 hpi) and titrated by plaque assay section (2.2.4a ) to choose the most efficient transfection reagent.

Page intentionally left blank

# Chapter 3

# Exploration of novel BacMam gene delivery vectors using occlusion-derived baculovirus particles

## 3.1 Introduction

Baculovirus technology has been exploited for recombinant protein production in insect cell cultures for more than three decades. However, baculoviruses are also able to transduce mammalian cells and express the target gene(s) efficiently if modified to include a mammalian cell active promoter. This technology is called BacMam and has been used as an attractive tool for gene delivery for *in vivo*, *ex vivo* and for therapeutic protein production applications (Mansouri and Berger, 2018). BacMam virus particle production is easier than for mammalian viruses, for instance, BacMam can reach titres of up to 1 x $10^8$ to 2 x $10^8$ pfu/ml as the BV particles bud out through the cell membrane into the culture media. In contrast, for example, adenovirus production requires cell lysis to release virions into the culture media (reviewed by Kost *et al.*, 2010). Hofmann *et al.* (1995) pioneered the use of recombinant baculovirus BV as a source of BacMam to deliver and express the target gene(s) in hepatic cell lines under the control of mammalian promoters. Since then efforts have been made to improve the transduction efficiency of BacMam-based recombinant baculovirus across a wide range of mammalian cells (reviewed by Mansouri and Berger, 2018). For example, it has been reported that BacMam can transduce primary rat chondrocytes efficiently without affecting their differentiation state (reviewed by Mansouri and Berger, 2018). In addition, BacMam is able to transduce and deliver the gene(s) of interest effectively into human osteosarcoma cell lines, human fibroblast neural cells, CHO, CV-1, HeLa, 293, Cos7, BHK and pancreatic islet cells in addition to fish cells (reviewed by Mansouri and Berger, 2018).

The aim of this chapter was to construct a recombinant baculovirus and investigate whether the ODV form of the virus, rather than BV, can be used as an alternative source of BacMam. While the use of the BV has been very successful, the need to use high multiplicities of infection (MOI) for some mammalian cell lines often requires that the virus is concentrated prior to transduction. Polyhedra can be produced to very high densities and contain many ODV per occlusion. Potentially, much higher concentrations of the virus could be available for transduction. It was also considered that similar technology might be used in the future to achieve display of antigens on the surface of ODV. In order to investigate whether baculovirus ODV can be employed as a BacMam, it was decided to produce a recombinant virus in which the Green Fluorescence Protein (GFP) reporter gene was expressed under the control of human cytomegalovirus immediate early promoter (CMV-ie1). This enables the production of GFP to be monitored by fluorescence microscopy in addition to immunoblotting. Furthermore, the BacMam needed to be polyhedrin-positive (*polh*+) in order to produce polyhedra in insect cell lines, from which the ODV could be isolated and purified.

## 3.2 Results

## 3.3 Construction of the transfer vectors

To generate recombinant ODV-based BacMams, it was necessary to create a transfer vector, which contained a copy of *polh* and the CMV-ie1 promoter to drive the production of GFP in mammalian cell lines. In order to achieve these goals, two plasmids pAcUW21, a dual expression vector that contains a copy of *polh* and the *p10* promoter, and pEGFP-N1 that expresses *gfp* under control of CMV-ie1 were used as transfer vector backbone and as a donor for the CMV.GFP expression cassette, respectively (supplied by R D Possee, OET Ltd).

### 3.3.1 Introducing new restriction enzyme sites into pAcUW21 and pEGFP-N1

To remove the *p10* promoter in pAcUW21 and replace it with the CMV-ie1 promoter and *gfp* sequences from pEGFP-N1, it was necessary to modify these plasmids by introducing new restriction sites *Not*I and *Xba*I, respectively. Three phosphorylated oligos RA1, RA2 and RA3 (Table 2.7, Methods 2.4.5) were used for this purpose. RA1 and RA2 were annealed to produce *Not*I flanked by *Bgl*II and *Xba*I (Figure 3.1 A).

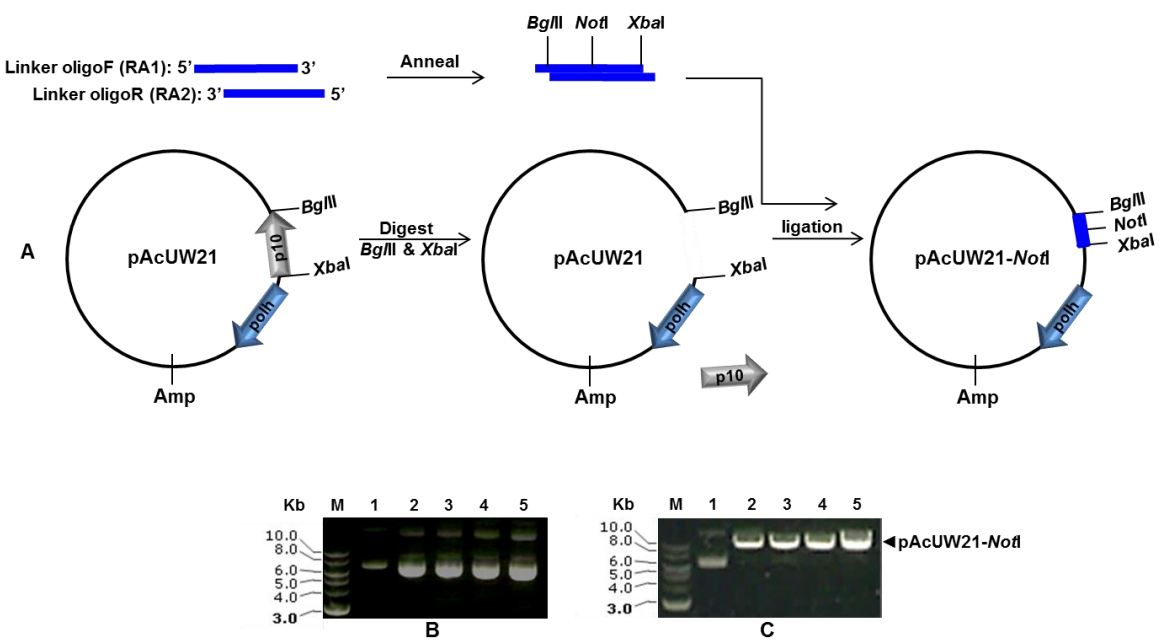


**Figure 3.1: Modification of pAcUW21.**
**A:** Schematic representation of the cloning strategy to modify pAcUW21 by introducing a *Not*I site into its genome. *E.coli* DH5α was transformed with modified pAcUW21-*Not*I. **B:** Analysis of DNA isolated from transformed colonies on a 1% agarose gel. M: 2-log ladder; lane 1: pAcUW21; lane 2-5: pAcUW21-*Not*I. **C:** Restriction digest analysis of pAcUW21-*Not*I genome purified from four colonies on a 1% agarose gel. The pAcUW21-*Not*I was digested with *Not*I for 1 hour at 37ºC before the analysis. M: 2 Log ladder; lane 1: pAcUW21-*Not*I (undigested); lane 2-5: pAcUW21-*Not*I digested with *Not*I.

Subsequently, pAcUW21 was digested with *Bgl*II and *Xba*I to remove the *p10* promoter. The linear fragment of pAcUW21 was purified from an agarose gel and ligated with the annealed oligos to introduce the *Not*I restriction site. Following transformation of *E. coli* DH5α and characterisation of colonies (Figure 3.1 B, C), one colony was selected to take forward and the plasmid was designated pAcUW21-*Not*I (Figure 3.1). In parallel, oligo RA3 was self-annealed to produce *Xba*I flanked by *Ase*I restriction sites. Next, pEGFP-N1 was digested with *Ase*I and dephosphorylated by Antarctic Phosphatase (NEB) as described in Methods (2.4.2b), purified and ligated with the annealed RA3 (Methods 2.4.2a and 2.4.4, respectively) to introduce *Xba*I; the newly modified plasmid was designated pEGFP-N1-*Xba*I (Figure 3.2).

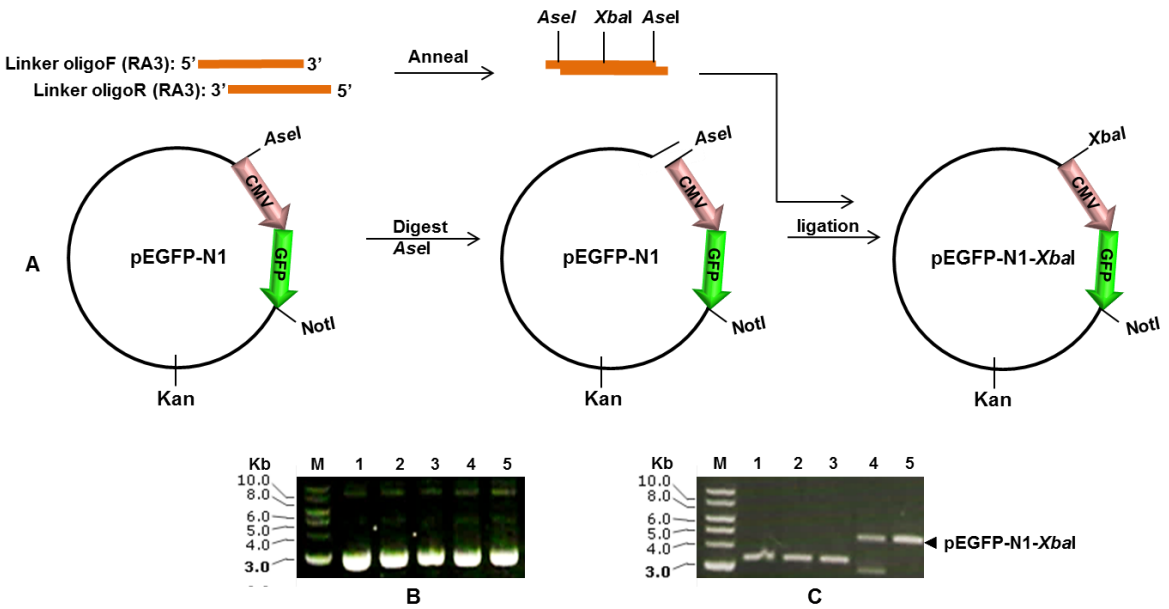


**Figure 3.2: Modification of pEGFP-N1.**
**A:** Schematic representation of the cloning strategy to modify the pEGFP-N1 by introducing *Xba*I flanked by *Ase*I into its genome. *E.coli* DH5α was transformed with modified pEGFP-N1-*Xba*I. **B:** Analysis of the DNA isolated from transformed colonies on a 1% agarose gel. M: 2-log ladder; lane 1: pEGFP-N1; lane 2-5: pEGFP-N1-*Xba*I. **C:** Restriction digest analysis of pEGFP-N1-*Xba*I from four colonies on a 1% agarose gel. pEGFP-N1-*Xba*I digested with *Xba*I for 1 hour at 37ºC before the analysis. M: 2-Log ladder; lane 1: pEGFP-N1-*Xba*I (undigested); lane 2-5: pEGFP-N1-*Xba*I digested with *Xba*I. Lane 5 shows that this plasmid has the *Xba*I restriction site.

### 3.3.2 Construction of pAcCMV.GFP transfer vector

In order to construct the recombinant transfer vector pAcCMV.GFP, both pAcUW21-*Not*I and pEGFP-N1-*Xba*I were digested with *Xba*I and *Not*I (Figure 3.3 A). Restriction digest analysis resulted in a large fragment of pAcUW21-*Not*I at the expected size. Digestion of pEGFP-N1-*Xba*I resulted in two fragments, the large one belonging to the pEGFP-N1 backbone and the smaller fragment the CMV.GFP expression cassette at the expected size (Figure 3.3 B). The CMV.GFP fragment and the pAcUW21-*Not*I backbone were isolated from a 1% agarose gel and purified as described in Methods (2.4.2a). Following ligation

(Figure 3.3 C) and *E.coli* transformation, plasmids from seven amplified colonies were purified and screened by PCR using primers RDP 213B and RDP 214B (Table 2.7, Methods 2.4.5). Two colonies contained the correct recombinant plasmid giving a single band of the insert target gene of about 3 kbp (Figure 3.3 D). Plasmids from these two colonies were screened by restriction digestion, which resulted in two fragments at expected sizes (data not shown). One colony was selected to amplify and purify the recombinant plasmid, which was also confirmed by DNA sequencing (data not shown).

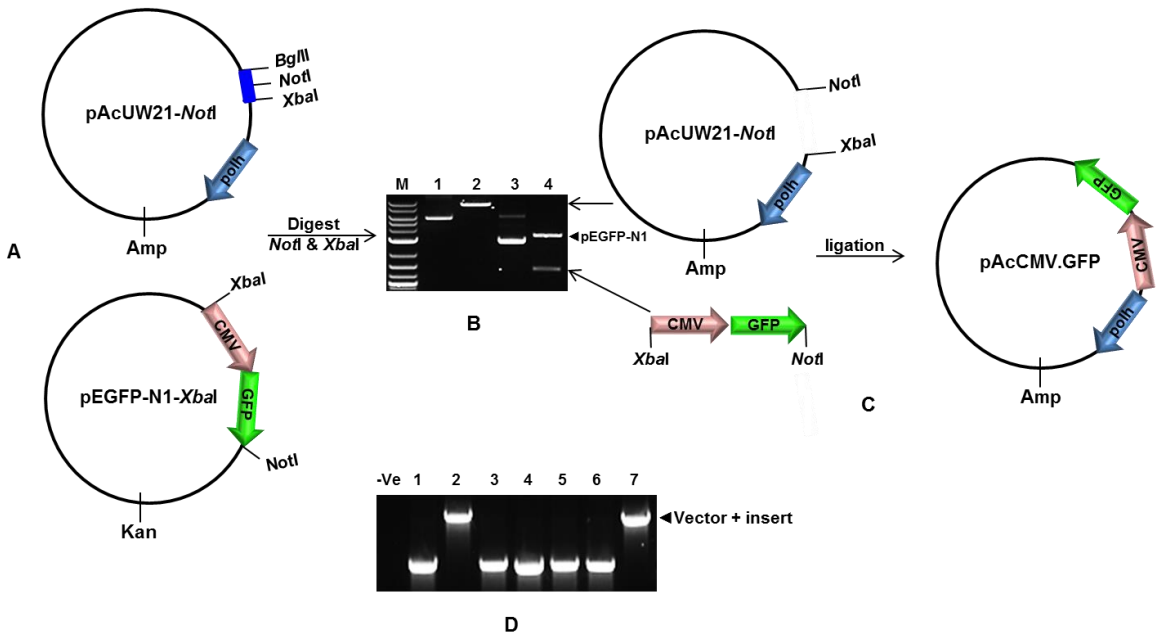


**Figure 3.3: Generation of pAcCMV.GFP transfer vector.**
**A:** Schematic representation of the cloning strategy to generate the pAcCMV.GFP by digesting the pAcUW21-*Not*I and pEGFP-*Xba*I with *Not*I *and Xba*I. **B** & **C:** pAcUW21-*Not*I and CMV-GFP fragments were purified from a 1% agarose gel and ligated using standard cloning protocol to produce pAcCMV.GFP recombinant vector. M: 2-Log ladder; lane 1: pAcUW21-*Not*I (undigested); lane 2: pAcUW21-*Not*I digested with *Not*I; Lane 3: pEGFP-N1-*Xba*I (undigested); lane 4: pEGFP-N1-*Xba*I digested with *Xba*I. **D:** Analysis of the DNA isolated from transformed picked colonies on a 1% agarose gel. -Ve: distilled water as a negative control for PCR reaction; lane 1-7: recombinant DNA screening by PCR amplification using RDP 213B and RDP 214B primers.

## 3.4 Construction of BacMam FBU-GFP$^{CMV}$ virus

To construct the *polh*+ BacMam FBU-GFP$^{CMV}$ in a single step without the need for purification of recombinant virus from the parental background by plaque assay, the *flash*BAC system was used (Hitchman *et al.*, 2007a) in particular, FBU (Hitchman *et al.*, 2011). Insect cells (Sf9) were co-transfected with a mixture of FBU DNA (OET Ltd) and pAcCMV.GFP transfer vector as described in Methods (2.2.3). Homologous recombination between these DNAs results in replacement of the BAC region within FBU DNA with the dual expression cassette and restoring the function of ORF1629 that enables the replication

of viral DNA to generate the recombinant BacMam (Figure 3.4). The BacMam BV was harvested from the culture medium 5 days after the co-transfection and was considered as virus seed stock passage 0 (P0). This BacMam virus stock was amplified further by infecting Sf9 insect cells in 50 ml of shaking culture to produce a P1 working stock of virus. This stock comprised a source of BV to confirm the expression of GFP under the CMV-ie1 promoter. The P1 titre was 1.8 x $10^8$ pfu/ml as titrated by plaque assay (Methods 2.2.4a). Insertion *of gfp* into the virus genome was confirmed by PCR using EGFPF and YGFPR primers in (Table 2.7, Methods 2.4.5) and DNA sequencing (data not shown).

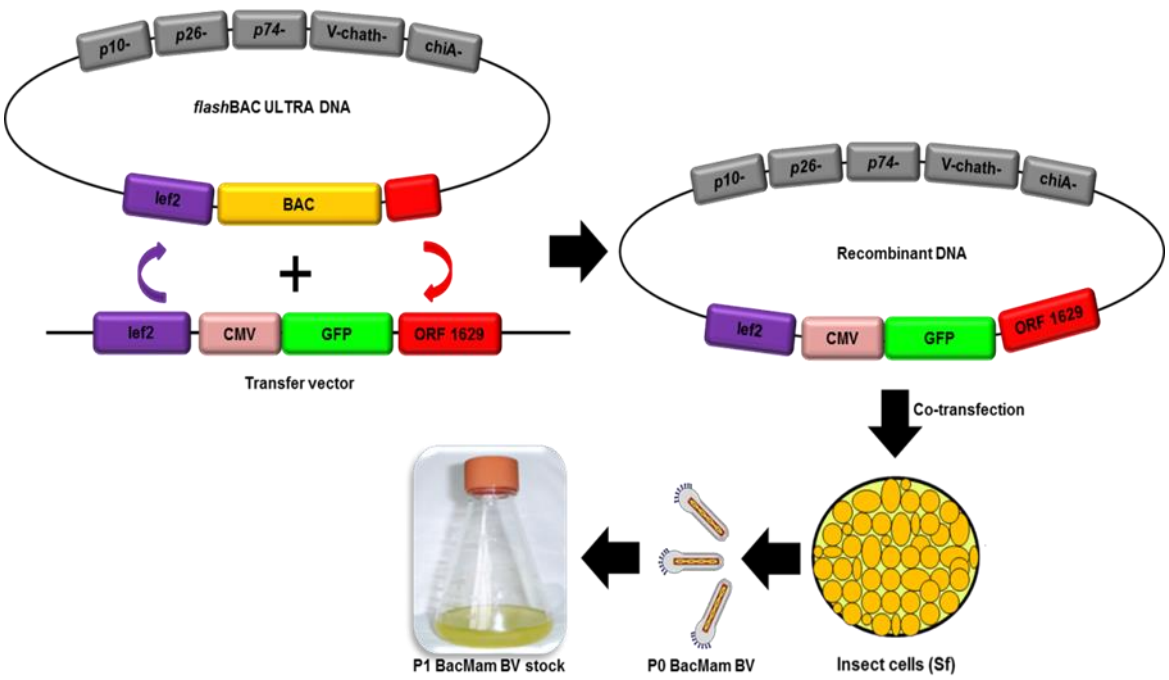


**Figure 3.4: Schematic representation of the P1 FBU-GFPCMV virus stock generation.**
FBU-GFP$^{CMV}$ virus was produced by the co-transfection of Sf9 cells with the pAcCMV.GFP transfer vector and baculovirus *flash*BACULTRA DNA. Homologous recombination, replacing the BAC gene with the expression cassette from the recombinant transfer vector, in addition to restoring the function of ORF1629 generates the recombinant FBU-GFP$^{CMV}$. The FBU-GFP$^{CMV}$ virus stock was harvested from the culture medium to produce a large volume of a P1 working stock of the recombinant virus.

## 3.5 Characterisation of polyhedra produced in AcMNPV and FBU-GFP$^{CMV}$ infected Sf9 cells using electron microscopy

A previous study by Wang *et al.* (2009) demonstrated that *p10, p26, p74* genes play an essential role in ODV occlusion in polyhedra of AcMNPV. They found that Sf21 cells infected with AcMNPV lacking these three genes produced empty polyhedra without occluded virions. Therefore, it was essential to investigate the significance of these gene deletions on virion occlusion in FBU-GFP$^{CMV}$-infected Sf9 cells, as the parental virus genome FBU also contains these three gene deletions (Hitchman *et al.*, 2011). Briefly, Sf9 cells were

infected with wild-type AcMNPV or FBU-GFP$^{CMV}$ at an MOI of 1pfu/cell (Methods 2.7.2a). After 3 days post-infection (dpi), infected cells were recovered by centrifugation and prepared for TEM analysis by (Methods 2.7.2a) to examine the ODV occlusion by polyhedra.

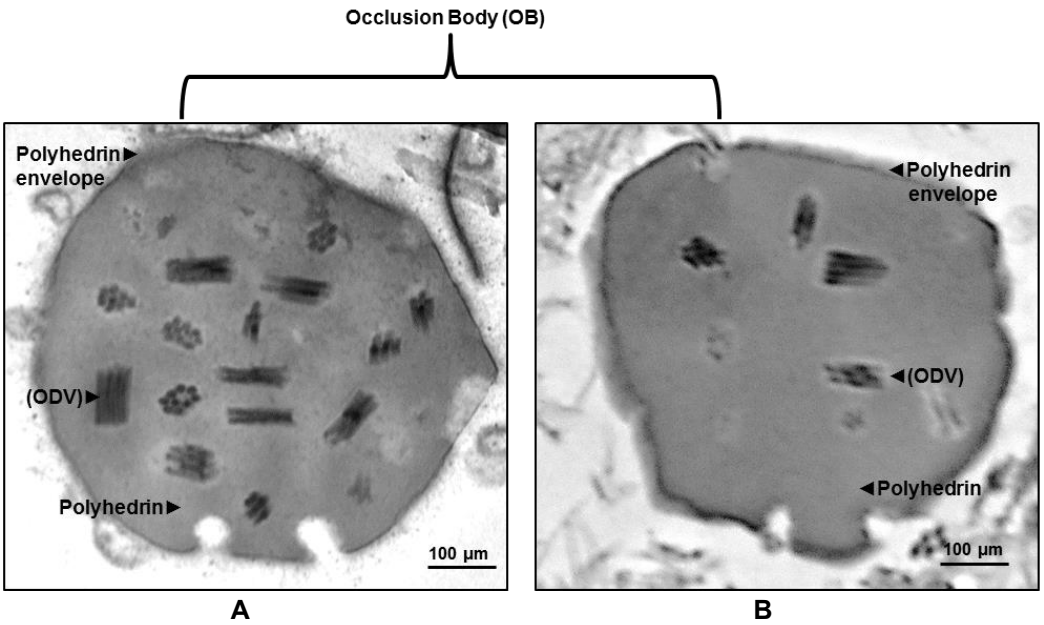


**Figure 3.5: Transmission electron microscopy analysis of ODV occlusion in polyhedra produced in infected Sf9 cells.**
Sf9 cells were infected with AcMNPV or FBU-GFP$^{CMV}$. At 3 dpi, cells were pelleted and prepared for TEM analysis to observe polyhedra structure using a Hitachi H7650 electron microscope. **A:** AcMNPV-derived polyhedra showed many ODV surrounded by the polyhedrin matrix. **B:** FBU-GFP$^{CMV}$ polyhedra showed fewer ODV surrounded by the polyhedrin matrix. Scale bar = 100 µm.

The TEM images confirmed that polyhedra in FBU-GFP$^{CMV}$–infected Sf9 cells occluded significantly fewer ODV than in wild-type virus-infected cells (Figure 3.5 B), which was confirmed by a t-test ($p<0.0001$). The average number of ODV per polyhedra was 10.61 or 2.74 for AcMNPV and FBU-GFP$^{CMV}$, respectively (Figure 3.6). However, the polyhedra diameter for both viruses was not significantly different ($p>0.05$; Figure 3.7, further information is presented in the discussion section 3.12, p65, last paragraph).

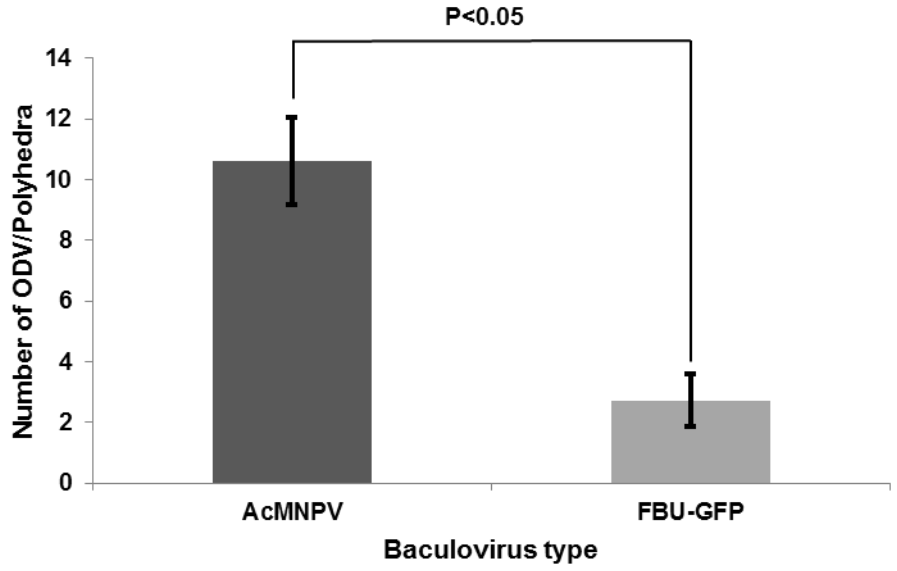


**Figure 3.6: Comparison of total ODV counts occluded by polyhedra in AcMNPV and FBU-GFP$^{CMV}$ infected cells.**
Sf9 cells were infected with AcMNPV or FBU-GFP$^{CMV}$. At 3 dpi, cells were pelleted and prepared for TEM analysis as described in Figure 3.5. The number of ODV embedded in sections of polyhedra was counted to give total ODV per polyhedra. Error bars represent mean ± SD (n=38 sections counted); p<0.05.

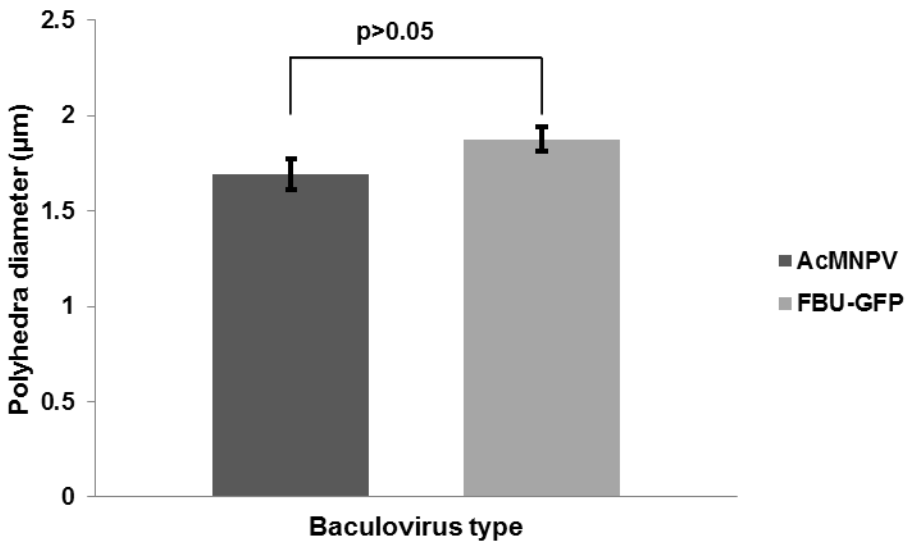


**Figure 3.7: Comparison of AcMNPV- and FBU-GFP$^{CMV}$-derived polyhedra diameter.**
Sf9 cells were infected with AcMNPV or FBU-GFP$^{CMV}$. At 3 dpi, cells were pelleted and prepared for TEM analysis (Figure 3.5). Polyhedra diameters were measured using ImageJ programme. Error bars represents mean ± SD (n=19), p>0.05.

## 3.6 Production of polyhedra in different insect cell lines

In order to explore the possibility of using FBU-GFP$^{CMV}$ ODV to transduce mammalian cells and express the reporter gene, it was necessary to produce a large number of polyhedra to obtain an adequate yield of ODV. As the results in section 3.4 showed that polyhedra produced in Sf9 cells did not contain many ODV, it was decided to investigate whether a different cell line might produce higher yields of both polyhedra and ODV. Therefore, two different insect cell lines, Tni Hi5 and Sf9 were seeded in triplicate in 35 mm tissue culture dishes. After the cells had settled, they were infected with FBU-GFP$^{CMV}$ or wild-type AcMNPV virus as a control, at an MOI of 1pfu/cell, and incubated at 28ºC for 5 days (Methods 2.7.3). As observed by light microscopy, after 3 days many of the Tni Hi5 cells infected with either FBU-GFP$^{CMV}$ or AcMNPV contained a large number of polyhedra (Figure 3.8). In contrast, few polyhedra were observed in the Sf9 cells at 3 dpi for either virus (Figure 3.8).

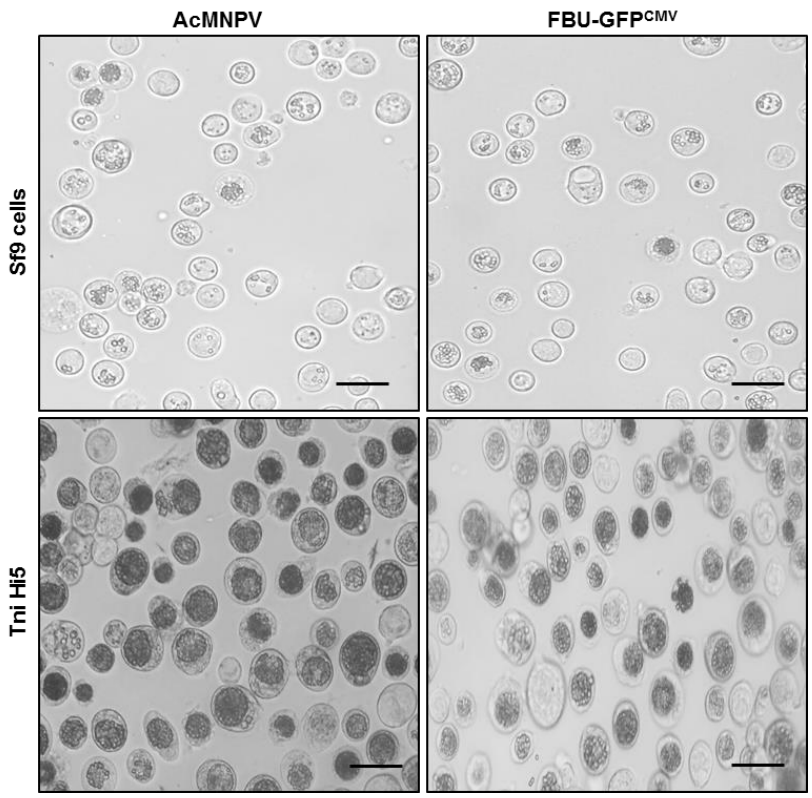


**Figure 3.8: Comparison of polyhedra production in FBU-GFP$^{CMV}$ and AcMNPV-infected cell lines.**
Sf9 and T.ni cells were infected with FBU-GFP$^{CMV}$ or AcMNPV in 35 mm tissue culture dishes and incubated at 28ºC. Infected cells were imaged using a Zeiss Axiovert 135 light microscope at 3 dpi to show polyhedra in the nucleus of these cells (100X). Scale bar = 20 µm.

To examine if the polyhedra number produced in Tni Hi5 cells was significantly higher than in Sf9 cells, the cells were harvested from the culture media and the polyhedra were purified (Methods 2.7.4). Then the number of polyhedra were counted using a haemocytometer and

the average number of polyhedra/cell were compared (Figure 3.9). A t-test showed that the number of AcMNPV polyhedra produced in Tni Hi5 (1.38 x $10^8$ / $10^6$ cells) was significantly higher ($p<0.05$) than in Sf9 cells (3.1 x $10^7$ / $10^6$ cells) (Figure 3.9). The number of polyhedra per infected cell was equivalent to 138 or 31 for Tni Hi5 and Sf9, respectively. Similar results were obtained for FBU-GFP$^{CMV}$; the number of polyhedra produced in Tni Hi5 (8.7 x $10^7$ / $10^6$ cells) was significantly higher ($p<0.05$) than in Sf9 cells (1.4 x $10^7$ / $10^6$ cells) (Figure 3.9). In addition, ODV were purified from polyhedra from both viruses and titrated using qPCR (Methods 2.2.4b). The results indicated that there was no significant difference between the AcMNPV and FBU-GFP$^{CMV}$ ODV titre produced in Tni Hi5 cells ($p>0.05$; Figure 3.10). However, the ODV titre of both viruses produced in Tni Hi5 cells was significantly higher ($P<0.0001$) than that in Sf9 cells (Figure 3.10). As a result, Tni Hi5 cells were selected for production and purification of polyhedra and ODVs in order to test the ability of the latter to transduce mammalian cells.

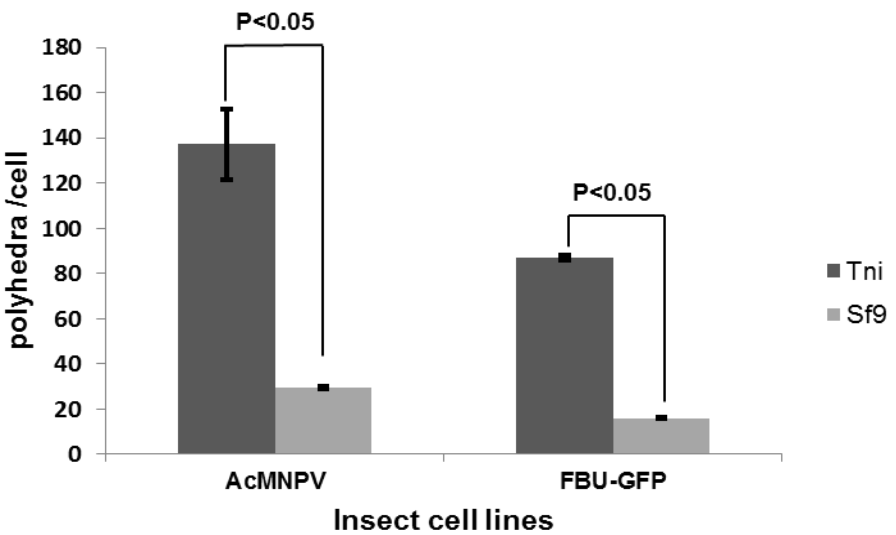


**Figure 3.9: Quantitative comparison of FBU-GFP$^{CMV}$ and AcMNPV polyhedra purified from different insect cell lines.**
Triplicate 35mm tissue culture dishes of Tni Hi5 and Sf9 seeded at 0.5 x $10^6$ and 1 x $10^6$cells/dish, respectively, were infected with AcMNPV or FBU-GFP$^{CMV}$. After 5 dpi, polyhedra were purified and re-suspended in 1ml of distilled water. Total polyhedra numbers from both infected cells were counted using a haemocytometer to give polyhedra/$10^6$ cells. The graph represents mean ± SD (n=9); $p<0.05$

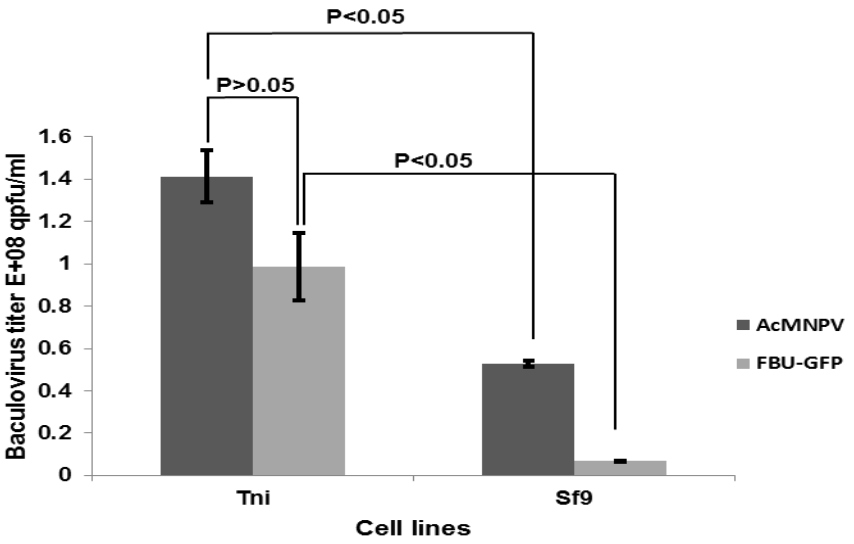


**Figure 3.10: Comparison of the ODV titre of FBU-GFP$^{CMV}$ and AcMNPV produced in different cell lines.**
Triplicate 35mm dishes of Tni Hi5 and Sf9 seeded at 0.5 x $10^6$ and 1 x $10^6$ cells/dish, respectively, were infected with AcMNPV or FBU-GFP$^{CMV}$. After 5 dpi, polyhedra were purified and treated with an alkaline buffer to release the ODV. The ODV titre was calculated using qPCR (Methods 2.2.4b). The graph represents the mean ± SD (n=6); $p<0.05$.

## 3.7 Production of polyhedra from FBU-GFP$^{CMV}$-infected Tni Hi5 cells

Based on findings obtained from section 3.5, Tni Hi5 (1 x $10^6$ cells/ml) in shake culture were infected with FBU-GFP$^{CMV}$ BV at an MOI of 1pfu/cell. Following incubation at 28ºC for 5 days, the cells were harvested by centrifugation and lysed with SDS to release polyhedra. The polyhedra were then harvested by centrifugation, resuspended in distilled water and the suspension applied onto a 50-60% (w/w) discontinuous sucrose gradient (Methods 2.7.4; Figure 3.11 A). A single, sharp white–milky band of pure polyhedra was obtained (Figure 3.11 B). Purified polyhedra were then dissolved in an alkaline buffer to release ODVs, which were then purified using a continuous 30-60% (w/w) sucrose gradient as described in method (section 2.7.4). Several ODV bands were observed in the gradient (Figure 3.11 C), which indicated that the number of nucleocapsids within a single ODV varied as has been previously described (Summers and Arnott, 1969).

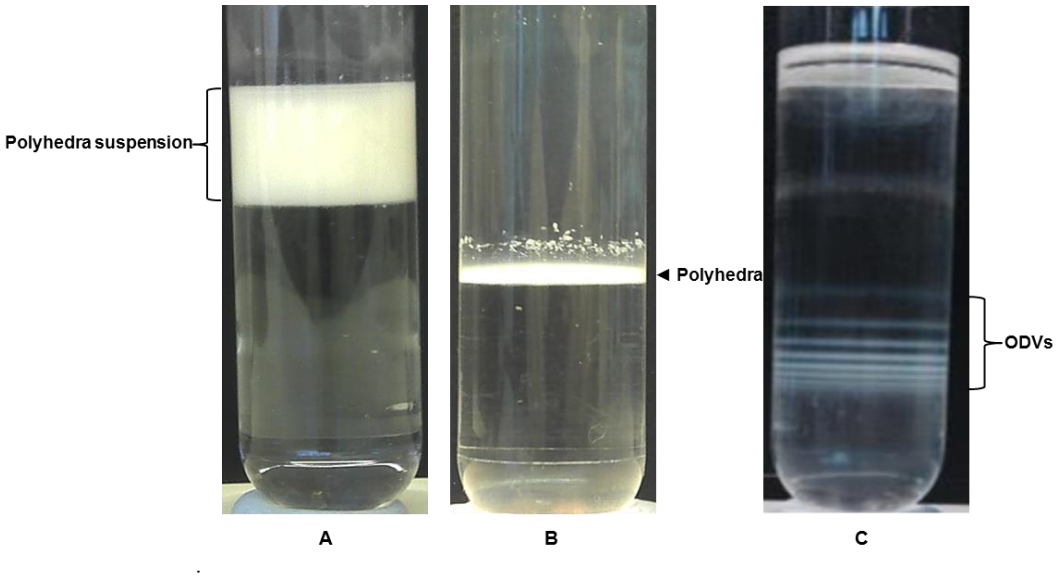


**Figure 3.11: Purification of FBU-GFP$^{CMV}$ polyhedra and ODV produced in Tni Hi5 cells.**
**(A & B):** Polyhedra produced in shaking culture of FBU-GFP$^{CMV}$-infected Tni Hi5 were harvested and purified by 50-60% (w/w) none continuous sucrose gradient. **(C):** Pure polyhedra were harvested and dissolved in an alkaline buffer to release ODVs, which were then purified using continuous 30-60% (w/w) sucrose gradient.

## 3.8 Analysis of *gfp* expression by transduction of mammalian cells with FBU-GFP$^{CMV}$ budded virus

Before testing the ability of ODV to transduce mammalian cells, HEK-293 cells were transduced with conventional FBU-GFP$^{CMV}$ BV in order to confirm the integrity of the *gfp* expression cassette within the FBU-GFP$^{CMV}$. Briefly, HEK-293 cells (0.5 x $10^5$ cells/well) in six-well plates were transduced with FBU-GFP$^{CMV}$ BV at different MOI (10, 30, 100 pfu/cell). In addition, mock-transduced (no virus) and AcMNPV-transduced cells were included as negative controls (Methods 2.7.5). Following incubation at 37ºC for 48 hours post-transduction (hpt), the cells were harvested by centrifugation. Crude cell lysates were separated by a 10% SDS-PAGE gel, following which the proteins were transferred onto a nitrocellulose membrane (Methods 2.5.2) for immunoblotting analysis using anti-GFP antibody (Table 2.8, Methods 2.5.2b). The Immunoblot identified a ~27 kDa band, corresponding to the expected size of recombinant GFP that increased in intensity with increasing MOI from 10 to 100 pfu/cell (Figure 3.12, arrow). As expected no GFP protein was detected in mock- or AcMNPV-transduced cells (Figure 3.12). The result confirmed that the recombinant BacMam was assembled correctly and that *gfp* was expressed under control of the CMV-ie1 promoter.

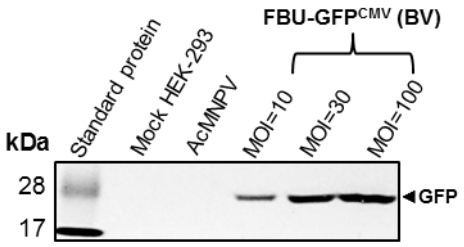


**Figure 3.12: Western blot analysis of the GFP production in FBU-GFP$^{CMV}$ BV-transduced HEK-293 cells.**
HEK-293 were transduced with FBU-GFP$^{CMV}$ BV at different MOI; mock- or AcMPNV-tranduced cells were included as controls. Cells were harvested at 48 hpt and total crude cell lysates were separated on a 10% SDS-PAGE gel and analysed by immunoblotting using anti-GFP antibody. Precision plus protein Western C standards (Bio-Rad). Arrow indicates the expected size of GFP.

## 3.9 Transduction of HEK-293 cells with ODV FBU-GFP$^{CMV}$

In order to examine whether FBU-GFP$^{CMV}$ ODV is able to transduce mammalian cells and express the *gfp* reporter gene, HEK-293 cells were transduced with FBU-GFP$^{CMV}$ ODV at an MOI of 100 qpfu/cell (Methods 2.7.5). FBU-GFP$^{CMV}$ BV-transduced cells at the same MOI were included as a positive control, a mock-transduced (no virus) and wild-type AcMNPV BV-transduced cells were included as negative controls. GFP production was visualized at 0, 24 and 48 hpt using a fluorescence microscope as shown in Figure 3.13. Fluorescence microscopy analysis revealed that GFP fluorescence level in HEK-293 cells transduced with FBU-GFP$^{CMV}$ BV (Figure 3.13, panel C) was considerably higher than in FBU-GFP$^{CMV}$ ODV-transduced cells (Figure 3.13, panel D) at both post transduction times. The fluorescence photomicrographs, shown in Figure 13.3, panel C also demonstrated the enhancing effect of post transduction time on transgene expression in FBU-GFP$^{CMV}$ For BV-transduced HEK-293 cells the GFP fluorescence level was notably increased after 48 hpt compared with 24 hpt. However, for the FBU-GFP$^{CMV}$ ODV-transduced cells (Figure 3.13, panel D), the fluorescence levels approximately was the same at both post transduction times. No fluorescence was observed in either the mock- or AcMNPV BV-transduced HEK-293 cells, at any time post-transduction, as expected (Figure 3.13, panel A, B), respectively.

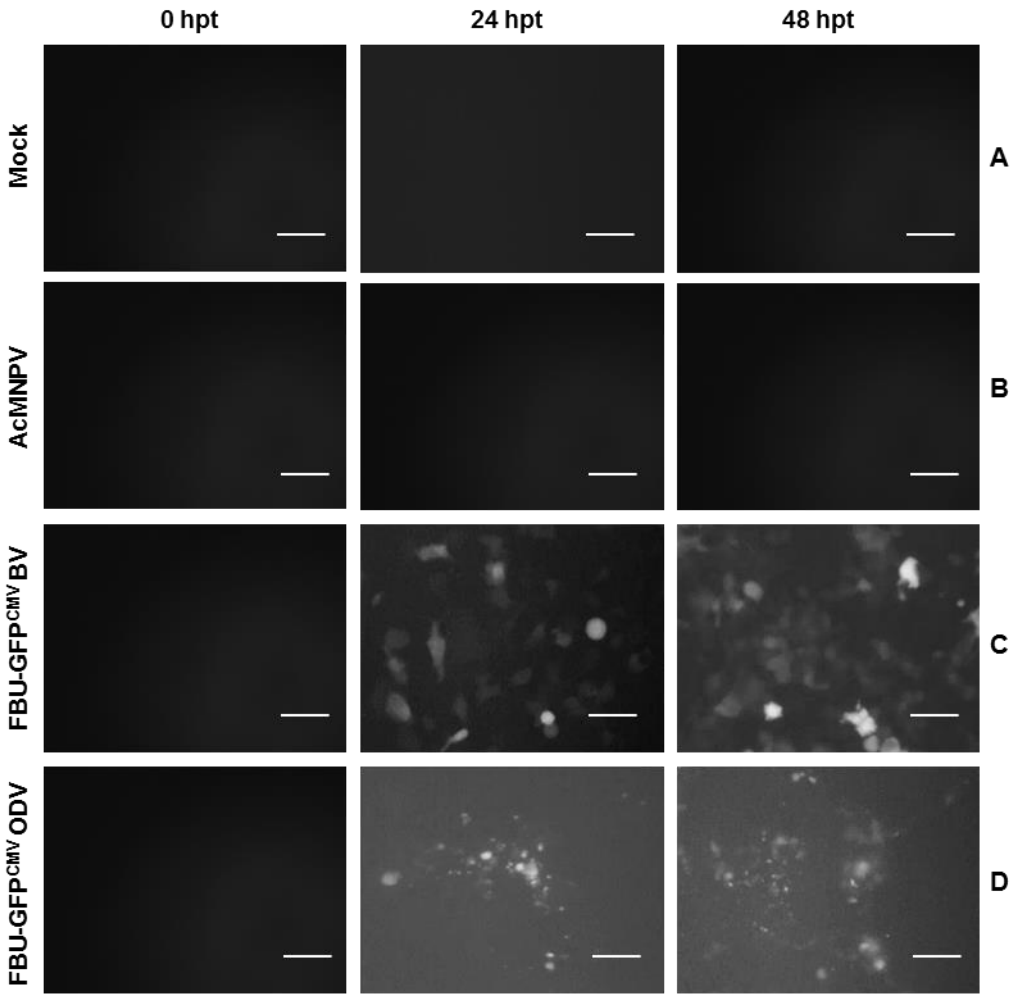


**Figure 3.13: Time course of GFP production in HEK-293 cells transduced with BV- or ODV-FBU-GFP$^{CMV}$.**
HEK-293 cells (0.5 x $10^5$ cells/well) were transduced with either FBU-GFP$^{CMV}$ BV **(C)** or ODV **(D)**. Mock- **(A)** and AcMNPV-transduced HEK-293 cells **(B)** were included as negative controls. Images were taken at 0, 24, 48 hpt as indicated using a Zeiss Axiovert Fluorescence Microscope (x100). Scale bar = 20 µm.

## 3.10 Analysis of *gfp* expression by FBU-GFP$^{CMV}$ ODV in HEK-293 cells

Fluorescence microscopy analysis, in section 3.8, showed that FBU-GFP$^{CMV}$ ODV-mediated transgene expression was very low even after 48 hpt (Figure 3.13 D). Therefore, it was decided to examine the GFP production in FBU-GFP$^{CMV}$ ODV- and BV-transduced cells by SDS-PAGE and immunoblotting. HEK-293 cells (0.5 x $10^5$ cells/well in a six-well plate) were transduced with FBU-GFP$^{CMV}$ ODV at an MOI of 100, 250, 400 qpfu/cell or with FBU-GFP$^{CMV}$ BV at an MOI of 100 pfu/cell as a positive control for GFP expression (Methods 2.7.5). Mock- and AcMNPV BV-transduced cells were included as negative controls. Following incubation at 37ºC for 48 hours, the cells were harvested and crude cell lysates were separated by a 10% SDS-PAGE gel. After that, the proteins were transferred onto a nitrocellulose membrane (Methods 2.5.2) for immunoblotting analysis using anti-GFP antibody (Table 2.8, Methods 2.5.2b). Expression of *gfp* for a single representative

experiment is shown in Figure 3.14. The anti-GFP antibody identified a ~27 kDa band corresponding to the expected size of recombinant GFP protein in cells transduced with BV at an MOI of 100 pfu/cells. However, no *gfp* expression was observed for any ODV-transduced cells at all tested MOI used in this experiment (Figure 3.14). No GFP was observed in both mock- and AcMNPV BV-transduced cells lysates as expected (Figure 3.14).

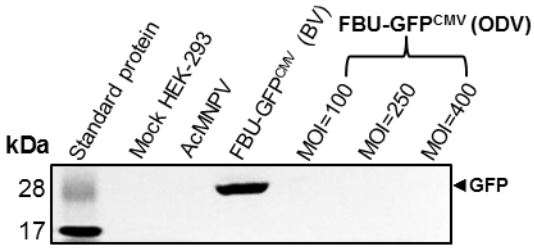


**Figure 3.14: Protein synthesis in FBU-GFP$^{CMV}$ ODV-transduced HEK-293 cells.**
HEK-293 cells (0.5 x $10^5$ cells/well) were transduced with FBU-GFP$^{CMV}$ ODV at different MOI. Mock-cells and AcMNPV BV-transduced cells were included as negative controls, FBU-GFP$^{CMV}$ BV-transduced cells as controls. Cells were harvested and the total proteins in crude cell lysates were separated on a 10% SDS-PAGE gel, followed by immunoblotting analysis and the GFP was detected by the anti-GFP antibody. Marker: Precision plus protein Western C standard (Bio-Rad). Arrow indicates the expected size of GFP.

## 3.11 Attempts to improve ODV transduction conditions

Several transduction protocols have been used to optimise BacMam efficiency to deliver and express the target gene(s) in mammalian cells, such as incubation temperature, culture medium used for inoculation, as well as inoculation time (reviewed by Jardin *et al.*, 2008). Therefore, a number of parameters were investigated in this chapter to determine whether transduction using ODV could be improved including incubation temperature, incubation time and transduction media.

### 3.11.1 Effect of incubation temperature

The effect of incubation temperature on FBU-GFP$^{CMV}$ transduction efficiency was investigated. Briefly, HEK-293 cells were transduced with FBU-GFP$^{CMV}$ ODV at an MOI of 400 qpfu/cell as described in section 3.9 with one exception when the incubation temperature of the virus inoculum and the cells were shifted from of 37ºC to room temperature for 1 hour, to determine whether a lower temperature can enhance the transduction efficiency. Following transduction, cells were incubated at 37ºC for 24 and 48 hpt and subsequently, transduced cells were examined by fluorescence microscopy. However, no improvement in ODV transduction was observed (data not shown) compared with that shown in Figure 3.13 D, indicating that reducing the temperature during transduction was not effective.

### 3.11.2 Effect of incubation time and cell culture medium

To examine whether the incubation time of FBU-GFP$^{CMV}$ ODV with HEK-293 cells had any effect on transduction efficiency, HEK-293 cells were transduced with the corresponding virus as described in section 3.10.1 for 1 or 4 hours. GFP synthesis in HEK-293 cells transduced with FBU-GFP$^{CMV}$ ODV remained low even when the incubation time was extended to 4 h, suggesting that incubation time has no effect on transduction efficiency. In contrast, control cells transduced with FBU-GFP$^{CMV}$ BV showed slightly increased expression levels after 4 h of incubation (data not shown). In the above experiments, DMEM medium was used to adjust the final volume of the virus to 100 µl. To examine whether the medium had any influence on transduction efficiency, HEK-293 cells were transduced as described in the protocol above, but in addition, PBS buffer was substituted for DMEM.

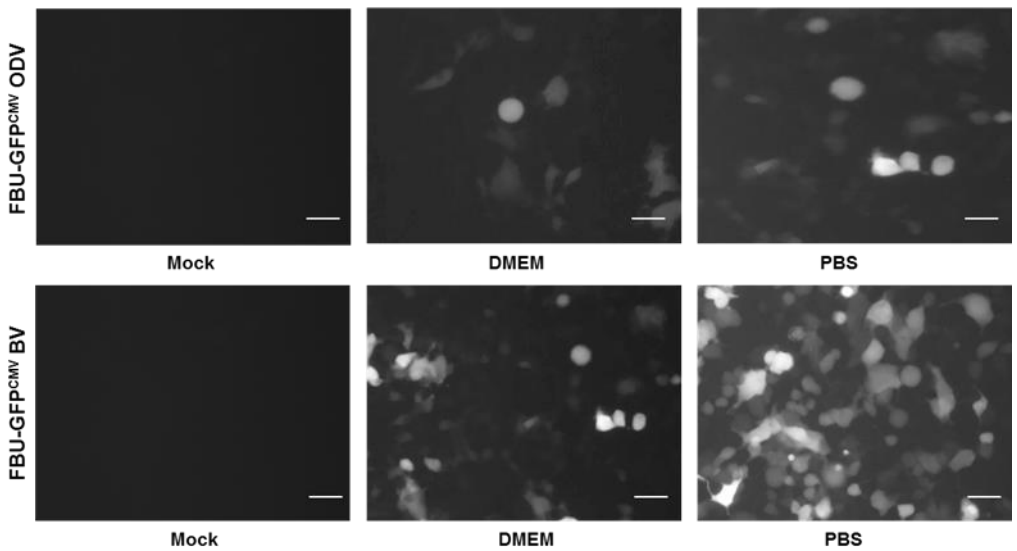


**Figure 3.15: Effect of transduction medium on FBU-GFP$^{CMV}$ ODV transduction efficiency in HEK-293 cells.**
HEK-293 cells 0.5 x $10^5$ cells/well were transduced with either FBU-GFP$^{CMV}$ ODV at MOI of 400 qpfu/cell or BV at MOI of 100 pfu/ml. Virus inoculum was diluted in DMEM or PBS prior to transduction. Mock-transduced HEK-293 cells were included as a negative control as well as BacMam BV-transduced HEK-293 as a positive control. Images were taken at 48 hpt as indicated using a Zeiss Axiovert Fluorescence Microscope (x100). Scale bar = 20 µm.

As shown in Figure 3.15, PBS was better as a transduction medium and resulted in a higher transduction efficiency and GFP synthesis, when compared to DMEM medium for both BV and ODV-transduced cells. Unfortunately, for this modification, the transduction efficiency of FBU-GFP$^{CMV}$ ODV remained low compared to BV, as indicated by *gfp* expression. FBU-GFP$^{CMV}$ BV transduction efficiency and gene expression were significantly increased by replacing DMEM with PBS in the transduced HEK-293 cells (Figure 3.15).

## 3.12 Discussion

BacMam recombinant baculovirus technology has received great attention and development over the last decade. Several studies have reported the use of these viruses as a successful gene delivery tool in many different applications (Paul *et al.*, 2014). However, the main disadvantage of using recombinant BacMams for gene delivery is the limitation of the gene expression that been mediated by these viruses (Shen *et al.*, 2008; Yang *et al.*, 2009). Many strategies have been exploited to enhance the performance of BacMam, to be used as a gene delivery vehicle for both *in vitro* and *in vivo* applications. These strategies include using high virus titre for transduction or by extending the virus incubation time with the transduced cell (Sprick *et al.*, 2017). Furthermore, high transduction efficiency has been reported using VSV-G pseudotyped recombinant BacMam (Levin *et al.*, 2016)

The main aim of the experiments described in this chapter was to construct and create a novel recombinant baculovirus. This virus can be used as a BacMam, which can deliver and express the target protein(s) under the control of a strong mammalian promoter, cytomegalovirus immediate early 1 (CMV-ie1) in human cells or as a novel vector to display protein(s) on the surface of ODV in the insect expression system. The potential advantage of using ODV vector is, it can be packaged into polyhedra, which may provide a useful transport mechanism to protect the targeted vaccine during storage and transport without the need for a cold supply chain.

The experimental work in this chapter has mainly relied on the use of the recombinant BacMam virus in which the reporter *gfp* gene has been driven by CMV-ie1. Several researchers have suggested using *gfp* as a reporter gene because the gene expression it is easy to monitor and quantify (reviewed by Locanto, 2014). Different approaches have been used to measure GFP fluorescence intensity and the expression level, for example using flow cytometry analysis, fluorescence microscopy or Western immunoblotting. Fluorescence microscopy was used in this thesis chapter to visualise the GFP fluorescence directly in the live transduced cells because it is specific and more sensitive. In addition, the level of GFP in total transduced cell lysates was detected by western immunoblot. The recombinant baculovirus was successfully constructed to express the GFP protein as a reporter gene under control of the CMV-ei1 promoter.

It has been reported in a previous study (Wang *et al.*, 2009) that AcMNPV lacking three genes (*p10, p74, p26*) produced empty polyhedra (with no ODVs) in infected Sf21 cells. This study suggested that these genes might play an essential role in the virion occlusion process in AcMNPV polyhedra. As the first step of this chapter was to produce a large number of polyhedra to obtain a high yield of ODV for transduction experiments. Therefore,

following the BacMam construction, it was essential to investigate whether infected Sf9 cells will behave the same as Sf21 cells regarding ODV occlusion. BacMam-infected Sf9 cells were investigated using TEM, and the results in Figure 3.5 B showed that some ODV were occluded by polyhedral although not as many as in wild-type virus. Interestingly, these results were different to the findings obtained by Wang *et al.* (2009) who characterised polyhedra of AcMNPV (*p10, p74, p26*) mutant in Sf21 cells; it is probable that this is a result of the difference in virion occlusion pathways between these two cell types.

After this finding, the polyhedra from recombinant baculovirus were characterized in a different insect cell line, Tni Hi5 cells (section 3.5) to compare the number of polyhedra produced in Sf9 cells. Sf9 cells are generally used for the propagation of wild-type and recombinant baculoviruses (Summers and Smith, 1987; Wang *et al.*, 1992). While Tni Hi5 cells are known to be used widely for the production of the recombinant proteins (Wickham *et al.*, 1992) It was shown that both cell lines infected with *polh*+ BacMam produced polyhedra in their nucleus after 3 days of infection (Figure 3.8). Almost all of the infected Tni Hi5 cells displayed the presence of a large number of polyhedra within each nucleus. In comparison, few polyhedra were observed within the nucleus of infected Sf9 cells (Figure 3.8).

The results of this study showed that polyhedra production is influenced by the host cell, which is similar to the observation of the most recent study by Graves (2016), which reported that a number of polyhedra produced in these cells are variable and infected Tni Hi5 cells showed a larger number of polyhedra compared to Sf9. The difference in polyhedra number between Tni Hi5 and Sf9 cell lines had also been observed in the earlier study by Kim *et al.* (2007), where Tni Hi5 cells also showed the largest number of polyhedra compared to Sf9 cells. It is likely that this variability is a result of the difference in the requirements that are needed for the expression of late/very late factor genes, which can affect the activity of *p10* and *polh* promoter directly (Morris and Miller, 1992; Lu and Miller, 1995). In addition, results shown in Figure 3.10 demonstrated that there was no different in baculovirus ODV titre obtained from AcMNPV or BacMam polyhedra produced in Tni Hi5 cells, however, the titre was significantly lower in Sf9 cells. For these reasons, Tni Hi5 cells were selected to be used for polyhedra production and ODV purification for the HEK-293 transduction experiments. Tni Hi5 cells were infected with BacMam and the ODVs were purified. It was shown in Figure 3.11 that the continuous sucrose gradients had several white-milky bands at different positions, suggesting that the polyhedra had occluded a large number of ODVs with variable numbers of nucleocapsids within a single ODV, as has been previously described (Summers and Arnott, 1969). Previous studies demonstrated that the number of ODVs occluded by polyhedra is variable and each one can include between 20-

80 ODVs. In addition, each ODV can contain between 1 to 15 nucleocapsids (Simon *et al.*, 2004; Clavijo *et al.*, 2009).

These results also confirmed that *p10, p26* and *p74* gene mutations had no significant effect on ODV occlusion by BacMam polyhedra in Tni Hi5 cells (Figure 3.11). This supports the hypothesis that ODV occlusion within polyhedra is host specific and possibly relies on an as yet unspecified host protein or pathway. It is perhaps worth noting that Tni Hi5 cells present as a near homologous host cell as AcMNPV is genetically almost identical to TniMNPV and therefore it is more likely that Tni Hi5 cells would support virus replication in full, compared to a heterologous host cell like Sf9 or Sf21 cells.

A preliminary experiment was performed to investigate the ability of *polh*+ BacMam BV to deliver and express the *gfp* reporter gene in the transduced HEK-293 cells. The immunoblotting analysis in Figure 3.12 showed that BacMam BV was able to transduce HEK-293 cells and express the GFP protein under the CMV-ie1 promoter efficiently at both low and high MOI. This was a promising result and encouraged me to carry on the next important step. To investigate whether BacMam ODV could mediate gene delivery in HEK-293 cells, purified ODV was used. The results in Figure 3.13 suggested that GFP expression was significantly lower in HEK-293 cells transduced with ODV compared to the cells transduced with BV at the same MOI and time post-transduction. Therefore, it was decided to investigate the effect of using low and high MOI on mammalian cell transduction efficiency. Initially, HEK-293 cells were transduced BacMam ODV at an MOI ranging from 100-400 qpfu/cell. No GFP expression was detected in any BacMam ODV- transduced cell lysate samples, at any MOI, as shown in Figure 3.14. Whereas clear evidence of GFP expression was observed in the sample obtained from cells transduced with BacMam BV at MOI of 100 pfu/cell.

The transduction conditions were optimised further by extending the incubation time of the virus with HEK-293 cells from 1 to 4 hours. No improvement was achieved in the transduction efficiency of ODV transduced cells with a slight improvement in BV transduced cells suggesting that the incubation time had no effect on the transduction efficiency. In addition, the effect of incubating at room temperature was examined to improve the transduction efficiency. However, GFP expression remained low in the case of ODV-transduced cells, while a remarkable increase in expression was observed in BV-transduced cells. A recent study by Sprick *et al.* (2017) reported a notable increase in the proportion of GFP+ cells transduced with BacMam BV up to 30.7% when they extended the incubation time from 5 to 24 h. In addition, they found out that using high MOI for transduction also increased the proportion of GFP+ cells up to 61.7% and for both modifications they also noticed an increase in the fluorescence intensity, represented by the mean fluorescence (Sprick *et al.*, 2017).

Furthermore, the effect of using different surrounding solutions for inoculum virus dilution on transduction efficiency was also investigated. Fluorescence imaging of transduced HEK-293 cells with BacMam ODV (Figure 3.15) showed a very low increase in GFP expressing cells when DMEM solution was replaced with PBS. In contrast, HEK-293 cells transduced with BacMam BV showed a high increase in GFP expression (Figure 3.15). An earlier study by Hsu *et al.* (2004) demonstrated that transduction efficiency of HeLa cells by recombinant BacMam BV significantly increased by 75-85% and the reporter gene was highly expressed when the transduction occurred at room temperature for 4 h using PBS as the surrounding solution. It was a challenge to compare between ODV-transduction results in this thesis and previous studies because to date, there has only been one previously published study that has mentioned the use of BacMam ODV as a delivery vehicle in mammalian cells. It was demonstrated that no GFP expression was observed in the ODV-transduced cells compared to the normal gene expression level in BV-transduced cells (Makela *et al.*, 2008). This study suggested that progression of ODV entry could be blocked at the periphery of the cytoplasm as indicated by the accumulation of viral capsids near the plasma membrane of the transduced mammalian cells.

It has been reported that baculovirus entry into both insect and mammalian cells is dependent on clathrin-mediated endocytosis (Matilainen *et al.*, 2005; Long *et al.*, 2006). However, a recent study reported that heparan sulfate proteoglycans (HSPG) may mediate BacMam entry in some mammalian cells (Makkonen *et al.*, 2013). They also reported that BacMam might interact with 6-O and N-sulfated chains of HSPG, bind to the receptor syndecan-1 and enter the vertebrate cells. Several studies have been suggested that GP64 envelope protein plays an important role in BacMam attachment and entry through direct fusion (Kataoka *et al.*, 2012). It has been found that increasing *gp64* levels in baculovirus vectors lead to enhance transduction efficiency (Tani *et al.*, 2001). On the other hand, any inhibition or blocking of the *gp64* will result in reducing or preventing the baculovirus ability to transduce mammalian cells (Schutz *et al.*, 2006).

## 3.13 Conclusion

The results in this chapter have shown that Tni Hi5 cells support more polyhedra and better occlusion of ODV. Furthermore, unlike the previous study by Wang *et al.* (2009) polyhedra of a baculovirus *p10*, *p26* and *p74* mutant (*flash*BACULTRA in this study) was shown some ODVs occlusion in Sf9 cells. In addition, transduction efficiency in HEK-293 cells has shown that BacMam BV was delivered and express the reporter gene efficiently at a high level using low and high MOI. While BacMam ODV showed very low transduction efficiency and transgene expression in the same transduced cell lines. It is possible that this is a result of poor uptake of ODV particles by HEK-293 cells or might be that higher MOI is needed for

cell transduction. Since ODV-based BacMam transduction of mammalian cells did not produce the results anticipated, the original exploration of novel BacMam gene delivery vectors or surface display using occlusion-derived baculovirus particles was not pursued further. Therefore, the project was directed to use recombinant baculovirus BV for development novel baculovirus display vectors for membrane glycoproteins and vaccine production as will be described in the following chapters.

Page intentionally left blank

# Chapter 4

# Development of novel baculovirus display vectors for membrane glycoproteins using influenza virus haemagglutinin as a target protein

## 4.1 Introduction

Surface display technology has become an attractive tool that can be utilized in different research platforms such as antibody and vaccine generation, protein-protein interactions, gene delivery and large peptide library screening. The technology has utilised phage (Smith, 1985), bacterial (Westerlund-Wikström, 2000) and yeast cell surface display (Mei *et al.*, 2017). Nevertheless, using these organisms as a display platform has experienced some drawbacks that have restricted the protein types used for display. For example, phage surface display is based on prokaryotic expression systems that mean the displayed protein(s) will not have any post-translational modifications that may be required for correct folding and function of mammalian proteins (Fields and Casey, 1995).

Baculovirus surface display technology offers an alternative system that may overcome many of these disadvantages. Recombinant proteins displayed on the baculovirus envelope can be produced at high yields using insect cell cultures that enable post-translational modifications for correct protein folding (Smith *et al.*, 1983; Bustos *et al.*, 1988). In 1995, a universal eukaryotic vector was developed to display target protein(s) on the surface of the baculovirus BV envelope by employing the GP64 glycoprotein (Boublik *et al.*, 1995). The target protein coding region was inserted in the locus between the signal peptide and the transmembrane domain (TMD) sequences of a copy of *gp64* (Boublik *et al.*, 1995). The native GP64 was left unmodified as it is essential for baculovirus infectivity (Blissard and Wenz, 1992).

This chapter uses baculovirus BV surface display to investigate new ways of producing influenza virus HA as a putative vaccine. Initially, three different recombinant baculoviruses were compared to optimise HA expression driven by the *polh* promoter in insect cell lines both within the cell cytoplasm and through surface display on the BV envelope. The very late *polh* promoter is most often used to drive high levels of recombinant protein production in insect cells (Matsuura *et al.*, 1987). The most common insect cell lines (Sf9 and Tni Hi5) for recombinant protein production were used throughout this study.

Three different parental baculovirus genomes were used to generate recombinant viruses: BacPAK6, BacPAK6$^{HT}$ and FBU. All generate recombinant viruses through homologous recombination. BacPAK6 was generated by modification of the wild-type AcMNPV genome in which the *polh* coding region was replaced with *lacZ*. In addition, three *Bsu*36I restriction sites were introduced so that the genome can be linearised (Kitts and Possee, 1993). The BacPAK6$^{HT}$ is similar to the BacPAK6 genome but includes a mutation within *fp-25* gene. A recent study has demonstrated that this mutation can result in an increase in baculovirus genome stability and produce a higher titre of infectious BV (Li *et al.*, 2015). In contrast, FBU is based on an AcMNPV genome that has deletions in five genes (*p10, p74, p26, chiA* and *v-cath*) that are non-essential for virus replication in cell culture. It has been reported

that deletion of these genes from the AcMNPV genome is beneficial for improving the yield and quality of some recombinant proteins especially those that are trafficked through the secretory pathway such as membrane proteins (Hitchman *et al.*, 2010a).

### 4.1.1 Construction of haemagglutinin surface display transfer vector

As native HA has its own signal peptide and TMD, it was decided to produce a truncated HA in which these domains were removed so that they would not interfere with the GP64 signal peptide and TMD. In order to construct the truncated HA surface display transfer vectors, sequences encoding HA of H1N1 influenza virus type A were amplified by PCR from the template pAcMP-1.HA (kindly provided by R D Possee, OET Ltd) using gene-specific primers in which 51 amino acids (aa), encoding the signal peptide and TMD were removed (Figure 4.1 A). During the PCR amplification process, both start and stop codons were removed to allow surface display as a fusion with GP64. The resultant HA fragment (HA51) was engineered to contain *Kpn*I and *Xma*I sites at the 5' and 3' ends, respectively (Figure 4.1 B). The HA51 fragment was inserted between the signal peptide and the TMD of a shortened version of GP64 ($GP64^{TRUN}$) in pBACsurf-1-*polh* (kindly provided by M. Aksular, OET Ltd; Figure 4.1 C).

The original version of pBACsurf-1, commercially available from Novagen, creates a full-length GP64-fusion protein (Boublik *et al.*, 1995). Aksular (2017) showed that truncating the GP64 sequence from 1479 bp (56.6kDa) to leave just the signal peptide and TMD (97 bp; 3.8 kDa) improved recombinant fusion or chimeric protein display pBACsurf-1-*polh* was digested with *Kpn*I and *Xma*I and dephosphorylated by Antarctic phosphatase (NEB; Methods 2.4.2b) to remove the 5´ phosphate group to prevent self-ligation prior to ligation with the HA51 fragment using conventional cloning techniques (Methods 2.4.4). DNA was purified from four transformed colonies and screened by PCR amplification with RDP213B and RDP214B primers (Table 2.7) to confirm the insertion of the HA51 fragment. The resulting surface display recombinant vector was specified pBACsurf-1-$HA51^{polh}$ (Figure 4.1 C) and was confirmed by restriction enzyme digestion (Figure 4.1 D) and DNA sequencing (data not shown).

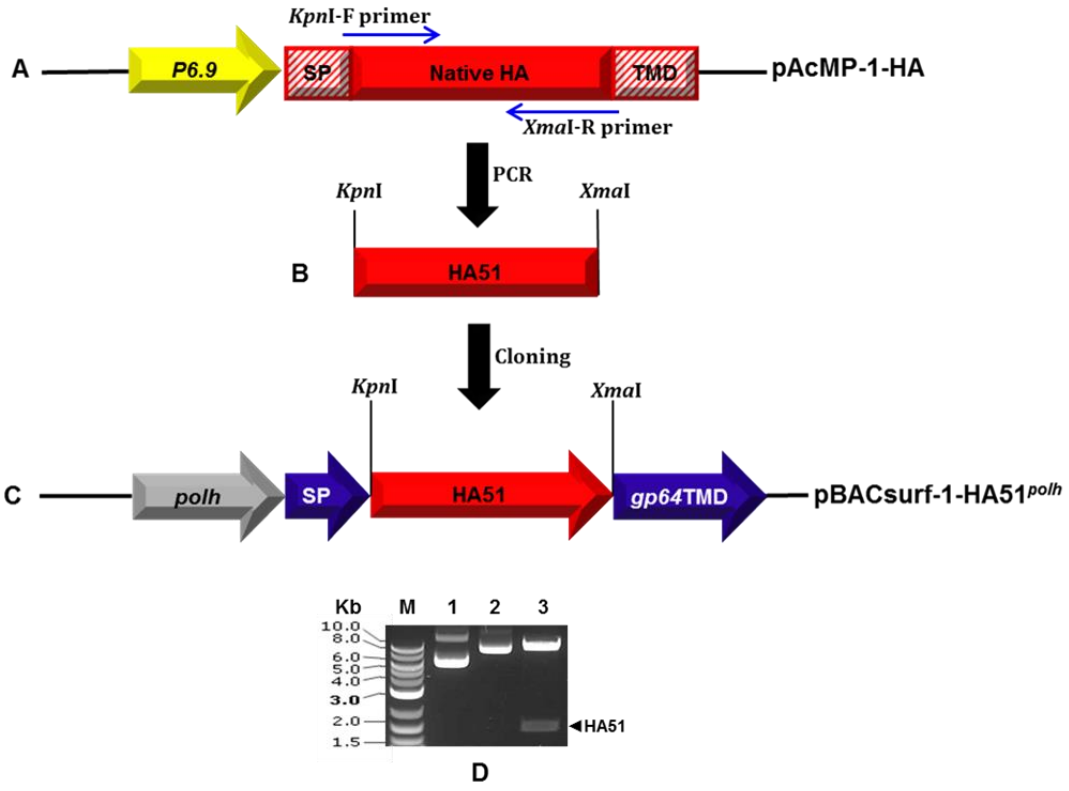


**Figure 4.1: Construction of pBACsurf-1-HA51polh.**
**A:** Schematic representation to show amplification of the HA51 fragment from pAcMP-1.HA by PCR using specific primers. **(B-C):** The HA51 fragment was cloned into the *KpnI* and *XmaI* multiple cloning sites between the upstream *gp64* signal peptide and downstream *gp64* TMD sequences in the pBACsurf-1-*polh* (HA51-GP64$^{TRUN}$) under the control of a *polh* promoter. **D:** Restriction digest analysis of pBACsurf-1-HA51$^{polh}$ plasmid purified from colony picks *of E.coli* in a 1% agarose gel. pBACsurf-1-HA51$^{polh}$ was digested with *KpnI* and *XmaI* for 1 hour at 37ºC before the analysis. M: 2 Log ladder; lane 1: pBACsurf-1-*polh* surface display plasmid, lane 2: pBACsurf-1-HA51$^{polh}$, lane 3: pBACsurf-1- HA51$^{polh}$ digested with *KpnI* and *XmaI.*

### 4.1.2 Generation of surface display recombinant baculoviruses

Following HA51 transfer vector construction, surface display recombinant baculoviruses were generated using three different parental viruses: BacPAK6, BacPAK6$^{HT}$ and FBU (section 2.2.3). After the generation of the first P0 virus seed stocks, 50 ml of P1 virus stocks was produced in Sf9 cells and titrated by plaque assay (Methods 2.2.2 and 2.2.4a, respectively) as summarised in Table 4.1.

**Table 4.1: Summary of HA51 surface display viruses**

| Surface display transfer plasmid with promoter | Virus genome | Gene deletion/modification in the virus genome | Surface display virus name |
|---|---|---|---|
| pBACsurf-1-HA51$^{polh}$ | BacPAK6 | Wild-type | AcSurfHA51$^{polh}$ |
| pBACsurf-1-HA51$^{polh}$ | BacPAK6$^{HT}$ | *fp25* | HTSurfHA51$^{polh}$ |
| pBACsurf-1-HA51$^{polh}$ | FBU | *p10*, *p26*, *p74*, *chiA*, *v-cath* | FBUSurfHA51$^{polh}$ |

## 4.2 Examination of HA51–GP64$^{TRUN}$ chimeric protein synthesis in Tni Hi5 and Sf9 cells infected with surface display viruses

Protein synthesis was analysed in recombinant virus-infected insect cell lines. Initially, production of HA51–GP64$^{TRUN}$ chimeric protein was analysed in AcSurfHA51$^{polh}$, HTSurfHA51$^{polh}$ or FBUSurfHA51$^{polh}$ infected Tni Hi5 cells. Negative controls included mock- and AcMNPV-infected cells and the positive control was AcRP19-HA$^{polh}$, which expresses the full-length HA under control of the *polh* promoter (Matsuura *et al.*, 1987; kindly provided by R. D Possee, OET Ltd). Cells were infected at an MOI of 5 pfu/cell. After incubation at 28°C for 72 hours, cells were harvested using low-speed centrifugation and cell pellets were prepared for SDS-PAGE (Methods 2.5.2). The culture medium was retained and stored at 4ºC for BV display analysis (Methods 2.2.2). Proteins in the crude cell lysates were separated in a 10% SDS-PAGE gel and immunoblotted using monoclonal antibody raised against HA protein (Methods 2.5.2 and 2.5.2b; Figure 4.2 A).

The cell lysates showed two specific bands, the lowest band at the expected molecular mass of the HA51-GP64$^{TRUN}$ chimeric protein of approximately 64 kDa, in addition to another band at ~70 kDa (Figure 4.2 A). The 70 kDa band could correspond to a glycosylated form of the HA51-GP64$^{TRUN}$ chimeric protein. Further investigation is required to identify the nature of the 70 kDa protein band. Based on band intensity, FBUSurfHA51$^{polh}$-infected cells gave the highest expression levels of the chimeric protein, followed by AcSurfHA51$^{polh}$ with very low levels observed with the HTSurfHA51$^{polh}$ virus (Figure 4.2 A). Overall, the 64 kDa band intensity was stronger than the 70 kDa in all surface display virus-infected cell lysate samples. In the positive control, the AcRP19-HA$^{polh}$-infected cell lysate showed one band only at approximately 70 kDa. As expected, no expression of HA was detected in either the AcMNPV- or mock-infected Tni Hi5 cells (Figure 4.2 A).

HA51-GP64$^{TRUN}$ chimeric protein synthesis was also examined in Sf9 cells, in order to compare with the expression in Tni Hi5 cells. The results of this analysis showed the same expression pattern as in Tni Hi5 infected cells, where two specific bands of 64 and 70 kDa were observed (Figure 4.2 B). However, the relative amounts of the two bands were the opposite of what was observed in the Tni Hi5 cells (Figure 4.2 A), with more of the 70 kDa protein. Based on band intensity, FBUSurfHA51$^{polh}$-infected Sf9 cells gave the highest chimeric protein expression level, followed by AcSurfHA51$^{polh}$ (Figure 4.2 B). Although the expression levels with the HTSurfHA51$^{polh}$ virus was the lowest, it was still much higher than that observed for this virus in Tni Hi5 (Figure 4.2 A). Comparisons have to be cautious, however, because the samples were analysed on separate gels. In the control AcRP19-HA$^{polh}$-infected cells, only one band at 70 kDa was observed. As expected, no expression was detected in either AcMNPV- or mock-infected Sf9 cells (Figure 4.2 A, B).

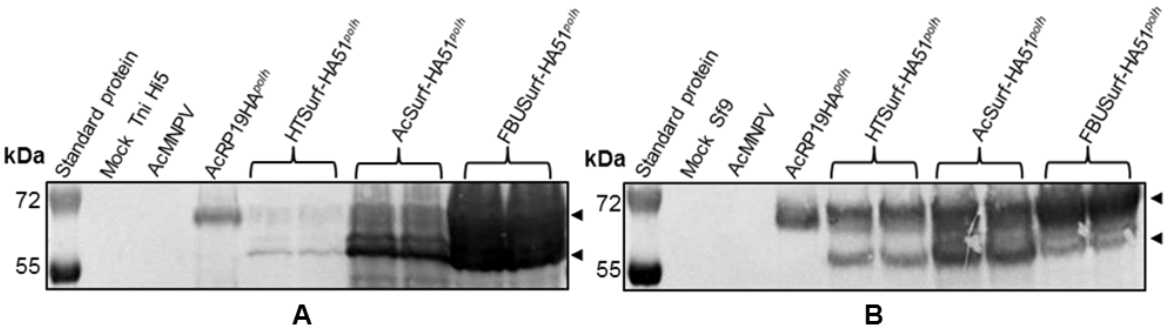


**Figure 4.2: Characterization of HA51-GP64TRUN chimeric protein synthesis in Tni Hi5 (A) or Sf9 (B) cells.**
Tni Hi5 or Sf9 cells were seeded in 35 mm dishes at a density of 0.5x10$^6$ or 1x10$^6$cells/dish, respectively, and infected with the corresponding recombinant surface display or control viruses. Negative controls were mock- and AcMNPV-infected cells and the positive control was AcRP19-HA$^{polh}$-infected cells. Cell pellets were harvested at 72 hpi and cell lysates were separated by an SDS-PAGE gel (10%) and analysed by immunoblotting. The blot was developed using primary full-length anti-mouse HA antibody (1:1000) and secondary anti-mouse alkaline phosphatase conjugated antibody (1:25,000). The blot also includes standard protein markers: Precision plus protein Western C standard (Bio-Rad). Arrowheads indicated 70 kDa and 64 kDa proteins.

## 4.3 Characterisation of the biological activity of the HA51-GP64$^{TRUN}$ chimeric protein

### 4.3.1 Haemagglutination assay

The HA surface glycoprotein of influenza virus can mediate haemagglutination of red blood cells (RBCs). Therefore, in order to examine the biological activity of the HA51-GP64$^{TRUN}$ chimeric protein, a haemagglutination assay was performed. Monolayer cultures of Tni Hi5 cells at a density of 0.5x10$^6$ cells/35 mm tissue culture dish were infected with HTSurfHA51$^{polh}$, AcSurfHA51$^{polh}$ or FBUSurfHA51$^{polh}$ at an MOI of 5 pfu/cell and incubated at 28°C for 48 h. The assay also included mock- and AcMNPV-infected cells as negative controls and AcRP19-HA$^{polh}$-infected cells as a positive control. Haemagglutination activity was analysed using intact (non-sonicated) or sonicated cells in addition to purified BV from the same recombinant surface display virus. Cells were harvested at 48 hpi and pelleted by low-speed centrifugation. BV samples were prepared for this assay as previously described (Methods 2.8.2). Samples (50 µl) from either cell pellets (sonicated or intact) or BV were added to the wells of a 96-well microtitre plate and two-fold serial dilutions were prepared across the plate and RBCs added as described (Methods 2.8.2).

Both intact and sonicated cell pellets of Tni Hi5 cells infected with each surface display virus, or positive control virus, showed evidence of haemagglutination activity as indicated by a lattice formation (Table 4.2). As expected, there was no haemagglutination activity in mock- or AcMNPV-infected cells (Table 4.2). Samples from the sonicated positive control AcRP19-HA$^{polh}$- infected cells showed the highest relative haemagglutination activity unit

(HAU) at a 1:256 dilution (Table 4.2); therefore, the haemagglutination titre of this virus was recorded as 256 HAU/50µl. Sonicated FBUSurfHA51$^{polh}$-infected Tni Hi5 cells showed the highest relative titre of HAU of the surface display viruses at 128 HAU/50µl, followed by AcSurfHA51$^{polh}$ with 64 HAU/50µl and HTSurfHA$^{polh}$ with 8 HAU/50µl (Table 4.2). This result was consistent with the results observed in immunoblotting assays (section 4.2.1).

It was noted that the HA titre in the non-sonicated infected cells was significantly lower than in the sonicated infected cells (Table 4.2). For example, the positive control AcRP19-HA$^{polh}$ showed the highest titre of 64 HAU/50µl, compared to 256 in sonicated cells. No haemagglutination activity was observed in either mock- or AcMNPV-infected cells as expected (Table 4.2). The BV samples obtained from the culture medium also showed clear evidence of haemagglutination activity that indicated HA51-GP64$^{TRUN}$ on the BV envelope was also able to agglutinate RBCs (Table 4.3). HA51-GP64$^{TRUN}$ displayed on FBUSurfHA51$^{polh}$ BV had the highest titre of 64 HAU/50µl compared to AcSurfHA51$^{polh}$ and HTSurfHA51$^{polh}$ with titres of 32 HAU/50µl and 16 HAU/50µl, respectively. AcRP19-HA$^{polh}$-BV showed the highest titre of 128 HAU/50µl, whereas no HA activity was detected the mock- or AcMNPV-infected cells (Table 4.3); the RBCs settled to form a sharp red dot at the centre of the well, which indicated the absence of agglutination activity in these samples.

**Table 4.2: Haemagglutination activity of recombinant virus-infected Tni Hi5 cells**

| Virus-infected cells | Intact cells HAU/50 µl | Sonicated cells HAU/50 µl |
|---|---|---|
| Mock | 0 | 0 |
| AcMNPV | 0 | 0 |
| AcRP19-HA$^{polh}$ | 64 | 256 |
| FBUSurfHA51$^{polh}$ | 32 | 128 |
| AcSurfHA51$^{polh}$ | 16 | 64 |
| HTSurfHA51$^{polh}$ | 4 | 8 |

**Table 4.3: Haemagglutination activity of the surface display BV**

| BV sample | HAU/50 µl |
|---|---|
| Mock | 0 |
| AcMNPV | 0 |
| AcRP19-HA$^{polh}$ | 128 |
| FBUSurfHA51$^{polh}$ | 64 |
| AcSurfHA51$^{polh}$ | 32 |
| HTSurfHA51$^{polh}$ | 16 |

### 4.3.2 Haemadsorption assay

Sf9 cells infected with HA51-GP64$^{TRUN}$ surface display recombinant viruses have shown the ability to express the chimeric protein on the BV surface. If the chimeric protein is biologically active, it will be able to adsorb RBCs on its surface due to HA activity. In order to examine this activity, virus-infected Sf9 cells were analysed using a haemadsorption assay. This assay was conducted by infecting monolayer cultures of Sf9 cells ($1x10^6$ cells/35mm dish) with AcSurfHA51$^{polh}$, HTSurfHA51$^{polh}$ or FBUSurfHA51$^{polh}$ at an MOI of 5pfu/cell. Negative

controls used in this experiment were mock- and AcMNPV-infected cells with AcRP19-HA$^{polh}$-infected Sf9 cells as a positive control. Virus-infected cells were incubated at 28°C for 48 hpi, and then washed twice with PBS before 0.5 ml of 0.5% freshly prepared chicken RBCs were added into each dish and incubated for 30 min. Subsequently, the cells were washed twice with PBS and examined under the light microscope. All the cells infected with AcRP19.HA$^{polh}$, FBUSurfHA51$^{polh}$, AcSurfHA51$^{polh}$ or HTSurfHA51$^{polh}$ showed clear evidence for RBCs haemadsoption on the cell surface (Figure 4.3). This result provided further evidence that the HA51 expressed as a fusion protein with a GP64 signal peptide and TMD is biologically active.

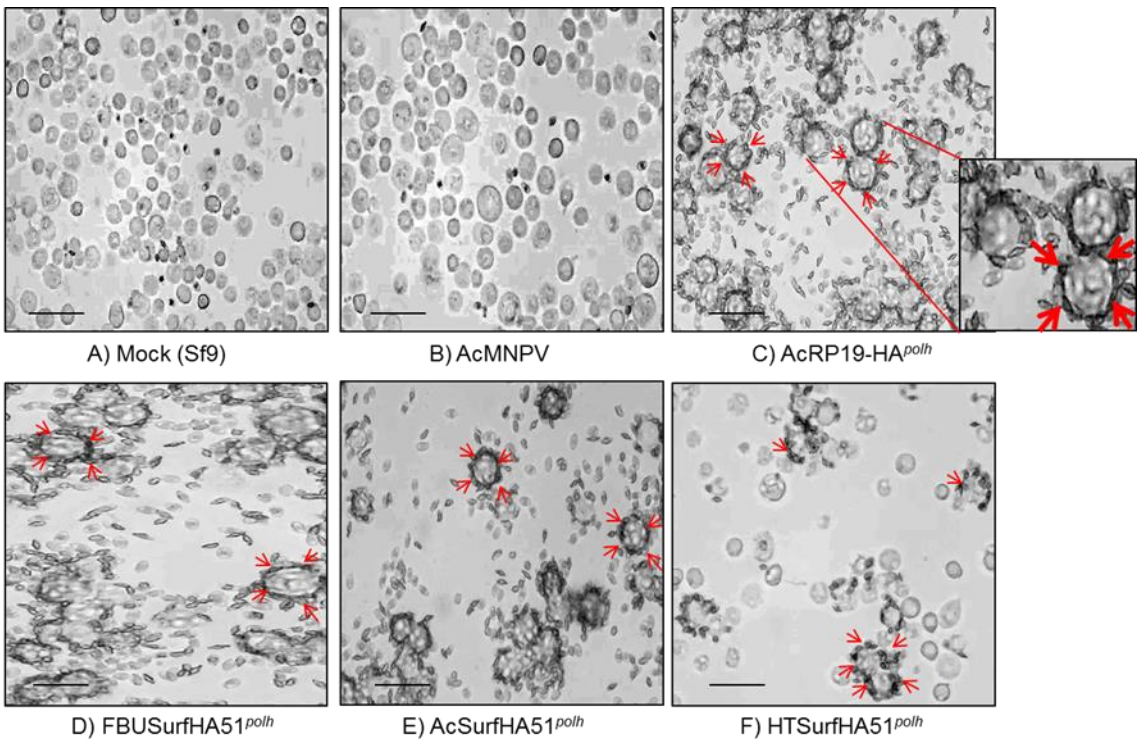


**Figure 4.3: Haemadsorption assays of HA51-GP64TRUN-surface display viruses infected Sf9 cells.**
Sf9 cells were dispensed in 35 mm tissue culture dishes at a density of 1x10$^6$ cell/dish and infected with corresponding recombinant surface display viruses. Negative controls were mock- and AcMNPV-infected Sf9 cells and the positive control was AcRP19-HA$^{polh}$-infected cells. The cells were examined using a light microscope Zeiss Axiovert 135 at 48 hpi to show RBCs haemadsorption (100X). Scale bar is 20 µm. Surface display and positive control infected Sf9 cells show haemadsorption activity on the surface indicated with red arrows.

There was no haemadsoption activity observed on the surface of mock-infected cells and cells infected with AcMNPV, as expected. The highest haemadsoption activity was observed on the cell surface infected with the full-length HA recombinant virus, providing further evidence that native HA had greater activity than the chimeric HA-GP64 protein from surface display viruses (Figure 4.3).

## 4.4 Confirmation of the translocation of the HA51-GP64$^{TRUN}$ to the Sf9 cell surface by immunofluorescence assay and confocal microscopy

In order to investigate whether the HA51-GP64$^{TRUN}$ chimeric protein was properly translocated to the plasma membrane, Sf9 cells were seeded on sterile coverslips in 6-well plates and prepared for immunofluorescence assay and confocal microscopy (Methods 2.6.1a). Subsequently, the Sf9 cells were infected with AcSurfHA51$^{polh}$, HTSurfHA51$^{polh}$ or FBUSurfHA51$^{polh}$ at an MOI of 5pfu/cell. The negative controls used in this experiment were mock- and AcMNPV-infected cells with AcRP19-HA$^{polh}$ as a positive control. After 48 hpi, infected or control cells were fixed, stained using an HA primary antibody and Alexa-fluor 488® secondary antibody (Methods 2.6.1a, 2.6.1b) and subjected to immunofluorescence imaging using a Zeiss LSM 510 meta laser scanning microscope. As shown in Figure 4.4, the HA51-GP64$^{TRUN}$ chimeric protein was clearly detected on the surface of Sf9 cells infected with all HA51 surface display viruses. No HA51-GP64$^{TRUN}$ was detected in mock- or AcMNPV-infected cells, as expected. Full-length HA was detected in AcRP19-HA$^{polh}$-infected cells (Figure 4.4). These results confirmed that both native HA and HA51-GP64$^{TRUN}$ chimeric protein were able to localise within the plasma membrane of Sf9 cells, demonstrating that HA proteins were successfully anchored on the surface of the infected cells. In addition, these results provide an explanation for their corporation into BV, as they bud out through the outer cell membrane.

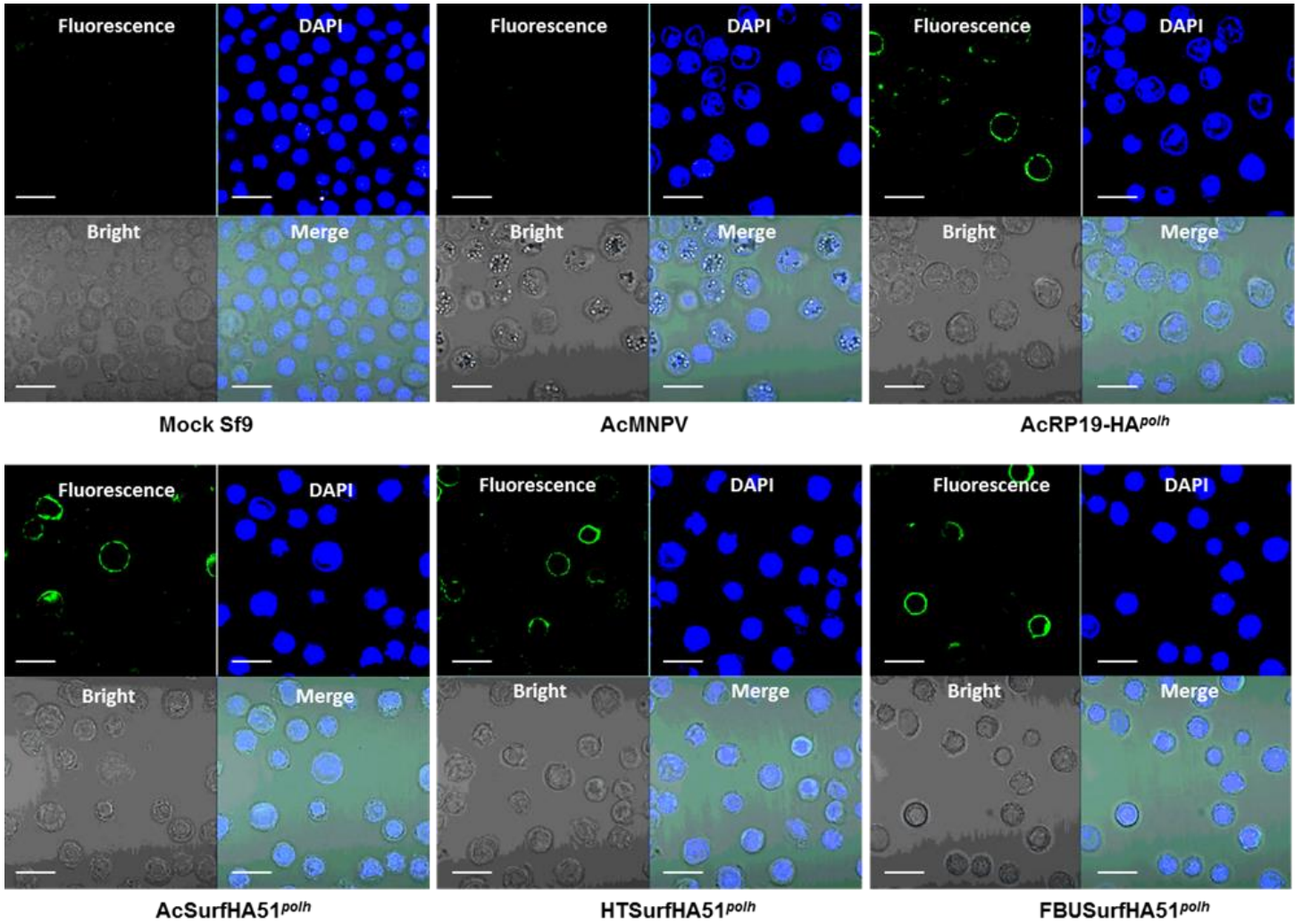


**Figure 4.4: Characterization of HA51-GP64TRUN surface display viruses in Sf9 cells by confocal microscopy.**
Sf9 infected with AcSurfHA51$^{polh}$, HTSurfHA51$^{polh}$ or FBUSurfHA51$^{polh}$ to observe HA51-GP64$^{TRUN}$ (green). Negative controls were mock- and AcMNPV-infected Sf9 cells and the positive control was AcRP19-HA$^{polh}$-infected cells. Infected cells were fixed at 48 hpi and stained by indirect immunofluorescence using an anti-HA antibody. A secondary antibody conjugated to an Alexa-fluor 488 was used to visualise the HA51-GP64$^{TRUN}$ translocated into infected cells plasma membrane using a confocal microscope (488 wavelength). No HA signal was detected in mock- and AcMNPV-infected cells. Scale bar 20µm.

## 4.5 Examination of HA51-GP64$^{TRUN}$ displayed on the BV envelope in recombinant virus-infected insect cells

### 4.5.1 Analysis of HA51-GP64$^{TRUN}$ displayed on the BV envelope in recombinant virus-infected Tni Hi5 cells

In order to investigate the incorporation of HA51-GP64$^{TRUN}$ chimeric protein into the surface of the BV envelope of recombinant viruses generated in 4.1.2 (Table 4.1), the BV particles from the stored culture medium (4.2.1) were pelleted at 15000 rpm at 4ºC for 40 minutes using an Eppendorf table-top centrifuge. Budded virus pellets were resuspended in distilled water and SDS-lysis buffer, and an equal amount of BV lysates was then separated using a 10% SDS-PAGE gel followed by immunoblotting. The blot was probed with specific antibodies raised against AcMNPV VP39, GP64, and the HA protein (Methods 2.5.2 and 2.5.2b). The results of this analysis indicated the positions of VP39 and GP64 (Figure 4.5) and demonstrated that there were approximately equivalent amounts of both proteins in AcSurfHA51$^{polh}$ or FBUSurfHA51$^{polh}$ BV samples at the expected sizes of 39 kDa and 64 kDa, respectively. However, greater quantities of both proteins were observed in the HTSurfHA51$^{polh}$ BV samples. This result was consistent with the increased production of BV per unit volume in Tni Hi5 cells infected with viruses harbouring a defective *fp*-25 (Harrison *et al*., 1995). This was confirmed by analysis of BV infectivity by plaque assay, which gave virus titres of 9 x $10^6$ pfu/ml for HTSurfHA51$^{polh}$, 3x$10^5$ pfu/ml for AcSurfHA51$^{polh}$ and 6 x$10^5$ pfu/ml for FBUSurfHA51$^{polh}$, which indicated that there was between 15-30-fold more BV per unit volume in the HT virus. Figure 4.5 shows two specific bands of approximately 64 kDa corresponding to HA51-GP64$^{TRUN}$ chimeric protein incorporated into the BV envelope in addition to another band at approximately 70 kDa, as previously described.

The amounts of HA51-GP64$^{TRUN}$ incorporated into the BV were variable; there was none evident in mock or AcMNPV BV samples as expected. The positive control AcRP19-HA$^{polh}$ BV sample showed one band only at approximately 70 kDa (Figure 4.5), suggesting that native HA was incorporated into the BV envelope. The results showed that FBUSurfHA51$^{polh}$ produced BV with the highest levels of HA51-GP64$^{TRUN}$ chimeric protein, followed by AcSurfHA51$^{polh}$, very little chimeric protein was observed within the HTSurfHA51$^{polh}$ BV envelope (Figure 4.5). This was surprising as FBUSurfHA51$^{polh}$ contained less BV than HTSurfHA51$^{polh}$ (Figure 4.5). However, HTSurfHA51$^{polh}$ contains a mutation within *fp-25*, which severely curtails expression from the *polh* promoter (reviewed by Shufen *et al*., 2015). It is also noteworthy that the full-length HA incorporated into BV envelope of AcRP19-HA$^{polh}$ was better than surface display viruses based on band intensity, which was significantly higher (Figure 4.5). It is unclear why HTSurfHA51$^{polh}$ and AcSurfHA51$^{polh}$ displayed different quantities of HA51-GP64$^{TRUN}$ chimeric protein on the envelope of BV. Nevertheless, BV

from HTSurfHA51$^{polh}$ might be expected to contain less chimeric protein as it has a mutation within *fp*-25, which limits *polh* promoter activity.

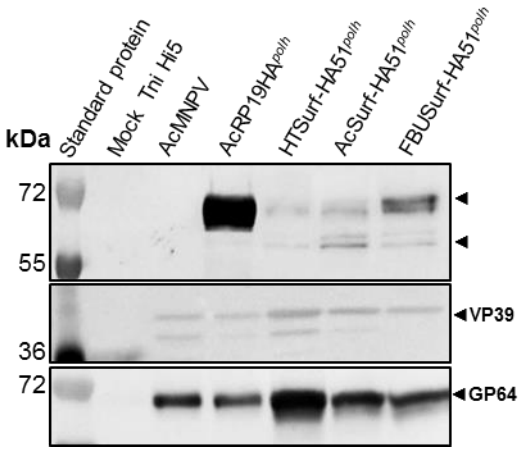


**Figure 4.5: Characterization of HA51-GP64TRUN incorporated into budded virus produced in Tni Hi5 cells.**
Tni Hi5 cells were seeded in 35 mm tissue culture dishes at a density of 0.5x10$^6$ cells/dish and infected with the corresponding recombinant surface display or control viruses. Negative controls were mock- and AcMNPV-infected Tni Hi5 cells and the positive control was AcRP19-HA$^{polh}$-infected cells. Culture medium was harvested at 72 hpi and the BV fractions were separated by SDS-PAGE gel (10%) and analysed by immunoblotting. The blot was developed using primary full-length anti-mouse HA antibody (1:1000), GP64 antibody (1:1000), VP39 antibody (1:5000) and secondary anti-mouse alkaline phosphatase conjugated antibody (1:25,000). The blot also includes standard protein markers: Precision plus protein Western C standard (Bio-Rad). Arrowheads indicated 70 kDa and 64 kDa bands.

### 4.5.2 Analysis of HA51-GP64$^{TRUN}$ displayed on the envelope of budded virus produced in Sf9 cells

The incorporation of HA51-GP64$^{TRUN}$ chimeric protein into BV envelope of recombinant surface display viruses produced in Sf9 cells was also examined (Figure 4.6). Analysis of BV recovery after centrifugation revealed that all virus samples contained approximately equivalent quantities of VP39 and GP64 (Figure 4.6). There was no HA protein evident in mock or AcMNPV BV samples as expected. The positive control AcRP19-HA$^{polh}$ BV sample showed one band only at ~ 70 kDa (Figure 4.6) and it is also confirmed that native HA was incorporated into the BV envelope of AcRP19-HA$^{polh}$ as in BV from Tni Hi5 (Figure 4.5). However, analysis of HA51-GP64$^{TRUN}$ incorporation into the BV envelope of recombinant surface display viruses showed that FBUSurfHA51$^{polh}$ and AcSurfHA51$^{polh}$ contained higher levels compared to the small amount of HA51-GP64$^{TRUN}$ chimeric protein that was incorporated into the HTSurfHA51$^{polh}$ BV envelope. This result was similar to that observed when these viruses were produced in Tni Hi5 cells (Figure 4.5). It was also noted that the HA51-GP64$^{TRUN}$ chimeric protein in BV from Sf9 cells appeared to be in one form as indicated by one band at 70 kDa (Figure 4.6), further suggesting that the likely glycosylated

form of HA5-GP64$^{TRUN}$ is important for membrane targeting. Overall, these results demonstrated that the HA TM compared to *gp64* TM, resulted in significant HA incorporation into baculovirus BV envelope (Figure 4.5, 4.6).

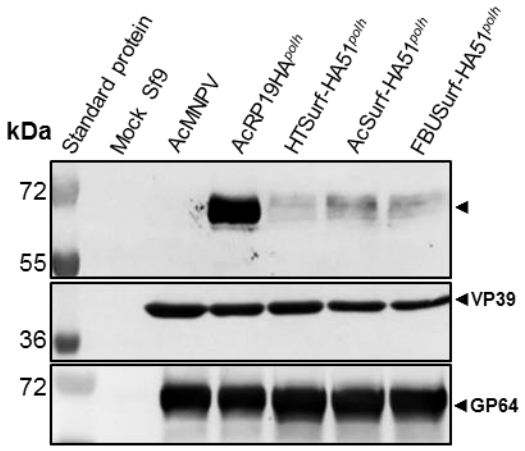


**Figure 4.6: Characterization of HA51-GP64$^{TRUN}$ incorporated into budded virus produced in Sf9 cells.**
Sf9 cells were seeded in 35 mm tissue culture dishes at a density of 1x10$^6$ cells/dish and infected with the corresponding recombinant surface display or control viruses. Negative controls were mock- and AcMNPV-infected Sf9 cells and the positive control was AcRP19-HA$^{polh}$-infected cells. Culture media were harvested at 72 hpi and the BV fractions were separated by SDS-PAGE gel (10%) and analysed by immunoblotting. The blot was developed using primary full-length anti-mouse HA antibody (1:1000), GP64 antibody (1:1000), VP39 antibody (1:5000) and secondary anti-mouse alkaline phosphatase conjugated antibody (1:25,000). The blot also includes standard protein markers: Precision plus protein Western C standard (Bio-Rad).

## 4.6 Analysis of the post-translational modification of HA51-GP64$^{TRUN}$ surface display protein

It was rationalised that the doublet band (64 and 70 kDa) observed in Figures 4.2 A, B and 4.5 could result from HA51-GP64$^{TRUN}$ glycosylation or might be due to non-specific binding. To investigate the glycosylation possibility, an online prediction programme (NetNGlyc 1.0 Server) was used to examine for any potential glycosylation sites on the HA51-GP64$^{TRUN}$ chimeric protein. Five glycosylation sites were predicted, which are mainly present on the HA51 carboxyl-terminal. To examine whether the doublet bands observed were due to glycosylation of the HA51-GP64$^{TRUN}$ chimeric protein, FBUSurfHA51$^{polh}$ BV particles were treated with either PNGase F or Endo H glycosidase. PNGase F enzyme cleaves and removes all types of N-linked (Asn linked) glycosylation such as high mannose, hybrid, bi, tri, and tetra-antennary, whereas Endo H cleaves and removes high mannose and some hybrid types of N-linked carbohydrates (reviewed by Aksular, 2017).

For the initial investigation, BV from FBUSurfHA51$^{polh}$–infected Tni Hi5 cells culture medium was analysed (in duplicate) for each enzyme reaction. One sample was mixed with distilled

water as a negative control, while the other sample was mixed with either PNGase F or Endo H (Methods 2.5.4). Following enzyme treatment, all samples were separated using a 10% SDS-PAGE gel followed by immunoblotting using HA or GP64 specific antibodies. Jarvis *et al.* (1998) demonstrated that baculovirus native GP64 glycoprotein has N-linked sugar residues, and therefore, it was included as a positive control for the enzyme activity and de-glycosylation tests.

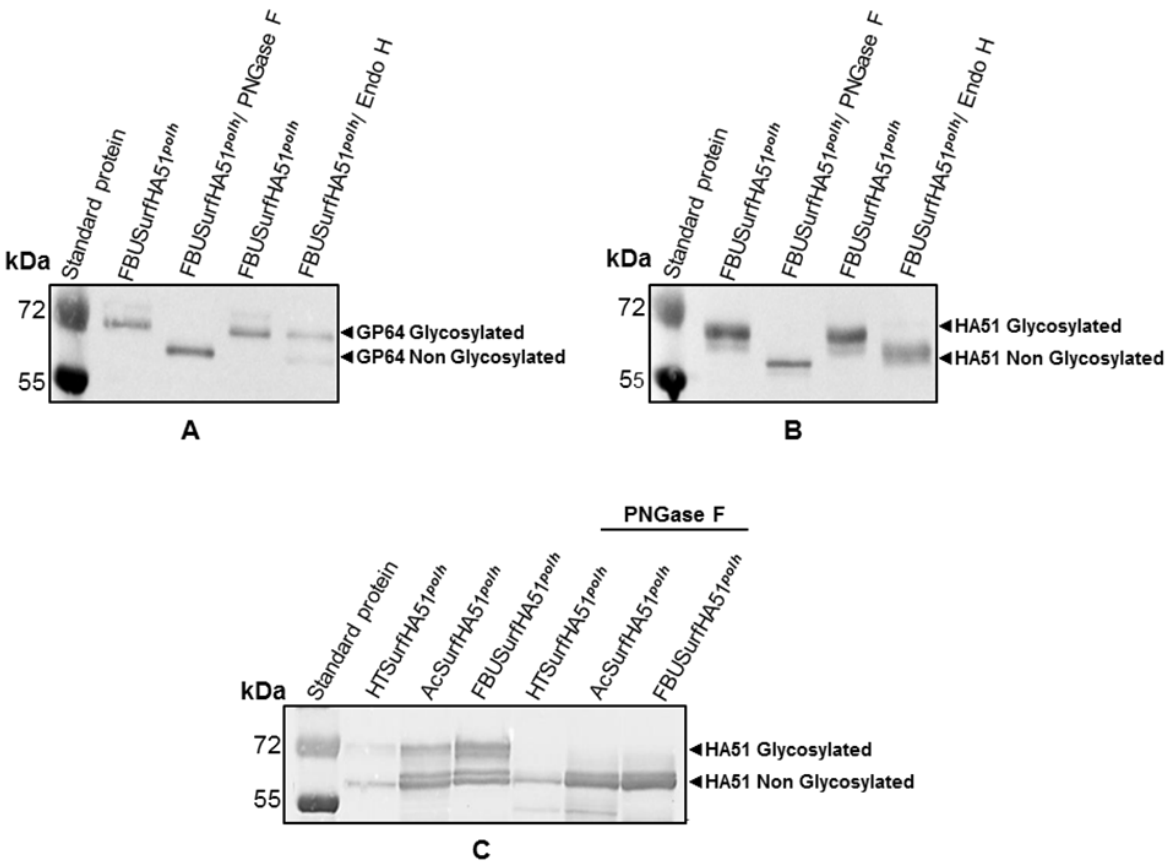


**Figure 4.7: Glycosylation analysis of HA51-GP64$^{TRUN}$ incorporated into a budded virus and in Tni Hi5 cell lysates.**
**(A, B):** BV fraction from FBUSurfHA51$^{polh}$-infected Tni Hi5 cells culture medium. **C:** crude cell lysate of surface display viruses infected cells. Following enzymes treatment, samples were separated by SDS-PAGE gel (10%) and analysed by immunoblotting. The blot was developed using primary anti-mouse GP64 antibody (1:1000) (A) or full-length HA antibody (1:1000) (B and C) and secondary anti-mouse alkaline phosphatase conjugated antibody. The blot also includes standard protein markers: Precision plus protein Western C standard (Bio-Rad).

The results in Figure 4.7 A and B showed very clear evidence of glycosylation, as there was a detectable difference in band size between the enzymes treated and control samples. Only one 64 kDa band was detected in the enzyme-treatment samples, which is the predicted size of the non-glycosylated HA51-GP64$^{TRUN}$ chimeric protein; the 70 kDa band disappeared. Using the same protocol as described above, the analysis was extended to crude cell lysates of HTSurfHA51$^{polh}$-, AcSurfHA51$^{polh}$- and FBUSurfHA51$^{polh}$-infected Tni Hi5 cells (Figure 4.7 C).

The results were consistent with FBUSurfHA51$^{polh}$ BV sample results (Figure 4.7 B), confirming that the 70 kDa protein is most likely an N-linked glycosylated form of the 64 kDa protein. The findings in Figure 4.7 A-C also confirmed that the difference in band size was a consequence of N-linked glycan residues, as indicated in blot A when GP64 treated with PNGase F showed one band only at 64 kDa while the Endo H treated sample showed two bands at 64 kDa and 70 kDa (Figure 4.7 A). The results confirmed the successful removal of carbohydrates as well as enzyme activity.

## 4.7 Analysis of AcSurfHA51$^{polh}$ vs AcRP19HA$^{polh}$ in Tni Hi5 cells during time course infection

In order to select the best recombinant virus that can be exploited as antigen candidate for influenza vaccine, it was decided to make a comparison between truncated HA51$^{TRUN}$ chimeric protein and the full-length HA incorporation into the BV envelopes of AcSurfHA51$^{polh}$ and AcRP19HA$^{polh}$, respectively during time course infection. Briefly, Tni Hi5 cells were prepared as described previously (Section 5.5), infected with AcSurfHA51$^{polh}$ and AcRP19HA$^{polh}$ viruses at an MOI of 5 pfu/cell and the HA incorporation into BV envelopes were monitored during the time course of infection (24-96 hpi). The BV particles were harvested from each time course and analysed by SDS-PAGE 10 % gel and western immunoblot. The result in Figure 5.8 A showed that HA51$^{TRUN}$ chimeric protein displayed on the BV envelope of AcSurfHA51$^{polh}$ virus starts from 48 hpi, during this time of infection three bands were observed on the blot at different molecular mass presenting chimeric protein at different glycosylation stage. The lowest band was observed at a molecular mass of a proximately 64 kDa representing the non-glycosylated form of HA51$^{TRUN}$ chimeric protein incorporated into BV envelope (Figure 5.8 A). While the other two bands were observed at a very close molecular mass of about 68-70 kDa, belong to a glycosylated form of HA51$^{TRUN}$ chimeric protein (Figure 5.8 A). Between 72 and 96 hpi, the glycosylated form seems to be targeted for degradation resulting in one band at a molecular mass of approximately 64 kDa. However, non-glycosylated chimeric protein incorporated into the BV was found to increase during this time of infection, as suggested by the intensity, and the maximum was at 96 hpi (Figure 5.8 A).

On the other hand, full-length HA on BV envelope AcRP19HA$^{polh}$ showed an opposite pattern of HA51$^{TRUN}$ chimeric protein incorporation at 48 hpi (Figure 5.8 B, A), respectively, where the glycosylated form incorporation was greater than non-glycosylated form (Figure 5.8 B). It is noteworthy, however, after 48 hpi the non-glycosylated form decreased due to degradation and remains constant until 96 hpi (Figure 5.8 B). In contrast, the amount of glycosylated form was found to increase within the time and reached the maximum level at 96 hpi (Figure 5.8 B). Furthermore, these results clearly demonstrated that glycosylation of

the HA protein occurs when it is overexpressed by AcRP19HA$^{polh}$ making it a promising candidate for the production of immunologically reactive HA.

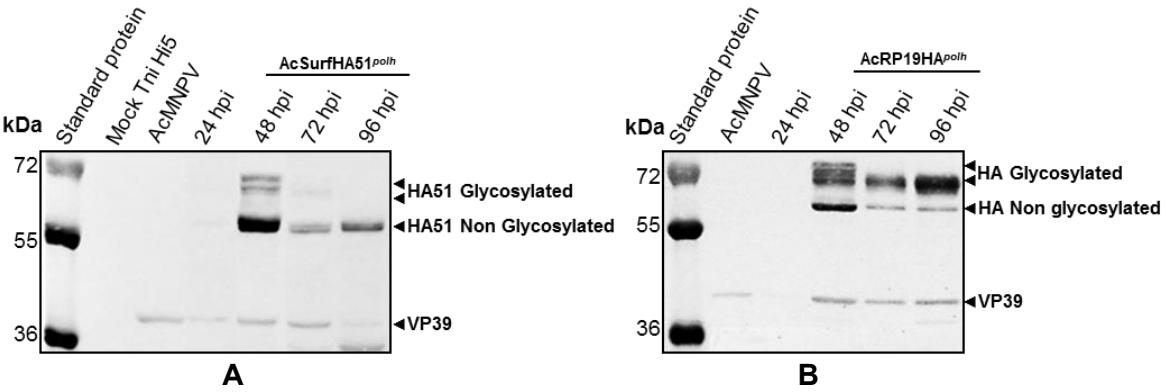


**Figure 4.8: Comparing the HA incorporation into AcSurfHA51$^{polh}$ (A) or AcRP19HA$^{polh}$ (B) BV envelopes during Tni Hi5 time course infection.**
Tni Hi5 cells were seeded in 35 mm tissue culture dishes at a density of 0.5x10$^6$ cells/dish and infected with the corresponding recombinant viruses, negative controls were mock- and AcMNPV-infected cells. Culture media were harvested at different time post infection (24-96 hpi) and the BV fractions were separated by SDS-PAGE gel (10%) and analysed by immunoblotting. The blot was developed using primary full-length anti-mouse HA antibody (1:1000), VP39 antibody (1:5000) and secondary anti-mouse alkaline phosphatase conjugated antibody (1:25000). The blot also includes standard protein markers: Precision plus protein Western C standard (Bio-Rad).

## 4.8 Discussion

Baculovirus GP64 signal peptide and TMD has been successfully used for protein surface display in several studies (Boublik *et al.*, 1995; Elliott, 2012; Aksular, 2017). Therefore, the main aim of the experimental work presented in this chapter was to develop a BEVS-based display vector that would efficiently display a truncated HA chimeric protein (HA51) on the BV envelope surface. This was achieved through a modified commercially available baculovirus surface display transfer vector, pBACsurf-1 (Novagen), in which GP64 sequence was truncated to leave only signal peptide and TMD. Gene expression in this vector was driven by the very late *polh* promoter. After the construction of this surface display transfer vector, three recombinant baculoviruses were successfully generated using BacPAK6, BacPAK$^{HT}$ or FBU as the AcMNPV parental virus genome; PCR screening confirmed the integrity of these constructs (Table 4.1).

AcSurfHA51$^{polh}$, HTSurfHA51$^{polh}$ and FBUSurfHA51$^{polh}$ surface display recombinant baculoviruses were characterised in Tni Hi5 and Sf9 insect cell lines to examine HA51-GP64$^{TRUN}$ chimeric protein synthesis in crude cell lysates and display in BV particles. The results demonstrated that HA51-GP64$^{TRUN}$ was synthesised and expressed in Sf9 and Tni Hi5 lysates using western immunoblotting. However, the protein yield was markedly different between the cell lines. HA51-GP64$^{TRUN}$ expressed in Tni Hi5 crude cell lysate was higher than in Sf9 cells (Figure 4.2 A, B). Even though the distinct reasons behind the difference in *polh* promoter-mediated gene expression activities and protein expression

profiles between these two cell lines are not well understood, it is probable that this is due to the fact that these two cell lines derived from different insect species. Therefore, the promoter activity and pathway process of recombinant protein production in these two cell lines are most likely different.

These findings are consistent with another study suggesting that the yield of recombinant proteins produced in Tni Hi5 is significantly higher than Sf9 (Aksular, 2017). Further, a study to develop an H5N1 HA VLP-based vaccine has confirmed the hyperexpression of HA protein in Tni Hi5 cells (Krammer *et al.*, 2010). They suggested that Tni Hi5 cell could be a good choice for the recombinant protein production, especially for vaccines, in terms of production cost as these cells can be easily maintained in serum-free medium (Krammer *et al.*, 2010). Another study by Elliott (2012) conducted a similar experiment where they compared the expression level of HAFLAG chimeric protein in two different insect cell lines. They found out that protein yields were significantly higher from infected Tni Hi5 cells (Elliott, 2012).

Samples obtained from the cell lysates of virus-infected cells consistently showed double bands on the western immunoblot. The first band was about 64 kDa, which was around the expected molecular mass of HA51-GP64$^{TRUN}$ chimeric protein and the second one was about 70 kDa. The two bands observed on the immunoblot in this experiment raised the question of whether it was due to post-translational protein modification or nonspecific antibody binding, which were investigated further in this chapter. It was shown that HA51-GP64$^{TRUN}$ was best expressed in FBUSurfHA51$^{polh}$-infected cells, both Sf9 and Tni Hi5, with lower levels obtained in AcSurfHA51$^{polh}$-infected cells as judged by immunoblotting. In comparison, very little expression was detected in the HTSurfHA51$^{polh}$-infected Tni Hi5 cells, however, HTSurfHA51$^{polh}$-infected Sf9 cells lysates showed better chimeric protein expression than Tni Hi5 cells.

It was reported that *fp-25* mutation can cause a significant reduction in *polh* transcription in Tni Hi5 and Sf9 cells, however, the reasons for this are still unknown (Cheng *et al.*, 2013). Previous studies demonstrated that *polh* mRNA stability remains the same when Sf9 cells infected with either wild-type or AcMNPV *fp-25* mutant, however, the rate of *polh* transcription significantly reduced in *fp-25* mutants infected cells. It is most likely that this difference could be due to low *polh* promoter activities of *fp25k* mutants compared to the wild-type AcMNPV (Jarvis *et al.*, 1992; Harrison and Summers, 1995).

The study by Cheng *et al.* (2013) suggested two possibilities for the difference in *polh* activities that can be observed in two different insect cell lines. The first possibility was this difference could be a result of viral or cellular factors that can control baculovirus *polh* promoter activities directly or indirectly. They suggested that the presence of these factors

in some insect cells might replace FP-25, which results in enhancing the activities of *the polh* promoter. In contrast, the absence of these factors from other insect cells will allow FP-25 to inhibit the *polh* promoter activities (Cheng *et al.*, 2013). The other plausible possibility for the difference in *polh* activities in some Sf21 and Sf9 cells and in the most of Tni Hi5 cells is that, these viral or cellular factors acting as operons that can bind to either *polh* promoter or to one or more LEFs, which result in a reduction in the protein synthesis under the control of *polh* promoter. In the vast majority of Sf21 cells and in some of Tni Hi5 cells, these factors might be present at very low levels or be missing. Therefore, the *polh* promoter activity is not influenced (Cheng *et al.*, 2013).

On the other hand, the superior expression of the HA51-GP64$^{TRUN}$ in FBUSurfHA51$^{polh}$-infected cells was probably due to lack of *p10*, *p74*, *p26*, *chiA* and *v-cath* genes included in the commercially available *flash*BACULTRA$^{TM}$ vector. It has been reported that *p10* promoter deletion or inhibition can result in a remarkable increase in the protein production under the control of the *polh* promoter, in addition to *polh* mRNA levels (Janssen *et al.*, 1988; Chaabihi *et al.*, 1993). Thus, removing *p10* from AcMNPV genome was expected to result in a notable increase in the transcription of the recombinant gene(s) driven by the *polh* promoter. Another study by Hawtin *et al.* (1997) demonstrated that chitinase and cathepsin play an important role in host liquefaction during the late phase of viral infection. However, in cell culture, it has been found that chitinase produced during baculovirus replication as a secretory protein may result in transportation blocking of the recombinant secretory protein(s) through the cell's secretory pathway (Thomas *et al.*, 1998; Possee *et al.*, 1999). While cathepsin results in recombinant protein degradation when released into the culture medium from lysed cells (Gotoh *et al.*, 2001). It has been demonstrated that deletion of both *chiA* and *cath* from the baculovirus genome boosts secreted recombinant proteins production and stability. This may be a result of facilitating the movement of the recombinant proteins via the cell's secretory pathway and the absence of serine protease encoded by the virus in cell culture media (Possee *et al.*, 1999; Kaba *et al.*, 2004). Hitchman *et al.* (2010a) observed that these five genes are non-essential for virus replication in insect cell culture. However, deletion of all these five genes has improved the yield and quality of the recombinant protein (Hitchman *et al.*, 2010a).

Influenza virus HA can agglutinate chicken RBCs and a haemagglutination assay is widely used to show the biological activity of HA and diagnosis of influenza virus infection. A haemagglutination assay was used to confirm the biological activity of the HA constructs produced in Tni Hi5 cells in this chapter. At 48 hpi, either intact or sonicated cells infected with the AcSurfHA51$^{polh}$, HTSurfHA51$^{polh}$ and FBUSurfHA51$^{polh}$ surface display recombinant baculoviruses were examined for the HA activity as it was not certain that HA in intact cells would be accessible for the HA assay. The haemagglutination activity for the pelleted BV

was also examined. Initial assay results indicated that AcSurfHA51$^{polh}$, HTSurfHA51$^{polh}$, and FBUSurfHA51$^{polh}$ are able to express the HA51-GP64$^{TRUN}$ chimeric protein in both sonicated and non-sonicated infected Tni Hi5 cells (Table 4.2). As shown using an HA assay and as compared to full-length HA expressed in the positive control virus, the HA51 chimeric protein expressed as a fusion with GP64 using baculovirus expression systems is functional as assessed by its ability to present influenza A virus haemagglutination activity. Therefore, it is suitable for future experiments in this study. The principle of haemagglutination assay is that the surface display baculoviruses will have HA51-GP64$^{TRUN}$ chimeric protein on its envelope and by infecting the cells with these viruses this protein will be synthesised and transported into the cell surface. The chimeric protein will then display on the BV envelope surface during the virus budding through the cell membrane. This displayed protein will also bind to sialic acid receptors of erythrocytes RBCs causing the formation of a lattice, which typically viewed as a diffuse reddish solution.

Sf9 cells infected with the surface display viruses were examined in this chapter for haemadsorption activity, the results showed the ability of all HA51-GP64$^{TRUN}$-recombinant viruses to induce RBCs haemadsorption on the plasma membrane of infected cells. The level of haemadsorption was significantly higher in Sf9 cells infected with FBUSurfHA51$^{polh}$ followed by AcSurfHA51$^{polh}$ (Figure 4.3 D and E, respectively). In contrast, very low haemadsorption activity was observed in Sf9 infected with HTSurfHA51$^{polh}$ virus (Figure 4.3 F). However, cells infected with the full-length HA positive virus was the best among the cells infected with surface display viruses (Figure 4.3 C). No RBCs were adsorbed on the Sf9 cells infected with wild-type AcMNPV or mock cells as expected. These results were quite similar to the haemagglutination activity observed from the same viruses. These findings suggest that chicken RBCs adsorbed on the surface of the infected cells is due to the HA expression not because of the virus infection. The result also demonstrated that the HA51 had fully functional haemadsorption activity and was successfully synthesised and expressed on the surface of the infected insect cells under the control of the *polh* promoter. This was consistent with previous studies where they found that HA expressed in insect cells infected with HA recombinant virus was biologically active (Cox, 2009; Elliott, 2012; Gadalla *et al.*, 2014). Both haemagglutination and haemadsorption assays confirmed immunoblotting results in relation to the best vectors. In fact that although FBU was the best over the surface display vectors, none of these surface display vectors was better than native HA as determined by immunoblotting, HA or haemadsorption assays.

The translocation of HA51-GP64$^{TRUN}$ chimeric protein into infected Sf9 cell surface membrane was confirmed by confocal microscopy (Figure 4.4). Sf9 cells infected with AcSurfHA51$^{polh}$, HTSurfHA51$^{polh}$, FBUSurfHA51$^{polh}$ or AcRP19-HA$^{polh}$ showed clear evidence of the chimeric protein translocation on its plasma membrane. The result also

indicated that HA51-GP64$^{TRUN}$ chimeric protein from either surface display viruses or full-length HA from AcRP19-HA$^{polh}$ was successfully synthesised, transported and translocated to the plasma membrane of infected Sf9.

To determine the efficient baculovirus system that can maximize the HA51-GP64$^{TRUN}$ chimeric protein display, the BV samples from infected Tni Hi5 and Sf9 cells were examined and the results showed that HA51 displayed by FBUSurfHA51$^{polh}$ was significantly higher followed by AcSurfHA51$^{polh}$ for the BV samples purified from infected TniHi5 culture media. In contrast, very little display was detected from the HTSurfHA51$^{polh}$-infected cells even when the virus titre was higher for this virus as detected by VP39 and Gp64 antibodies and by plaque assay. FBUSurfHA51$^{polh}$ was superior over other viruses, which might be due to the same reason discussed previously. In contrast, results in Figure 4.6 reveals that the BV form FBUSurfHA51$^{polh}$ and AcSurfHA51$^{polh}$-infected Sf9 culture medium showed approximately equal display levels. While HTSurfHA51$^{polh}$ display remains very low, the reasons behind that might be due to the *fp*-25 mutation in the baculovirus genome. High titre of BV production from *fp*-25 mutant baculovirus-infected cells was also reported by previous studies. They found that mutant virus was about three times higher than the non-mutant virus titre (Harrison and Summers, 1995; Li *et al.*, 2015). In addition, Li *et al*. reported that the *fp*-25 mutation resulted in a significant change in the accumulation of some baculovirus proteins. The envelope glycoprotein GP64 and ODV-E26 expression level increased in the cells infected with FP mutants, while the production level of polyhedrin decreased (Li *et al.*, 2015).

The immunoblotting analysis in Figure 4.5, 4.6 showed that native HA incorporation into the envelope surface of AcRP19HA$^{polh}$ was significantly higher than the truncated version in surface displayed viruses. Interestingly, the results observed with full-length HA conflicted with the previous study that demonstrated the incorporation of avian influenza virus truncated HA fused to *gp64* TMD into baculovirus BV envelope was significantly higher than native HA (Yang *et al.*, 2007). Another study also found that the display of HA chimeric protein including baculovirus GP64 TMD and the signal peptide was higher than the HA contain its own TMD (Zhou and Blissard, 2008). This is the first study to investigate the influence of different baculovirus expression vectors and the origin of TM on the chimeric protein incorporation into the recombinant baculovirus BV envelope. It has been found that the influenza virus HA is subject to many post-translational modifications in insect cells, which include disulfide bonds formation (Segal *et al.*, 1992) and N-glycosidic oligosaccharide side chains addition (Keil *et al.*, 1985).

Two bands of the expressed HA51-GP64$^{TRUN}$ chimeric protein were observed in the western immunoblot at different molecular mass. One was estimated as 64 kDa, which could correspond to the non-glycosylated HA51 version (HA51+ Gp64 TMD). The other was

estimated as 70 kDa, which was larger than its predicted molecular mass of 64 kDa, suggesting that the expressed protein from insect cells could have posttranslational modifications such as glycosylation. This hypothesis was confirmed by treating BV particles obtained from FBUSurfHA51$^{polh}$ infected Tni Hi5 cells with either PNGase F or endoglycosidase H to remove the glycans. In both cases, the 70 kDa band was absent and only one band was observed at the expected molecular mass of 64 kDa.

This result confirmed that the expressed chimeric protein using baculovirus expression systems was glycosylated. In addition, the results were identical with predictions by the online programme NetNGlyc 1.0 Server, that the HA51 chimeric protein included five glycosylation sites. Recently, Hsieh *et al.* (2018) reported that HA protein from the avian influenza virus expressed in insect culture was glycosylated and they predicted that this protein could have three to four glycosylation sites on the C-terminus (Hsieh *et al.*, 2018). Glycosylation of recombinant HA in insect culture was also reported by a previous study (Elliott, 2012). They investigated the nature of 65 kDa and 74 kDa HA from infected insect cells lysate detected in western immunoblot. They suggested that the difference in the molecular mass was due to glycosylation (Elliott, 2012). Matrosovich and co-workers demonstrated that 4-6 glycosylation sites of HA protein of H5 and H7 can be glycosylated (Matrosovich *et al.*, 1999).

The results in this thesis are in agreement with the early study by Wang *et al.* (2006), which suggested that using BEVS for recombinant HA production in insect cells produced at least two bands at a different molecular mass on western immunoblot. In addition, they demonstrated that the recombinant protein is glycosylated and biologically active (Wang *et al.*, 2006). Another study by Shi and Jarvis (2007) demonstrated that the HA glycan produced in insect culture could include six monosaccharides, resulting in an additional molecular mass of approximately 1.1 kDa. Several changes in the antigenic structure of both seasonal and pandemic human influenza H1N1 virus have been detected. These include either an increase or decrease in the glycosylation sites 142 and 177 on the HA head. These changes block the HA protein antigenic sites from the antibody neutralisation produced by the host immune response, which can cause more antigenic differences in some influenza virus serotypes (Sun *et al.*, 2011). It was decided to make the final comparison between full-length HA virus and truncated form HA51-GP64$^{TRUN}$ chimeric protein where both were expressed under *polh* promoter to select the best antigen candidate for vaccination experiment. The result suggested that full-length HA virus is best for the HA display, which gave two stable HA forms from early till very late time post infection compared to the HA51 virus that showed these form at 48 hpi only and after that, the glycosylated form was degraded.

## 4.9 Conclusion

It could be concluded from the results obtained in this chapter that among the three baculovirus expression vectors tested, FBU offers superior intracellular HA, however, this does not translate into better display on the BV envelope surface. The results also showed that HA51-GP64$^{TRUN}$ chimeric protein, produced by all recombinant surface display viruses, and full-length HA protein was biologically active when translocated on the surface of the infected cell. Unexpectedly, the use of baculovirus GP64 signal peptide and TMD appear to be detrimental to the surface display of HA. However, HA was displayed on the cell surface, the block appeared to be in incorporation into the budded virus particles. Immunoblotting analysis also showed that full-length HA protein display was better than that for the HA51-GP64$^{TRUN}$ chimeric protein. Finally, HA display by AcRP19HA$^{polh}$ was surprisingly good. This virus has a native HA gene with its own signal peptide and TMD, which was shown to be better than using GP64 signal peptide and TMD. Therefore, further experimental work of the study was directed towards optimising full-length HA for influenza A vaccine development, which will be described in chapters five and six.

# Chapter 5

# Optimizing the surface display of influenza virus haemagglutinin by baculovirus budded virus

## 5.1 Introduction

The development of novel baculovirus vectors for glycoprotein and vaccine production using baculovirus surface display technology is the major interest of this thesis. For this purpose, the influenza HA surface glycoprotein was the test protein investigated. Chapter 4 of this thesis demonstrated that use of a chimeric protein comprising HA51 glycoprotein with a GP64 signal peptide and TMD was not effective at targeting HA to the BV membrane. Unexpectedly, full-length HA from the original virus (AcRP19HA$^{polh}$) showed better results. This suggests that native HA, using its own signal peptide and TMD, is the better choice for surface display on the BV envelope. It was therefore decided to optimise full-length HA display by firstly comparing the use of three baculovirus vectors with different parental genomes: BacPAK6, BacPAK6$^{HT}$ or FBU, which were described in Chapter 4 (section 4.1). It was also decided to compare the effectiveness of three different baculovirus promoters: the late *p6.9* (Wilson *et al.*, 1987) and the very late *p10* (Weyer and Possee, 1989) or *polh* (Possee and Howard, 1987).

Based on previous studies, the AcMNPV late gene promoters have been extensively used for target protein(s) production. These promoters showed high expression levels of recombinant protein (reviewed by Premanand *et al.*, 2018). In addition, it has been reported that late gene promoters have been advantageous for production of secreted recombinant proteins such as juvenile hormone esterase (JHE) (Bonning *et al.*, 1994) and human urokinase (Lawrie *et al.*, 1995). The late phase of the baculovirus replication cycle is when viral glycoproteins are being synthesised, such as GP64, and therefore it is possible that this phase may also be optimal for the production of recombinant glycoproteins. In addition, the late phase sees a maximum production of BV (Chapter 1, section 1.3.1), so it might be predicted that incorporation of glycoprotein into BV may be optimised by using a late gene promoter. Hence, these findings highlight the importance of investigation of AcMNPV late promoter for high yield HA protein expression and for improving incorporation of this protein into the BV envelope surface.

An improved HA surface display construct could help with immunogenic investigations in vaccination experiments, as will be discussed in detail in Chapter 6 of this thesis. This chapter also sought to optimise the production of BV in shake and monolayer cultures using low and high MOI, to examine HA stability and to improve full-length HA incorporation into BV envelope using RNAi technology. RNA interference (RNAi) is a new approach that has facilitated gene function studies. It is a natural defence process used by different organisms such as fungi, insects, plants and mammals towards viral disease (reviewed by Valdes *et al.*, 2003). It was first employed as a tool for studying biological and disease-related processes and later it has been employed in medicine and biotechnology to silence essential virus gene expression aiming to develop an effective drug for infectious diseases

(reviewed by Lee *et al.*, 2015). In addition, this technology has recently been exploited for enhancing several expression systems to produce high yield and good quality of recombinant proteins (Chavez-Pena and Kamen, 2018). It has been reported that introducing double-stranded RNA (dsRNA) into different cells (including insect cells) results in specific gene(s) silencing (Valdes *et al.*, 2003; Lee *et al.*, 2015). In this chapter, RNAi technology is used to down-regulate *gp64* expression to determine whether reducing the amount of GP64 incorporated into BV enables more HA to be displayed.

## 5.2 Generation of recombinant baculoviruses expressing full-length HA

Two recombinant transfer vectors pAcMPHA$^{p6.9}$ and pAcUW3HA$^{p10}$ (kindly provided by Professor R. Possee) in which HA expression was under control of the late *p6.9* or very late *p10* promoters, respectively, were used to generate recombinant baculoviruses encoding the full-length HA glycoprotein. Briefly, Sf9 cells were co-transfected with each transfer vector and either BacPAK6, BacPAK6$^{HT}$ or FBU to generate six recombinant HA-baculoviruses (Methods 2.2.3). Virus stocks were harvested from the culture media 5 days after the co-transfection. The virus stocks from co-transfection with FBU and each transfer vector were considered as virus seed stock passage 0 (P0), as only the recombinant virus can be produced during the co-transfection (Hitchman *et al.*, 2007a). On the other hand, co-transfection with BacPAK6 or BacPAK6$^{HT}$ produced a mixture of recombinant viruses; clear plaques from recombinant virus and blue plaques from the parental virus expressing *lacZ* in the presence of X-gal (Figure 5.1; Kitts and Possee, 1993). Therefore, to obtain a genetically homogeneous stock of HA-recombinant viruses clear plaques were isolated and subjected to plaque purification until no blue plaques were observed (Methods 2.2.5).

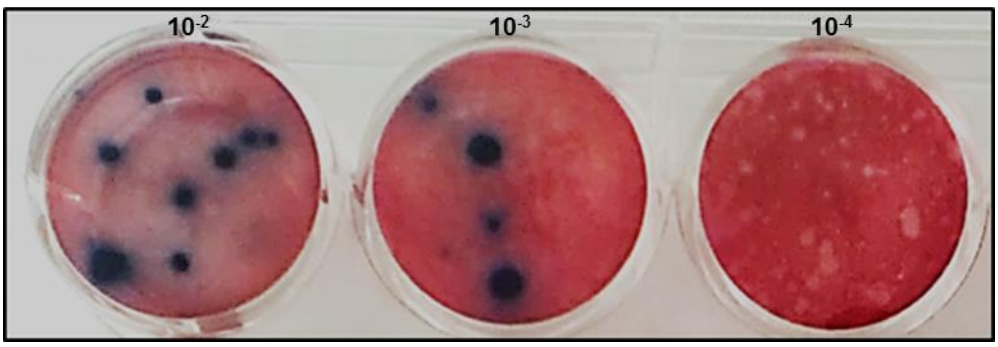


**Figure 5.1: Identification of HA recombinant baculovirus using plaque assay.**

The image shows a typical plaque assay with serial dilutions ($10^{-2}$, $10^{-3}$, $10^{-4}$) of virus harvested from the culture medium of Sf9 cells co-transfected with BacPAK6 or BacPAK6$^{HT}$ and either pAcMPHA$^{p6.9}$ or pAcUW3HA$^{p10}$ to produce recombinant baculoviruses. The dishes were stained with X-gal and neutral red after 4 days to differentiate between recombinant virus (clear plaques) and parental virus (blue plaques).

The virus harvested from the final plaque purification round was used to infect Sf9 cells in 35 mm tissue culture dishes (Methods 2.5.1). After 5 dpi, HA-recombinant viruses were harvested from the culture media and considered as the P0. In order to confirm that the recombinant viruses obtained from plaque purifications were genetically homogenous and free from parental virus, DNA was isolated from each virus and PCR screening was undertaken using RDP213B and RDP214B (Table 2.7; section 2.2.4b, 2.4.5). This indicated that the recombinant viruses were generated correctly (data not shown). After the generation of the first P0 virus seed stocks, 50 ml of P1 virus stocks were produced in Sf9 cells and titrated by plaque assay (Methods 2.2.2 and 2.2.4a, respectively), as summarised in Table 5.1. Recombinant viruses expressing full-length HA under control of the *polh* promoter, FBUHA$^{polh}$ constructed in this study and AcRP19HA$^{polh}$have been described previously (Chapter 4, section 4.2) but are included in Table 5.1 for completeness.

**Table 5.1: Summary of recombinant baculoviruses expressing HA**

| Transfer display vector | BEVS | Wild-type of gene(s) deleted | Recombinant virus name |
|---|---|---|---|
| pAcMPHA$^{p6.9}$ | BacPAK6 | Wild-type | AcHA$^{p6.9}$ |
| pAcMPHA$^{p6.9}$ | BacPAK6$^{HT}$ | *fp25* | Ac$^{HT}$HA$^{p6.9}$ |
| pAcMPHA$^{p6.9}$ | FBU | *p10, p26, p74, chiA, v-cath* | FBUHA$^{p6.9}$ |
| pAcUW3HA$^{p10}$ | BacPAK6 | Wild-type | AcHA$^{p10}$ |
| pAcUW3HA$^{p10}$ | BacPAK6$^{HT}$ | *fp25* | Ac$^{HT}$HA$^{p10}$ |
| pAcUW3HA$^{p10}$ | FBU | *p10, p26, p74, chiA, v-cath* | FBUHA$^{p10}$ |
| pAcRP19.HA$^{polh}$ | BacPAK6 | Wild-type | AcRP19HA$^{polh}$ |
| pOET1-HA$^{polh}$ | FBU | *p10, p26, p74, chiA, v-cath* | FBUHA$^{polh}$ |

## 5.3 Influence of promoter choice on full-length HA synthesis and display in insect cell lines infected with recombinant viruses

### 5.3.1 Examination of HA synthesis in Tni Hi5 and Sf9 cells

In order to determine the influence of the promoter activity on HA synthesis, Tni Hi5 and Sf9 cells were infected with the full-length HA recombinant viruses based on BacPAK6 backbone at an MOI of 5 pfu/cell and in which the HA gene was driven by either *p6.9*, *p10* or *polh* promoters (AcHA$^{p6.9}$, AcHA$^{p10}$ and AcRP19HA$^{polh}$, respectively; Table 5.1). In addition, mock- and AcMNPV-infected cells were included as negative controls. After incubation at 28°C for 72 hours, cells were harvested using low-speed centrifugation and cell pellets were prepared for SDS-PAGE (Methods 2.5.2). The culture media were retained and stored at 4ºC for BV analysis (Methods 2.2.2). Proteins in the crude cell lysates were separated in 10% SDS-PAGE gels followed by transfer onto nitrocellulose membrane for immunoblotting analysis. The blots were then probed with specific antibodies raised against HA and VP39 proteins (Methods 2.5.2 and 2.5.2b). The cell lysates of virus-infected Sf9 cells showed two specific bands in both AcHA$^{p10}$- and AcRP19HA$^{polh}$-infected cells. The

lowest band was at the expected molecular mass of the full-length HA protein of approximately 64 kDa, with the other band at 70 kDa corresponding to the HA glycosylated form. The expression profile also showed that there was more non-glycosylated than glycosylated HA produced in both AcRP19HA$^{polh}$- and AcHA$^{p10}$-infected Sf9 cells (Figure 5.2 A).

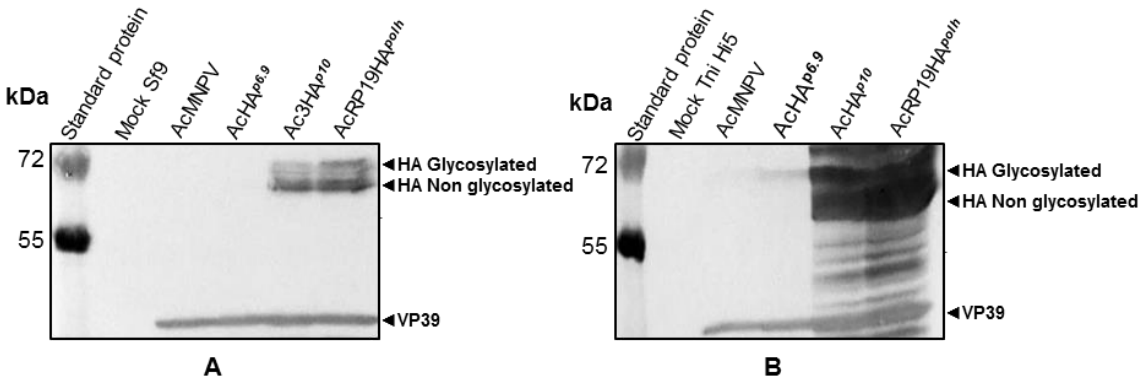


**Figure 5.2: Characterization of full-length HA protein synthesis in Sf9 (A) or Tni Hi5 cells (B).** Sf9 or Tni Hi5 cells were seeded in 35 mm dishes at a density of 1x10$^6$ or 0.5x10$^6$cells/dish, respectively. Cells were infected with the corresponding recombinant viruses. Negative controls were mock- and AcMNPV-infected cells. Cell pellets were harvested at 72 hpi and cell lysates were separated by an SDS-PAGE gel (10%) and analysed by immunoblotting. The blot was developed using primary full-length anti-mouse HA antibody (1:1000), VP39 antibody (1:5000) and secondary anti-mouse alkaline phosphatase conjugated antibody (1:25000). The blot also includes standard protein markers: Precision plus protein Western C standard (Bio-Rad).

Based on band intensity, the AcRP19HA$^{polh}$-Sf9 infected cells gave the highest expression levels, followed by the AcHA$^{p10}$-Sf9 infected cells (Figure 5.2 A). In contrast, no expression was detected in AcHA$^{p6.9}$-infected cell lysates and, as expected, no expression of HA was detected in either the AcMNPV- or mock-infected Sf9 cells (Figure 5.2 A). The HA protein synthesis was also examined in virus-infected Tni Hi5 cell lysates in order to compare with the expression in Sf9 cells. Crude cell lysates showed hyper-expression of HA protein in both AcRP19HA$^{polh}$- and AcHA$^{p10}$-infected Tni Hi5 cells at molecular masses ranging from approximately 64-74 kDa, corresponding to HA and its glycosylated forms (Figure 5.2 B). Based on band intensity, AcHA$^{p10}$ and AcRP19HA$^{polh}$-Tni Hi5 infected cells gave approximately the same expression levels. In contrast, very little expression was observed in AcHA$^{p6.9}$-infected cells (Figure 5.2 B). These results suggested that very late (*p10* and *polh*) promoters drive higher HA protein expression levels in both cell lines compared to the late *p6.9* promoter and that the *polh* was the best among these promoters. In addition, Tni Hi5 cells showed the best support for protein expression and glycosylation in comparison to Sf9 cells. Furthermore, this result suggested that HA expression yields seem to depend on the promoter and host cells used.

### 5.3.2 Examination of the HA incorporation on the envelope of BV produced in Sf9 and Tni Hi5 cells

To examine the influence of the promoter activity on the incorporation of full-length HA protein into the recombinant virus envelope surface, BV particles from the culture medium of virus-infected Sf9 cells were prepared as described previously (section 5.2). Immunoblotting analysis (Chapter 4, section 4.5.1) revealed that all BV samples contained a near equivalent amount of VP39 (Figure 5.3 A). However, analysis of HA protein incorporation into the BV envelope showed approximately similar amounts in both AcRP19HA$^{polh}$ and AcHA$^{p10}$ (Figure 5.3 A). In contrast, only a very small amount of HA protein was incorporated into the AcHA$^{p6.9}$ BV envelope. It was also noted that the HA protein anchored in the BV envelope of all three viruses appeared to be only in the glycosylated form, as indicated by the single band at ~70 kDa (Figure 5.3 A).

The effect of promoter activity on the incorporation of HA protein into BV envelope of recombinant viruses produced in Tni Hi5 cells was also analysed (Figure 5.3 B). There were approximately equivalent amounts of VP39 capsid protein in AcHAp10 and AcRP19HA$^{polh}$ recombinant viruses BV samples at the expected 39 kDa (Figure 5.3 B). However, the quantity of VP39 protein observed in the AcHA$^{p6.9}$ BV sample was a little higher (Figure 5.3 B) suggesting relatively more BV was loaded into these lanes. The blot in Figure 5.3 B showed two specific bands of HA protein incorporated into the AcRP19HA$^{polh}$ BV envelope, at 64 kDa and 70 kDa corresponding to full-length HA and glycosylated forms, respectively. In addition, the results showed that AcRP19HA$^{polh}$ BV envelope has the highest incorporation of HA protein, followed by the AcHA$^{p10}$ with very little protein observed on AcHA$^{p6.9}$ BV envelope (Figure 5.3 B). It is also noteworthy that only the glycosylated form of HA protein was incorporated into the AcHA$^{p6.9}$ and AcHA$^{p10}$ BV envelope ~70 kDa, whereas AcRP19HA$^{polh}$ BV showed both full length and glycosylated HA forms (Figure 5.3 B). There was no HA evident in mock or AcMNPV BV samples, as expected (Figure 5.3 B). Overall, the results showed that *polh* and *p10* support better HA incorporation into BV envelope than *p6.9* in BV obtained from both Sf9 and Tni Hi5 infected cells culture media as indicated on the western immunoblot (Figure 5.3 A and B, respectively).

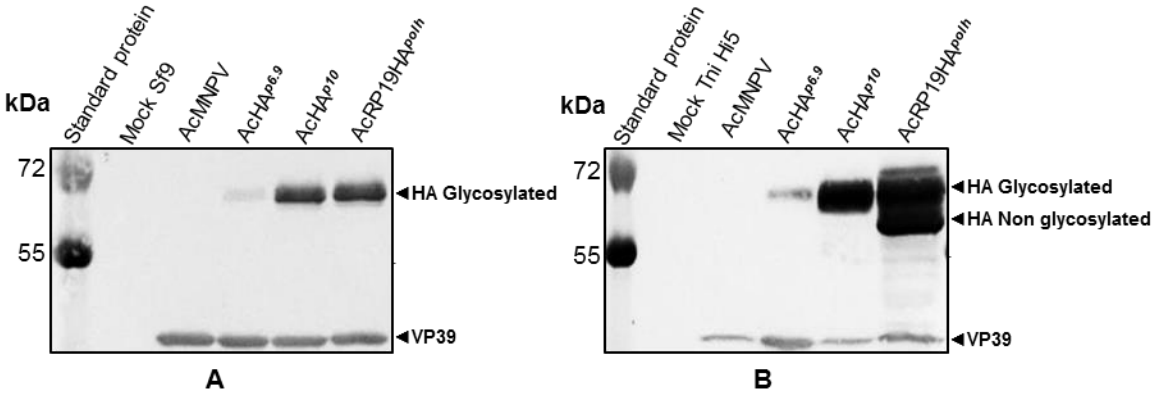


**Figure 5.3: Characterization of full-length HA incorporated into AcRP19HA$^{polh}$ AcHA$^{p10}$ and AcHA$^{p6.9}$ budded virus produced in Sf9 (A) or Tni Hi5 cells (B).**
Sf9 and Tni Hi5 cells were seeded in 35 mm tissue culture dishes at a density of 1x10$^6$ or 0.5X10$^6$ cells/dish, respectively. Cells were infected with the corresponding recombinant viruses, negative controls were mock- and AcMNPV-infected cells. Culture media were harvested at 72 hpi and the BV fractions were separated by SDS-PAGE gel (10%) and analysed by immunoblotting. The blot was developed using primary full-length anti-mouse HA antibody (1:1000), VP39 antibody (1:5000) and secondary anti-mouse alkaline phosphatase conjugated antibody (1:25000). The blot also includes standard protein markers: Precision plus protein Western C standard (Bio-Rad).

## 5.4 Comparison between HA incorporation into AcRP19HA$^{polh}$ and AcHA$^{p10}$ BV envelopes produced in Tni Hi5 cells

Both AcRP19HA$^{polh}$ and AcHA$^{p10}$ viruses showed good incorporation of HA into BV envelopes when they were produced in Tni Hi5 cells, although in the former the HA was a mix of the glycosylated and non-glycosylated forms whereas in AcHA$^{p10}$ only the glycosylated form was incorporated. Therefore, it was decided to further investigate these two viruses during a time course of infection to identify the best promoter that can support HA synthesis and display. Briefly, Tni Hi5 cells were seeded and infected with recombinant viruses as described previously in this chapter (section 5.2). The BV was collected during different periods from 24-96 hpi. An equal amount of BV was then separated using 10% SDS-PAGE gel, followed by immunoblotting analysis. The blots were probed with specific antibodies raised against VP39 and the HA protein (Methods 2.5.2 and 2.5.2b). Interestingly, after 48 hpi HA displayed on the envelopes from both recombinant BVs showed several reactive bands at different molecular mass ranging from (64-72 kDa) (Figure 5.4 A and B) suggesting different glycosylation levels of the HA protein. At 72 and 96 hpi, AcHA$^{p10}$ BV envelope showed one band only corresponding to the HA glycosylated form at ~70 kDa (Figure 5.4 A). Whereas, BV from AcRP19HA$^{polh}$ showed two specific bands of HA at 64 kDa and glycosylated HA ~70 kDa at 72 hpi (Figure 5.4 B). However, the relative intensity of the 64 kDa protein band started to decrease after 48 hpi. No HA-specific

bands were detected at 24 hpi in either AcHA$^{p10}$ or AcRP19HA$^{polh}$ BV samples (Figure 5.4 A and B).

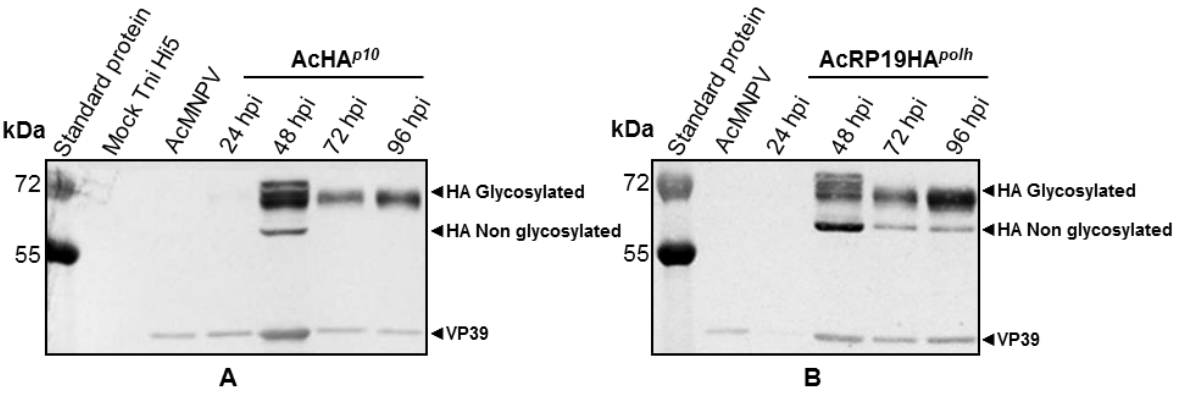


**Figure 5.4: Comparing the HA incorporation into AcHA$^{p10}$ (A) and AcRP19HA$^{polh}$ (B) BV envelopes during a Tni Hi5 time course infection.**
Tni Hi5 cells were seeded in 35 mm tissue culture dishes at a density of 0.5x10$^6$ cells/dish and infected with the corresponding recombinant viruses, negative controls were mock- and AcMNPV-infected cells. Culture media were harvested at different time post infection (24-96 hpi) and the BV fractions were separated by SDS-PAGE gel (10%) and analysed by immunoblotting. The blot was developed using primary full-length anti-mouse HA antibody (1:1000), VP39 antibody (1:5000) and secondary anti-mouse alkaline phosphatase conjugated antibody (1:25000). The blot also includes standard protein markers: Precision plus protein Western C standard (Bio-Rad).

This experiment also indicated that HA is most likely stably integrated into the BV envelope as levels were not significantly reduced even at very late times (96 hpi; Figure 5.6 A and B). Additionally, the result showed that non-glycosylated HA in AcHA$^{p10}$ appeared unstable as after 48 hpi, only BV with the glycosylated form of HA was detected (Figure 5.4 A). On the other hand, non-glycosylated HA produced under *polh* promotor appeared to be stably incorporated even at 96 hpi (Figure 5.4 B). These results also showed that the 70 kDa bands intensity from both BV samples increased from 72-96 hpi time point (Figure 5.4 A and B).

## 5.5 Examination of HA protein synthesis in AcRP19HA$^{polh}$-infected Tni Hi5 cells in defined 24 hour periods after infection

In section 5.4, the incorporation of HA protein into BV that had accumulated at different times after infection was investigated. This showed that in AcRP19HA$^{polh}$ both the glycosylated and non-glycosylated forms of HA was displayed in the BV envelope. To investigate whether these forms are incorporated differentially throughout infection, the experiment was repeated with modifications. Essentially, in one set of samples, the total accumulation of HA in BV was assessed by collecting medium at 24, 48, 72 and 96 hpi as before. Alternatively, in the second set of samples, BV production was examined in 24 h periods between 0-24, 24-48, 48-72 or 72-96 hpi to monitor HA display. This was achieved

by collecting medium and then replacing it with an identical volume of fresh medium to allow accumulation of virus in the next 24 h period prior to the next harvest.

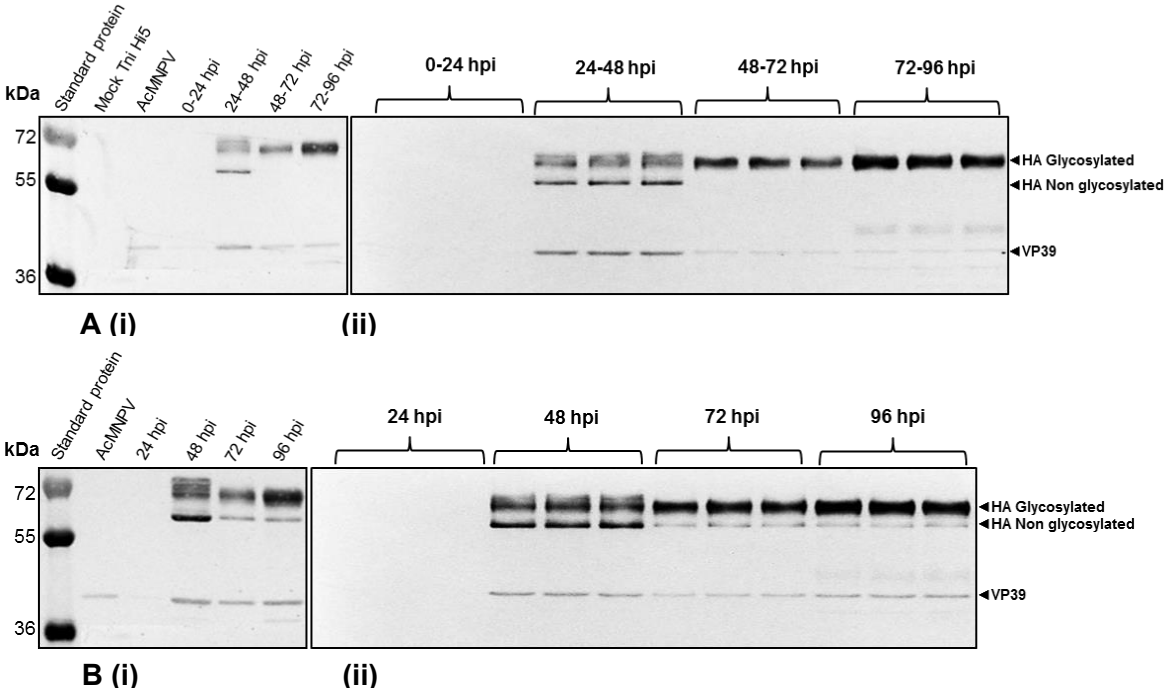


**Figure 5.5: Comparing the HA incorporation into AcRP19HA$^{polh}$ BV envelopes during time windows and time course Tni Hi5 infection.**
Tni Hi5 cells were seeded in 35 mm tissue culture dishes at a density of 0.5x10$^6$ cells/dish and infected with the corresponding recombinant viruses, negative controls were mock- and AcMNPV-infected cells. **A.** Culture media were harvested every 24 h pi and replaced with fresh medium to enable subsequent collection at the end of the next 24 h period from the same dish. **B.** Culture media were collected at 24, 48, 72 and 96 h pi from separate dishes to monitor total BV accumulation. The BV fractions were separated by SDS-PAGE gel (10%) and analysed by immunoblotting. The blot was developed using primary full-length anti-mouse HA antibody (1:1000), VP39 antibody (1:5000) and secondary anti-mouse alkaline phosphatase conjugated antibody (1:25000). The blot also includes standard protein markers: Precision plus protein Western C standard (Bio-Rad). Left panels in both A (i) and B (i) blots represent single replicate. These results were confirmed by the analysis of triplicate samples (Figure. 5.5 A [ii], B[ii]).

Two sets of Tni Hi5 cells were seeded in 35 mm tissue culture dishes at a density of 0.5x10$^6$ cells/dish in triplicate for both experiments. The cells were then infected with AcRP19HA$^{polh}$ at an MOI of 5 pfu/cell and incubated at 28ºC for the required time before harvesting BV as described above. A preliminary analysis of BV samples showed negligible incorporation of HA into BV by 24 hpi (Figure 5.5 A(i), B(i). Between 24-48 hpi both glycosylated and non-glycosylated forms of HA were evident in BV (Figure 5.5 A(i). While this indicated that the non-glycosylated HA might be unstable, its presence in BV that had accumulated at both 72 and 96 h pi (Figure 5.5 B[ii]).

## 5.6 The effect of the parental virus genome composition on full-length HA display on the BV envelope

It was shown in Chapter 4 that the baculovirus genome could influence the HA51GP64$^{TRUN}$ chimeric protein surface display within the BV envelope. Therefore, it was decided to investigate the effects of the virus backbone on full-length HA display. Briefly, Sf9 and Tni Hi5 cells were infected with recombinant baculoviruses (Table 5.1) at an MOI of 5 pfu/cell. After incubation at 28°C for 72 hours, cells were harvested using low-speed centrifugation (Methods 2.5.2). The culture medium was retained and stored at 4ºC for BV display analysis (Methods 2.2.2).

### 5.6.1 The impact of virus backbone on the incorporation of *p6.9* gene promoter-expressed HA in the BV envelope

The incorporation into BV of full-length HA expressed under control of the *p6.9* promoter was investigated in Sf9 cells. Briefly, BV particles from the stored culture medium (Section 5.6) were pelleted and prepared for immunoblotting (Chapter 4, section 4.5.1). The blot was probed with specific antibodies raised against AcMNPV VP39 (as a loading control) and the HA protein (Methods 2.5.2 and 2.5.2b). Immunoblotting analysis indicated the positions of VP39 and demonstrated that there were approximately equivalent amounts of this protein in AcHA$^{p6.9}$, FBUHA$^{p6.9}$ and Ac$^{HT}$HA$^{p6.9}$ BV samples at the expected molecular mass of 39 kDa (Figure 5.6 A). However, the amounts of HA incorporated into the BV envelope were varied. The results showed that FBUHA$^{p6.9}$ produced BV with the highest levels of HA protein, which is indicated by the strong band. A very faint band of HA protein was detected on AcHA$^{p6.9}$ BV envelope (Figure 5.6 A). In contrast, no HA band was observed in the Ac$^{HT}$HA$^{p6.9}$ BV sample (Figure 5.6 A). It was also noted that the HA protein in all the BV samples appeared as one band at ~70 kDa corresponding to the glycosylated form of HA (Figure 5.6 A). However, it seems that FBU supports the best HA incorporation into BV envelope when compared with the other two backbones (Figure 5.6 A).

The incorporation of HA into the surface of the BV envelope of recombinant viruses produced in Tni cells was also investigated (Figure 5.6 B). There were approximately equivalent amounts of VP39 protein in the AcHA$^{p6.9}$ and FBUHA$^{p6.9}$ BV fractions (Figure 5.6 B). However, only a small quantity of VP39 protein was observed in the Ac$^{HT}$HA$^{p6.9}$ and AcMNPV BV samples suggesting less BV had been loaded in these lanes. Overall, compared to the Sf9 samples in Figure 5.6 A, there appeared to be less BV purified from Tni cells, as evidenced by comparison of the VP39 loadings. However, HA protein incorporation into the BV envelope was greater in AcHA$^{p6.9}$ and FBUHA$^{p6.9}$ BV samples from Tni Hi5 cells (Figure 5.6 B). In addition, Ac$^{HT}$HA$^{p6.9}$ BV samples from Tni Hi5 cells showed good protein incorporation compared to the same virus in Sf9 cells, which did not show any

HA protein incorporation into BV (Figure 5.6 B, A, respectively). The blot in Figure 5.2 B showed one specific band at ~70 kDa, the same as in Sf9 cells.

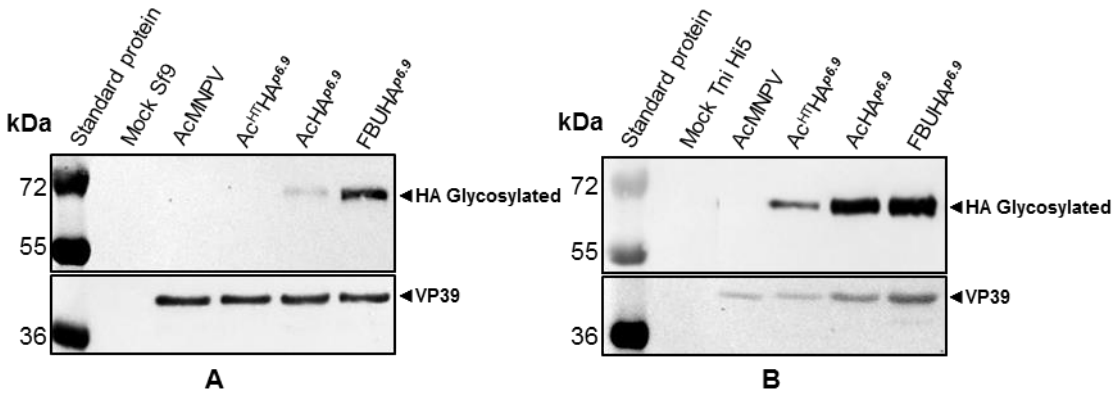


**Figure 5.6: Characterization of HA incorporated into budded virus produced in Sf9 (A) or Tni Hi5 cells (B) using the p6.9 promoter.**
Sf9 and Tni Hi5 cells were seeded in 35 mm tissue culture dishes at a density of $1x10^6$ or $0.5x10^6$ cells/dish, respectively. The cells were infected with the corresponding recombinant viruses. Negative controls were mock- and AcMNPV-infected cells. Culture media were harvested at 72 hpi and the BV fractions were separated by SDS-PAGE gel (10%) and analysed by immunoblotting. The blot was developed using primary full-length anti-mouse HA antibody (1:1000), VP39 antibody (1:5000) and secondary anti-mouse alkaline phosphatase conjugated antibody (1:25000). The blot also includes standard protein markers: Precision plus protein Western C standard (Bio-Rad).

Overall, the results demonstrated that FBUHA$^{p6.9}$ BV envelope had the highest levels of HA protein and that this was greatest when the BV was produced in Tni Hi5 cells. It is also noteworthy that HA protein incorporated into all of the BV samples appeared to be glycosylated (Figure 5.6 B), similar to that observed when these viruses were produced in Sf9 cells (Figure 5.6 A). The result also suggests that the glycosylated form of HA is essential for membrane targeting.

### 5.6.2 Analysis of the incorporation of HA on the BV envelope in recombinant virus-infected Sf9 and Tni Hi5 cells under the control of the *p10* promoter

Expression of full-length HA under control of the *p10* promoter was also investigated in BV obtained from the culture medium of infected cells, in a similar manner to that described above for the *p6.9* promoter. The BV obtained from infected Sf9 culture medium were analysed for HA protein incorporation. The results (Figure 5.7 A) showed that BV of FBUHA$^{p10}$ accommodates the highest amount of HA protein. Whereas, based on band intensity, AcHA$^{p10}$ BV had approximately half the amount of HA protein in its envelope (Figure 5.7 A). Furthermore, no HA protein was detected in the Ac$^{HT}$HA$^{p10}$ BV sample, which could be due to very low protein concentration or no HA protein has incorporated into the BV envelope (Figure 5.7 A). Analysis of BV recovery after centrifugation revealed that all BV samples contained approximately equivalent quantities of VP39 (Figure 5.7 A). In

addition, it was also noted that the HA protein incorporated into FBUHA$^{p10}$ and AcHA$^{p10}$ BV envelope appeared as one band at a molecular mass of ~70 kDa of the glycosylated form (Figure 5.7 A).

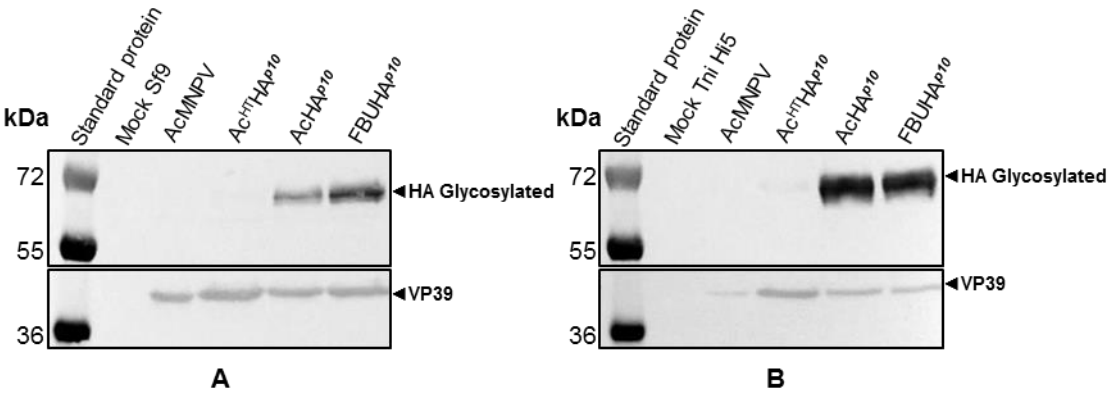


**Figure 5.7: Characterization of HA incorporated into budded virus produced in Sf9 (A) or Tni Hi5 cells (B) under control of a p10 promoter.**
Sf9 and Tni Hi5 cells were seeded in 35 mm tissue culture dishes at a density of 1x10$^6$ or 0.5x10$^6$ cells/dish, respectively. The cells were infected with the corresponding recombinant viruses. Negative controls were mock- and AcMNPV-infected cells. Culture media were harvested at 72 hpi and the BV fractions were separated by SDS-PAGE gel (10%) and analysed by immunoblotting. The blot was developed using primary full-length anti-mouse HA antibody (1:1000), VP39 antibody (1:5000) and secondary anti-mouse alkaline phosphatase conjugated antibody (1:25000). The blot also includes standard protein markers: Precision plus protein Western C standard (Bio-Rad).

There was no evidence of HA protein in mock- or AcMNPV-infected BV samples, as expected. HA incorporation into BV from Tni Hi5 culture media was also examined. The results (Figure 5.7 B) showed that the incorporation of HA protein into the BV envelopes of both FBUHA$^{p10}$ and AcHA$^{p10}$ viruses was approximately the same. In contrast, a very faint band of HA protein on the BV envelope of the Ac$^{HT}$HA$^{p10}$ virus was observed. This result was very similar to that observed when HA was expressed under the control of the *p6.9* promoter (Figure 5.6 B).

## 5.7 Examining the effect of MOI and cell culture system on BV production and HA display

In this thesis, an MOI of 5 pfu/cell was exploited for HA protein production in insect cells grown in monolayer cultures for all experiments. However, this system is less amenable for scale up and consumes large amounts of virus inoculum. If a low MOI (e.g. 0.1 pfu/cell) and insect cells in shake/suspension cultures could be used this would be more economical for antigen production for vaccine formulation. Therefore, the level of HA protein production was compared in 2 ml or 25 ml of monolayer and shake cultures, respectively of TnHi5 cells infected with either 0.1 or 5 MOI (section 2.5.1).

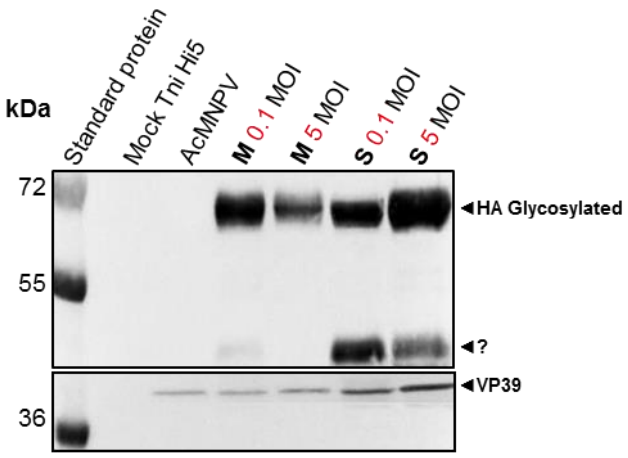


**Figure 5.8: Immunoblot analysis of HA from BV produced in TnHi5 cells infected with low (0.1 pfu/cell) or high (5 pfu/cell) MOI in either monolayer or shake cultures.**
Tni Hi5 cells were seeded in 35 mm tissue culture dishes at a density of (1x10$^6$cells/dish) or in 25 ml conical flasks at a density of (1x10$^6$cells/ml) in monolayer (M) or shake cultures (S), respectively. Cells were infected with an AcRP19HA$^{polh}$ virus using 0.1 or 5 MOI. The cultures infected with 0.1 MOI were harvested at 5 dpi and the cultures infected with 5 MOI were harvested at 3 dpi. Proteins from BV faction samples were separated by SDS-PAGE gel (10%) and analysed by immunoblotting. The blot was developed using primary VP39 (1:5000) antibody or full-length HA antibody (1:1000) and secondary anti-mouse alkaline phosphatase conjugated antibody (1:25000). Mock- and AcMNPV were included as negative controls. The blot also includes standard protein markers: Precision plus protein Western C standard (Bio-Rad).

The proteins from BV fractions were separated by 10% SDS-PAGE and analysed using western immunoblot (Sections 2.5.2 and 2.5.2a). HA glycosylated protein was observed from both MOI and cultures samples at the expected molecular mass of approximately 70 kDa (Figure 5.8). However, a strong band was observed at expected a molecular mass of HA1 subunit of approximately 42 kDa from shaking culture samples (Figure 5.8). This band has raised the question of whether it was due to proteolytic activity or nonspecific antibody binding, which was investigated further in this chapter.

## 5.8 Construction of FBUHA$^{polh}$ recombinant virus

As an extra band at a molecular mass of approximately 42 kDa was observed on immunoblotting from AcRP19HA$^{polh}$ BV samples obtained from shaking cultures, it was decided to investigate the nature of this band. The AcRP19HA$^{polh}$ recombinant virus was based on the AcMNPV genome where the *polh* coding region was replaced with *lacZ* gene (Kitts and Possee, 1993) but all other virus genes remained intact. Therefore, it was hypothesised that this band may be because of the protease activity of cathepsin enzyme produced by the AcRP19HA$^{polh}$ virus during the late phase of infection and released into cell culture after cell lysis. In order to investigate this hypothesis, a new recombinant virus expressing full-length HA protein under control of the *polh* promoter in FBU was

constructed. FBU is a baculovirus vector based on an AcMNPV genome that has deletions in five genes *p10, p74, p26, chiA* and *v-cath* (Hitchman *et al.*, 2010b). Following the success of the FBUHA$^{polh}$ construction, Tni Hi5 cells were infected in shake culture with either AcRP19HA$^{polh}$ or FBUHA$^{polh}$ at an MOI of 0.1 pfu/cell; mock- and AcMNPV-infected cells were also included as negative controls. After incubation at 28°C for 72 hpi and 96 hpi, cells were harvested using low-speed centrifugation.

The BV particles from the culture medium were pelleted and prepared for immunoblotting analysis as described previously (section 4.5.1). The blot was probed with a specific monoclonal antibody raised against the HA protein (Methods 2.5.2 and 2.5.2b). The results of this analysis indicated the positions of two bands with molecular masses of approximately 70 kDa and 42 kDa from AcRP19HA$^{polh}$ BV samples. The relative intensities of the bands were approximately equal at 72 hpi. At 96 hpi the 70 kDa band decreased in intensity, which was accompanied by an increasing amount of the 42 kDa band (Figure 5.9 A). In contrast, one band only was detected at ~70 kDa from FBUHA$^{polh}$ BV samples at both 72 and 96 hpi (Figure 5.9 A).

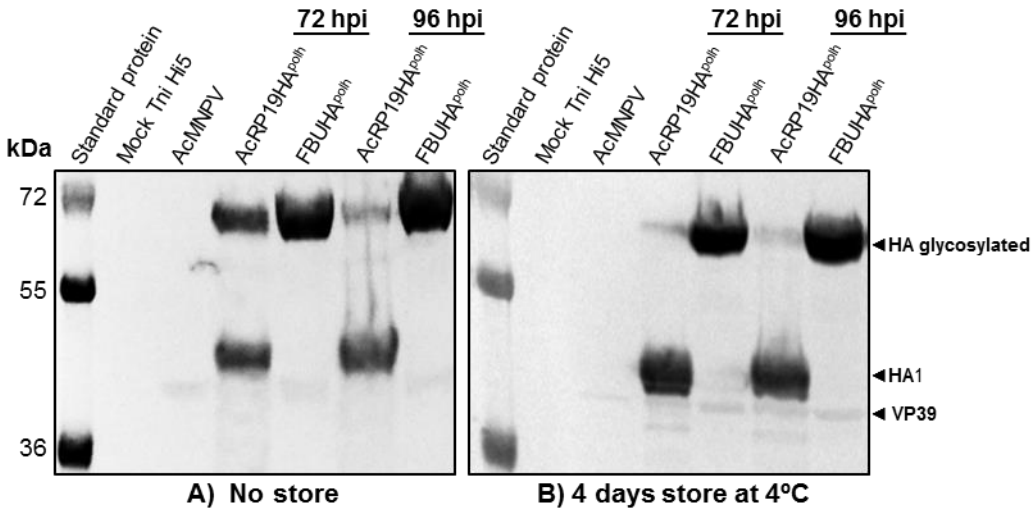


**Figure 5.9: Western immunoblot analysis of the proteolytic degradation of HA in BV produced in TnHi5 cells before storage at 4ºC (A) and after storage at 4ºC for 4 days (B).**
Tni Hi5 cells were seeded in 25 ml conical flasks at a density of (1x10$^6$cells/ml) in shake cultures. Cells were infected with AcRB19HA$^{polh}$ or FBUHA$^{polh}$ at an MOI of 5 pfu/cells. The cultures were harvested at two different time points (72 and 96 hpi). Proteins from BV fraction samples were separated by SDS-PAGE gel (10%) and analysed by immunoblotting for proteolytic activity and stability. The blot was developed using primary anti-mouse full-length HA (1:1000) and VP39 (1:5000) antibody and secondary anti-mouse alkaline phosphatase conjugated antibody (1:25000). Mock- and AcMNPV were included as negative controls. The blots also include standard protein markers: Precision plus protein Western C standard (Bio-Rad).

The stability of the HA protein was also examined using the same BV samples that were stored at 4ºC for 4 days (Figure 5.9 B). As shown in Figure 5.9 B, HA from FBUHA$^{polh}$ BV samples remained stable and the band intensity from 72 and 96 hpi was approximately

identical. On the other hand, clear evidence of proteolytic activity was observed in AcRP19HA$^{polh}$ BV samples at both post-infection times in which the vast majority of HA protein was converted into HA1 subunit (Figure 5.9 B).

## 5.9 Attempts to improve full-length HA incorporation on FBUHA$^{polh}$ BV envelope by reducing GP64 production using RNA interference technology

Previous studies have demonstrated that baculovirus replication and BV assembly can be downregulated using a double-stranded RNA (dsRNA) approach to target and knockdown *gp64* gene expression (Valdes *et al.*, 2003; Lee *et al.*, 2015). This technique may be beneficial to reduce baculovirus particles that contaminate the final products of recombinant proteins and VLPs (Lee *et al.*, 2015). In this study, it was decided to use this approach to determine whether knockdown of GP64 synthesis might lead to increased levels of HA incorporated into BV; the assumption being that there may be a finite amount of glycoprotein that can be targeted to the virion envelope. As GP64 has been shown to be essential for budding of BV in Sf9 cells (Mangor *et al.*, 2001). It was important to monitor BV production and determine whether the same effect was observed in Tni cells. As transfection reagents have been shown to have different efficiency in insect cells, it was decided to optimise three different transfection reagents and select the best one for future experiments.

### 5.9.1 Optimisation of the transfection efficiency

To examine the transfection reagents and determine the most efficient one that can achieve high transfection efficiency, three different transfection reagents were used according to the supplier's recommended protocol: Lipofectine®, Lipofectamine® RNAiMAX (Invitrogen) or TransIT®-Insect transfection reagent (Mirus). In this experiment, the *p35* anti-apoptosis gene was employed as a target gene to monitor the cells for apoptosis under the light microscope. To do this, the *p35* gene sequence was amplified by PCR from wild-type AcMNPV DNA template using specific primers (Table 2.7, Section 2.4.5). After that, dsRNA targeting the *p35* gene was synthesised according to the supplier's recommended protocol using the HiScribe™ T7 High Yield RNA Synthesis Kit (NEB). The uptake of dsRNA by Sf21 insect cells in 6-well tissue culture plates was analysed as described (Methods 2.9.2). Then the cells were infected with AcMNPV virus at MOI of 1 pfu/cell; mock-, AcMNPV-infected cells plus control dsRNA were included as negative controls. Then the infected cells were monitored for signs of apoptosis (membrane blebbing) over a time course and imaged using a light microscope at 24 and 48 hpi.

A time course analysis of cell apoptosis would enable selecting the best transfection reagent. As shown in Figure 5.10 A, a small increase in blebbing was observed in the Sf21 cells from 24-48 hpi when transfected with TransIT®-Insect and *p35* dsRNA. In the case of Lipofectine® and *p35* dsRNA transfected Sf21 cells, clear signs of apoptosis were detected at 24 hpi and the population of apoptotic cells had increased by 48 hpi (Figure 5.10 B). The same profile was observed with Lipofectamine® RNAiMAX and *p35* dsRNA transfected Sf21 cells, where the population of apoptotic cells increased from 24 hpi to 48 hpi (Figure 5.10 B). However, compared to Lipofectine® a larger population of apoptotic cells was observed at 24 hpi and the number significantly increased by 48 hpi (Figure 5.10 B).

A quantitative analysis was carried out using a plaque assay (Methods 2.2.4a), which allowed a comparison between three transfection reagents based on the virus titre. As shown in Figure 5.11 there was a 10-fold decrease in AcMNPV titre in the case of Sf21 cells transfected with Lipofectamine® RNAiMAX, followed by a 5-fold decrease when the cells were transfected with Lipofectine® transfection reagent (Figure 5.11). The virus titre remained close to the control infection when the cells were transfected with TransIT®-Insect transfection reagent (Figure 5.11). These findings suggested that Lipofectamine® RNAiMAX was the best transfection reagent because it improved the transfection of cells and increased the dsRNA uptake by Sf21 cells. As expected no apoptosis signs were detected in mock-, AcMNPV- and AcMNVP+ control dsRNA- infected cells for all transfection reagents experiments (Figure 5.11 A, B).

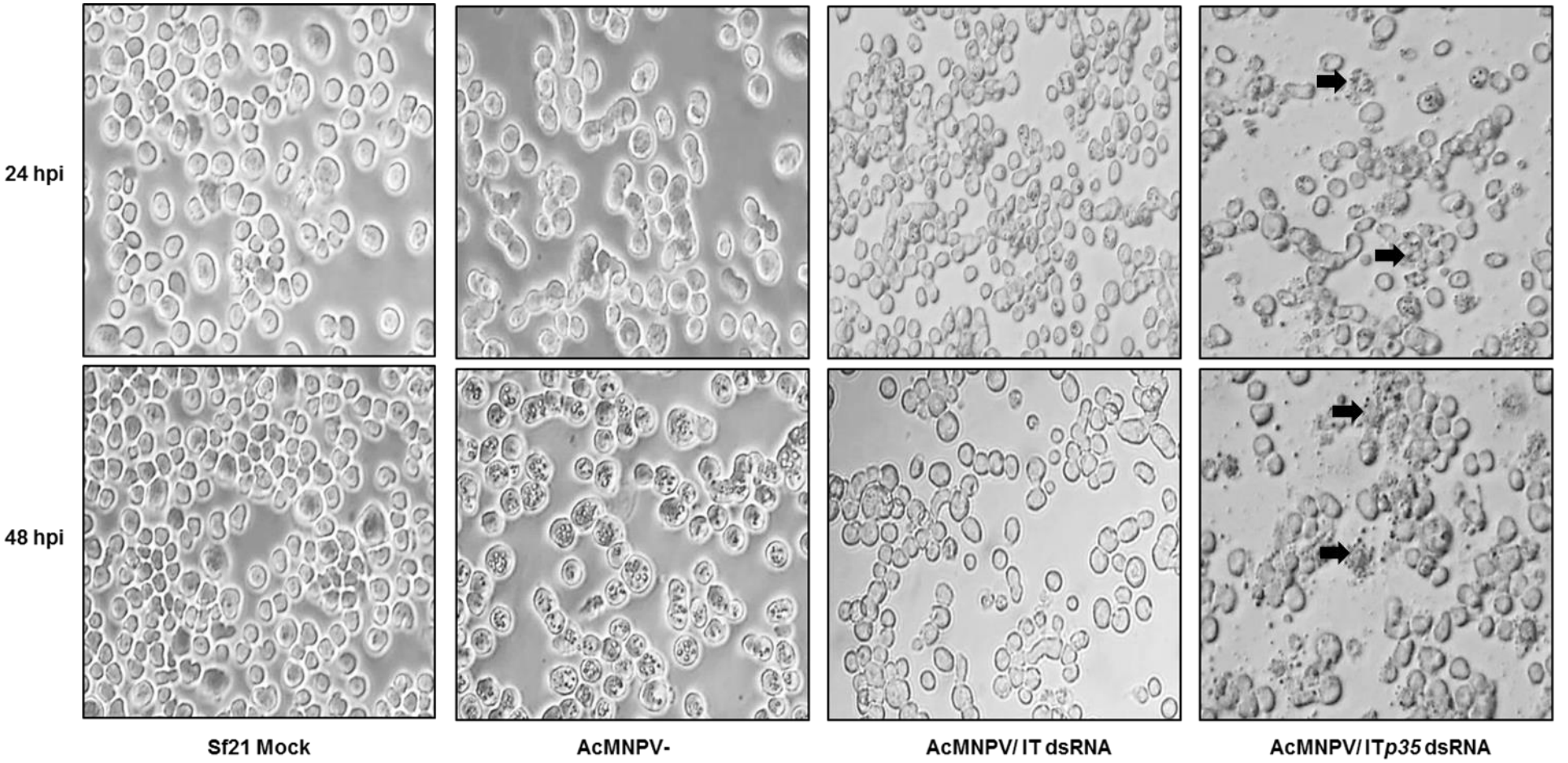


**Figure 5.10: Optimisation of transfection efficiency by apoptosis.**

Examination of the transfection efficiency of TransIT®-Insect transfection reagent (IT) in Sf21 cells. The cells were seeded in 6-well tissue culture plates at a density of 1 x $10^6$ cells/well and transfected with a mixture of (IT) and *p35* dsRNA or standard dsRNA as a control. The cells were then incubated overnight at 28ºC, after that the cells were infected with AcMNPV virus at an MOI of 1pfu/cell. At 24 and 48 hpi, the infected cells were visualized and imaged by a light microscope. Mock- and AcMNPV- infected Sf21 cells were included as negative controls. Arrow points to cell blebbing, which is indicative of apoptosis

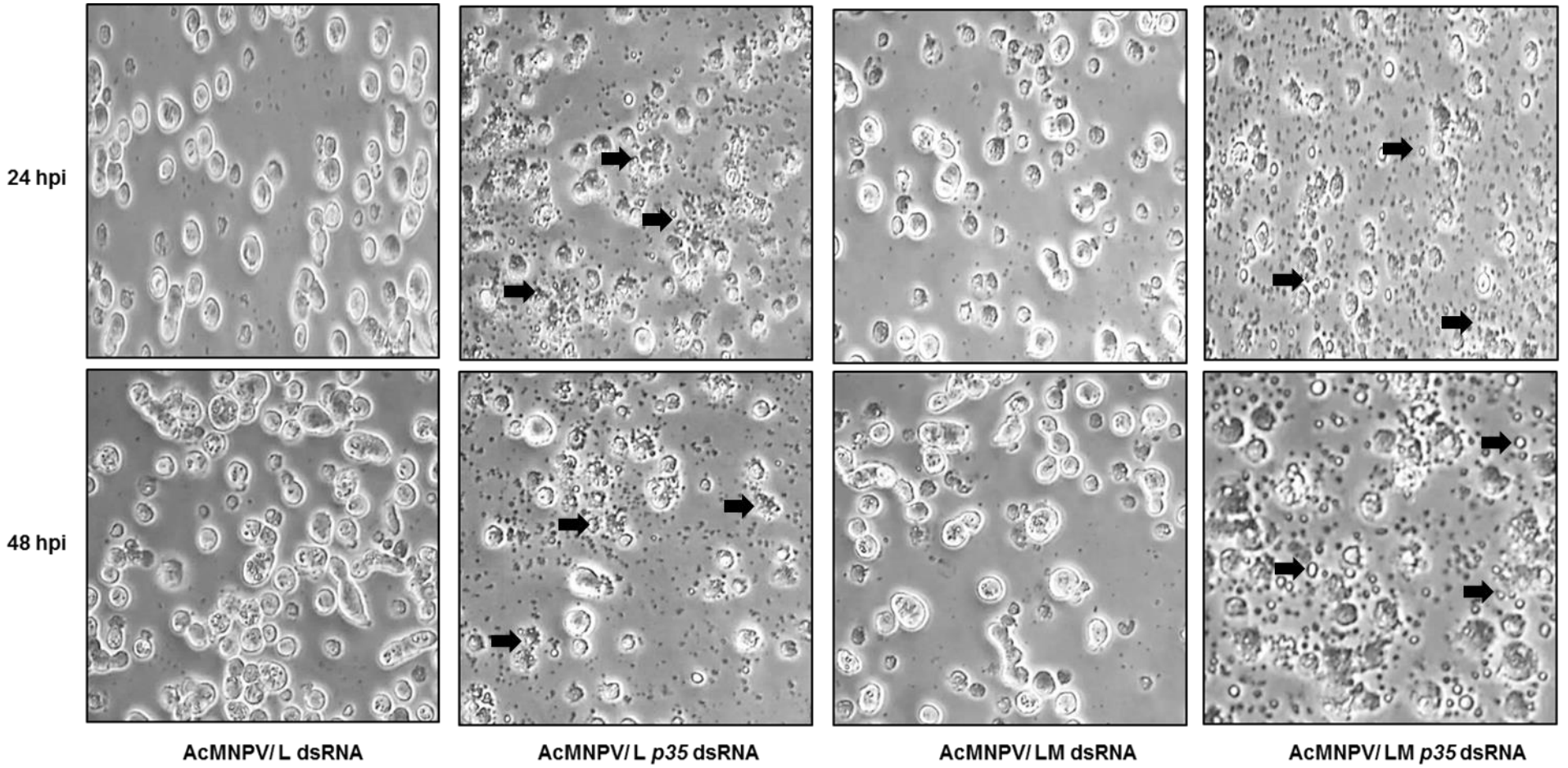


**Figure 5.11: Optimisation of transfection efficiency by apoptosis.**

Examination of the transfection efficiency of Lipofectine® (L) or Lipofectamine® RNAiMAX (LM) in Sf21 cells. The cells were seeded in 6-well tissue culture plates at a density of 1 x $10^6$ cells/well and transfected with a mixture of L or LM and *p35* dsRNA or standard dsRNA as a control. The cells were then incubated overnight at 28ºC, after that the cells were infected with AcMNPV virus at an MOI of 1pfu/cell. At 24 and 48 hpi, the infected cells were visualized and imaged by a light microscope. Mock- and AcMNPV- infected Sf21 cells were included as negative controls. Arrow points to cell blebbing, which is indicative of apoptosis.

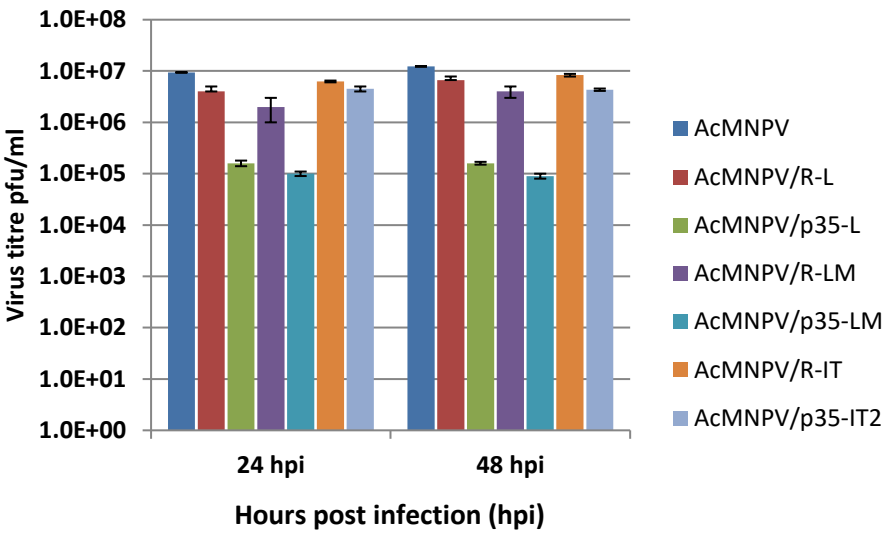


**Figure 5.12: Quantify of transfection efficiency by plaque assay.**
Examine the transfection efficiency of three different transfection reagents (Lipofectine® (L), Lipofectamine® RNAiMAX (LM) and TransIT®-Insect (IT)). Sf21 cells were seeded in 6-well tissue culture plate at a density of 1 x $10^6$ cells/well and transfected with a mixture of one transfection reagent and *p35* dsRNA or scrambled dsRNA (R). The cells were then incubated overnight at 28ºC, after that the cells were infected with AcMNPV virus at an MOI of 1pfu/cell. At 24 and 48 hpi, BV was harvested from the culture medium of infected cells and titrated by plaque assay. Mock- and AcMNPV- infected Sf21 cells were included as negative controls.

The HA display on the BV envelope surface was examined in Sf21 and Tni Hi5 cells in parallel with the optimisation of the transfection efficiency in Sf21 cells. Results demonstrated that HA synthesis in Tni Hi5 was much better than Sf21 cells (data not shown). Therefore, it was decided to examine the effect of *gp64* dsRNA on HA incorporation into BV in the next section using LM transfection reagent in Tni Hi5 cells without repeating the transfection efficiency optimisation in this cells. This was due to the high cost of the transfection reagents in addition to the time limitation.

### 5.9.2 Examination the effect of *gp*64 dsRNA on the full-length HA incorporation into FBUHA$^{polh}$ BV envelope surface

To examine whether targeting the *gp64* gene using dsRNA could inhibit or reduce GP64 glycoprotein production and improve full-length HA incorporation into the FBUHA$^{polh}$ BV envelope surface, Tni Hi5 cells were transfected overnight with 1µg of *gp64* dsRNAs or scrambled dsRNA using Lipofectamine® RNAiMAX transfection reagent. Cells were then infected with the FBUHA$^{polh}$ virus, mock-, FBUHA$^{polh}$-, FBUHA$^{polh}$-infected cells plus scrambled dsRNA were included as negative controls. After incubation at 28°C for 48 hours, BVs were harvested from the infected cell culture media and prepared for SDS-PAGE (Methods 2.5.2).

BV particles were analysed by immunoblotting as described previously in Chapter 4 Section 4.5.1. Immunoblotting analysis revealed that BV samples from FBUHA$^{polh}$ and scrambled samples contained an approximately equivalent amount of VP39 and GP64 at the expected molecular mass (Figure 6.9). In contrast, the amount of GP64 protein was decreased and it was undetectable on the BV envelope surface of GP64 dsRNA treated samples. VP39 also decreased compared to controls (Figure 5.13). However, HA incorporated into BV envelope remained approximately similar to control samples (Figure 5.13).

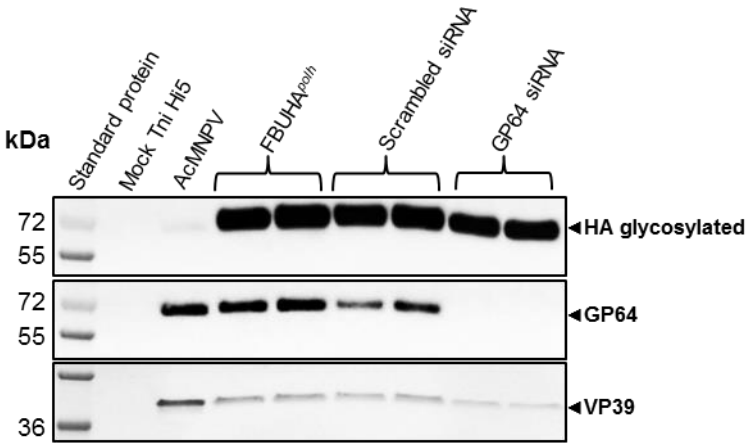


**Figure 5.13: Analysis of the HA incorporation into FBUHA$^{polh}$ BV envelope after *gp64* knockdown by dsRNA.**
Tni Hi5 cells were seeded in 6-well tissue culture plate at a density of 0.5 x $10^6$ cells/well and transfected with a mixture of either *gp64* dsRNA or with scrambled dsRNA plus transfection reagent and incubated at 28ºC for overnight. Subsequently, the transfected cells were infected with FBUHA$^{polh}$ virus at an MOI of 1 pfu/cell. At 48 hpi, BV was harvested from the culture medium of infected cells and proteins from BV particles were separated by SDS-PAGE gel (12%) and analysed by immunoblotting. The blot was developed using full-length HA (1:1000), GP64 (1:1000), VP39 (1:5000) primary antibodies and secondary alkaline phosphatase conjugated antibody (1:25000). Mock-, AcMNPV- and FBUHA$^{polh}$-infected cells were included as controls. The blot also includes standard protein markers: Precision plus protein Western C standard (Bio-Rad). Samples were presented in duplicates.

As previous studies in Sf21 cells have shown that knockdown of *gp64* can lead to reductions in BV titre (Schultz and Friesen, 2009; Lee *et al*. 2015), it was investigated whether *gp64* silencing using *gp64* dsRNA can result in preventing baculovirus assembly and reduce BV infectivity in Tni cells. Viruses from the culture media were titrated by plaque assay (Methods 2.2.4a). These results derived infectious virus titres of 6.6 x$10^3$ pfu/ml for *gp64* dsRNA treated samples, 5.8x$10^5$ pfu/ml for scrambled dsRNA samples and 6.4x$10^5$ pfu/ml for non-treated samples, which indicated that there was between 90-100 fold less infectious BV in the former sample than the latter two. This result was consistent with the immunoblotting (Figure 5.13) where less VP39 production was observed and non-detectable GP64 protein in BV produced in Tni Hi5 cells transfected with *gp64* dsRNA. These results suggest that *gp64* dsRNA inhibited the baculovirus GP64 expression and resulted in reduced the BV assembly and decreased the viral transmission between the

cells. However, HA incorporation into the BV envelope surface remains similar to scrambled dsRNA and non-treated BV, which is a promising result for improving the surface display technology.

## 5.10 Discussion

The main objective of this chapter was to investigate the incorporation of full-length HA into the baculovirus BV envelope surface using its own signal peptide and TMD, which were otherwise incorporated and displayed in low level as shown in Chapter 4 of this thesis when the truncated HA version (HA51) was inserted between signal peptide sequences and TMD of *gp64*. Furthermore, late *p6.9* and very late *p10* and *polh* promoters were used to drive HA expression. In addition to the aim of improving the HA incorporation into BV envelope, the best full-length HA recombinant virus will be also exploited as a platform for investigating the antigenicity of HA protein and serve as potential vaccine candidates for H1N1 type A influenza virus. Six HA recombinant baculoviruses were successfully generated using BacPAK6, BacPAK$^{HT}$ or FBU as the AcMNPV parental virus genome; PCR screening confirmed the integrity of these constructs (Table 5.1).

The effect of late and very late promoters activity on HA expression and the display was examined in Sf9 and Tni Hi5 cells in this study. Initially, the results showed that very late promoters *polh* and *p10* drive high HA protein expression better than the late promoter *p6.9* in both cell lines. However, the expression driven by the very late promoters was significantly higher in Tni Hi5 than Sf9 cell. Surprisingly, very little HA incorporation into AcHA$^{p6.9}$ BV envelope was observed compared to very strong display in AcRP19HA$^{polh}$ and AcHA$^{p10}$ BV. It was expected that the late *p6.9* promoter would exhibit the best HA display among the other viruses as during this time of infection, the vast majority of baculovirus BV would be produced (Rice and Miller, 1986), however, the reason behind that in this study is unknown.

As AcRP19HA$^{polh}$ and AcHA$^{p10}$ BV showed the best HA incorporation, it was decided to make a comparison between these two viruses during infection time course between 24-96 hpi. The result demonstrated that HA incorporation into AcRP19HA$^{polh}$ BV was increased from 48 hpi and achieved the maximum display level at very late times. In addition, this virus had shown consistently both glycosylated and non-glycosylated forms. In contrast, HA the non-glycosylated form in AcHA$^{p10}$ was unstable, beginning at 48 hpi and degraded after 72 hpi. However, AcRP19HA$^{polh}$ showed the highest HA display on its BV envelope, therefore, it was selected for the next investigations in this chapter.

To investigate the time of HA incorporation into AcRP19HA$^{polh}$ BV envelope, BV was harvested during time windows (0-96 hpi) and during the time course (24-96). The results

of this experiment demonstrated that HA incorporation starts from 24-48 hpi and increased to the maximum at 72-96 hpi. What was surprising in this study was how HA incorporation into BV continued in the very late phase of gene expression. It is usually assumed that the peak period of BV production is in the late phase of baculovirus replication (between 18 – 30 hpi). However, in this study, BV release from cells continued well into the very late phase. This may be a particular feature of virus replication in Tni Hi5 cells. Most studies on AcMNPV replication are carried out using *S. frugiperda* cell lines. It would be interesting to perform the analysis of BV production in one of these cell lines using the 24 hpi window sampling method that was used for Tni Hi5 cells in the chapter (Figure 5.5).

The recombinant baculoviruses containing full-length HA (Table 5.1) were characterised in Tni Hi5 and Sf9 insect cell lines to examine the native HA protein display in BV particles. The first set (AcHA$^{p6.9}$, Ac$^{HT}$HA$^{p6.9}$, FBUHA$^{p6.9}$), HA protein expression was driven by *p6.9* whereas the second set (AcHA$^{p10}$, Ac$^{HT}$HA$^{p10}$ FBUHA$^{p10}$) HA protein expression driven by *the p10* promoter.

To determine the efficient baculovirus system that can maximize the HA protein display, the BV samples from infected Tni Hi5 and Sf9 cells were examined and the results of immunoblotting analysis using HA-specific antibody demonstrated that HA protein under either *p6.9* or *p10* promoter was incorporated into BV envelope surface (Figures 5.6 and 5.7 A, B), respectively. The results showed that FBU was the best baculovirus expression vector for HA display over BacPAK6 and BacPAK6$^{HT}$ in both BV particles from Sf9 and Tni Hi5 cells from *p6.9* or *p10* promoter (Figures 5.6 and 5.7 A, B), respectively. However, this study also revealed that BV samples from Tni Hi5 infected cells culture medium showed significantly higher HA incorporation than Sf9 samples as judged by band intensities (Figure 5.6 and 5.7 B, A), respectively. Interestingly, the results observed by comparing different baculovirus expression vectors for displaying full-length HA in two different cell lines were consistent with Chapter 4, where FBU from Tni Hi5 cells was the best for the displaying HA51$^{TRUN}$ chimeric protein between other expression vectors. The possible reasons for this difference between the baculovirus expression vectors and two cell lines were discussed in detail in Chapter 4, therefore, no further discussion will be included in this chapter. Surprisingly, recombinant viruses using the BacPAK6$^{HT}$ baculovirus expression vector showed similar behaviour to what was observed in Chapter 4 of this thesis even when the HA was driven by either the *p6.9* or *p10* promoter. This observation may suggest that the *fp-25* mutation could affect the activity of these promoters in baculoviruses genomes. Further work needs to be done to test this hypothesis. Interestingly, HA protein from all BV particles was in the glycosylated form as detected at a molecular mass of approximately 70 kDa (Figures 5.6 and 5.7 A, B) whereas HA51-GP64$^{TRUN}$ chimeric protein showed both glycosylated and non-glycosylated forms (Chapter 4).

It is well known that most recombinant proteins produced in insect cell cultures are correctly folded and glycosylated (reviewed by Aksular, 2017). Several studies have demonstrated that glycosylation plays an essential role in the survival and spread of particular influenza virus subtypes (Seidel *et al.*, 1991; Schulze, 1997; Skehel and Wiley, 2000). On the other hand, it has been found that lack of glycosylation in the head of HA can limit H2N2 IAV virus circulation in humans (Tsuchiya *et al.*, 2001). In contrast, the ability of H1N1 and H3N2 influenza viruses to modify and acquire more glycosylation additional sites on the HA head results in their persistence and escape of the immune pressure and the neutralisation by antibodies (Abe *et al.*, 2004).

The full-length HA expressed under *polh* showed the best display on the AcRP19HA$^{polh}$ surface. Therefore, the production of BV was compared in Tni Hi5 cells infected with low or high MOI using monolayer or shake culture. It was demonstrated that HA produced in Tni Hi5 shake culture infected with low or high MOI showed two specific bands on western blot, the high molecular mass band was detected at the expected size of glycosylated HA 70 kDa, whereas the second band was detected at a molecular mass of ~ 42 kDa (Figure 6.1). This raised the question of whether the low molecular mass band represents the HA1 subunit resulting from protease activity encoded by *cath* in baculovirus genome or possibly due to non-specific antibody binding. In order to investigate this further, a new recombinant baculovirus-based on FBU system was constructed.

Subsequently, the new recombinant FBUHA$^{polh}$ BV was characterised in Tni Hi5 cells shake culture during a time course of 72 and 96 hpi. A western immunoblot analysis was carried out to make a comparison between FBUHA$^{polh}$ and AcRP19HA$^{polh}$ BV under the same conditions, Low molecular mass band 42 kDa in AcRP19HA$^{polh}$ BV sample was detected in addition to 70 kDa band of full-length HA. Only one band was detected in FBUHA$^{polh}$ samples at 70 kDa as shown in Figure 5.9 A. These results strongly suggested that the 42 kDa band come from full-length HA cleavage to produce HA1. In addition, the results in Figure 5.9 B showed that HA displayed on AcRP19HA$^{polh}$ BV envelope was unstable during the storage as most of HA 70 kDa protein was cleaved into HA1subunit. In contrast, HA from FBUHA$^{polh}$ BV samples showed only one band at 70 kDa. It has been previously reported that the serine protease encoded by baculovirus produced during the late phase of the viral infection is released into the cell culture medium when the virus-infected cells lyse (Gotoh *et al.*, 2001). Earlier studies established that this enzyme caused recombinant protein degradation in cell culture. They found that deletion of *v-cath* from the genome of the baculovirus result in the protection of recombinant protein from degradation and increase its stability (Possee *et al.*, 1999; Kaba *et al.*, 2004; Hitchman *et al.*, 2010a).

In this study, we hypothesised that targeting *gp64* gene by dsRNA could reduce the native GP64 glycoprotein protein expression, which may provide more space in the BV envelope

that can be occupied by full-length HA and result in better HA display. In order to examine this hypothesis, dsRNA targeting baculovirus GP64 envelope protein was designed and used for Tni Hi5 cells transfection. Subsequently, the cells were infected with FBUHA$^{polh}$, the results performed on BV samples showed that GP64 expression was suppressed by *gp64* dsRNAs and it was difficult to detect the protein on the western immunoblot. However, HA expression was unaffected. In addition, FBUHA$^{polh}$ infectious BV production was reduced by about 90-100 fold as indicated by plaque assay compared to untreated and scrambled dsRNAs samples. A similar observation was also reported by Valdes *et al.* (2003), when insect cells were transfected with *gp64* dsRNA, no GP64 protein was detected by either immunoblotting analysis or by confocal microscopy. They suggested that new viral progeny budding out through transfected cell membrane would lack GP64 protein from its envelope surfaces (Valdes *et al.*, 2003). In addition, they did more confirmation for these findings by testing the viral infectivity and they found that very low pfu compared to controls (Valdes *et al.*, 2003). Other studies had confirmed the inhibition of baculovirus replication in insect cells previously transfected with dsRNAs targeting *gp64* (Flores-Jasso *et al.*, 2004; Schultz and Friesen, 2009).

A more recent study by Lee *et al.* (2015) demonstrated that targeting *gp64* could reduce baculovirus BV assembly and budding-out through the infected cell membrane, however, the target gene expression under *polh* promoter was not affected. Therefore, the RNAi technology can be employed in baculovirus GP64 biological functions studies in insect culture, for instance, viral assembly, gene expression and baculovirus DNA replication result from inhibition of GP64 expression. Reducing baculovirus assembly in insect culture can be beneficial for reducing baculovirus virions, which can result in simplify purification process of recombinant proteins or VLPs in addition to reducing the cost during the purification and the minimization of adverse effects in clinical trials.

## 5.11 Conclusion

Overall from this chapter, It was shown that when choosing a promoter for full-length HA display using baculovirus expression system, the very late *polh* promoter has driven the highest expression levels and achieved the best HA incorporation into the FBUHA$^{polh}$ BV envelope surface. The Tni Hi5 cells were the most efficient for both protein production and HA display. Therefore, these optimum conditions were taken forward to investigate the antigenic nature of FBUHA$^{polh}$ BV and Tni Hi5 cells in chapter 6 of this thesis. In addition, the data presented in this chapter clearly demonstrated that the full-length HA displayed on FBUHA$^{polh}$ BV envelope surface was stable compared to HA displayed on AcRP19HA$^{polh}$ BV and can be used as antigen for mice vaccination experiment. Furthermore, the result

confirmed our hypothesis that silencing *gp64* using RNAi technology can reduce the native GP64 and enhance the HA incorporation into BV envelope surface.

Page intentionally left blank

# Chapter 6

# Antibody responses to baculovirus-displayed HA in a mouse model

## 6.1 Introduction

The utilisation of recombinant, human viral vectors to elicit an immune response in both animals and humans has experienced problems related to pre-existing immunity and toxicity (reviewed by Heinimaki *et al.*, 2017). Surface display technology based on invertebrate-specific baculovirus has the potential to produce novel vectors for recombinant subunit vaccine development (Musthaq *et al.*, 2014; Premanand *et al.*, 2018). The main concern raised about using these vaccines in man is the biosafety of baculoviruses for immunisation. Biosafety tests with baculoviruses, however, have indicated that there are no harmful effects on human health and the virus is non-pathogenic, replicative or carcinogenic in humans or mammalian cells (Chen *et al.*, 2011; Premanand *et al.*, 2018). Recombinant subunit vaccines based on influenza HA have been developed using an insect cell expression system and evaluated in humans and animals (reviewed by Premanand *et al.*, 2018). The US FDA approved Flublok®, the first influenza vaccine to be produced in insect cell culture for human use, in January 2013 (reviewed by Thompson *et al.*, 2015).

However, recombinant subunit vaccines based on purified proteins experience some issues. For instance, the hydrophobic nature of some recombinant proteins is one of the major obstacles in recombinant sub-unit vaccine development. In addition, these recombinant vaccines need to be used at high doses with adjuvants to promote immune responses (reviewed by Premanand *et al.*, 2018). Therefore, vaccine development based on baculovirus surface display technology may overcome some of these issues. By using this technology large complexes of the target protein(s) can be presented on the baculovirus BV envelope surface with no effect on virus replication and infectivity (Madhan *et al.*, 2010; Musthaq *et al.*, 2014). Furthermore, baculovirus-infected insect cells maintain the correct formation of the recombinant vaccine due to post-translational modifications such as glycosylation (Xianzong and Donald, 2007), phosphorylation (Hericourt *et al.*, 2000) and disulphide bond formation (Hodder *et al.*, 1996) that are essential for most eukaryotic proteins to maintain their stability and biological activity (Fiedler and Simons, 1995; Phizicky and Fields, 1995). Additionally, it has been reported that subunit vaccines based on the baculovirus display platform are capable of eliciting a strong immune response against foreign antigens without using adjuvants (Hervas-Stubbs *et al.*, 2007).

Budded virus display of full-length HA was optimised in Chapter 5 of this thesis, which concluded that the highest yield of displayed HA was achieved when gene expression was driven by the *polh* promoter in FBUHA$^{polh}$ virus produced in Tni Hi5 cells. Therefore, the aims of this chapter were to analyse the immune or antibody response to HA displayed within BV and compare that to the responses raised against recombinant virus-infected whole cells.

## 6.2 Antigen preparation

Prior to preparing the antigens for immunisation studies, a feasibility test was completed using BV samples obtained from monolayer and shake/suspension cultures of FBUHA$^{polh}$-infected Tni Hi5 cells at low or high MOI. Samples were prepared and treated as described previously in Chapter 5 (section 5.7). Glycosylated HA was detected on western blots from low and high MOI samples at the expected molecular mass of approximately 70 kDa (Figure 6.1). Based on band intensities, the shake culture was better than the monolayer culture in producing BV with HA displayed on its envelope at both MOI used. However, no discernible differences were observed between these two samples. This result suggested that infecting Tni Hi5 at low MOI could be used to produce sufficient BV for antigen preparation.

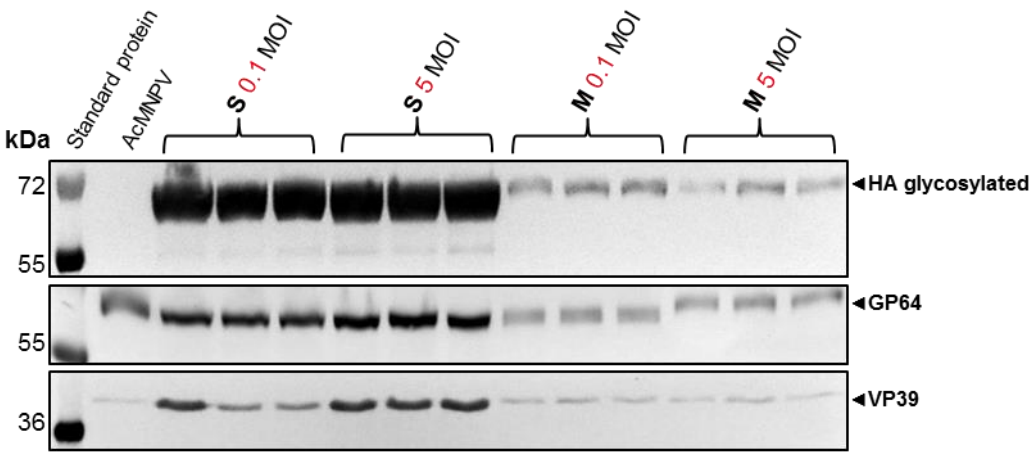


**Figure 6.1: Immunoblot analysis of HA from BV produced in TnHi5 cells infected with low (0.1 pfu/cell) or high (5 pfu/cell) MOI in either monolayer or shake cultures.**
Tni Hi5 cells were seeded in 35 mm tissue culture dishes at a density of (1x10$^6$ cells/dish) or in 25 ml conical flasks at a density of (1x10$^6$ cells/ml) in monolayer or shake cultures, respectively. Cells were infected with FBUHA$^{polh}$ virus at either 0.1 or 5 MOI. The cultures infected at 0.1 MOI were harvested at 5 dpi and the cultures infected at 5 MOI were harvested at 3 dpi. Proteins from the BV fraction were separated by SDS-PAGE gel (10%) and analysed by immunoblotting. The blot was developed using primary anti-mouse GP64 (1:1000), VP39 (1:5000) or HA antibody (1:1000) and secondary anti-mouse alkaline phosphatase conjugated antibody (1:25000). Mock- and AcMNPV were included as negative controls. The blot also includes standard protein markers: Precision plus protein Western C standard (Bio-Rad). M= monolayer culture, S= shake culture.

## 6.3 Preparation of test and negative control antigens for immunisation studies

To prepare antigen for immunisation studies, Tni Hi5 cells were seeded in shake cultures at a density of 1x10$^6$ cells/ml, infected with FBUHA$^{polh}$ or FBUNull (no HA as a negative control; kindly provided by, OET Ltd ) virus at an MOI of 0.1 pfu/cell and incubated at 28ºC. After 5 days, virus-infected cells were harvested from the culture medium using low-speed centrifugation, washed twice with PBS, re-pelleted at low-speed centrifugation and stored at -80ºC until immunization (Methods 2.2.6). BV particles were purified from the clarified

culture media using sucrose-gradients (Methods 2.2.6). Subsequently, BV particles were titrated by QPCR (Methods 2.2.4b). The viruses titres were; FBUHA$^{polh}$: 6x10$^{8}$ qpfu/ml and FBUNull: 5x108 qpfu/ml. Purified BV particles were diluted to a final concentration of 1x10$^{7}$ or 1x10$^{8}$ pfu/ well. In addition, FBUHA$^{polh}$- and FBUNull-infected cells pellets were prepared to a final density of 1x10$^{5}$ and 5 x 10$^{5}$ cells/well. To check HA production, both BV and whole Tni Hi5 cell pellets were separated in a 10% SDS-PAGE gel followed by immunoblotting using a monoclonal antibody raised against the protein (Methods 2.5.2 and 2.5.2b). Native influenza H1N1 antigen (Bio-Rad) was included as a positive control. Figure 6.2 shows one strong band of glycosylated HA at the expected ~70 kDa in both FBUHA$^{polh}$ BV and FBUHA$^{polh}$-infected cells. Therefore, these were taken forward as the antigen dose to be used for purified BV and whole cell antigens in the immunization study. There was none evident in the negative control samples as expected. The positive control H1N1 antigen sample showed a faint band at approximately 64 kDa (Figure 6.2). The immunoblotting profile in Figure 6.2 confirmed the presence of antigens in the purified BV particles and virus-infected cells samples, it is also helped to choose the antigen dose for the immunisation experiments. Band intensities were stronger from 2.5x10$^{5}$ cells/well and 1x10$^{8}$ pfu/well from FBUHA$^{polh}$ virus BV and FBUHA$^{polh}$-infected cells samples, respectively (Figure 6.2). Therefore, after consultation with BioServ Ltd, these amounts were considered as suitable antigen doses to be used for immunization experiments.

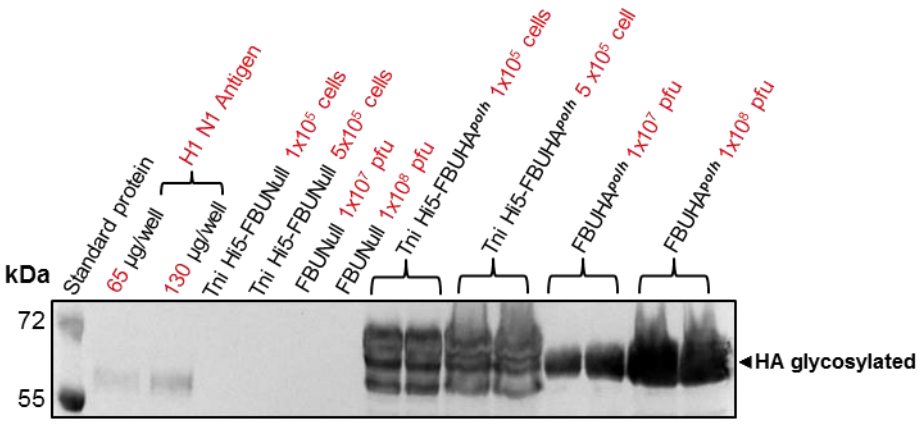


**Figure 6.2: Immunoblotting analyses of FBUHA$^{polh}$ BV and infected cell samples.**
Tni Hi5 cells were seeded in shake culture and infected with FBUHA$^{polh}$, the cells were harvested by centrifugation. The BV particles from culture medium were purified using 10-50% sucrose gradient. Proteins from BV particles and cell lysates were separated by SDS-PAGE gel (10%) and analysed by immunoblotting. The blot was developed using primary anti-mouse full-length HA antibody (1:1000) and secondary anti-mouse alkaline phosphatase conjugated antibody (1:25000). FBUNull, FBUNull-infected cells were included as negative controls and H1N1 antigen as a positive control. The blot also includes standard protein markers: Precision plus protein Western C standard (Bio-Rad). Samples were presented in duplicates.

### 6.3.1 Mouse immunisation studies

Mouse immunisations were carried out by BioServ Ltd in Sheffield, UK through collaboration with Oxford Expression Technologies Ltd. All work was performed under BioServ Home Office licences and ethics approvals. Unfortunately, BioServ, owing to their internal protocols, were unable to use the positive control antigen characterised in Figure 6.2, even though this had been sourced as an inactivated virus. Therefore, no positive control was used in the immunisation study; only purified FBUHA$^{polh}$ BV and FBUHA$^{polh}$-infected Tni Hi5 cells were evaluated for their potential to produce an immune response in mice. Briefly, 12 female BALB/c mice, aged eight weeks and certified pathogen-free were divided randomly into four groups. Blood sera were collected from each group on day 0 and were considered as pre-immunisation sera. The 12 mice were then immunised subcutaneously with each antigen prepared in section 6.2 combined with Freund's complete adjuvant (Sigma) in the ratio 1:1. Table 6.1 summarises the antigen doses used for the immunization test.

After the first immunisation, sera were collected via venepuncture at 21 days post vaccination (dpv). Thereafter, mice received the same antigen/dose (Table 6.1) as a booster immunization. Two weeks later (35 dpv), immunised mouse sera were collected and the mice received the final booster immunisation dose. After 60 days, mice were sacrificed and sera were collected from the whole blood. Sera received from BioServ were examined by ELISA for serum antibodies.

**Table 6.1: Summary of antigens and doses used for immunization**

| Group | Antigen | Dose/mouse |
|---|---|---|
| 1 | FBUNull BV (BV-Null) | $1x10^8$ pfu |
| 2 | FBUNull-infected Tni Hi5 cells (Tni-Null) | $5x10^5$ cells |
| 3 | FBUHA$^{polh}$ BV (BV-HA) | $1x10^8$ pfu |
| 4 | FBUHA$^{polh}$-infected Tni Hi5 cells (Tni-HA) | $5x10^5$ cells |

### 6.3.2 Post-vaccination serum antibodies analysis

In order to investigate whether influenza HA-specific antibodies had been elicited by the recombinant baculovirus BV constructs produced in this study, indirect standard enzyme-linked immunosorbent assay (ELISA) was performed to examine the sera from vaccinated mice. To ensure optimum ELISA performance, it was essential to determine the best sera concentration that can give a strong detectable signal with low background noise. Briefly, post-immunisation sera from mice vaccinated with BV-HA antigen was optimised by preparing serial dilutions (Figure 6.3).

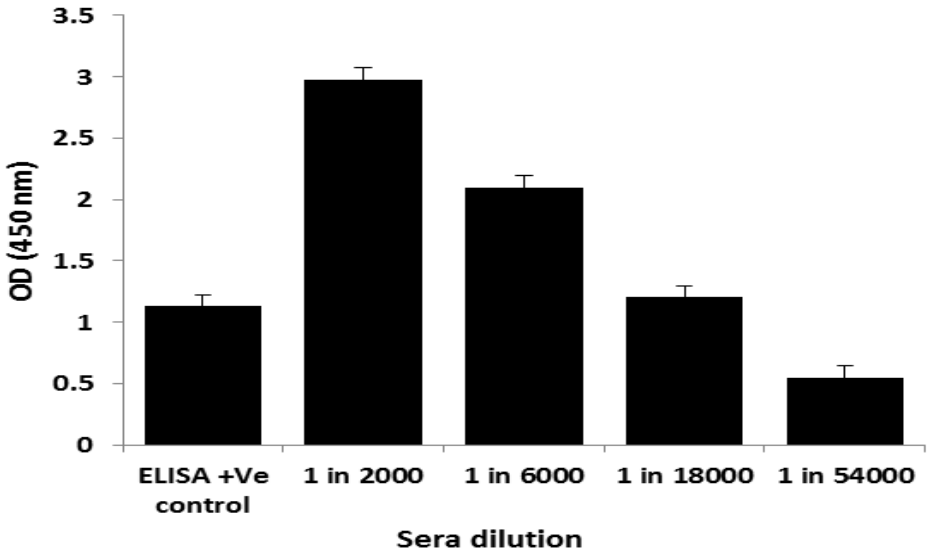


**Figure 6.3: Optimisation of post-vaccination serum antibodies dilutions using ELISA.**
To determine the dilution of HA-specific antibodies that produce optimum ELISA performance, sera from mice group vaccinated with BV-HA antigens were diluted three-fold in ELISA blocking buffer. A 96-well plate was coated overnight with 20 ng/well of native influenza H1N1 antigen prepared in coating buffer. Subsequently, ELISA examined each sera dilution in triplicate against the antigen. HA antibody (Abcam Ltd) was included as ELISA positive (+ve) control. Error bars represents mean ± SD (n=4)

The result showed that the signal from the 1:2000 dilution was saturated and gave an OD value of 2.98 (Figure 6.3). In contrast, a 1:6000 dilution or higher gave a detectable signal; interestingly even a very high dilution of 1:54000 gave a strong detectable signal with OD about 0.55 (Figure 6.3). It was decided to use 1:10000 dilutions in ELISA to examine all sera from vaccinated mice groups.

Following the detection of the best sera dilution, indirect ELISA was performed to analyse the serum antibodies from blood collected on 0, 21, 31 and 60 dpv. Mice vaccinated with BV-HA elicited a high level of total HA-specific antibodies on day 21 post vaccination with an OD value of 2.02 compared to Tni-HA OD value of 1.67 (Figure 6.4 A), however, the difference between the OD values was found not to be statistically different when evaluated by t-test $P>0.05$ (Figure 6.4 A). Pre-immunisation sera (day 0) and sera from the negative controls, BV-Null and Tni-Null antigens, did not elicit any HA-specific antibodies at any time point (Figure 6.4 A).

When the serum antibodies from 31 dpv were evaluated by ELISA, both BV and infected cells samples showed a significant increase in the OD values (2.52, 2.24), respectively, compared to day 21. However, the level of antibodies elicited by BV-HA antigen after the booster vaccination was significantly higher than that elicited by Tni-HA antigen ($p<0.05$, Figure 6.4 B). Sera collected after the third and final immunisation were also examined by ELISA and no significant difference was observed in the OD values (2.59, 2.23, $p>0.05$) for

both BV and infected cells antigens, respectively (Figure 6.4 C). Overall, these results showed that there was no significant difference in the immune response between the mice group vaccinated with purified BV-HA or whole Tni-HA cells antigens.

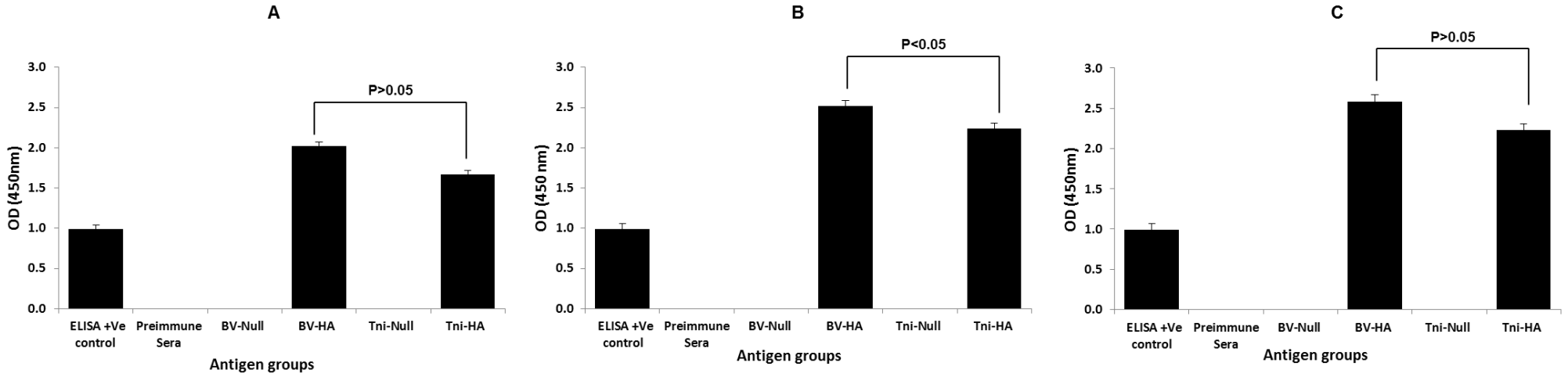


**Figure 6.4: Analysis of post-vaccination sera antibodies using an ELISA.**

To examine HA-specific antibodies in sera collected from vaccinated mice on 21 **(A)**, 31 **(B)** and 60 **(C)** dpv using an indirect ELISA, a 96-well ELISA plate was coated overnight with 20 ng/well of native influenza H1N1 antigen prepared in coating buffer. Subsequently, 1:10000 dilution from each serum was examined in triplicate against the antigens. Each antigen group is represented by the average value of data obtained from four group-specific mice. Group 1: BV-Null, Group 2: Tni-Null, Group 3: BV-HA, Group 4: Tni-HA. HA antibody (Abcam Ltd) and pre-immune sera were included as ELISA positive (+ve) control and as HA-specific antibodies negative control, respectively. Error bars represents mean ± SD (n=4).

## 6.4 Haemagglutination inhibition (HAI) assay

In order to examine whether the post-vaccination sera antibodies are able to inhibit attachment of the influenza virus to red blood cells and prevent haemagglutination, an HAI assay (Webster *et al*., 1991) was performed using New Caledonia 20/99 H1N1 influenza A virus (Bio-Rad, Methods 2.8.2) as antigen. Overall, serum samples from vaccinated mouse groups at 21 dpv with $1x10^8$ pfu BV-HA vaccine showed that a dilution of 1:160, but not higher was able to block haemagglutination of influenza virus compared to sera diluted from the mice group vaccinated with $5x10^5$ Tni-HA (≥80, Figure 6.5). No HAI antibody responses were detected in BV-Null or Tni-Null serum samples (Figure 6.5). These results were consistent with the ELISA for the same serum samples (Figure 6.4). These results suggest that the HA antigens are immunogenic and able to elicit a strong humoral immune response in the experimental vaccinated mice and suggested that sera antibodies might be able to neutralise influenza A virus.

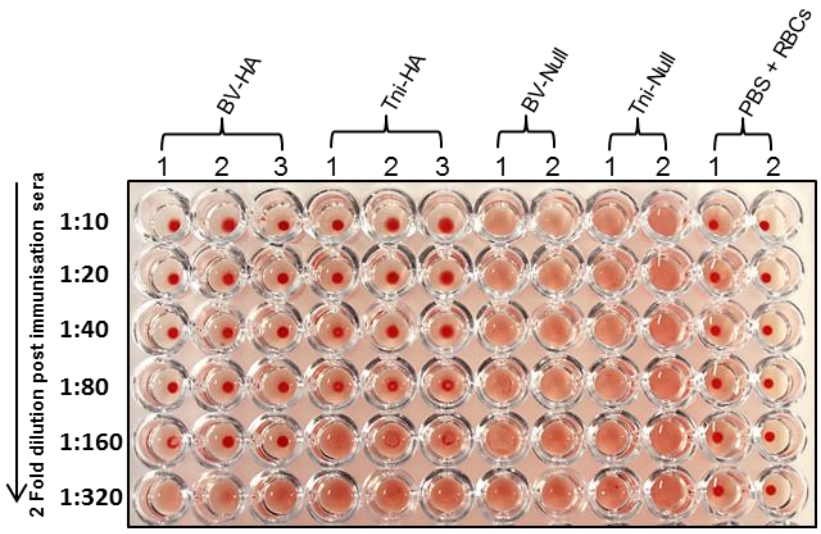


**Figure 6.5: Haemagglutination inhibition assay.**
In this assay 25 µl of 4HAU of H1N1 influenza A virus (Bio-Rad) was incubated with 25 µl of 2-fold serially diluted first sera post vaccination from each antigen in 96- well plate for 30 minutes at room temperature. Then 50 µl of chicken RBCs at a concentration of 0.5% were added and mixed gently and the plate incubated at room temperature for 60 minutes before assessing the assay. PBS and chicken RBCs were included as a control for RBCs.

## 6.5 Discussion

In recent years, large numbers of research studies have focused on exploring the baculovirus expression system as a tool for vaccine development. The production of recombinant vaccines based on the baculovirus platform offers several advantages, such as higher active recombinant protein(s) yields, low cost of production, easy to generate and scale up (Musthaq *et al.*, 2014). Also important is the fact that baculoviruses are non-

pathogenic for humans in contrast to conventional human vaccines based on live attenuated viruses such as (polio, measles, yellow fever, influenza virus; Premanand *et al.*, 2018). Additionally, baculoviruses exhibit proper glycosylation and other post-translation modifications essential to elicit systemic, mucosal and cellular immune responses (Treanor *et al.*, 2007; Lu *et al.*, 2012).

It has been reported by several studies that full-length protein(s) and domains of protein(s) could be displayed successfully on the recombinant baculovirus BV envelope surface as a fusion protein when it is fused to the baculovirus *gp64* (Mottershead *et al.*, 1997; Grabherr and Ernst, 2010). These BV particles produced a good immune response in experimental animals (Lindley *et al.*, 2000; Yoshida *et al.*, 2003; Yang *et al.*, 2007). In addition, it was reported that live recombinant baculovirus displaying HA protein could be employed as an effective antigen to elicit a great humoral and cellular immune response against influenza virus infection (Prabakaran *et al.*, 2013). By presenting the targeted vaccine on the baculovirus envelope surface, it might be more easily recognised by the immune system and is more likely to elicit antibodies (Prabakaran *et al.*, 2010).

The full-length HA expressed under *polh* prompter control showed the best display on the FBUHA$^{polh}$ surface in the results presented in Chapter five of this thesis. Therefore, the main object of this chapter was to explore the antigenicity of FBUHA$^{polh}$ BV *in vivo* in mice by a pilot vaccination experiment. Initially, the production of BV was compared in Tni Hi5 cells infected with low or high MOI using monolayer or shake culture. It was demonstrated that HA produced in Tni Hi5 shake culture infected with low or high MOI showed identical HA display on BV envelope. This result suggested that sufficient BV could be produced in the antigen preparation using low MOI. This approach conserves virus stocks and makes future scale-up more cost-effective.

The analysis of post-vaccination serum antibodies by indirect ELISA revealed that both live purified BV-HA and Tni-HA cells were capable of eliciting high levels of HA-specific antibodies against influenza virus H1N1 from the first booster immunization in the experimental mouse groups. In addition, high levels of specific HAI antibodies were observed after the first vaccination in mice immunised with BV-HA or Tni-HA antigens. Interestingly, BV-HA antigens elicited the highest levels of influenza A/New Caledonia specific HAI antibodies 160 compared to Tni-HA antigens, which was ≥80. Cox (2013) reported that HAI antibody response ≥40 would be able to provide the populations with about 50% protection against influenza infection or disease.

These results were consistent with the previous studies where the mice immunised with live baculovirus displaying full-length recombinant HA protein elicited a high level of serum HA-specific antibodies against influenza virus compared to inactivated influenza virus vaccines.

They suggested that the significant increase in the immune response was due to baculovirus BV, which acts as a strong adjuvant (Musthaq *et al.*, 2014; Sim *et al.*, 2016; Heinimaki *et al.*, 2017). Several studies have reported the effectiveness of baculovirus surface display technology to present viral envelope proteins on the BV envelope. These recombinant viruses have shown their ability to induce both humoral and cellular immune responses against foreign antigens in the vaccinated animal (Yang *et al.*, 2010; Musthaq *et al.*, 2014; Sim *et al.*, 2016). Early studies have reported the efficacy of baculovirus displaying HA to elicit a high level of anti-HA antibodies against H1N1 and H5N1 influenza viruses in the mouse model after vaccination (Yang *et al.*, 2007; Prabakaran *et al.*, 2010). Furthermore, a study by Prabakaran *et al*. demonstrated that a high level of specific IgG and IgA antibodies could be induced in the vaccinated mice with live recombinant baculovirus BacHA due to systemic and mucosal immune responses stimulation, respectively (Prabakaran *et al.*, 2010). In contrast, mice vaccinated with inactivated BacHA elicited a low level of immune responses (Prabakaran *et al.*, 2010). In addition, live BacHA vaccine results in higher HAI antibodies against the H5N1 influenza virus infection compared to inactivated BacHA (Prabakaran *et al.*, 2010). They assumed that these differences between the immunogenicity of live BacHA and inactivated BacHA in the vaccinated mice could be due to retaining the functional oligomeric conformation of the HA displayed on the live BV envelope surface, which can result in enhancement of immune responses in comparisons with inactivated baculovirus.

To our knowledge, this is the first study to investigate Tni Hi5 cells to produce recombinant BV as an antigen for HA vaccine development. Researchers do not normally use these for BV production because of the *fp25* mutation effect on gene expression under the *polh* promoter, in addition to the production of lower BV titre. However, this study has shown that even though the BV titre per ml was less than using Sf9 cells, more HA was displayed on the BV envelope. This may be because, in Tni Hi5 cells, processing of membrane proteins to the cell surface and incorporation into BV is more efficient, perhaps because less BV is being made. While *S. frugiperda* cells have been used extensively for fundamental studies on AcMNPV replication owing to ease of culture and high BV titres, they do represent a heterologous cell type for this virus. In addition, this study has shown for the first time use Tni Hi5 cells as an antigen to elicit the immune response in the animal model. However, further studies are required to analyse the cell-mediated immune response and protection in animal models before a solid conclusion could be drawn.

## 6.6 Conclusion

In conclusion, data presented in this chapter has clearly shown the potential use of FBUH$^{Apolh}$ BV or FBUHA$^{polh}$-infected-Tni Hi5 expressing HA as antigens to elicit a strong

immune response (HA-specific antibodies) in experimental vaccinated mice from the first immunization. Furthermore, post-immunisation sera evaluation using indirect ELISA and HAI assay using H1N1 human influenza virus as an antigen demonstrated that the antibodies react efficiently against the antigen even at high dilutions, suggesting that these antigens could be promising vaccine candidates and an alternative strategy that can enhance broad and persistent protection against H1N1 influenza virus infection.

Taken together, the surface display technology described here allows fast and cost-effective production of large amounts of target antigen(s). Furthermore, this technology could be exploited to produce seasonal influenza vaccines or any new emerging pandemic influenza outbreaks. Due to time limitations, challenging with H1N1 influenza virus could not be evaluated in the immunised experimental mice.

# Chapter 7

# Final Discussion and Future Work

## 7.1 Introduction

Since the 1918 pandemic, influenza has been considered as a serious threat to human health (reviewed by Premanand *et al.*, 2018). To date, vaccination is the most effective method to prevent and control the spread of the influenza virus. However, conventional human inactivated influenza virus vaccines produced in embryonated chicken eggs face several challenges. For instance, the vaccine production process is considered time-consuming. It takes several months from virus amplification to vaccine validation (Gerdil, 2003). In addition, the immune responses that result from these vaccines are not completely effective and are maintained for only a short duration after vaccination. Furthermore, some individuals are allergic to the residual egg proteins present in this vaccine (Behzadian *et al.*, 2013).

To overcome the challenges mentioned above, alternative vaccine development platforms are under consideration or have already been introduced. For example, Flublok® comprises influenza virus HA proteins synthesised using the baculovirus expression system (reviewed by Thompson *et al.*, 2015). Owing to the fact that vaccine production can be scaled-up rapidly in insect cells without the need first to derive a reassortant influenza virus for use in embryonated eggs, development time is only a few months. The vaccine is recommended for those with an allergy to egg proteins.

A further development of the insect virus expression system is a platform based on baculovirus surface display technology to develop a subunit vaccine. This exhibits several advantages: a subunit protein vaccine displayed on the BV envelope surface is easily recognised by the immune system and elicits high levels of antibodies (Yoshida *et al.*, 2003; Yang *et al.*, 2007). In addition, no pre-existing immunity has been observed in humans to the BV compared with mammalian viral vectors. The virus genome is silent in mammalian cells, meaning that BV cannot replicate in mammalian cells and produce infectious virus. Furthermore, large-scale vaccine production is readily achieved in insect cells in serum-free medium at low cost (Strauss *et al.*, 2007). The purification of BV is quite straightforward, although the long-term stability of a vaccine based on this approach remains to be demonstrated. However, the baculovirus surface display technology remains a promising tool for vaccine development.

The overall aim of this thesis was to explore factors that might improve the surface display of influenza virus haemagglutinin on baculovirus budded virus particles and its potential as a vaccine. To achieve this aim, HA was expressed under late and very late baculovirus promoters using different insect cell lines. This study was the first to compare different baculovirus expression systems, surface display techniques and examined different promoters and HA coding structure to express the HA protein.

## 7.2 Discussion of thesis results and future work

In this thesis, several HA surface display recombinant baculoviruses were generated. The expression and biological activity of HA protein were monitored using an immunoblotting assay with an HA-specific antibody, and haemagglutination and haemadsorption assays, respectively. Previous studies have demonstrated that target protein(s) fused to the GP64 transmembrane protein can be incorporated into the baculovirus BV envelope surface (Grabherr and Ernst, 2010). Furthermore, it has been reported that using a short version of GP64 containing just the signal peptide and TMD only were enough to achieve surface display of a target protein. By avoiding the need to use the full-length GP64 this strategy should avoid the obstacles resulting from using a large transfer vector (Pidre *et al.*, 2013) and permit the display of recombinant proteins in their native form, free of most GP64 components.

Early work conducted in this thesis examined the feasibility of using the occluded form of baculovirus enveloped virions for both transduction of mammalian cells and potentially as surface display vectors. This option was quickly dismissed owing to the difficulty in obtaining sufficient ODV from polyhedra for experimental work and the realisation that the mechanisms for inclusion of glycoproteins into these structures are not known in sufficient detail to permit them to be applied to recombinant proteins. However, it maybe that ODV could be used for display of proteins via the use of capsid structures as has already been achieved by displaying GFP protein on baculovirus capsid to track the virus transduction in mammalian cells (Kukkonen *et al.*, 2003).

The major aim of this study, therefore, was to examine strategies for improving the HA display on the BV. Initially, sequences encoding HA were amplified by PCR so that the regions encoding the signal peptide and TMD could be removed. In order to display the truncated HA version on the baculovirus BV envelope surface, the target gene was inserted between the signal peptide and the TMD of a shortened version of GP64 in pBACsurf-1-*polh* under the control of the *polh* promoter. Subsequently, surface display recombinant baculoviruses were generated using three different parental viruses: BacPAK6, BacPAK6$^{HT}$ and FBU as described in detail previously in this thesis. These were compared with AcRP19HA$^{polh}$, which comprised a wild-type virus genome producing HA, also under the control of the *polh* promoter. It was anticipated that at least one of the new viruses would be superior for HA surface display. Amongst the recombinant viruses tested, FBUSurfHA51$^{polh}$ showed the best intracellular HA, which was superior in Tni Hi5 compared to Sf9 cells. However, this did not translate into better HA51-GP64$^{TRUN}$ chimeric protein display on the BV envelope surface compared to full-length HA displayed on wild-type AcRP19HA$^{polh}$ BV. This suggested that using the native HA signal peptide and TMD was

the most efficient way to display this protein instead of using the GP64 signal peptide and TMD.

This result conflicts with previous findings because Yang *et al.* (2007) reported that substituting the signal peptide and cytoplasmic domain (CTD) of HA (rHA) with a signal peptide and (CTD) derived from *gp64* (rHA*gp64*) resulted in greater HA incorporation into virion envelopes. Utilising the CTD of the HA with the *gp64* signal peptide impaired HA display, suggesting that the HA expression was adversely affected by the non-baculovirus CTD. It is hypothesised that perhaps the rHA and rHA*gp64* experience different levels of palmitoylation. Consequently, rHA is more likely to be trapped within the lipid rafts, while rHAgp64 may be eliminated, which might result in more HA incorporation into the baculovirus BV envelope surface. Alternatively, as demonstrated in this thesis, superior full-length HA incorporation into BV may be directly related to using a native signal peptide, coding sequence and native TMD. The structure of this protein may be ideal for transport through the cellular pathways to the plasma membrane and subsequent incorporation into AcRP19HA$^{polh}$, compared to the truncated HA surface display baculoviruses (Chapter 4). However, in this thesis, the HA51-GP64$^{TRUN}$ chimeric protein and full-length native HA were found to be translocated to the membrane of the infected cell and biologically active as indicated by confocal microscopy, haemagglutination and haemadsorption, respectively. Therefore, it remains unclear why the display of the hybrid HA was less efficient than that of the native protein.

A result that was perhaps less surprising was the relatively poor synthesis and display of the truncated HA by BacPAK6$^{HT}$. This virus is essentially wild-type, but in addition to being polyhedrin-negative has a mutation within *fp25*, which reduces transcription by the *polh* promoter but enhances BV production. However, it was hoped that subsequent experiments where different baculovirus gene promoters were utilised for HA expression would produce better results.

The effectiveness of baculovirus late and very late promoters in different insect cell lines was also investigated (Chapter 5). It had been anticipated that there might be some advantage in using late gene promoters for producing displayed HA since these are active in the phase of virus replication where most baculovirus glycoproteins are synthesised, particularly GP64. Further, other studies had shown superior production of some secreted recombinant proteins in the late phase compared with the same protein made in the very late phase. A previous study by Lin and Jarvis (2013) reported that the production of secreted alkaline phosphatase (SEAP) was significantly higher in Sf9 cells co-transfected with the delayed early *39*K promoter than cells co-transfected with the late *p6.9* and very late *polh* promoter constructs after baculovirus infection. It was surprising, therefore, that the late *p6.9* promoter was unable to surpass or even match HA production by the *polh*

promoter. It might have been interesting to use the *gp64* promoter, but *p6.9* is considered one of the strongest late promoters and has been used successfully to produce other recombinant proteins previously.

The very late *p10* promoter was also used to express HA for BV display. This came close to matching the results with the *polh* promoter. Since *p10* is expressed slightly earlier than *polh*, beginning in the late phase of virus replication it had been expected to surpass the use of *polh*.

The results obtained when using baculovirus gene promoters in the late phase challenge the initial assumption that they would be better than the use of the *polh* promoter. The experiments that analysed BV production and HA display in 24 hour windows after infection showed that these both continue to very late times (72 hp.i.). It is generally assumed that BV synthesis declines significantly in the very late phase, but this idea may have to be modified in view of the results obtained in this study.

Another result that was surprising and a little disappointing was the failure of a virus with a mutation in *fp25* to enhance BV HA display. Although this virus backbone is not recommended for use with the *polh* promoter, other promoters such as *p6.9* or *p10* should be unaffected by FP25 deficiency. The production of BV is enhanced by *fp25* mutations, particularly in *T. ni* cells. However, this increased BV output was not accompanied by a higher HA display.

Ultimately, these results demonstrated that more HA was incorporated into the recombinant baculovirus BV envelope using *flash*BACULTRA, a virus with multiple gene deletions and when the HA was expressed under the control of the *polh* promoter in Tni Hi5 cells. There were significant advantages also for the stability of the displayed HA, which escaped proteolytic degradation to the HA1 subunit. This conclusion was based purely on the estimated size of the degraded protein and requires confirmation using other methods such as protein sequencing.

A very preliminary study in this thesis examined the use of dsRNA to reduce the synthesis of GP64 in an attempt to maximise HA display. The rationale for this work was that by reducing the amount of GP64 in a BV hat this would allow more HA to be displayed. The results showed that GP64 incorporation in BV could be reduced but it is unclear yet whether or not HA display was increased. The large reduction in GP64 content by BV does pose the question of how much of this protein is required to attain virus budding from the plasma membrane. The limits of the immunoblotting technique used here are probably too crude to detect very small quantities of protein. Further work should use a combination of qPCR and ELISA to assess the amount of virus that buds from virus-infected cells. Transfection of cells with a *gp64*-deficient AcMNPV would also provide an absolute answer as to whether GP64

is required for budding. If a virus can still bud from cells without GP64, this would suggest that another virus protein (such as influenza HA) can serve as a signal for this step in virus replication. If *gp64* negative viruses cannot bud from cells using a virus that is *gp64*-deficient by adding the HA gene we could assess if a heterologous TMD can be a substitute.

The antigenicity of the full-length HA described in this thesis (Chapter 6) used live BV displaying HA and infected Tni H5 cells containing HA as antigens. This investigation was based on serial experiments carried out in previous Chapters of this thesis. Although it was a preliminary study, it demonstrated that mice vaccinated with the antigens mentioned above were able to elicit HA-specific antibodies from the first immunisation booster when sera samples were examined by indirect ELISA suggesting that live BV and infected cells are able to induce humoral immune responses *in vivo* against H1N1influenza virus antigen. This was a preliminary experiment and additional work in this *in vivo* mouse model requires further optimisation, including vaccinating mice with inactivated BV and infected cells. Future work could also be directed towards challenging vaccinated mice with H1N1 influenza virus. Furthermore, the results in this thesis showed a significant haemagglutination inhibition titre in post-vaccination sera against influenza A/New Caledonia virus from both mice groups vaccinated with either BV-HA or Tni Hi5-HA antigens. Recent studies suggested that live baculovirus BV appeared to be a good adjuvant that can enhance both humoral and cellular immune responses against foreign antigens in the vaccinated animal (Musthaq *et al.*, 2014; Sim *et al.*, 2016; Heinimaki *et al.*, 2017). It will be interesting to investigate this feature in future work.

## 7.3 Conclusion

In conclusion, this thesis has shown the potential of using the signal peptide and TMD of HA for maximising the display of this protein on the baculovirus BV envelope surface. Furthermore, it was clearly demonstrated that FBU is the best choice for full-length HA display to be used as an antigen for animal vaccinations. Finally, siRNA technology has great potential for reducing GP64 glycoprotein and improving the HA incorporation into BV envelope.

Although baculovirus BV display of proteins appears very attractive for further development as vaccines, there are many obstacles to overcome before its use in humans. Perhaps the most important will be the response of both regulators and the general public to the idea of using a live virus as a vaccine. While vaccines based on attenuated viruses are well accepted there can be inherent resistance to anything that has been genetically manipulated. In addition, clinical evaluation to study safety and efficacy must be conducted in humans before approval for widespread use of any new vaccine(s) can take place. This usually takes several years from Phase I of a clinical study until the vaccine is approved

and licensed. Therefore, it may be that the best chance of demonstrating the use of baculovirus BV as a recombinant vaccine lies in its use either in veterinary applications or to combat some of the most deadly human diseases such as Ebola or Lassa that need novel approaches to generate vaccines. The recent outbreak of the former showed how pitifully unprepared we are for such threats to human health.

# References

## References


Abe, Y., Takashita, E., Sugawara, K., Matsuzaki, Y., Muraki, Y.and Hongo, S. (2004). Effect of the addition of oligosaccharides on the biological activities and antigenicity of influenza A/H3N2 virus hemagglutinin. *J Virol,* 78**,** 9605-11.

Adam, J. R.and Mcclintock, J. T. 1991. *Baculoviridae, nuclear poluhedrosisviruses Part 1. Nuclear polyhedrosis viruses of insects*, In "Atlas of Invertebrate Viruses".

Airenne, K. J., Hu, Y. C., Kost, T. A., Smith, R. H., Kotin, R. M., Ono, C.and Yla-Herttuala, S. (2013). Baculovirus: an insect-derived vector for diverse gene transfer applications. *Mol Ther,* 21**,** 739-49.

Aksular, M. 2017. *Use of baculovirus surface display for further characterization of AHSV4-VP2 antigenic structure.* PhD Thesis., Oxford Brookes University

Anthony, E., Fiore, M., David, K., Shay, M., Karen, B., John, K. I.and Nancy, J. C. (2008). Prevention and Control of Influenza, Recommendations of the Advisory Committee on Immunization Practices. *Morb Mortal Wkly Rep,* 57**,** 1-60.

Ayres, M. D., Howard, S. C., Kuzio, J., Lopez-Ferber, M.and Possee, R. D. (1994). The complete DNA sequence of Autographa californica nuclear polyhedrosis virus. *Virology,* 202**,** 586-605.

Bak, X. Y., Lam, D. H., Yang, J., Ye, K., Wei, E. L., Lim, S. K.and Wang, S. (2011). Human embryonic stem cell-derived mesenchymal stem cells as cellular delivery vehicles for prodrug gene therapy of glioblastoma. *Human Gene Therapy,* 22**,** 1365-77.

Barrett, P. N., Mundt, W., Kistner, O.and Howard, M. K. (2009). Vero cell platform in vaccine production: moving towards cell culture-based viral vaccines. *Expert Rev Vaccines,* 8**,** 607-18.

Barsoum, J., Brown, R., Mckee, M.and Boyce, F. M. (1997). Efficient transduction of mammalian cells by a recombinant baculovirus having the vesicular stomatitis virus G glycoprotein. *Human Gene Therapy,* 8**,** 2011-8.

Behzadian, F., Goodarzi, Z., Fotouhi, F.and Saberfar, E. (2013). Baculoviral Co-Expression of HA, NA and M1 Proteins of Highly Pathogenic H5N1 Influenza Virus in Insect Cells. *Jundishapur Journal of Microbiology,* 6.

Belongia, E. A., Simpson, M. D., King, J. P., Sundaram, M. E., Kelley, N. S., Osterholm, M. T.and Mclean, H. Q. (2016). Variable influenza vaccine effectiveness by subtype: a systematic review and meta-analysis of test-negative design studies. *The Lancet Infectious Diseases,* 16**,** 942-951.

Blissard, G. W.and Rohrmann, G. F. (1990). Baculovirus diversity and molecular biology. *Annual Review of Entomology,* 35**,** 127-55.

Blissard, G. W.and Wenz, J. R. (1992). Baculovirus gp64 envelope glycoprotein is sufficient to mediate pH-dependent membrane fusion. *Journal of Virology,* 66**,** 6829-35.

Bonning, B. C.and Hammock, B. D. (1992). Development and potential of genetically engineered viral insecticides. *Biotechnology and Genetic Engineering Reviews,* 10**,** 455-89.

Bonning, B. C., Roelvink, P. W., Vlak, J. M., Possee, R. D.and Hammock, B. D. (1994). Superior expression of juvenile hormone esterase and β-galactosidase from the basic protein promoter of Autographa californica nuclear polyhedrosis virus compared to the p10 protein and polyhedrin promoters. *Journal of General Virology,* 75**,** 1551-1556.

Boublik, Y., Di Bonito, P.and Jones, I. M. (1995). Eukaryotic virus display: engineering the major surface glycoprotein of the Autographa californica nuclear polyhedrosis virus (AcNPV) for the presentation of foreign proteins on the virus surface. *Bio/Technology,* 13**,** 1079-84.

Bouvier, N. M.and Palese, P. (2008). The biology of influenza viruses. *Vaccine & Immunization News,* 26**,** D49-D53.

Boyce, F. M.and Bucher, N. L. (1996). Baculovirus-mediated gene transfer into mammalian cells. *Proceedings of the National Academy of Sciences of the United States of America,* 93**,** 2348-52.

## References


Brands, R., Visser, J., Medema, J., Palache, A.and Van Scharrenburg , G. (1999). Influvac: a safe Madin Darby Canine Kidney (MDCK) cell culture-based influenza vaccine. *Dev Biol Stand,* 98**,** 93-100.

Braunagel, S. C.and Summers, M. D. (2007). Molecular biology of the baculovirus occlusion-derived virus envelope. *Current Drug Targets,* 8**,** 1084-95.

Bustos, M. M., Luckow, V. A., Griffing, L. R., Summers, M. D.and Hall, T. C. (1988). Expression, glycosylation and secretion of phaseolin in a baculovirus system. *Plant Molecular Biology,* 10**,** 475-88.

Carbonell, L. F., Klowden, M. J.and Miller, L. K. (1985). Baculovirus-mediated expression of bacterial genes in dipteran and mammalian cells. *Journal of Virology,* 56**,** 153-60.

Carpentier, D. C., Griffiths, C. M.and King, L. A. (2008). The baculovirus P10 protein of Autographa californica nucleopolyhedrovirus forms two distinct cytoskeletal-like structures and associates with polyhedral occlusion bodies during infection. *Virology,* 371**,** 278-91.

Carstens, E. B., Williams, G. V., Faulkner, P.and Partington, S. (1992). Analysis of polyhedra morphology mutants of Autographa californica nuclear polyhedrosis virus: molecular and ultrastructural features. *Journal of General Virology,* 73 ( Pt 6)**,** 1471-9.

Cdc. 2018. *Types of Influenza Viruses [Online]* [Online]. Available: https://www.cdc.gov/flu/about/viruses/types.htm [Accessed 25 February 2018 2018].

Chaabihi, H., Ogliastro, M. H., Martin, M., Giraud, C., Devauchelle, G.and Cerutti, M. (1993). Competition between baculovirus polyhedrin and p10 gene expression during infection of insect cells. *Journal of Virology,* 67**,** 2664-71.

Chambers, A. C. 2012. *The role of ODV structural proteins in baculovirus replication.* PhD Thesis., Oxford Brookes University.

Chapple, S. D.and Jones, I. M. (2002). Non-polar distribution of green fluorescent protein on the surface of Autographa californica nucleopolyhedrovirus using a heterologous membrane anchor. *Journal of Biotechnology,* 95**,** 269-75.

Charlton, C. A.and Volkman, L. E. (1986). Effect of tunicamycin on the structural proteins and infectivity of budded Autographa californica nuclear polyhedrosis virus. *Virology,* 154**,** 214-8.

Charlton, C. A.and Volkman, L. E. (1991). Sequential rearrangement and nuclear polymerization of actin in baculovirus-infected Spodoptera frugiperda cells. *Journal of Virology,* 65**,** 1219-27.

Charlton, C. A.and Volkman, L. E. (1993). Penetration of Autographa californica nuclear polyhedrosis virus nucleocapsids into IPLB Sf 21 cells induces actin cable formation. *Virology,* 197**,** 245-54.

Chavez-Pena, C.and Kamen, A. A. (2018). RNA interference technology to improve the baculovirus-insect cell expression system. *Biotechnol Adv,* 36**,** 443-451.

Chen, C. Y., Lin, C. Y., Chen, G. Y.and Hu, Y. C. (2011). Baculovirus as a gene delivery vector: recent understandings of molecular alterations in transduced cells and latest applications. *Biotechnology Advances,* 29**,** 618-31.

Chen, C. Y., Lin, S. Y., Cheng, M. C., Tsai, C. P., Hung, C. L., Lo, K. W.and Hu, Y. C. (2013). Baculovirus vector as an avian influenza vaccine: hemagglutinin expression and presentation augment the vaccine immunogenicity. *J Biotechnol,* 164**,** 143-50.

Chen, P., Hutter, D., Liu, P.and Liu, Y. (2002). A mammalian expression system for rapid production and purification of active MAP kinase phosphatases. *Protein Expression and Purification,* 24**,** 481-8.

Cheng, X. H., Hillman, C. C., Zhang, C. X.and Cheng, X. W. (2013). Reduction of polyhedrin mRNA and protein expression levels in Sf9 and Hi5 cell lines, but not in Sf21 cells, infected with Autographa californica multiple nucleopolyhedrovirus fp25k mutants. *J Gen Virol,* 94**,** 166-76.

Chiron, V. 2002. *Agrippal Product Monograph. Adis International Limited, Starnberg, Germany.*

Choi, Y., Kwon, S. Y., Oh, H. J., Shim, S., Chang, S., Chung, H. J.and Lee, Y. (2017). Application of recombinant hemagglutinin proteins as alternative antigen standards for pandemic influenza vaccines. *Biotechnology Letters,* 39**,** 1375-1380.

Clavijo, G., Williams, T., Simon, O., Munoz, D., Cerutti, M., Lopez-Ferber, M.and Caballero, P. (2009). Mixtures of complete and pif1- and pif2-deficient genotypes are required for increased potency of an insect nucleopolyhedrovirus. *Journal of Virology,* 83**,** 5127-36.

Condreay, J. P., Witherspoon, S. M., Clay, W. C.and Kost, T. A. (1999). Transient and stable gene expression in mammalian cells transduced with a recombinant baculovirus vector. *Proceedings of the National Academy of Sciences of the United States of America,* 96**,** 127-32.

Cook, S. P., Webb, R. E., Podgwaite, J. D.and Reardon, R. C. (2003). Increased mortality of gypsy moth Lymantria dispar (L.) (Lepidoptera: Lymantriidae) exposed to gypsy moth nuclear polyhedrosis virus in combination with the phenolic glycoside salicin. *Journal of Economic Entomology,* 96**,** 1662-7.

Cox, M.and Subbarao, K. (2003). Global epidemiology of influenza: past and present. *Annual Review of Medicine,* 51**,** 407-421.

Cox, M. M. (2012). Recombinant protein vaccines produced in insect cells. *Vaccine,* 30**,** 1759-66.

Cox, M. M.and Hollister, J. R. (2009). FluBlok, a next generation influenza vaccine manufactured in insect cells. *Biologicals,* 37**,** 182-9.

Cox, M. M. J. 2009. *Development of an influenza virus vaccine using the baculovirus-insect cell expression system.* PhD Thesis, Wageningen University.

Cox, R. J. (2013). Correlates of protection to influenza virus, where do we go from here? *Hum Vaccin Immunother,* 9**,** 405-8.

Dong, S., Wang, M., Qiu, Z., Deng, F., Vlak, J. M., Hu, Z.and Wang, H. (2010). Autographa californica multicapsid nucleopolyhedrovirus efficiently infects Sf9 cells and transduces mammalian cells via direct fusion with the plasma membrane at low pH. *Journal of Virology,* 84**,** 5351-9.

Doroshenko, A.and Halperin, S. (2009). Trivalent MDCK cell culture-derived influenza vaccine Optaflu (Novartis Vaccines). *Expert Rev Vaccines,* 8**,** 679-88.

Duisit, G., Saleun, S., Douthe, S., Barsoum, J., Chadeuf, G.and Moullier, P. (1999). Baculovirus vector requires electrostatic interactions including heparan sulfate for efficient gene transfer in mammalian cells. *Journal of Gene Medicine,* 1**,** 93-102.

Elias, C. B., Zeiser, A., Bedard, C.and Kamen, A. A. (2000). Enhanced growth of Sf-9 cells to a maximum density of 5.2 x 10(7) cells per mL and production of beta-galactosidase at high cell density by fed batch culture. *Biotechnology and Bioengineering,* 68**,** 381-8.

Elliott, A. 2012. *Comparing influenza virus hemagglutinin (HA) expression in three different baculovirus expression systems.* MSc MSc.Thesis, University of Guelph.

Entwistle, P. F.and Evans, H. F. 1985. *Viral control. In Comprehensive Insect Physiology Biochemistry and Physiology*, Oxford: Pergamon Press.

Europe, F. N. 2018. *Online* [Online]. Available: https://flunewseurope.org/PrimaryCareData [Accessed 25 February 2018].

Federici, B. A.and Hice, R. H. (1997). Organization and molecular characterization of genes in the polyhedrin region of the Anagrapha falcifera multinucleocapsid NPV. *Archives of Virology,* 142**,** 333-48.

Felberbaum, R. S. (2015). The baculovirus expression vector system: A commercial manufacturing platform for viral vaccines and gene therapy vectors. *Biotechnology Journal,* 10**,** 702-14.

Fiedler, K.and Simons, K. (1995). The role of N-glycans in the secretory pathway. *Cell,* 81**,** 309-12.

Fields, T. A.and Casey, P. J. (1995). Phosphorylation of Gz alpha by protein kinase C blocks interaction with the beta gamma complex. *Journal of Biological Chemistry,* 270**,** 23119-25.

## References


Flannery, B., Reynolds, S. B., Blanton, L., Santibanez, T. A., O'halloran, A., Lu, P.-J.and Fry, A. M. (2017). Influenza Vaccine Effectiveness Against Pediatric Deaths: 2010–2014. *Pediatrics,* 139**,** e20164244.

Flores-Jasso, C. F., Valdes, V. J., Sampieri, A., Valadez-Graham, V., Recillas-Targa, F.and Vaca, L. (2004). Silencing structural and nonstructural genes in baculovirus by RNA interference. *Virus Research,* 102**,** 75-84.

Fraiser, M. J. (1986). Ultrastructural observations of virion maturation in Autographica californicanuclear polyhedra virus infected Spodoptera frugiperdacull cultures. *Journal of Ultrastructre, Molecular Structure Research,* 95.

Fraser, M. J., Cary, L., Boonvisudhi, K.and Wang, H. G. (1995). Assay for movement of Lepidopteran transposon IFP2 in insect cells using a baculovirus genome as a target DNA. *Virology,* 211**,** 397-407.

Funk, C. J., Braunagel, S. C.and Rohrmann, G. F. 1997. Baculovirus Structure. *In:* MILLER, L. K. (ed.) *The Baculoviruses.* Boston, MA: Springer US.

Gadalla, M. R., El-Deeb, A. H., Emara, M. M.and Hussein, H. A. (2014). Insect cell surface expression of hemagglutinin (HA) of Egyptian H5N1 avian influenza virus under transcriptional control of whispovirus immediate early-1 promoter. *J Microbiol Biotechnol,* 24**,** 1719-27.

Gao, R., Mccormick, C. J., Arthur, M. J., Ruddell, R., Oakley, F., Smart, D. E.and Mann, D. A. (2002). High efficiency gene transfer into cultured primary rat and human hepatic stellate cells using baculovirus vectors. *Liver,* 22**,** 15-22.

Geisler, C.and Jarvis, D. (2009). Insect cell glycosylation patterns in the context of biopharmaceuticals. Post-translational Modification of Protein *Biopharmaceuticals***,** 165-191.

Gerdil, C. (2003). The annual production cycle for influenza vaccine. *Vaccine,* 21**,** 1776-1779.

Gotoh, T., Miyazaki, Y., Sato, W., Kikuchi, K.and Bentley, W. E. (2001). Proteolytic activity and recombinant protein production in virus-infected Sf-9 insect cell cultures supplemented with carboxyl and cysteine protease inhibitors. *Journal of Bioscience and Bioengineering,* 92**,** 248-55.

Grabherr, R.and Ernst, W. (2010). Baculovirus for eukaryotic protein display. *Current Gene Therapy,* 10**,** 195-200.

Grabherr, R., Ernst, W., Oker-Blom, C.and Jones, I. (2001). Developments in the use of baculoviruses for the surface display of complex eukaryotic proteins. *Trends in Biotechnology,* 19**,** 231-6.

Granados, R. R. (1978). Early events in the infection of Hiliothis zea midgut cells by a baculovirus. *Virology,* 90**,** 170-4.

Granados, R. R., Li, G. X., Derksen, A. G.and Mckenna, K. A. (1994). A new insect cell line from Trichoplusia ni (BTI-Tn-5B1-4) susceptible to Trichoplusia ni single enveloped nuclear polyhedrosis virus. *J Invertebr Pathol,* 64**,** 260-266.

Graves, L. P. 2016. *Taking a closer look: Exploring the functional roles of P10 in baculovirus-infected cells.* PhD PhD Thesis, Oxford Brookes University.

Gross, C. H., Russell, R. L.and Rohrmann, G. F. (1994). Orgyia pseudotsugata baculovirus p10 and polyhedron envelope protein genes: analysis of their relative expression levels and role in polyhedron structure. *Journal of General Virology,* 75 ( Pt 5)**,** 1115-23.

Haas-Stapleton, E. J., Washburn, J. O.and Volkman, L. E. (2004). P74 mediates specific binding of Autographa californica M nucleopolyhedrovirus occlusion-derived virus to primary cellular targets in the midgut epithelia of Heliothis virescens Larvae. *J Virol,* 78**,** 6786-91.

Haase, S., M, Leticia, M.and Romanowski, V. (2013). Baculovirus Display: A Novel Tool for Vaccination *Current Issues in Molecular Virology - Viral Genetics and Biotechnological Applications*.

Hahn, T. J., Webb, B., Kutney, J., Fix, E., Nidel, N., Wong, J.and Sowers, M. (2015). Rapid Manufacture and Release of a GMP Batch of Zaire Ebolavirus Glycoprotein Vaccine

Made Using Recombinant Baculovirus-Sf9 Insect Cell Culture Technology. *BioProcessing Journal,* 14.

Harrap, K. (1972). The structure of nuclear polyhedrosis viruses: I. The inclusion body. *Virology (Auckland),* 50**,** 114-123.

Harrison, R. L.and Summers, M. D. (1995). Mutations in the Autographa californica multinucleocapsid nuclear polyhedrosis virus 25 kDa protein gene result in reduced virion occlusion, altered intranuclear envelopment and enhanced virus production. *Journal of General Virology,* 76 ( Pt 6)**,** 1451-9.

Hawtin, R. E., Zarkowska, T., Arnold, K., Thomas, C. J., Gooday, G. W., King, L. A.and Possee, R. D. (1997). Liquefaction of Autographa californica nucleopolyhedrovirus-infected insects is dependent on the integrity of virus-encoded chitinase and cathepsin genes. *Virology,* 238**,** 243-53.

Heinimaki, S., Tamminen, K., Malm, M., Vesikari, T.and Blazevic, V. (2017). Live baculovirus acts as a strong B and T cell adjuvant for monomeric and oligomeric protein antigens. *Virology,* 511**,** 114-122.

Hericourt, F., Blanc, S., Redeker, V.and Jupin, I. (2000). Evidence for phosphorylation and ubiquitinylation of the turnip yellow mosaic virus RNA-dependent RNA polymerase domain expressed in a baculovirus-insect cell system. *Biochemical Journal,* 349**,** 417-25.

Herniou, E. A.and Jehle, J. A. (2007). Baculovirus phylogeny and evolution. *Current Drug Targets,* 8**,** 1043-50.

Herniou, E. A., Olszewski, J. A., Cory, J. S.and O'reilly, D. R. (2003). The genome sequence and evolution of baculoviruses. *Annual Review of Entomology,* 48**,** 211-34.

Hervas-Stubbs, S., Rueda, P., Lopez, L.and Leclerc, C. (2007). Insect baculoviruses strongly potentiate adaptive immune responses by inducing type I IFN. *Journal of Immunology,* 178**,** 2361-9.

Hiscock, D.and Upton, C. (2000). Viral Genome DataBase: storing and analyzing genes and proteins from complete viral genomes. *Bioinformatics,* 16**,** 484-5.

Hitchman, R. B., Locanto, E., Possee, R. D.and King, L. A. (2011). Optimizing the baculovirus expression vector system. *Methods,* 55**,** 52-7.

Hitchman, R. B., Possee, R. D., Crombie, A. T., Chambers, A., Ho, K., Siaterli, E.and King, L. A. (2010a). Genetic modification of a baculovirus vector for increased expression in insect cells. *Cell Biol Toxicol,* 26**,** 57-68.

Hitchman, R. B., Possee, R. D.and King, L. A. (2007a). Improved Baculovirus Expression Vectors. In: Methods Express: Expression Systems, Eds. Dyson, MR and Durocher, Y pp. 147-167. Scion Publishing Ltd, Oxford. .

Hitchman, R. B., Possee, R. D.and King, L. A. (2009). Baculovirus expression systems for recombinant protein production in insect cells. *Recent Pat Biotechnol,* 3**,** 46-54.

Hitchman, R. B., Possee, R. D., Siaterli, E., Richards, K. S., Clayton, A. J., Bird, L. E.and King, L. A. (2010b). Improved expression of secreted and membrane-targeted proteins in insect cells. *Biotechnology and Applied Biochemistry,* 56**,** 85-93.

Hitchman, R. B., Siaterli, E. A., Nixon, C. P.and King, L. A. (2007b). Quantitative real-time PCR for rapid and accurate titration of recombinant baculovirus particles. *Biotechnology and Bioengineering,* 96**,** 810-4.

Ho, Y. C., Chung, Y. C., Hwang, S. M., Wang, K. C.and Hu, Y. C. (2005). Transgene expression and differentiation of baculovirus-transduced human mesenchymal stem cells. *Journal of Gene Medicine,* 7**,** 860-8.

Hodder, A. N., Crewther, P. E., Matthew, M. L., Reid, G. E., Moritz, R. L., Simpson, R. J.and Anders, R. F. (1996). The disulfide bond structure of Plasmodium apical membrane antigen-1. *Journal of Biological Chemistry,* 271**,** 29446-52.

Hofmann, C., Sandig, V., Jennings, G., Rudolph, M., Schlag, P.and Strauss, M. (1995). Efficient gene transfer into human hepatocytes by baculovirus vectors. *Proceedings of the National Academy of Sciences of the United States of America,* 92**,** 10099-103.

## References


Hohmann, A. W.and Faulkner, P. (1983). Monoclonal antibodies to baculovirus structural proteins: determination of specificities by Western blot analysis. *Virology,* 125**,** 432-44.

Horton, H. M.and Burand, J. P. (1993). Saturable attachment sites for polyhedron-derived baculovirus on insect cells and evidence for entry via direct membrane fusion. *Journal of Virology,* 67**,** 1860-8.

Hoss, A., Moarefi, I., Scheidtmann, K. H., Cisek, L. J., Corden, J. L., Dornreiter, I.and Fanning, E. (1990). Altered phosphorylation pattern of simian virus 40 T antigen expressed in insect cells by using a baculovirus vector. *Journal of Virology,* 64**,** 4799-807.

Hsieh, M. S., He, J. L., Wu, T. Y.and Juang, R. H. (2018). A secretary bi-cistronic baculovirus expression system with improved production of the HA1 protein of H6 influenza virus in insect cells and Spodoptera litura larvae. *J Immunol Methods,* 459**,** 81-89.

Hsu, C. S., Ho, Y. C., Wang, K. C.and Hu, Y. C. (2004). Investigation of optimal transduction conditions for baculovirus-mediated gene delivery into mammalian cells. *Biotechnol Bioeng,* 88**,** 42-51.

Janssen, J. J., Van De Ven, W. J., Van Groningen-Luyben, W. A., Roosien, J., Vlak, J. M.and De Grip, W. J. (1988). Synthesis of functional bovine opsin in insect cells under control of the baculovirus polyhedrin promoter. *Molecular Biology Reports,* 13**,** 65-71.

Jarvis, D. L., Bohlmeyer, D. A.and Garcia, A., Jr. (1991). Requirements for nuclear localization and supramolecular assembly of a baculovirus polyhedrin protein. *Virology,* 185**,** 795-810.

Jarvis, D. L., Bohlmeyer, D. A.and Garcia, A., Jr. (1992). Enhancement of polyhedrin nuclear localization during baculovirus infection. *Journal of Virology,* 66**,** 6903-11.

Jarvis, D. L.and Garcia, A., Jr. (1994). Biosynthesis and processing of the Autographa californica nuclear polyhedrosis virus gp64 protein. *Virology,* 205**,** 300-13.

Jarvis, D. L., Wills, L., Burow, G.and Bohlmeyer, D. A. (1998). Mutational analysis of the N-linked glycans on Autographa californica nucleopolyhedrovirus gp64. *Journal of Virology,* 72**,** 9459-69.

Jehle, J. A., Blissard, G. W., Bonning, B. C., Cory, J. S., Herniou, E. A., Rohrmann, G. F.and Vlak, J. M. (2006). On the classification and nomenclature of baculoviruses: a proposal for revision. *Archives of Virology,* 151**,** 1257-66.

Jin, H., Leser, G. P., Zhang, J.and Lamb, R. A. (1997). Influenza virus hemagglutinin and neuraminidase cytoplasmic tails control particle shape *EMBO Journal,* 16**,** 1236-1247.

Kaba, S. A., Salcedo, A. M., Wafula, P. O., Vlak, J. M.and Van Oers, M. M. (2004). Development of a chitinase and v-cathepsin negative bacmid for improved integrity of secreted recombinant proteins. *J Virol Methods,* 122**,** 113-8.

Kaname, Y., Tani, H., Kataoka, C., Shiokawa, M., Taguwa, S., Abe, T.and Matsuura, Y. (2010). Acquisition of complement resistance through incorporation of CD55/decay-accelerating factor into viral particles bearing baculovirus GP64. *J Virol,* 84**,** 3210-9.

Kataoka, C., Kaname, Y., Taguwa, S., Abe, T., Fukuhara, T., Tani, H.and Matsuura, Y. (2012). Baculovirus GP64-mediated entry into mammalian cells. *J Virol,* 86**,** 2610-20.

Katsuma, S., Noguchi, Y., Zhou, C. L., Kobayashi, M.and Maeda, S. (1999). Characterization of the 25K FP gene of the baculovirus Bombyx mori nucleopolyhedrovirus: implications for post-mortem host degradation. *Journal of General Virology,* 80 ( Pt 3)**,** 783-91.

Katz, J., M, Naeve, C., Wand Webster, R., G (1987). Host cell-mediated variation in H3N2 influenza viruses. *Virology (Auckland),* 156**,** 386-95.

Keddie, B., Aponte, G.and Volkman, L. (1989). The pathway of infection of Autographa californica nuclear polyhedrosis virus in an insect host. *Science,* 243**,** 1728-1730.

Keil, W., Geyer, R., Dabrowski, J., Dabrowski, U., Niemann, H., Stirm, S.and Klenk, H. D. (1985). Carbohydrates of influenza virus. Structural elucidation of the individual glycans of the FPV hemagglutinin by two-dimensional 1H n.m.r. and methylation analysis. *The EMBO Journal,* 4**,** 2711-2720.

Kida, H., Webster, R., Gand Yanagawa, R. (1983). Inhibition of virus-induced hemolysis with monoclonal antibodies to different antigenic areas on the hemagglutinin molecule of A/seal/Massachusetts/1/80 (H7N7) influenza virus. *Archives of Virology,* 76**,** 91-9.

Kim, J. S., Choi, J. Y., Roh, J. Y., Lee, H. Y., Jang, S. S.and Je, Y. H. (2007). Production of recombinant polyhedra containing Cry1Ac fusion protein in insect cell lines. *Journal of Microbiology and Biotechnology,* 17**,** 739-44.

King, L. A.and Possee, R. D. 1992. *The Baculovirus Expression System. A Laboratory Guide,* London, Chapman & Hall.

Kioukia, N., Nienow, A. W., Emery, A. N.and Al-Rubeai, M. (1995). Physiological and environmental factors affecting the growth of insect cells and infection with baculovirus. *Journal of Biotechnology,* 38**,** 243-51.

Kitts, P. A., Ayres, M. D.and Possee, R. D. (1990). Linearization of baculovirus DNA enhances the recovery of recombinant virus expression vectors. *Nucleic Acids Research,* 18**,** 5667-72.

Kitts, P. A.and Possee, R. D. (1993). A method for producing recombinant baculovirus expression vectors at high frequency. *Biotechniques,* 14**,** 810-7.

Klenk, H.-D. (1996). Post-translational modifications in insect cells. Insect Cell Culture: Fundamental and Applied Aspects. Springer.

Kost, T. A., Condreay, J. P.and Ames, R. S. (2010). Baculovirus gene delivery: a flexible assay development tool. *Current Gene Therapy,* 10**,** 168-73.

Kost, T. A., Condreay, J. P.and Jarvis, D. L. (2005). Baculovirus as versatile vectors for protein expression in insect and mammalian cells. *Nature Biotechnology,* 23**,** 567-75.

Krammer, F., Schinko, T., Palmberger, D., Tauer, C., Messner, P.and Grabherr, R. (2010). Trichoplusia ni cells (High Five) are highly efficient for the production of influenza A virus-like particles: a comparison of two insect cell lines as production platforms for influenza vaccines. *Mol Biotechnol,* 45**,** 226-34.

Kukkonen, S. P., Airenne, K. J., Marjomaki, V., Laitinen, O. H., Lehtolainen, P., Kankaanpaa, P.and Yla-Herttuala, S. (2003). Baculovirus capsid display: a novel tool for transduction imaging. *Molecular Therapy,* 8**,** 853-62.

Laakkonen, J. P., Makela, A. R., Kakkonen, E., Turkki, P., Kukkonen, S., Peranen, J.and Marjomaki, V. (2009). Clathrin-independent entry of baculovirus triggers uptake of E. coli in non-phagocytic human cells. *PLoS ONE,* 4**,** e5093.

Lamb, R., A. and Krug, R., M. 2001. *Orthomyxoviridae: The viruses and their replication. In Knipe DM, Howley PM, Griffin DE et al, editors. Fields Virology, 4th edn. Lippincott Williams & Wilkins: pp. 1487-531.*

Lamontagne, J., R, Noble, G., Rand Quinnan, G., V (1983). Summary of clinical trials of inactivated influenza vaccine-1978. *Rev Inf Dis,* 5**,** 723-36.

Lawrie, A. M., King, L. A.and Ogden, J. E. (1995). High level synthesis and secretion of human urokinase using a late gene promoter of the Autographa californica nuclear polyhedrosis virus. *Journal of Biotechnology,* 39**,** 1-8.

Lee, Lee, H., Y., Kim, Y., J, Jung, H., D, Choi, K., J, Yang, J., Mand Kim, K. (2015). Small interfering (Si) RNA mediated baculovirus replication reduction without affecting target gene expression. *Virus Res,* 199**,** 68-76.

Lee, S. Y., Poloumienko, A., Belfry, S., Qu, X., Chen, W., Macafee, N.and Krause, M. (1996). A common pathway for p10 and calyx proteins in progressive stages of polyhedron envelope assembly in AcMNPV-infected Spodoptera frugiperda larvae. *Archives of Virology,* 141**,** 1247-58.

Levin, E., Diekmann, H.and Fischer, D. (2016). Highly efficient transduction of primary adult CNS and PNS neurons. *Scientific Reports,* 6**,** 38928.

## References


Li, S., Wang, M., Shen, S., Hu, Z., Wang, H.and Deng, F. (2015). The FP25K Acts as a Negative Factor for the Infectivity of AcMNPV Budded Virus. *PLoS ONE,* 10**,** e0128471.

Licari, P.and Bailey, J. E. (1991). Factors influencing recombinant protein yields in an insect cell-baculovirus expression system: multiplicity of infection and intracellular protein degradation. *Biotechnology and Bioengineering,* 37**,** 238-46.

Lin, C. H.and Jarvis, D. L. (2013). Utility of temporally distinct baculovirus promoters for constitutive and baculovirus-inducible transgene expression in transformed insect cells. *Journal of Biotechnology,* 165**,** 11-7.

Lindley, K. M., Su, J. L., Hodges, P. K., Wisely, G. B., Bledsoe, R. K., Condreay, J. P.and Kost, T. A. (2000). Production of monoclonal antibodies using recombinant baculovirus displaying gp64-fusion proteins. *Journal of Immunological Methods,* 234**,** 123-35.

Locanto, E. 2014. *Baculovirus as a gene delivery and expression vector in mammalian cells.* PhD Thesis., Oxford Brookes University.

Long, G., Pan, X., Kormelink, R.and Vlak, J. M. (2006). Functional entry of baculovirus into insect and mammalian cells is dependent on clathrin-mediated endocytosis. *Journal of Virology,* 80**,** 8830-3.

Lu, A.and Miller, L. K. (1995). Differential requirements for baculovirus late expression factor genes in two cell lines. *Journal of Virology,* 69**,** 6265-72.

Lu, H.-Y., Chen, Y.-H.and Liu, H.-J. (2012). Baculovirus as a vaccine vector. *Bioengineered,* 3**,** 271-274.

Luckow, V. A., Lee, S. C., Barry, G. F.and Olins, P. O. (1993). Efficient generation of infectious recombinant baculoviruses by site-specific transposon-mediated insertion of foreign genes into a baculovirus genome propagated in Escherichia coli. *Journal of Virology,* 67**,** 4566-79.

Lynn, D. E.and Hink, W. F. (1978). Cell cycle analysis and synchronization of the TN-368 insect cell line. *In Vitro,* 14**,** 236-8.

Madhan, S., Prabakaran, M.and Kwang, J. (2010). Baculovirus as vaccine vectors. *Current Gene Therapy,* 10**,** 201-13.

Makela, A. R., Tuusa, J. E., Volkman, L. E.and Oker-Blom, C. (2008). Occlusion-derived baculovirus: interaction with human cells and evaluation of the envelope protein P74 as a surface display platform. *J Biotechnol,* 135**,** 145-56.

Makkonen, K. E., Turkki, P., Laakkonen, J. P., Yla-Herttuala, S., Marjomaki, V.and Airenne, K. J. (2013). 6-o- and N-sulfated syndecan-1 promotes baculovirus binding and entry into Mammalian cells. *Journal of Virology,* 87**,** 11148-59.

Mangor, J. T., Monsma, S. A., Johnson, M. C.and Blissard, G. W. (2001). A GP64-null baculovirus pseudotyped with vesicular stomatitis virus G protein. *Journal of Virology,* 75**,** 2544-56.

Mansouri, M.and Berger, P. (2018). Baculovirus for gene delivery to mammalian cells: Past, present and future. *Plasmid,* 98**,** 1-7.

Matilainen, H., Rinne, J., Gilbert, L., Marjomaki, V., Reunanen, H.and Oker-Blom, C. (2005). Baculovirus entry into human hepatoma cells. *Journal of Virology,* 79**,** 15452-9.

Matrosovich, M., Zhou, N., Kawaoka, Y.and Webster, R. (1999). The surface glycoproteins of H5 influenza viruses isolated from humans, chickens, and wild aquatic birds have distinguishable properties. *Journal of Virology,* 73**,** 1146-55.

Matsuura, Y., Possee, R. D., Overton, H. A.and Bishop, D. H. (1987). Baculovirus expression vectors: the requirements for high level expression of proteins, including glycoproteins. *Journal of General Virology,* 68 ( Pt 5)**,** 1233-50.

Mei, M., Zhou, Y., Peng, W., Yu, C., Ma, L., Zhang, G.and Yi, L. (2017). Application of modified yeast surface display technologies for non-Antibody protein engineering. *Microbiological Research,* 196**,** 118-128.

Miller, L. K. (1997). Baculovirus interaction with host apoptotic pathways. *Journal of Cellular Physiology,* 173**,** 178-82.

## References


Monsma, S. A., Oomens, A. G.and Blissard, G. W. (1996). The GP64 envelope fusion protein is an essential baculovirus protein required for cell-to-cell transmission of infection. *Journal of Virology,* 70**,** 4607-16.

Monteiro, F., Carinhas, N., Carrondo, M. J., Bernal, V.and Alves, P. M. (2012). Toward system-level understanding of baculovirus-host cell interactions: from molecular fundamental studies to large-scale proteomics approaches. *Frontiers in Microbiology,* 3**,** 391.

Morris, T. D.and Miller, L. K. (1992). Promoter influence on baculovirus-mediated gene expression in permissive and nonpermissive insect cell lines. *Journal of Virology,* 66**,** 7397-405.

Moscardi, F. (1999). Assessment of the application of baculoviruses for control of Lepidoptera. *Annual Review of Entomology,* 44**,** 257-89.

Mottershead, D., Van Der Linden, I., Von Bonsdorff, C. H., Keinanen, K.and Oker-Blom, C. (1997). Baculoviral display of the green fluorescent protein and rubella virus envelope proteins. *Biochemical and Biophysical Research Communications,* 238**,** 717-22.

Murphy, F. A., Fauquet, C. M., Bishop, D. H., Ghabrial, S. A., Jarvic, A. W., Martelli, G. P.and Summers, M. D. 1995. *Virus Taxonomy.*, Vienna: Springer-Verlag.

Musthaq, S. K., Kumar, S. R., Szyporta, M.and Kwang, J. (2014). Immunization with baculovirus displayed H6 hemagglutinin vaccine protects mice against lethal H6 influenza virus challenge. *Antiviral Res,* 109**,** 42-53.

Neumann, G., Noda, T.and Kawaoka, Y. (2009). Emergence and pandemic potential of swine-origin H1N1 influenza virus. . *Nature,* 459**,** 931-939.

Nhs. 2012. *Unique new flu virus found in bats [online]* [Online]. Available: https://www.nhs.uk/news/heart-and-lungs/unique-new-flu-virus-found-in-bats/ [Accessed 25 February 2018].

Nichol, K., L, Margolis, K., L, Wuorenma, J.and Von Stenberg, T. (1994). The efficacy and cost effectiveness of vaccination against influenza among elderly persons living in the community. . *New England Journal of Medicine,* 331**,** 778-84.

Nichol, K., L, Nordin, J., Mullooly, J., Lask, R., Fillbrandt, K.and Iwane, M., N (2003). Influenza Vaccination and Reduction in Hospitalizations for Cardiac Disease and Stroke among the Elderly. *Engl J Med,* 348**,** 1322-32.

Odindo, M. O. (1983). Epizootiological observations on a nuclear polyhedrosis of the African armyworm Spodoptera exempta (Walk.). *Insect Science and Its Application,* 4**,** 291–298.

Okano, K., Vanarsdall, A. L., Mikhailov, V. S.and Rohrmann, G. F. (2006). Conserved molecular systems of the Baculoviridae. *Virology,* 344**,** 77-87.

Oomens, A. G.and Blissard, G. W. (1999). Requirement for GP64 to drive efficient budding of Autographa californica multicapsid nucleopolyhedrovirus. *Virology,* 254**,** 297-314.

Passarelli, A. L.and Miller, L. K. (1993). Identification of genes encoding late expression factors located between 56.0 and 65.4 map units of the Autographa californica nuclear polyhedrosis virus genome. *Virology,* 197**,** 704-14.

Patmanidi, A. L., Possee, R. D.and King, L. A. (2003). Formation of P10 tubular structures during AcMNPV infection depends on the integrity of host-cell microtubules. *Virology,* 317**,** 308-20.

Patterson, R. M., Selkirk, J. K.and Merrick, B. A. (1995). Baculovirus and insect cell gene expression: review of baculovirus biotechnology. *Environmental Health Perspectives,* 103**,** 756-9.

Paul, A., Hasan, A., Rodes, L., Sangaralingam, M.and Prakash, S. (2014). Bioengineered baculoviruses as new class of therapeutics using micro and nanotechnologies: principles, prospects and challenges. *Adv Drug Deliv Rev,* 71**,** 115-30.

Paul, M., Ophorst, C., Koldijk, M., Schouten, G., Mehtali, M.and Uytdehaag, F. (2001). The human cell line PER.C6 provides a new manufacturing system for the production of influenza vaccines. *Vaccine & Immunization News,* 19**,** 2716-21.

## References


Peng, K., Van Oers, M. M., Hu, Z., Van Lent, J. W.and Vlak, J. M. (2010). Baculovirus per os infectivity factors form a complex on the surface of occlusion-derived virus. *Journal of Virology,* 84**,** 9497-504.

Phizicky, E. M.and Fields, S. (1995). Protein-protein interactions: methods for detection and analysis. *Microbiol Rev,* 59**,** 94-123.

Pidre, M. L., Ferrelli, M. L., Haase, S.and Romanowski, V. 2013. Baculovirus Display: A Novel Tool for Vaccination. *Current Issues in Molecular Virology - Viral Genetics and Biotechnological Applications.*

Plonsky, I., Cho, M. S., Oomens, A. G., Blissard, G.and Zimmerberg, J. (1999). An analysis of the role of the target membrane on the Gp64-induced fusion pore. *Virology,* 253**,** 65-76.

Poinar, G., Jr.and Poinar, R. (2005). Fossil evidence of insect pathogens. *Journal of Invertebrate Pathology,* 89**,** 243-50.

Possee, R. D., Hitchman, R. B., Richards, K. S., Mann, S. G., Siaterli, E., Nixon, C. P.and King, L. A. (2008). Generation of baculovirus vectors for the high-throughput production of proteins in insect cells. *Biotechnology and Bioengineering,* 101**,** 1115-22.

Possee, R. D.and Howard, S. C. (1987). Analysis of the polyhedrin gene promoter of the Autographa californica nuclear polyhedrosis virus. *Nucleic Acids Res,* 15**,** 10233-48.

Possee, R. D., Thomas, C. J.and King, L. A. (1999). The use of baculovirus vectors for the production of membrane proteins in insect cells. *Biochemical Society Transactions,* 27**,** 928-32.

Prabakaran, M., Kolpe, A. B., He, F.and Kwang, J. (2013). Cross-protective efficacy of bivalent recombinant baculoviral vaccine against heterologous influenza H5N1 challenge. *Vaccine,* 31**,** 1385-92.

Prabakaran, M., Madhan, S., Prabhu, N., Qiang, J.and Kwang, J. (2010). Gastrointestinal delivery of baculovirus displaying influenza virus hemagglutinin protects mice against heterologous H5N1 infection. *J Virol,* 84**,** 3201-9.

Premanand, B., Zhong Wee, P.and Prabakaran, M. (2018). Baculovirus Surface Display of Immunogenic Proteins for Vaccine Development. *Viruses,* 10.

Pritchett, D. W., Young, S., Yearian, W.and (1984). Some factors involved in the dissolution of Autographa californica nuclear polyhedrosis virus polyhedra by digestive fluids of Trichoplusia ni larvae. *Journal of Invertebrate Pathology* 43**,** 160-168.

Rajakumar, A., Swierkosz, E.and Schulze, I. (1990). Sequence of an influenza virus hemagglutinin determined directly from a clinical sample. *Proc Natl Acad Sci,* 87**,** 4154-8.

Reperant, L., A, Rimmelzwaan, G., Fand Osterrhaus, A., D (2014). Advance in influenza vaccination. *F1000prime Rep,* 6**,** 47.

Rice, W. C.and Miller, L. K. (1986). Baculovirus transcription in the presence of inhibitors and in nonpermissive Drosophila cells. *Virus Research,* 6**,** 155-72.

Rohrmann, G. F. 2013a. *Baculovirus Molecular Biology* [Online]. Bethesda (MD): National Center for Biotechnology Information (US). Available: https://www.ncbi.nlm.nih.gov/books/NBK114593/ [Accessed 25 September 2018 2018].

Rohrmann, G. F. (2013b). Characterization of baculoviruses from the Martignoni collection. *Journal of Invertebrate Pathology,* 114**,** 61-4.

Rohrmann, G. F. 2011. *Baculovirus molecular biology [online] 2nd ed* [Online]. Available: www.ncbi.nlm.nih.gov/books/NBK49500. [Accessed 1 March 2018].

Saito, T., Dojima, T., Toriyama, M.and Park, E. Y. (2002). The effect of cell cycle on GFPuv gene expression in the baculovirus expression system. *Journal of Biotechnology,* 93**,** 121-9.

Sambrook, J.and Russell, D. W. (2006). Preparation and Transformation of Competent E. coli Using Calcium Chloride. *CSH Protoc,* 2006.

Samji, T. (2009). Influenza A: understanding the viral life cycle. *Yale J. Biol. Med,* 82**,** 153-159.

Schindelin, J., Rueden, C. T., Hiner, M. C.and Eliceiri, K. W. (2015). The ImageJ ecosystem: An open platform for biomedical image analysis. *Molecular Reproduction and Development,* 82**,** 518-529.

Schultz, K. L.and Friesen, P. D. (2009). Baculovirus DNA replication-specific expression factors trigger apoptosis and shutoff of host protein synthesis during infection. *Journal of Virology,* 83**,** 11123-32.

Schulze, I. T. (1997). Effects of Glycosylation on the Properties and Functions of Influenza Virus Hemagglutinin. *The Journal of Infectious Diseases,* 176**,** S24-S28.

Schutz, A., Scheller, N., Breinig, T.and Meyerhans, A. (2006). The Autographa californica nuclear polyhedrosis virus AcNPV induces functional maturation of human monocyte-derived dendritic cells. *Vaccine,* 24**,** 7190-6.

Segal, M. S., Bye, J. M., Sambrook, J. F.and Gething, M. (1992). Disulfide bond formation during the folding of influenza virus hemagglutinin. *J. Cell Biol,* 118**,** 227-244

Seidel, W., Kunkel, F., Geisler, B., Garten, W., Herrmann, B., Dohner, L.and Klenk, H. D. (1991). Intraepidemic variants of influenza virus H3 hemagglutinin differing in the number of carbohydrate side chains. *Arch Virol,* 120**,** 289-96.

Shen, H. C., Yeh, C. N., Chen, G. Y., Huang, S. F., Chen, C. Y., Chiu, Y. C.and Hu, Y. C. (2008). Sustained baculovirus-mediated expression in myogenic cells. *Journal of Gene Medicine,* 10**,** 1190-7.

Shi, X.and Jarvis, D. L. (2007). Protein N-glycosylation in the baculovirus-insect cell system. *Current Drug Targets,* 8**,** 1116-25.

Shi, Y., Zhang, C., Xie, C., Quan, Y., Nie, Z., Chen, J.and Yu, W. (2015). The effect of BM67 gene deletion on Bombyx mori nuclear polyhedrosis virus replication. *Acta Virologica,* 59**,** 40-8.

Shoji, I., Aizaki, H., Tani, H., Ishii, K., Chiba, T., Saito, I.and Matsuura, Y. (1997). Efficient gene transfer into various mammalian cells, including non-hepatic cells, by baculovirus vectors. *Journal of General Virology,* 78 ( Pt 10)**,** 2657-64.

Sim, S. H., Kim, J. Y., Seong, B. L., Nguyen, H. H.and Chang, J. (2016). Baculovirus Displaying Hemagglutinin Elicits Broad Cross-Protection against Influenza in Mice. *PloS One,* 11**,** e0152485.

Simon, O., Williams, T., Lopez-Ferber, M.and Caballero, P. (2004). Genetic structure of a Spodoptera frugiperda nucleopolyhedrovirus population: high prevalence of deletion genotypes. *Applied and Environmental Microbiology,* 70**,** 5579-88.

Skehel, J. J.and Wiley, D. C. (2000). Receptor binding and membrane fusion in virus entry: the influenza hemagglutinin. *Annu Rev Biochem,* 69**,** 531-69.

Slack, J.and Arif, B. M. (2007). The baculoviruses occlusion-derived virus: virion structure and function. *Advances in Virus Research,* 69**,** 99-165.

Slack, J. M., Kuzio, J.and Faulkner, P. (1995). Characterization of v-cath, a cathepsin L-like proteinase expressed by the baculovirus Autographa californica multiple nuclear polyhedrosis virus. *Journal of General Virology,* 76 ( Pt 5)**,** 1091-8.

Smith, G. E., Summers, M. D.and Fraser, M. J. (1983). Production of human beta interferon in insect cells infected with a baculovirus expression vector. *Molecular and Cellular Biology,* 3**,** 2156-65.

Smith, G. P. (1985). Filamentous fusion phage: novel expression vectors that display cloned antigens on the virion surface. . *Science,* 228**,** 1315-7.

Sprick, G., Weidner, T., Salzig, D.and Czermak, P. (2017). Baculovirus-induced recombinant protein expression in human mesenchymal stromal stem cells: A promoter study. *New Biotechnology,* 39**,** 161-166.

Stiles, B., Wood, H.and Hughes, P. (1983). Effect of tunicamycin on the infectivity of Autographa californica nuclear polyhedrosis virus. *Journal of Invertebrate Pathology,* 41**,** 405-408.

Strauss, R., Huser, A., Ni, S., Tuve, S., Kiviat, N., Sow, P. S.and Lieber, A. (2007). Baculovirus-based vaccination vectors allow for efficient induction of immune responses against plasmodium falciparum circumsporozoite protein. *Molecular Therapy,* 15**,** 193-202.

## References


Summers, M.and Smith, G. 1987. *A manual of methods for baculovirus vectors and insect cell culture procedures.*, Tex. Agric. Exp. Stn. Bull.

Summers, M. D.and Arnott, H. J. ( 1969). Ultrastructural studies on inclusion formation and virus occlusion in nuclear polyhedrosis and granulosis virus-infected cells of Trichoplusia ni (Hubner). *Journal of Ultrastructure Research,* 28**,** 462-480.

Sun, S., Wang, Q., Zhao, F., Chen, W.and Li, Z. (2011). Glycosylation site alteration in the evolution of influenza A (H1N1) viruses. *PLoS ONE,* 6**,** e22844.

Tani, H., Nishijima, M., Ushijima, H., Miyamura, T.and Matsuura, Y. (2001). Characterization of cell-surface determinants important for baculovirus infection. *Virology,* 279**,** 343-53.

Thomas, C. J., Brown, H. L., Hawes, C. R., Lee, B. Y., Min, M. K., King, L. A.and Possee, R. D. (1998). Localization of a baculovirus-induced chitinase in the insect cell endoplasmic reticulum. *Journal of Virology,* 72**,** 10207-12.

Thompson, C. M., Petiot, E., Mullick, A., Aucoin, M. G., Henry, O.and Kamen, A. A. (2015). Critical assessment of influenza VLP production in Sf9 and HEK293 expression systems. *BMC Biotechnology,* 15**,** 31.

Treanor, J. J., Schiff, G. M., Hayden, F. G., Brady, R. C., Hay, C. M., Meyer, A. L.and Cox, M. (2007). Safety and immunogenicity of a baculovirus-expressed hemagglutinin influenza vaccine: a randomized controlled trial. *JAMA,* 297**,** 1577-82.

Tsai, C. T., Chuang, C. K.and Hu, Y. C. (2009). Baculovirus-mediated gene transfer into mesenchymal stem cells. *Methods in Molecular Biology,* 515**,** 339-51.

Tsuchiya, E., Sugawara, K., Hongo, S., Matsuzaki, Y., Muraki, Y., Li, Z. N.and Nakamura, K. (2001). Antigenic structure of the haemagglutinin of human influenza A/H2N2 virus. *Journal of General Virology,* 82**,** 2475-84.

Valdes, V. J., Sampieri, A., Sepulveda, J.and Vaca, L. (2003). Using double-stranded RNA to prevent in vitro and in vivo viral infections by recombinant baculovirus. *J Biol Chem,* 278**,** 19317-24.

Van Loo, N. D., Fortunati, E., Ehlert, E., Rabelink, M., Grosveld, F.and Scholte, B. J. (2001). Baculovirus infection of nondividing mammalian cells: mechanisms of entry and nuclear transport of capsids. *Journal of Virology,* 75**,** 961-70.

Van Oers, M. M., Pijlman, G. P.and Vlak, J. M. (2015). Thirty years of baculovirus-insect cell protein expression: from dark horse to mainstream technology. *J Gen Virol,* 96**,** 6-23.

Vaughn, J. L.and Fan, F. (1997). Differential requirements of two insect cell lines for growth in serum-free medium. *In Vitro Cellular and Developmental Biology: Animal,* 33**,** 479-82.

Volkman, L. E. (1997). Nucleopolyhedrovirus interactions with their insect hosts. *Advances in Virus Research,* 48**,** 313-48.

Volkman, L. E.and Goldsmith, P. A. (1983). In Vitro Survey of Autographa californica Nuclear Polyhedrosis Virus Interaction with Nontarget Vertebrate Host Cells. *Applied and Environmental Microbiology,* 45**,** 1085-93.

Volkman, L. E., Goldsmith, P. A., Hess, R. T.and Faulkner, P. (1984). Neutralization of budded Autographa californica NPV by a monoclonal antibody: identification of the target antigen. *Virology,* 133**,** 354-62.

Volkman, L. E., Summers, M. D.and Hsieh, C. H. (1976). Occluded and nonoccluded nuclear polyhedrosis virus grown in Trichoplusia ni: comparative neutralization comparative infectivity, and in vitro growth studies. *Journal of Virology,* 19**,** 820-832.

Wang, K., Holtz, K. M., Anderson, K., Chubet, R., Mahmoud, W.and Cox, M. M. (2006). Expression and purification of an influenza hemagglutinin--one step closer to a recombinant protein-based influenza vaccine. *Vaccine,* 24**,** 2176-85.

Wang, L., Salem, T. Z., Campbell, D. J., Turney, C. M., Kumar, C. M.and Cheng, X. W. (2009). Characterization of a virion occlusion-defective Autographa californica multiple nucleopolyhedrovirus mutant lacking the p26, p10 and p74 genes. *J Gen Virol,* 90**,** 1641-8.

## References


Wang, M., Katz, J.and Webster, R. (1989). Extensive heterogeneity in the hemagglutinin of egg-grown influenza viruses from different patients. . *Virology (Auckland),* 171**,** 275-9.

Wang, P., Granados, R. R.and Shuler, M. L. (1992). Studies on serum-free culture of insect cells for virus propagation and recombinant protein production. *J. Invertebr. Pathol,* 59**,** 46-53.

Wang, Q., Bosch, B. J., Vlak, J. M., Van Oers, M. M., Rottier, P. J.and Van Lent, J. W. M. (2016). Budded baculovirus particle structure revisited. *J Invertebr Pathol,* 134**,** 15-22.

Wang, Z., Yang, Z. Q.and Chacko, S. (1997). Functional and structural relationship between the calmodulin-binding, actin-binding, and actomyosin-ATPase inhibitory domains on the C terminus of smooth muscle caldesmon. *Journal of Biological Chemistry,* 272**,** 16896-903.

Westerlund-Wikström, B. (2000). Peptide display on bacterial flagella: Principles and applications. *International Journal of Medical Microbiology,* 290**,** 223-230.

Weyer, U.and Possee, R. D. (1989). Analysis of the Promoter of the Autographa californica Nuclear Polyhedrosis Virus p10 Gene. *Journal of General Virology,* 70**,** 203-208.

Whitford, M., Stewart, S., Kuzio, J.and Faulkner, P. (1989). Identification and sequence analysis of a gene encoding gp67, an abundant envelope glycoprotein of the baculovirus Autographa californica nuclear polyhedrosis virus. *Journal of Virology,* 63**,** 1393-9.

Whitt, M. A.and Manning, J. S. (1988). A phosphorylated 34-kDa protein and a subpopulation of polyhedrin are thiol linked to the carbohydrate layer surrounding a baculovirus occlusion body. *Virology,* 163**,** 33-42.

Who 2018. Weekly Epidemiological Record. 12 January 2018 ed.

Wickham, T. J., Davis, T., Granados, R. R., Shuler, M. L.and Wood, H. A. (1992). Screening of insect cell lines for the production of recombinant proteins and infectious virus in the baculovirus expression system. *Biotechnology Progress,* 8**,** 391-6.

Wickham, T. J.and Nemerow, G. R. (1993). Optimization of growth methods and recombinant protein production in BTI-Tn-5B1-4 insect cells using the baculovirus expression system. *Biotechnology Progress,* 9**,** 25-30.

Wilson, I., Skehel, J.and Wiley, D. (1981). Structure of the haemagglutinin membrane glycoprotein of influenza virus at 3angstrom resolution. *Nature,* 289**,** 366-373.

Wilson, M. E., Mainprize, T. H., Friesen, P. D.and Miller, L. K. (1987). Location, transcription, and sequence of a baculovirus gene encoding a small arginine-rich polypeptide. *Journal of Virology,* 61**,** 661-6.

Xianzong, S.and Donald, L. J. (2007). Protein N-Glycosylation in the Baculovirus-Insect Cell System. *Current Drug Targets,* 8**,** 1116-1125.

Xu, X., Zhu, X., Dwek, R. A., Stevens, J.and Wilson, I. A. (2008). Structural characterization of the 1918 influenza virus H1N1 neuraminidase. *Journal of Virology,* 82**,** 10493-501.

Xu, X. G.and Liu, H. J. (2008). Baculovirus surface display of E2 envelope glycoprotein of classical swine fever virus and immunogenicity of the displayed proteins in a mouse model. *Vaccine,* 26**,** 5455-60.

Xu, X. G., Tong, D. W., Chiou, M. T., Hsieh, Y. C., Shih, W. L., Chang, C. D.and Liu, H. J. (2009). Baculovirus surface display of NS3 nonstructural protein of classical swine fever virus. *Journal of Virological Methods,* 159**,** 259-64.

Xu, X. G., Tong, D. W., Wang, Z. S., Zhang, Q., Li, Z. C., Zhang, K.and Liu, H. J. (2011). Baculovirus virions displaying infectious bursal disease virus VP2 protein protect chickens against infectious bursal disease virus infection. *Avian Diseases,* 55**,** 223-9.

Yang, D. G., Chung, Y. C., Lai, Y. K., Lai, C. W., Liu, H. J.and Hu, Y. C. (2007). Avian influenza virus hemagglutinin display on baculovirus envelope: cytoplasmic domain affects virus properties and vaccine potential. *Molecular Therapy,* 15**,** 989-96.

## References


Yang, J., Yoshida, R., Kariya, Y., Zhang, X., Hashiguchi, S., Nakashima, T.and Sugimura, K. (2010). Characterization of human single-chain antibodies against highly pathogenic avian influenza H5N1 viruses: mimotope and neutralizing activity. *Journal of Biochemistry,* 148**,** 507-15.

Yang, Y., Lo, S. L., Yang, J., Yang, J., Goh, S. S., Wu, C.and Wang, S. (2009). Polyethylenimine coating to produce serum-resistant baculoviral vectors for in vivo gene delivery. *Biomaterials,* 30**,** 5767-74.

Yoden, S., Kida, H., Kuwabara, M., Yanagawa, R.and Webster, R., G (1986). Spin-labeling of influenza virus hemagglutinin permits analysis of the conformational change at low pH and its inhibition by antibody. *Virus Research,* 4**,** 251-64.

Yoshida, S., Kondoh, D., Arai, E., Matsuoka, H., Seki, C., Tanaka, T.and Ishii, A. (2003). Baculovirus virions displaying Plasmodium berghei circumsporozoite protein protect mice against malaria sporozoite infection. *Virology,* 316**,** 161-70.

Zeng, J., Du, J., Zhao, Y., Palanisamy, N.and Wang, S. (2007). Baculoviral vector-mediated transient and stable transgene expression in human embryonic stem cells. *Stem Cells,* 25**,** 1055-61.

Zhang, G. (1994). Research, development and application of Heliothis viral pesticide in China. *Resour. Environ. Yangtze Valley,* 3**,** 1-6.

Zhou, J.and Blissard, G. W. (2008). Display of heterologous proteins on gp64null baculovirus virions and enhanced budding mediated by a vesicular stomatitis virus G-stem construct. *Journal of Virology,* 82**,** 1368-77.